U.PORTO

DOUTORAMENTO

CIÊNCIAS BIOMÉDICAS

Hierarchical electrospun nanostructures for skin regeneration

Juliana Rosa Dias

D

2017

U.PORTO

Juliana Dias. Hierarchical electrospun nanostructures for skin regeneration

Hierarchical electrospun nanostructures for skin regeneration

Juliana Rosa Dias

INSTITUTO DE CIÊNCIAS BIOMÉDICAS ABEL SALAZAR

Juliana Rosa Dias

Hierarchical electrospun nanostructures for skin regeneration

Tese de candidatura ao grau de Doutor em Ciências Biomédicas do Instituto de Ciências Biomédicas submetida ao Instituto de Ciências Biomédicas de Abel Salazar da Universidade do Porto.

Orientadores

Paulo Jorge da Silva Bártolo
Categoria – Professor Catedrático
Afiliação – Universidade de Manchester

Pedro Lopes Granja
Categoria –Professor Afiliado
Afiliação –Instituto de Ciências
Biomédicas Abel Salazar da Universidade do Porto

The works are supported by a research grant (SFRH/BD/91104/2012) awarded by Portuguese FCT.

“It always seems impossible until it’s done.”

Nelson Mandela

Acknowledgements

Four years passed …

This challenge became a long journey with ups and downs, smiles and tears, happiness and sadness. However, at the end, looking back, I realized how difficult this journey was…the relieved feeling taking over me as I had crossed the finishing line of a marathon. Now, it is time for me to thank all those who supported me during my journey as a doctoral student.

First of all, I would like to thank to my Family (Mum, Dad, Brother, Sister in law and my lovely godson) without them I'm sure I would not be here, they were always my safe harbour, my refuge, my emotional support. Part of my family but a vital part of my heart, I am grateful everyday to the man of my life. Never gave up on me, on us, stayed stronger on my side, listening to my words and drying my tears. Every day I love you more.

I would also like to thank my supervisors, for their responsibility to make my dream come true. To Professor Paulo Bártolo who introduced me to the research field and followed my research course since I finished my degree. To Professor Pedro Granja, who accepted to be my supervisor even without knowing me, for his important support especially in the last two years that we worked together at i3s/INEB. Thanks for the daily encouragement to do things better and more, making me believe in myself to do a good job than a mere supervisor …a true friend. I could thanks millions time that I cannot demonstrate my gratitude to you, Pedro.

To Biocarrier group, my team, I would like to thanks to ALL, each one in different ways for supporting me during my time in Porto far from my family and comfort zone. Thanks for the guffaws and teachings, all of you will stay in my heart forever.

Collaborations are always welcome, but sometimes reveals more than a simple exchange of knowledge I would like to thank to the Universidade Católica Portuguesa, namely to Professor Ana Leite Oliveira, Doctor Sara Silva and Doctor Sandra Borges. Thanks for the support, friendship and for welcoming me so well that I felt part of our team.

I would like to thank the CDRsp-IPL for supporting my research work since 2009, was the first institution that I belonged and, therefore had an important role in my journey as a researcher. The time spent at the institution was a privilege for my growing as a professional and as human being.

Last, but not the least I would like to thank my lovely friends Daniela Barros, Victoria Leiro, Vidhura Mahendra, Tatiana Patrício, Joana Valente, Ana Isabel Pinto, Elodie Pinto and Mauro

Sousa… how good friends you are. Thanks for supporting me with all my dramas, you are right... in the end everything will be ok.

Agradecimentos

Quatro anos se passaram ...

Este desafio transformou-se numa longa viagem repleta de altos e baixos, sorrisos e lágrimas, alegrias e tristezas. Neste momento, tão perto do fim, olho para o passado e percebo o quanto foi difícil...o sentimento de alívio toma conta de mim como cruzasse a linha da meta ao terminar uma maratona. Agora, é tempo para agradecer a todos que de alguma forma apoiaram-me neste percurso enquanto aluna de doutoramento.

Em primeiro lugar, gostaria de agradecer há minha família (mãe, pai, irmão, cunhada e ao meu amoroso afilhado), sem eles, tenho a certeza que não estaria aqui, foram sempre o meu porto seguro, o meu refúgio, o meu apoio emocional. Igualmente parte da minha família, mas uma parte vital do meu coração, sou grata todos os dias ao homem da minha vida. Nunca desistiu de mim, de nós, manteve-se forte do meu lado, ouvindo os meus desabafos e secando as minhas lágrimas. Amo-vos cada dia mais.

Gostaria, também, de agradecer aos meus supervisores, eles são os responsáveis por tornar o meu sonho realidade. Ao professor Paulo Bártolo que me introduziu na investigação e acompanhou todo o meu percurso desde que terminei a Licenciatura. Ao Professor Pedro Granja, que aceitou ser meu supervisor mesmo sem me conhecer bem, pelo seu importante apoio especialmente nos últimos dois anos que trabalhamos juntos na i3s / INEB. Agradeço a paciência e o seu apoio todas as semanas para fazer mais e melhor. Por me fazer acreditar que é possível fazer um bom trabalho mesmo quando tudo corre mal e, por ser mais do que um orientador...um verdadeiro amigo. Poderia agradecer-lhe um milhão de vezes que mesmo assim não seria suficiente para lhe demonstrar a minha gratidão por si… Obrigada Pedro.

Ao grupo Biocarrier, a minha equipa, gostaria de agradecer a todos, a cada um das mais diversas formas apoiaram-me durante o tempo que estive no Porto longe da minha família e da minha zona de conforto. Obrigada pelas gargalhadas e pelos ensinamentos ficarão no meu coração para sempre.

Colaborações são sempre bem-vindas, mas às vezes revelam-se mais do que a simples troca de conhecimentos. Gostaria de agradecer à Universidade Católica Portuguesa, nomeadamente à Professora Ana Leite Oliveira, à Doutora Sara Silva e à Doutora Sandra Borges. Obrigada pelo apoio, amizade e por me terem feito sentir parte da vossa equipa.

Gostaria de agradecer ao CDRsp-IPL por apoiar os meus trabalhos de investigação desde 2009. Foi a primeira instituição a que pertenci e, portanto, teve um papel importante no meu

percurso como investigadora. Crescer com a instituição foi um privilégio que me permitiu crescer profissionalmente e pessoalmente.

Em último lugar, mas não menos importante, gostaria de agradecer aos meus adoráveis amigos Daniela Barros, Victoria Leiro, Vidhura Mahendra, Tatiana Patrício, Joana Valente, Ana Isabel Pinto, Elodie Pinto and Mauro Sousa…que bons amigos vocês são. Obrigado por me terem apoiado em todos os meus dramas, estavam certos ... no final tudo iria ficar bem.

Abstract

Hybrid electrospun structures based on Polycaprolactone (PCL) and Gelatin (Ge) were developed and optimized to create a biofunctional wound dressing to promote skin regeneration. To improve the electrospinning apparatus reproducibility the home-made system was re-designed. The major production drawback has related to the metallic parts present in the initial system. Those components reduce the stability of the main jet, due to the interference with electric field, making it unstable and depositing all around the system Other than the collector. The re-design allowed obtain at laboratory scale an apparatus more versatile allowing the fiber production using vertical or horizontal configuration. After apparatus re-design, materials processing was optimized varying solution parameters (polymer concentration and solvent system) and processing parameters (distance between collector and needle, voltage and feed rate). According to the different processing conditions a myriad of samples were obtained, from simple droplets to homogeneous fibers without beads. Scanning electron Microscopy (SEM) images allowed define as best meshes (with homogenous fibers and high fiber density, without beads or drops,) the PCL prepared with 17wt-% of polymer in Dimethylaketone (DMK) solution, far from the collector 12 cm, a controlled feed rate of 3.17 mL/h and a voltage of 10kV, and Ge solution prepared with 15 wt-% of polymer in Acetic acid plus 2v/v-% of Triethylamine (TEA) with 12 cm between collector and needle, 0.4 mL/h of feed rate and under 12kV of voltage. We faced two parallel challenges subsequent to electrospun fiber optimization, the first one comprises the degradation behavior of electrospun PCL fibers and the second one was the selection of a proper gelatin crosslinker, able to keep the fiber morphology without toxicity. Being PCL one of the most used synthetic polymers in tissue engineering (TE) the degradation kinetics have been explored by several research teams. However, looking to the literature there are controversial results most of them due to the polymer molecular weight, some authors described slow degradation in enzymatic medium, only reach 18 % of weight loss in 18 weeks, however, decreasing the amount of PCL in 30% other study demonstrated a complete degradation over 12 weeks. Based on this we investigated the hydrolytic and enzymatic degradation in vitro vs in vivo degradation. Our main goal was to describe the PCL electrospun mesh degradation kinetic in different condition to clarify its potential to be use in short term applications, namely to the skin regeneration. According to our in vitro assay the hydrolytic degradation reached only 1.44 ± 0.7 % of weight loss after 91 days, however, in enzymatic medium, after the degradation period, a weight loss of 97.11 ± 5.1% was achieved. *In vivo* assays demonstrated that occured an initial slight reaction to the implanted electrospun samples and cells stayed concentrated in the membranes surface. At day 60 and 90 the hematoxylin and eosin (H&E) stainning shows

the cells infiltration across the electrospun meshes and its colonization demonstrating that electrospun meshes does not inhibited the cellular infiltration. After 90 days of implantation is visible the the extracellular matrix components production, probably, replacing the degraded PCL electrospun fibers.

One of the major drawbacks to use gelatin in TE field is its instability in aqueous medium, to overcome this inconvenience crosslinking is needed. There are several crosslinkers available but, most of them present toxicity and the common protocols used to crosslinking (by vapor or bath) induce changes in fiber morphology. To our study we select 1,4-butanediol diglycidyl ether (BDDGE) because it is a well-known hyaluronic acid crosslinker and the used of small amounts does not induce toxicity. To keep the fiber morphology, we explore the *in situ* crosslinking, which means we added the crosslinker to the polymeric solution and only then the fibers were produced. Using this approach, the crosslinker is encapsulated inside the fibers that makes the crosslinking reaction inside keeping the fiber morphology. Ranging the amount of crosslinker (2, 4 or 6 v/v-%) and the reaction time (24, 48 or 72h) we obtained fibers with different diameters and, consequently, different properties. The crosslinking degree can be tuned by varying the crosslinker amount and/or the reaction time and, consequently, adjust the fiber diameter and mechanical properties. Fibers with 4% and 6% of BDDGE (both incubated for 72h) provided gelatin fibers with high crosslinking degree and stable diameters of 339 ± 91 and 276 ± 88 nm, respectively. Nevertheless, the sample with 4% of BDDGE resulted in the best combination of mechanical properties. Cytotoxicity assays revealed non toxicity and proliferation assays showed that fibroblasts (hDNF) were able to attach and proliferate, producing new extracellular matrix within the electrospun meshes.

With the knowledge acquired related to PCL electrospun mesh degradation and gelatin fibers crosslinking we move forward towards the development of hybrid structures combining PCL and Ge fibers.

Three different methologies were established to develop the hybrid structures that combined the same materials (PCL and Ge) through different processing strategies. The first approach called multilayer combine, at the same structure, 5 distinct layers. The coated is the second approach, in which PCL fibers are dipped in a gelatin bath and, the last methodology was called blend, in this approach the PCL and Ge were mixed in the same solution prior to fiber production with a ratio of 1:1. Based on these approaches and using PCL and Ge meshes as controls structures, were performed several characterizations to evaluate the potential of each structure to be use as bioactive wound dressing. From the characterizations performed all hybrid structures presented better mechanical and biological properties than controls. However, taking into account the final application the coated structure showed poor water vapor permeability and the lowest porosity, consequence of the gelatin coating that closed most of the pores. Regarding Multilayer and blend methodologies both structures

demonstrated a huge potential to mimic the skin ECM and its properties, due to the fiber diameters in the range of native ECM filaments, mechanical properties similar to the human skin and structures with the ability to promote cell adhesion and proliferation and, fibronectin deposition. However, in the multilayer structure, the combination of distinct layers provides different porosities and pore sizes throughout the structure resulting in a thicker structure, easy handle without damage and avoiding fibers packaging, a drawback commonly associated with the electrospun meshes.

Keywords: Electrospun fibers, hybrid meshes, Polycaprolactone, Gelatin, wound dressings.

Resumo

Estruturas híbridas obtidas por electrospinning com base de Policaprolactona (PCL) e gelatina (Ge) foram desenvolvidas e otimizadas de modo a criar um curativo biofuncional com capacidade para promover a regeneração da pele. Para aumentar a reprodutibilidade do sistema laboratorial de electrospinning disponível foi redefinido o seu design de montagem. A maior desvantagem no processamento relacionava-se com a presença de partes metálicas no sistema, reduzindo as mesmas a estabilidade do jato principal foi melhorada aumentando, assim, a densidade de fibras depositadas no coletor. O novo design confere mais versatilidade ao sistema permitindo a produção de fibras na vertical e na horizontal. Após as alterações no sistema o processamento de materiais foi otimizado variando os parâmetros da solução (concentração polimérica e solventes) e os parâmetros de processamento (distância entre o coletor e a agulha, caudal e tensão). De acordo com as diferentes condições foram obtidas diversas amostras desde pequenas gotas até malhas de fibras com deposição aleatória e fibras homogéneas sem a presença de gotas de solvente. Recorrendo à Microscopia Eletrónica de Varrimento (SEM) definiu-se como a melhor malha (com filamentos homogéneos, elevada densidade de fibras e sem gotas de solvente nos filamentos ou na malha) a amostra com 17 wt-% de PCL dissolvido em acetona (DMK), com o coletor a uma distância de 12 cm da agulha, um caudal de 3,17 mL/h e uma tensão de 10kV e a amostra de Ge preparada com 15 wt-% de polímero numa solução de acido acético (AA) e adicionado 2 v/v-% de trietilamina (TEA), as fibras foram produzidas com o coletor a 12 cm da agulha, um caudal constante de 0,4 mL/h e uma tensão de 12kV. Após a otimização da produção enfrentámos dois desafios, o primeiro compreendia a degradação do PCL e o segundo a seleção de um reticulante para a gelatina que mantivesse a morfologia das fibras e não apresentasse toxicidade. Sendo o PCL um dos polímeros sintéticos mais usados na engenharia de tecidos a sua cinética de degradação tem vindo a ser explorada por diversas equipas de investigação. Contudo de acordo com a literatura os resultados apresentam-se bastante controversos muito devido às discrepâncias dos pesos moleculares do polímero usado, alguns autores descrevem uma degradação lenta em meio enzimático atingindo apenas 18 % de perda de massa em 18 semanas, por outro lado diminuindo a concentração de PCL em 30% outro estudo alcança a degradação completa em 12 semanas. Com base nestes resultados decidimos investigar a degradação hidrolítica e enzimática *in vitro* e *in vivo* para as estruturas desenvolvidas. O nosso objetivo principal é descrever a cinética de degradação das malhas de electrospinning feitas com PCL em diferentes condições e clarificar o seu potencial para ser usado em aplicações de curto prazo. De acordo com os testes *in vitro*, durante 91 dias, a degradação hidrolítica apenas resultou na perda de massa

de 1,44 ± 0,7 % no entanto a degradação enzimática induziu uma perda de massa de 97,11 ± 5,1%. Os ensaios *in vivo* demonstraram que ocorreu uma reacção inicial ligeira às amostras de electrospun implantadas e as células permaneceram concentradas na superfície das membranas. Ao dia 60 e 90 a coloração com hematoxilina e eosina (H & E) mostra a infiltração das células através das malhas electrospun e a sua colonização demonstrando que as malhas não inibem a infiltração celular. Após 90 dias de implantação é visível a produção de componentes da matriz extracelular, provavelmente, substituindo as fibras de PCL degradadas.

Um dos maiores inconvenientes na utilização da gelatina na área da Engenharia de Tecidos deve-se à sua instabilidade em meio aquoso, para tal é necessário reticulá-la para se tornar estável. Existem diversos reticulantes estudados, contudo a maioria deles são tóxicos e as metodologias comumente utilizadas (vapor e banho) induzem alterações na morfologia das fibras. Para o nosso estudo selecionamos 1,4-butanodiol diglicidil éter (BDDGE) pois é um reticulante bem conhecido na reticulação do ácido hialurónico e em pequenas quantidades não induz toxicidade. Para manter a morfologia das fibras exploramos a metodologia da reticulação *in situ*, que se baseia na adição do reticulante na solução polimérica antes de produzir as fibras. Utilizando esta metodologia o reticulante é encapsulado dentro das fibras e a reação ocorre mantendo a morfologia das mesmas. Variando a quantidade de reticulante (2,4 ou 6 v/v-%) e o tempo de reação (24,48 ou 72h) obtivemos fibras com diferentes diâmetros e, consequentemente, diferentes propriedades. O grau de reticulação pode ser adequado alterando a quantidade de reticulante e/ou o tempo de reação permitindo o controlo sobre o diâmetro das fibras e suas propriedades. Fibras com 4% ou 6% de BDDGE (72h de reação) resulta em fibras de gelatin com elevado grau de reticulação (~70%) e diametros estáveis de 339 ± 91 e 276 ± 88 nm, respectivamente, embora 4% BDDGE resulte na melhor combinação de propriedades mecânicas. Os testes de citotoxicidade, revelaram não toxicidade e os ensaios de proliferação demonstraram que os fibroblastos (hDNF) tiveram a capacidade para aderir e proliferar, produzindo matriz extracelular dentro das malhas.

Com base no conhecimento adquirido através do estudo do perfil de degradação das malhas de PCL e como é possível reticular as fibras de gelatina mantendo a sua morfologia e adjustando as suas propriedades prosseguimos os nossos estudos para o desenvolvimento de estruturas híbridas combinando fibras de PCL e Ge.

Para o desenvolvimento das estruturas híbridas foram estabelecidas três metodologias diferentes que combina os mesmos materiais (PCL e Ge). A primeira abordagem denominada Multilayer combina, na mesma estrutura, 5 camadas distintas. O Coated, é a segunda estratégia, na qual as fibras de PCL são mergulhadas num banho de gelatina resultando em filamentos duplos, em que o material interior é o PCL e o exterior a Ge. A última metodologia, denominada de Blend, combina o PCL e a Ge, num rácio de 1:1, na mesma solução antes da

produção das fibras. Com base nas estratégias definidas e tendo as malhas de PCL e Ge como controlos foram realizadas diversas caracterizações para avaliar qual das estratégias apresentava maior potencial para ser usado como curativo com capacidade para promover a regeneração da pele. As estruturas hibridas desenvolvidas demonstraram que, independentemente da estratégia utilizadas, o seu comportamento mecânico e biológico é melhor do que as estruturas de controlo. Contudo, tendo em conta a aplicação final a metodologia coated demonstrou fraca permeabilidade ao vapor de água e a mais baixa porosidade, consequência do banho de Ge que poderá ter fechado alguns poros. As estruturas Multilayer e Blend demonstraram grande potencial para mimetizar a matriz extracelular e as características de pele. Os filamentos das estruturas compreendiam diametros na gama da matriz extracelular nativa, as propriedades mecânicas são similares às do tecido humano e as estruturas híbridas permitiram a adesão e proliferação celular bem como a deposição de fibronetina. Contudo a estrutura Multilayer, devido à combinação de diferentes graus de porosidades e tamanhos de poros consequência das camadas distintas confere maior espessura à estrutura tornando-se mais fácil de manusear sem induzir dano e evita o empacotamento das fibras comumente associado às malhas de electrospinning.

Palavras-chave: Fibras de electrospinning; malhas hibridas, policaprolactona, gelatina, curativos

Preface

This thesis was organized in 5 parts including 7 chapters, which reflects the development of research work. All chapters were related to each other and the aims and methodology chosen in each chapter were indeed dependent on the conclusions brought about in previous one(s). Overall, the work described in this thesis includes development and characterization of hybrid electrospun structures to promote skin regeneration.

Part 1 includes **Chapter I**, addresses the state of the art of the electrospun meshes as skin substitutes. The main aim of this chapter is to give an overview about the advances in this field to better understand the potential of electrospun meshes as wound dressings. This chapter highlights, also, novel approaches to combine different techniques and methodologies to develop biomimetic structures with capability to better mimic the native ECM. In **Chapter II** the project aims were detailed to be a guideline of the work major core.

In **Part 2** – **Chapter III** a re-designed electrospinning apparatus was assembled to increase the process reproducibility and stability. PCL and Ge process optimization was performed, studying different solvent systems, polymer concentrations and processing parameters (feed rate, distance between the collector and needle and voltage). The optimized conditions were used in further studies to prepare the electrospun meshes with random fiber deposition without the formation of beads or drops.

Part 3 - **Chapter IV** was evaluated the in vitro and in vivo PCL electrospun meshes degradation. It is well-known that bulk PCL takes around 24 months to degrade being a slow degradation rate for skin application. However, the electrospun meshes present fibers with low diameter and high surface area which increase the degradation rate exponentially. The literature related to different rates depending on the material molecular weight and supplier. For that reason, we study the degradation kinetics regarding the electrospun meshes developed. **Chapter V** explores the use of BDDGE as a gelatin crosslinker *in situ*. Gelatin is water soluble and for that reason it is necessary crosslinking to improve its stability in aqueous medium. BDDGE is commonly used to crosslink the hyaluronic acid and collagen. To crosslinking gelatin was only evaluated to food packing films applications. In this chapter, were explored different amounts of crosslinker and reaction time, and correlated the meshes properties with the crosslinking degree.

In **Part 4**, **Chapter VI** is based on electrospun hybrid structure development, combining the knowledge of Chapter III, IV and V was possible establish three different methodologies to

prepare hybrid structures merging PCL and Gelatin. In this chapter, the hybrid structures were tested and evaluated to identify the structure with major potential to promote skin regeneration according to physicochemical, mechanical and biological properties.

Finally, in **Part 5**, the overall conclusions and future perpectives were presented in **Chapter VII**.

Most information presented in the chapters that constitute this dissertation has been already disseminated through submission to international peer review, via publication in scientific journals or attendance to conferences in the field, according to the following list:

Chapter I – State of the art

J.R. Dias, P.L. Granja, P.J. Bártolo, Advances in electrospun skin substitutes. Progress in Materials Science, 84 **(**2016), 314-334.

Chapter III – Re-design of electrospinning apparatus and PCL and Ge processing optimization

J.R. Dias, C. dos Santos, J. Horta, P.L. Granja, P.J. Bártolo. A new design of an electrospinning apparatus for tissue engineering applications. International Journal of Bioprinting, 3(2) (2017), 1-9.

J.R. Dias, F.E. Antunes, P.J. Bártolo, Influence of the rheological behaviour in electrospun PCL nanofibres production for tissue engineering applications. Chemical Engineering Transactions, 32 (2013), 1015-1020.

JR Dias, PJ Bártolo. Morphological characteristics of electrospun pcl meshes – the influence of solvent type and concentration. Procedia CIRP, 5 (2013), 216-221.

JR Dias, A Gloria, PJ Bártolo. Mechanical and biological characteristics of electrospun PCL meshes – the influence of solvent type and concentration. Advanced Materials Research, 683 (2013), 137-140.

Chapter IV - In vitro and In vivo degradation profile of PCL electrospun meshes

J.R. Dias, A. Sousa, P.L. Granja, P.J. Bártolo. In vitro and In vivo degradation profile of PCL electrospun meshes. *Under preparation*

Oral presentation

Enzymatic degradation of PCL electrospun meshes. 25th -27th of June 2015.4th International Conference on Tissue Engineering (ICTE), Lisboa, Portugal,

Controlled enzymatic degradation of Electrospun PCL network. 29th – 31st of July 2015: 2nd CIRP conference on Biomanufacturing (CIRP-Bio 2015), Manchester, UK;

Chapter V - *In situ* crosslinked electrospun gelatin nanofibers for skin regeneration

J.R. Dias, S. Baptista-Silva, C.M.T. de Oliveira, A. Sousa, A.L. Oliveira, P. J. Bártolo, P.L. Granja, *In situ* crosslinked electrospun gelatin nanofibers for skin regeneration. 2017. European Polymer Journal, 95 **(**2017), 161-173.

Poster communication

Internal crosslinking evaluation of gelatin electrospinning fibers with 1,4 – butanediol Diglycidyl ether.17th – 22nd of May,2016, WBC2016 – 10th world Biomaterials Congress, Montréal, Canadá,

Oral communication

Evaluation of Gelatin Electrospun Fibers Crosslinked with 1,4 – butanediol Diglycidyl Ether for Skin Regeneration. 30th of June to 1st of July, 2016, MDA2016 – 1st International conference on Materials design and applications.

Chapter VI – Hybrid electrospun structures for skin regeneration

J.R. Dias, S. Baptista-Silva, A. Sousa, A.L. Oliveira, P. J. Bártolo, P.L. Granja, Hybrid electrospun structures for skin regeneration.2017. Under preparation

Oral communication

Hybrid electrospun meshes for skin regeneration.28th of June – 1st of July, 2016, Electrospin2016 – 4th International Conference on Electrospinning 2016, Otranto, Italy.

Table of contents

List of Figures

List of Tables

List of abbreviations

%Xc – Cristallinity degree;

ΔH_c- Cold crystallization enthalpy;

ΔH_m - Enthalpies of fusion;

ΔH_m^0 - Enthalpy of melting of 100% crystalline material;

AA - Acetic acid;

Ag-MSNs - Mesoporous silica nanoparticles;

AM - Additive manufacturing;

ATR - Attenuated total reflectance;

Au/Pd - Gold/palladium;

BAECs - Bovine aortic endothelial cells;

BDDGE - 1,4-butanediol diglycidyl ether;

BSA - Bovine serum albumin;

CA – Contact angle;

CAD - Computer aided design;

CDRsp – Centro para o Desenvolvimento Rápido e Sustentado de Produto;

CEMUP - Centro de materiais da universidade do porto;

COMPETE - Programa Operacional Factores de Competitividade;

CS – Chitosan;

DAPI - 40,6-diamidino-2-phenylindole dihydrochloride;

DC - Direct contact;

DGV - Animal Welfare and Experimentation;

DMEM - Dulbecco's modified eagle medium;

DMK - Dimethyl ketone;

DNA - Deoxyribonucleic acid;

dsDNA - Double-stranded DNA;

DTA/DSC - Differential thermal analysis and differential scanning calorimetry;

E - Young's modulus;

EC - Emulsion-core;

ECM – Extracellular matrix;

EDTA - Ethylenediamine tetraacetic acid;

ENC - Enteric neural crest;

ε_B - Elongation at maximum strain;

F-actin – Filamentous actin;

FCT - Fundação para a Ciência e a Tecnologia;

FDM - Fused deposition modeling;

FEDER - European Fonds Européen de Développement Régional;

FN – Fibronectin;

FTIR - Fourier transform infrared;

GA – Glutaraldehyde;

GPC/SEC - Gel permeation/size exclusion chromatographer system;

H&E - Hematoxylin and Eosin;

hDNF - Human dermal neonatal fibroblasts;

I3s – Instituto em investigação e inovação em saúde;

IC - Indirect contact;

ICBAS – Instituto de Ciências Biomédicas Abel Salazar;

INEB – Instituto Nacional de Engeneharia Biomédica;

Ki-67 – Biomarker for proliferation;

LCD - Liquid crystal display;

LMM - Linear mixed model;

NH_0 - Free amino groups before crosslinking;

NHN – Ninhydrin;

NH_t - Free amino groups after crosslinking;

PBS - Phosphate buffered saline;

PCL – Polycaprolactone;

PDMS – Polydimethylsiloxane;

PELCL - Methoxy polyethylene glycol-b-poly(l-lactide-co-e-caprolactone);

PEO - Poly(ethylene oxide);

PES – Polyethersulfone;

PFA – Paraformaldehyde;

PGS - Poly(glycerolsebacate);

PLA - Poly(lactic acid);

PLGA - Poly(lactic-co-glycolic acid);

PLLA - Poly(L-lactide);

PLLCL - Poly(l-lactid acid)co-poly-(e-caprolactone);

PMMA – Polymethlylmethacrylate;

PVA - Poly(vinyl alcohol);

RGD - Arg–Gly–Asp;

RT – Room temperature;

SA:Vol - Surface area to volume ratio;

SD - Standard deviation;

SEM - Scanning electron microscopy;

STA - Simultaneous thermal analysis;

TCH - Tetracycline hydrochloride;

Tdeg. – Degradation temperature;

TE – Tissue engineering;

TE - Tris-EDTA;

TEA – Triethylamine;

TG – Thermogravimetry;

THF – Tetrahydrofuran;

T_m – Melting temperature;

TSB - Tensile strength at break;

w/o - Water-in-oil;

W_0 - Initial weight;

W_d - dry weight;

WHO – World health organization;

WVP – Water vapour permeability;

W_w - Wet weight;

X_c - Crystallinity degree;

ΔH – Enthalpy;

Part 1

Chapter I

State of the art

Contents

1. Introduction

The first shield between the external environment and the human body is the skin. This tissue plays a crucial role in body protection and, when damaged at full-size, the human life could be in risk [1, 2]. According to the World Health Organization (WHO) it is estimated that every year 265,000 deaths occurs caused by burns and, annually about 6 million people were burned requiring medical attention [3-6].The average length of stay in the hospital is 8.4 days, thus resulting in a considerable social and economic burden for the health care systems worldwide. Therefore, innovative strategies are required to promote skin tissue regeneration, despite the encouraging recent developments in wound dressings and tissue engineering-based products [7]. Electrospun meshes have been gaining increasing attention through the combination of materials and processing strategies of great potential for skin regeneration [8]. Wound dressings prepared from electrospun nanofibers have been claimed to present exceptional properties compared to conventional dressings, such as similarity to architecture of the natural extracellular matrix (ECM), improved promotion of hemostasis, absorption of wound exudates,

permeability, conformability to the wound, and avoidance of scar induction [9]. New processing strategies are thus being explored in which natural and synthetic materials are combined with new design approaches allowing the incorporation of substances that turn not electrospinnable materials into electrospinnable ones. In this review skin regeneration strategies will be revised with a focus on electrospinning methodologies and materials.

2. Skin tissue and wound healing process

The human body comprises several organs each one with specific functions, dimensions and shapes. The largest vital organ in the body is the skin that represents 7% of the total body weight and has the main function of protecting the human being against the external environment. It also helps protecting the body against excessive water loss, against attacks from chemicals and other harmful substances, and ultraviolet radiation [1, 8, 10-12]. In spite of the protective function of the skin, this tissue plays other important functions namely: (i) control of body temperature, by secreting sweat through the sweat glands, thereby lowering the temperature; (ii) sensory, through different receptors able to detect touch, pain, pressure and temperature; and (iii) synthesis of vitamin D (after exposure to sunlight), a precursor of calcitriol hormone that is converted in the liver and kidneys and plays an important role in the calcium absorption in the small intestine [10, 13]. Although the skin works as a barrier it is not totally impermeable: some substances are transferred across the skin, such as sweat, drugs and biomolecules [10, 14].

Skin functions are carried out by specialized cells and structures found in the two main skin layers, epidermis and dermis (Fig. I.1). Besides these two layers, beneath the dermis there is the hypodermis that provides support to the dermis [10, 15]. The epidermis, the outermost skin layer, is around 120 micrometer thick and is composed by numerous cells closely linked in different stages of differentiation, which form the stratified squamous epithelium [10]. The epidermis is avascular (nourished through diffusion from the dermis), consists of 4 different types of cells (keratinocytes, melanocytes, Langerhans cells and merkels cells) and presents 5 distinct cell layers (stratum basale, spinosum, granolosum, lucidum and corneum) [16, 17]. The dermis layer is composed by a complex mesh of ECM material that provides structure and resilience to the skin. The thickness of this layer varies according to the body region but is in average of 2 mm [10, 17]. The dermis is composed by a nanometer-sized network of structural proteins (collagen, which provides strength and flexibility, and elastin, which provides elasticity), blood and lymph vessels, and specialized cells (mast cells that help

in the healing process and protect against pathogenic organisms, and fibroblasts that produce collagen and elastin). This ECM network is engaged in a ground substance that is mostly composed by glycosaminoglycans and plays an important role in hydration and in maintaining moisture levels in the skin [10, 14]. The ECM is also highly dynamic, being constantly synthesized and re-organized by the cellular components, but in turn also having a prominent role in directing cellular behavior through direct and indirect signaling. For instance, ECM molecules control cell adhesion through specific cell binding sites, cell migration through proteolytically sensitive functionalities, and cell differentiation through bound and soluble signaling biomolecules. With relevance for the present topic is the nanometer scale of the several pores and fibers (collagen, hyaluronic acid, elastin, laminin, fibronectin, proteoglycans) that constitute the ECM, highlighting the relevance of mimicking the physical nanometer scale fibrillar nature of this structure through electrospinning. ECM fibers are reported to exhibit diameters between 10 and 300 nm, and the minimum fiber diameter required for fibroblast adhesion and migration, and maximum interfiber distance that fibroblasts are able to bridge, have been described as approximately 10 and 200 μm, respectively, which lie within parameters achievable by electrospinning but hardly achievable using alternative cell culture settings [18, 19] . Furthermore, due to their intrinsic ability to synthesize their own ECM, skin cells are known to be able to self-organize even in the absence of molecular cues provided that an adequate 3D nucleation structure exists to enable their self-organization, thereby reinforcing the stimulating role of electrospun nanofibrous structures for skin regeneration [19, 20].

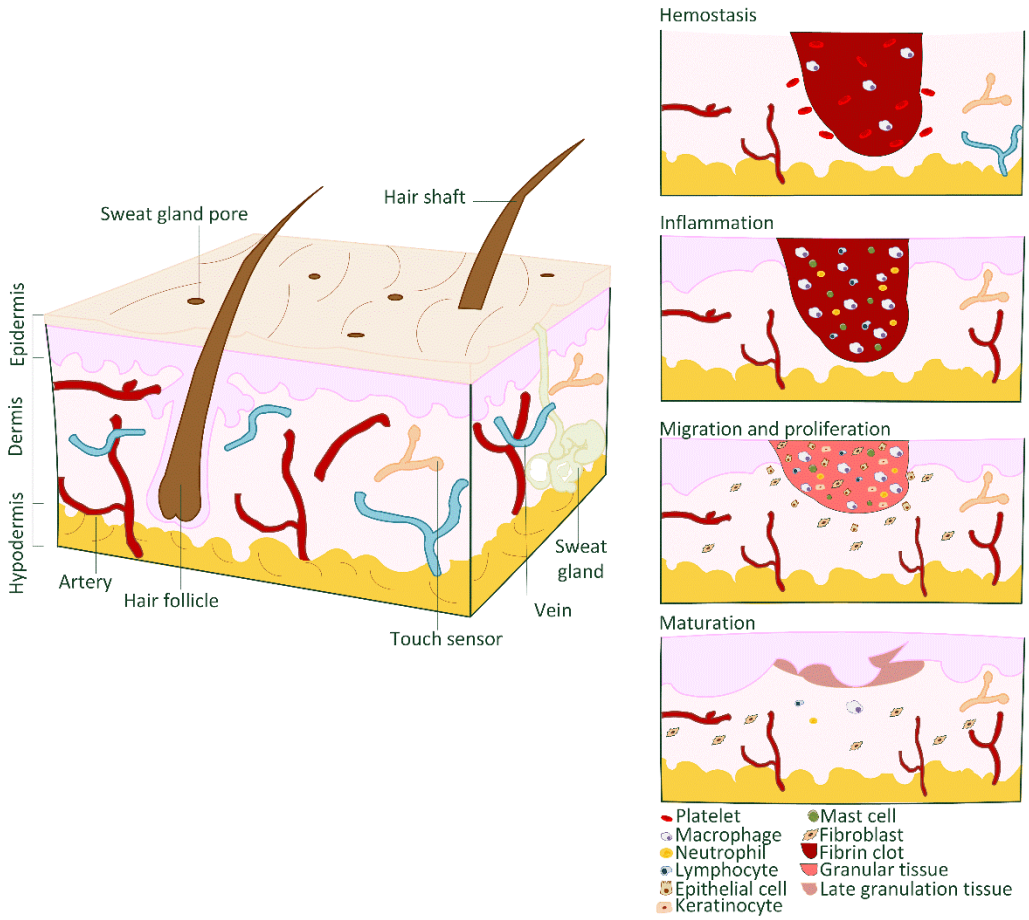

Figure I.1. Skin structure and wound healing phases.

When skin damage occurs a consecutive cascade of events called wound healing takes place to restore the skin structure and function [17, 21]. A wound can result from burns, contusion, hematoma or a disease process, causing chronic wounds. At present, due to the increasing life expectancy, diseases with high incidence such as diabetes have been considerably increasing the incidence of chronic wounds and thus making it of high social relevance [11, 21].

The wound healing process consists, in general, in five different phases, namely hemostasis, inflammation, migration, proliferation and maturation, occurring sequentially after damage [9, 21] (Fig I.1). During hemostasis, platelets suffer aggregation to promote clotting and stop any bleeding. Delivery of important growth factors to the inflammation process occurs, which trigger the wound healing process through attraction and activation of neutrophils, lymphocytes, macrophages and mast cells [22, 23]. The inflammation phase occurs at the same time as hemostasis. In this phase, blood neutrophils followed by phagocytes enter and penetrate inside to the injured area to destroy bacteria and eliminate debris from dying cells and damaged matrix [14, 24] . The

following phases, migration and proliferation, are considered by several authors as the same phase due to their interdependence [22, 25]. Migration is characterized by infiltration of new epithelial cells moving on to the damaged area to replace the dead cells and during the migration the inflammation decreases. The proliferation phase consist on covering all damaged area with epithelial cells and macrophages, while simultaneously fibroblasts and endothelial cells move to the damaged area forming a granular tissue composed by a new matrix and blood vessels, respectively [22, 25]. The last phase, maturation, comprises the remodeling process, in which fibroblasts cover all the damaged surface with a new skin layer and ideally leaving no evidence of scar [14, 23]. Through this elaborate process of wound healing the skin has self-regeneration ability although this capacity is strongly reduced in the case of full-thickness lesions, requiring the use of a graft or dressing [11].

3. Skin regeneration products

3.1 Autografts and allografts

When skin lesions result in large full-thickness defects the standard clinical procedure is the autologous skin transplantation based on transplanting split-thickness grafts [7, 8, 26]. However, this transplantation contains all of the epidermis layer but only a small part of the dermis often leading to scar formation [15]. This process has the obvious restriction of total amount of autologous skin that can be removed and the split-skin donor site takes one week to heal and can be used for split skin harvesting up to 4 times. Frequent harvests also lead to scars in donor sites and hospital stays for long periods of time [6, 27, 28]. Allografts are grafts removed from other individuals and constitute efficient alternatives to prevent fluid loss and infection, reduce pain and promote the healing of underlying tissues. However, this type of graft presents several ethical problems and is influenced by the donor's availability and potential disease transmission [26].

3.2 Wound dressings

The first procedure when skin damage occurs consists in applying a wound dressing due their efficiency on preventing wound infection and promoting exudate absorption, low cost and availability. The main functions of a dressing are promoting a moist environment in the wound, and protecting the wound against mechanical injury and microbial contamination, especially during the inflammatory stage [7, 29]. Ideally, the dressing should be able to fit the wound shape, absorb wound fluid without increasing bacterial proliferation or causing excessive dehydration, provide pressure for hemostasis, and

prevent leakage from the bandage. The dressing should also support the wound and surrounding tissues, eliminate pain, promote re-epithelialization during the reparative phase, and be easily applied and removed with minimal injury to the wound [30].

Wound dressings can be categorized according to different characteristics. One possible classification relies in classifying the wound dressings in passive or interactive [9, 31]. The passive ones correspond to the common wound dressings and their main function is covering the wound and allowing the regeneration beneath the dressing. Some examples are tulle dressings (made of cotton or viscose gauze impregnated with paraffin) and low-adherence dressings (made of materials as knitted viscose or polyester fabric) [32]. On the other hand, the interactive wound dressings present some advantages like the capability to modify the wound chemical environment facing to the physiological conditions of the wound for a faster healing process. Although in some cases this modification could take long periods of time [9, 33]. Commercial available interactive wound dressings, according the a widely accept classification, are divided into hydrocolloids, hydrofibers, hydrogels, foams, alginates and bioactive/biological dressings [32].

3.3 Tissue engineering-based products

During the past few years, the progress and evolution on tissue engineering (TE) field have been growing exponentially. This field has been exploring the regeneration of several tissues, including skin, involving knowledge from different disciplines. TE includes the combination of live cells, tissues or organs, with structures and materials designed to mimic the structure of a particular tissue [34, 35]. The use of TE strategies for skin tissue regeneration consists essentially in expanding skin cells in the laboratory, cultivating them on a scaffold and applying cell-scaffold construct for restoring the barrier function (first step in burn patients), or to promote wound healing (for instance in chronic non-healing ulcers), thereby reducing pain and promoting optimal conditions for a correct healing [11]. Several products for skin regeneration based on TE are already clinically available that meet the essential requirements for a clinical product, namely be safe for the patient, clinically effective and conveniently handled and applied by health care professionals [6, 11].

TE skin substitutes present several advantages when compared with other available solutions including less required vascularisation in the wound bed, increased dermal component of the healed wound, reduced presence of inhibitory factors and faster and safe coverage [8]. TE skin substitutes available in the market can be classified according

to different features. The most common classification is related with the anatomical structure to be regenerated, resulting in epidermal, dermal or dermal/epidermal (or composite) substitutes [6, 26]. An important phase in the production of epidermal substitutes is the isolation of keratinocytes, obtained through a 2-5 cm^2 skin biopsy from the donor. The epidermis is separated and *in vitro* cultured on top of fibroblasts [6, 36]. There are several epidermal substitutes available for clinical applications using cells either of autologous or allogenic origin, with the allogenic products presenting reduced manufacturing costs compared to autologous substitutes. Some of the commercial epidermal substitutes available are MySkin® (CellTran ltd, UK) a synthetic silicone support layer with surface coated and seeded with keratinocytes, Epicel® (Genzyme Biosurgery, USA), sheets of autologous keratinocytes attached to the petrolatum gauze support, and Epidex® (Eurodern GA, Switzerland), an epidermal equivalent from the patient's own outer root sheath, where the keratinocytes are cultured in silicone membranes. Despite their efficiency in proving epidermal coverage, autologous and allogenic epidermal substitutes are claimed to present poor attachment rates that can lead to blister formation [26].

The development of dermal substitutes emerged due the lack of dermal tissue in full thickness wounds and the poor quality of the scars after treatment with split thickness autografts or cultured epithelial grafts which contain little or no dermal component, respectively [37]. There are several products available in the market that have been demonstrating great effectiveness in dermal regeneration, such as Dermagraft® (Shire Regenerative Medicine, Inc, USA), a cryopreserved human fibroblast-derived dermal substitute, generated by the culture of neonatal dermal fibroblasts onto a bioresorbable poly(lactic-co-glycolic acid) (PLGA) mesh scaffold [38], Integra™ (Integra LifeSciences, USA), which is a nanofibrous bilayer mesh specifically designed to be used in conjunction with negative pressure wound therapy, comprising crosslinked bovine tendon collagen and glycosaminoglycan and a semi-permeable polysiloxane layer, and Karoderm™ (Karocell Tissue Engineering AB company, Sweden), a human donated cell free dermis that can also be used as a biological scaffold for autologous keratinocytes.

To mimic skin layers (dermis and epidermis) in the same construct dermal/epidermal substitutes have been explored. Several studies have been carried out with different cell types to evaluate their performance although only autologous keratinocytes were claimed effective to achieve permanent closure of skin defects [6, 26]. Dermal/epidermal substitutes available in the market include PermaDerm® (Regenicin Inc., USA), composed by cultured fibroblasts and keratinocytes on an absorbable collagen substrate, and Apligraf® (Novartis, USA), that combines two distinct nanofibrous layers,

the lower dermal layer containing bovine type I collagen and human fibroblasts and the upper epidermal layer formed by culturing human keratinocytes.

In spite of the great progress achieved on TE-based skin substitutes several challenges still need to be overcome to achieve the optimal skin substitute, such as: to avoid use animal-derived materials (e.g. serum), to improve the adhesion of cultured keratinocytes to the wound bed, to improve the rate of neovascularization of tissue engineered skin and to enhance the scaffolds materials to resist wound contraction and fibrosis [7, 8, 34, 39, 40].

3.4 Advanced skin substitutes

Advanced skin regeneration strategies have been emerging combining cells, growth factors and scaffolds overcoming some of the problems associated to the clinical application of skin grafts, dressings and TE-based products [7]. Scaffolds are a crucial component because the isolated cells on their own are not able to restore the native structure of the skin without support to guide the ECM growth [1]. For scaffolds fabrication, there are two main strategies: the top-down and bottom-up approaches [41, 42]. The top-down is considered the traditional approach and is based on cells seeded in a porous scaffold generating a cellular construct, which is later subjected to the maturation process in a bioreactor. With this methodology is expected that the cells adhere, proliferate and differentiate inside the scaffold creating an appropriate ECM stimulated by the growth factors and mechanical or other types of stimulation [41, 43]. Most of TE products described before are based on this strategy.

The bottom-up approach consists on developing biomimetic modular structures that can be created through self-assembled aggregation, microfabrication of cell-laden hydrogels, fabrication of cell sheets or direct printing with specific microarchitectural features [41, 44, 45]. The major advantages of this approach are better control over cell seeding, increasing cell density and complexity of microarchitecture than with top-down approaches. Major disadvantages of using bottom-up approaches include the fact that some cell types are unable to produce enough ECM, migrate or form cell-cell junctions, and the great difficulty in developing assembly techniques able to generate engineered tissues with clinically relevant length scales and mechanical properties [7, 41, 46] .

4. Electrospun skin substitutes

Although the electrospinning technique is under growing development in the biomedical field its principles emerged around 1600s. However, since 1980s, several research

groups demonstrated that it is possible to produce electrospun fibers with organic polymers increasing, since then, the number of publications exponentially [47, 48]. Some of the most important milestones are summarized on Table I.1. Further details about electrospinning's history are available elsewhere [47, 49-52].

Table I.1. Historical milestones of electrospinning.

Year	Author	Historical milestone	Reference
Around 1600s	W. Gilbert	Study of the magnetic behaviour and electrostatic phenomena.	[49]
Late 1800s	L. Rayleigh	Investigation of liquid jet hydrodynamic stability, with or without applied electric field.	[47, 50]
1902	J.F. Cooley	Patent registration entitled "Apparatus for electrically dispersing fluids", considered as the first description of a process recognizable as electrospinning.	[53, 54]
1914	J. Zeleny	Study of the fluid droplets behaviour at the end of metal capillaries.	[51, 52]
1934-1944	A. Formhals	Publication of several patents describing important developments towards electrospinning commercialization.	[55-65]
1936	C.L. Norton	Patented the use of melted polymers.	[49, 66]
1964 - 1969	G.I. Taylor	Development of theoretical electrospinning underpinning, which allowed the mathematical modeling of the cone shape formed by the liquid droplet that became known as Taylor's cone.	[51, 67]

Electrospinning is a technique allowing to create submicron to nanometer scale fibers from polymer solutions or melts and was developed from a basis of electrospraying, widely used for more than 100 years [65, 68]. It is also known as electrostatic spinning, with some common characteristics to electrospraying and the traditional fiber drawing process [69].

The conventional setup for an electrospinning system consists of three major components: a high voltage power supply, a spinneret and a collector that can be used with horizontal or vertical arrangement [47, 65, 70]. The syringe contains a polymeric solution or a melt polymer, pumped at a constant and controllable rate. The polymer jet

is initiated when the voltage is turn on and the opposing electrostatic forces overcome the surface tension of the polymer solution. Just before the jet formation, the polymer droplet under the influence of the electric field assumes the cone shape with convex sides and a rounded tip, known as the Taylor cone [51, 69, 71]. During the jet's travel, the solvent gradually evaporates, and charged polymer fibers are randomly deposited or oriented in the collector [71].

The electrospinning process can be influenced by several parameters, such as: solution parameters (viscosity, concentration, type of solvent), processing parameters (flow rate, distance between needle and collector, voltage supply, type of collector) and ambient parameters (temperature and humidity), as summarized in Table I.2 [47]. It should be emphasized that the acceleration of fiber formation is up to 600 m/s^2, which is much higher than the value of acceleration of gravitational forces on earth (at sea level and at 45º of latitude it corresponds to 9.80665 m/s^2), meaning that gravity does not influence the process [72, 73].

Table I.2. Effect of electrospinning parameters in fiber formation.

	Parameter	**Effect**	**References**
Solution	Viscosity	Determines the fiber formation.	[74-77]
	Surface tension	Determines the applied voltage; it must be higher than surface tension of the solution to initiate the process.	[76-78]
	Conductivity	Higher conductivity avoids droplet deposition in the fibers.	[75-77]
	Dielectric effect	High dielectric properties reduce bead formation and fiber diameter.	[77, 78]
Processing	Applied Voltage	Influences the jet stretching and acceleration and consequently fiber morphology.	[75, 77]
	Flow Rate	Influences the fiber diameter, its geometry and mesh porosity.	[75-77]
	Needle diameter	A small internal diameter reduces droplet formation in the fibers.	[77, 78]
	Distance needle-collector	Influences the solvent evaporation rate.	[75, 77]
Ambient	Temperature	The increase of temperature favors the solvent evaporation rate.	[67, 77]
	Humidity	If too high induces morphological changes increasing the surface heterogeneity and for hydrophilic polymers is unable form fibers and electrospraying occurs.	[47, 67, 77, 78]

	Atmosphere types	Some gases are influenced by the electrostatic field blocking the process.	[77]
	Pressure	If pressure is lower than atmospheric one the solution exists through the needle causing jet instability.	[77]

The technique is also highly versatile since, in addition to the conventional fiber configuration, it is possible to obtain a variety of other configurations, namely core/shell (co-axial) or emulsion configurations and, according to the fiber orientation, it is possible to produce aligned or randomly oriented fibers depending the type of the collector used (Fig. I.2). [11]

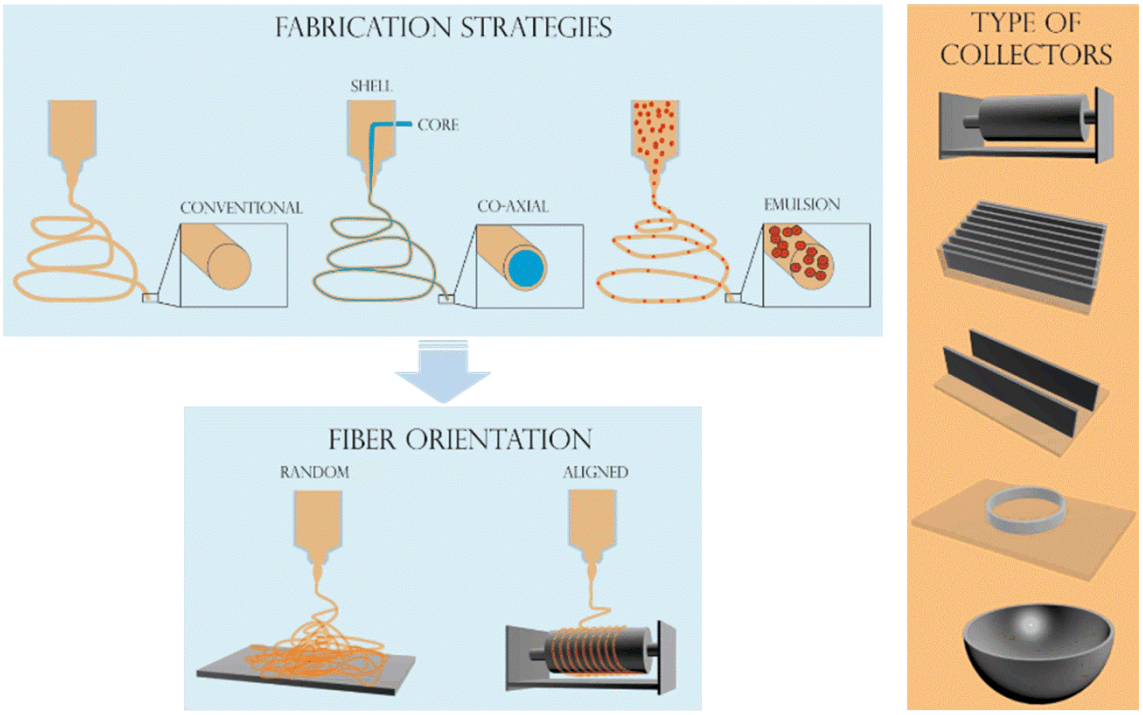

Figure I.2. Electrospinning fabrication strategies, fiber orientation types and types of collectors used.

The use of electrospinning to regenerate damaged tissues rose in the last decade due to its simplicity to produce meshes and its capacity to mimic the micro-nanostructure of the natural ECM. The nanofibers produced through electrospinning confer a high surface area to the structure, high interconnectivity which is beneficial for regenerative tissue growth and cell migration and great potential for effective delivery of biomolecules, [47, 79]. According to tissue engineering principles an ideal scaffold should hold cellular activities, and should disappear over time while tissue regeneration occurs. To enable this, scaffolds should mimic native tissue regarding its structure, appropriate mechanical strength, porosity for cellular infiltration and growth [35, 69].

Traditional scaffolding methodologies like solvent casting and particulate leaching, freeze drying and gas foaming have limited ability to form scaffolds that mimic the native tissue nanostructural architecture [80, 81]. However, electrospinning presents an unique ability to fabricate nanofiber-based scaffolds that best mimic the nanometer scale of the native ECM as well as the mechanical properties of the native skin. Electrospun skin substitutes have been claimed to have increased potential to promote better cellular attachment, growth and differentiation due the high surface area, high aspect ratio and high microporosity provided by the low fiber diameter structure [35, 52, 82]. The versatility of this technology further allows tuning of fibrous scaffold design in terms of mechanical properties, fiber diameter, density and orientation to mimic the physical features of the ECM, as shown in several examples ahead.

The mechanical properties of skin *in vitro* and *in vivo* have been evaluated using different techniques (ultrasounds, indentation, tensile tests, suction and torsion) [83-85]. Human skin is a complex tissue due its heterogeneity, viscoelasticity, anisotropy, adhesive properties and non-linear stress-strain behaviour [83, 84, 86]. Table I.3 presents the mechanical properties of skin tissue in comparison to electrospun meshes made by different materials and production strategies, showing that the mechanical properties of electrospun meshes are similar to those of skin, thus demonstrating the potential of this technology to mimic skin tissue due not only due to its similarity in terms of organization (nanofibrous mesh-like structure) but also mechanical properties.

Table I.3. Mechanical properties of skin tissue and electrospun meshes.

Structure	Young's Modulus (MPa)	Tensile strength (MPa)	Elongation at break (%)	Ref.
Human Skin	2.9-150	1-32	17-207	[87-90]
PCL	21.42 ± 0.04	6.87 ± 0.25	116.0 ± 6.53	[91]
PCL/collagen	82.08 ± 17.86	8.63 ± 1.44	24.0 ± 7.16	[91]
PLCL	47.66 ± 2.24	7.24 ± 0.16	158.54 ± 66.67	[90]
CA/pullulan	2.91 ± 0.21	0.13 ± 0.08	22.2 ± 0.01	[92]
HA/PLGA core/shell	28.0	1.52	60.07	[93]

CA – cellulose acetate; HA - hyaluronic acid; PCL – poly (Ɛ-caprolactone); PLCL - poly(Ɛ-caprolactone-co-lactide); PLGA - poly(lactic-co-glycolic acid).

Additionally, the high specific surface area and porosity of electrospun meshes constitute additional functional advantages by providing tunable fluid absorption and drug and

biomolecule delivery, adequate oxygen, water and nutrient diffusion coupled with efficient metabolic waste removal.

In spite of the significant advances in electrospinning, in the biomedical field only a few companies provide customized nanofibers production either as single or bi-layers combining different materials. Commercially available products also include cell culture well-plates integrating electrospun structures and meshes for stent coverage [94-96]. Specifically for skin regeneration, a clinical trial was carried out for the treatment of diabetic foot ulcers using a multilayer polyurethane electrospun transdermal patch releasing nitric oxide [97]. However no clinical trials using the electrospinning technique for skin regeneration are ongoing [98].

4.1 Randomly oriented fiber meshes

Conventional electrospinning set-up configuration consists in fibers randomly deposited over the grounded collector, which is usually a metal plate [47, 79, 99]. The random deposition is a consequence of the jet instability resulting from the electric field applied to overcome the polymeric solution surface tension [51, 100].

There are several studies comparing random and aligned deposition strategies in terms of nanofibers morphology, hydrophilicity, mechanical properties and cell adhesion and proliferation [101, 102].

In terms of biological response numerous studies demonstrated that aligned fibers usually exert a more relevant influence on cellular behaviour including cell morphology, cellular density and gene expression. In terms of mechanical properties the elongation at break presents better results when fibers are randomly oriented [101-104]. Although both strategies allow producing structures with suitable properties to promote skin regeneration, skin is generally characterized by a meshlike random orientation of fibrils, making random meshes the electrospun structures the more suited to mimic native skin's ECM [18]. Jha and colleagues explored the application of randomly oriented fiber meshes to improve wound healing, in which they assessed skin regeneration promoted by collagen electrospun fibers crosslinked with glutaraldehyde on adult guinea pigs [105]. *In vitro* and *in vivo* results showed that the created wounds closed after 16 days of implantation and no adverse inflammatory reactions or other antigenic complications were observed, showing the great potential of this strategy for dermal reconstruction. Said and co-workers (2011 and 2012) also investigated randomly oriented electrospun fibers for wound healing by combining PLGA with different substances as antimicrobial wound dressing. *In vivo* results after application of fusidic acid (FA)-loaded PLGA

electrospun ultrafine fibers showed high efficacy of this strategy to promote wound healing and reduced infection (Fig. I.3) [106, 107]. A study performed by Coskun et al. evaluated the performance of randomly oriented electrospun poly (vinyl alcohol)/sodium alginate as wound dressing *in vivo.* This study compared commercially available wound dressings (tulle gras, Eczacibasi), woven cotton antibacterial bactigras (Smith & Nephew) and nonwoven Suprasorb-A (Lohmann) made from calcium alginate fibers to the electrospun meshes during 21 days. In the early time-points (4 and 6 days) no significant differences were observed, although after the following time-points (15 and 21 days) important differences were observed. Electrospun meshes presented the best healing performance as shown through epithelization, epidermis characteristics, vascularization and formation of hair follicles (Fig. I.4) [108].

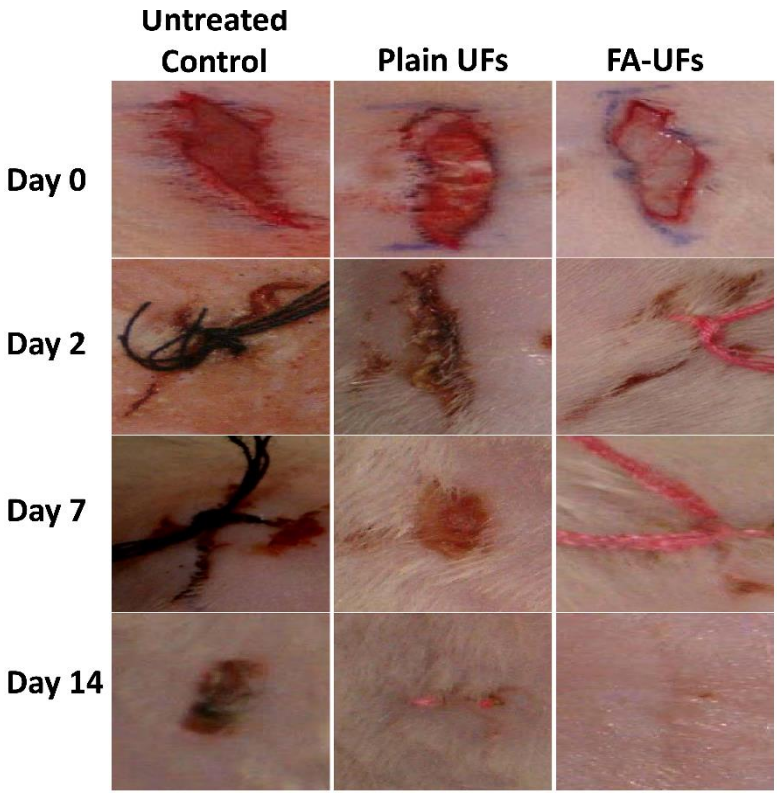

Figure I.3. Effect of plain and fusidic acid loaded PLGA ultrafine fibers on the healing of wounds in rats [107].

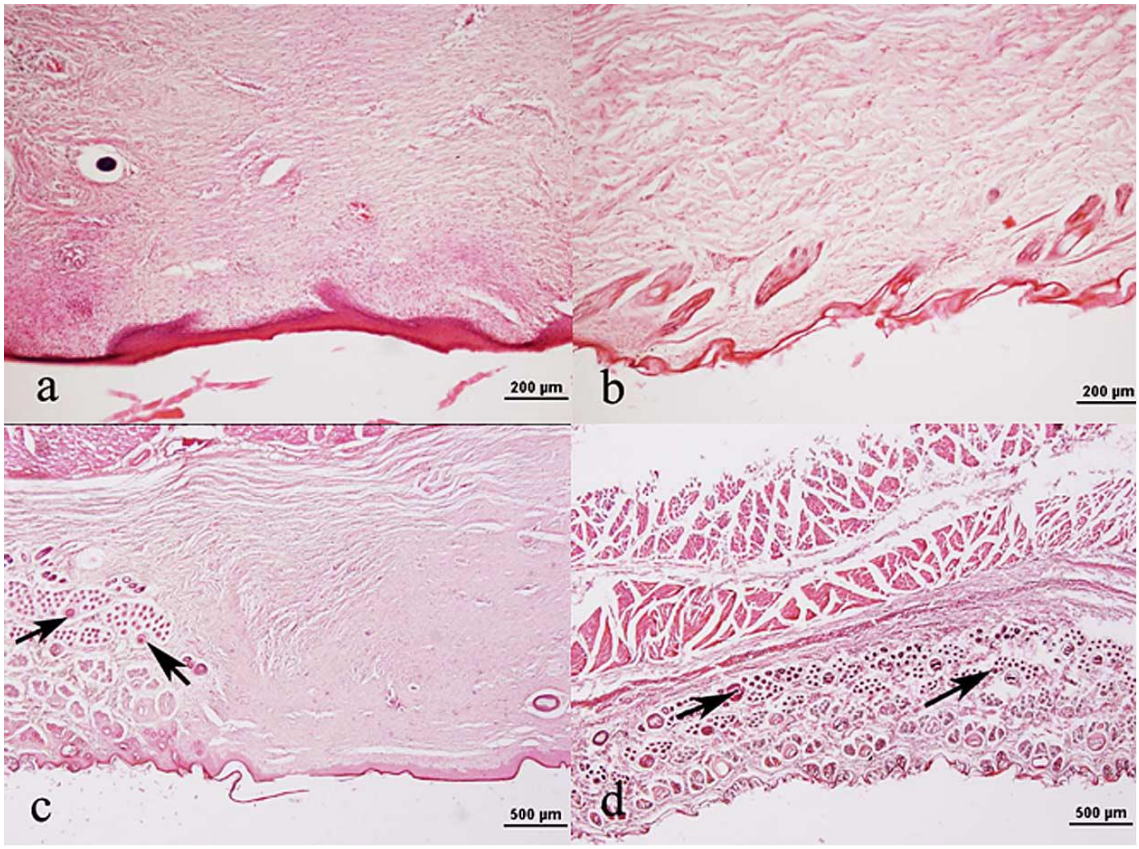

Figure I.4. Histological cross-sections of tissues obtained from regions covered by wound dressings on the 21st postoperative day. (a) Tulle grass; (b) Bactigras ; (c) Suprasorb-A ; (d) Electrospun poly (vinyl alcohol)/sodium alginate mesh . *Arrows*: hair follicies [108].

These studies demonstrate the importance of the nanostructure provided by randomly oriented electrospun meshes to promote wound healing. In fact the electrospinning technique allows production of nanostructures with similar diameter (native range between 10 to 300 nm), porosity and random orientation similar to the collagen fibrils in the ECM of skin [18, 108].

4.2 Aligned fiber meshes

In the TE field one of the most important criteria to design the optimal scaffolds relies in mimicking the tissue ECM, which may involve a considerable degree of orientation, depending on the tissue type and ECM. Hence, random fiber deposition may not be adequate when mimicking tissues where specific fiber orientation is required [72, 79]. Therefore several alternative set-ups to conventional electrospinning have been developed to achieve optimized architectures. To obtain aligned fibers by electrospinning several collectors with varied configurations have been designed to match the desired

orientation (Fig. I.2). Fiber alignment can also be achieved using near electrospinning or melt electrospinning. In both cases the collector is moving in X and Y directions to induce filament orientation and the process is characterized by short distances between the tip of the needle and the collector. To achieve a stable jet region for controllable deposition the average distance of near electrospinning lies between 500 µm and 3 mm and for melt electrospinning between 3 and 5 cm [109-111].

Compared to randomly oriented fibers, aligned fibers present significantly higher resistance to tensile stress, when tested parallel to fiber alignment, and also exert a distinct influence on cell behaviour [70]. Since a variety of tissues are constituted by oriented fibers the development of support structures capable of influencing cellular behaviour at the right orientation is of significant importance. These tissues include ligaments, tendons, brain, muscles, cardiac and vascular tissues [112]. Recent studies demonstrated the influence of aligned fibers over cell organization and function [113-115].

Despite the general random orientation of native skin tissue, Annaidh and colleagues have reported the relevance of the orientation of collagen fibers in the dermis due to the correlation between their orientation and Langer Lines [85]. In the past, Cox and Stark already concluded that the Langer lines have an anatomical basis, since they remained after removal of skin from the body and after tension tests [116, 117]. A few studies have investigated the use of aligned fiber meshes to promote wound healing. Patel et al. developed aligned and bioactive nanofibrous scaffolds by immobilizing extracellular matrix protein and growth factor onto poly(L-lactide) (PLLA) nanofibers, which simulated the physical and biochemical properties of native matrix fibrils. The aligned nanofibers significantly induced neurite outgrowth and enhanced skin cell migration during wound healing compared to randomly oriented nanofibers. Furthermore, the immobilized biochemical factors (as efficient as soluble factors) synergized with aligned nanofibers to promote highly efficient neurite outgrowth but had less effect on skin cell migration [118]. Kurpinski and co-authors showed that aligned PLLA nanofibers enhanced bovine aortic endothelial cells (BAECs) infiltration as a result of a high pore openness, which facilitated cell migration across the structure. *In vitro* and *in vivo* tests on a dermal wound healing model showed the importance of nanofiber alignment coupled with the effect of added heparin as effective biophysical and biochemical cues, respectively, to regulate the cellular behaviour and tissue remodeling [119]. In terms of wound size reduction no significant improvements were observed after 7 days. However, histological findings revealed that in aligned fibers the epidermal layer grew, migrating from the wound edge towards nanofibrous graft [119].

4.3 Fibers with core/shell structure

The core/shell technology emerged among the most promising set-ups in the field of electrospinning since it is based on the combination of two different materials or substances. Using this approach, the same filament may have distinct inner and outer layers, allowing different compositions such as a material surrounded by another material or by a matrix loaded with dispersed particles [79, 120]. This design was developed to incorporate substances (e.g. drugs, enzymes, growth factors or other biomolecules) inside the nanofibers. It presents two main advantages [52]: i) substances can be incorporated in the inner layer being protected from environmental factors, such as the organic solvents usually used in the electrospinning technique; ii) and the incorporated substance can be released from the inner layer and past the outer shell layer in a more controlled and sustained pattern [70]. The design parameters, selected materials, thickness and microstructure of the shell will directly influence the release pattern of the substance contained inside of the fibers. The core/shell design is also being widely explored to improve the surface properties of nanofibers, such as the hydrophilicity, which in turn will influence the biological response [70].

There are two different processes to produce core/shell fibers: co-axial electrospinning and emulsion electrospinning. Co-axial electrospinning consists on a capillary concentrically inserted inside the other capillary, resulting in a co-axial configuration in which each capillary is connected to a reservoir containing a given material. Similarly to the conventional electrospinning set-up this approach can work in the vertical or horizontal positions [120]. Through this process, several structures can be produced, such as bicomponent fibers, hollow fibers and fibers with microparticles (Figs. I.2 and I.5). Bicomponent fibers with core/shell configuration can be obtained from two electrospinnable materials or the combination of a spinable material with other non-spinable. This approach presents as major advantages the obtention of a final fiber presenting unique properties and the use of materials that on their own could not be used in the electrospinning process. Using this approach, the range of materials used in electrospinning considerably increases, overcoming the limitations to obtain electrospun fibers from specific materials due their low molecular weight, limited solubility, unsuitable molecular arrangement, or lack of required viscoelastic properties [120]. For instance, Nguyen and co-workers (2011) developed electrospun meshes of chitosan (CS) (core) and poly(lactic acid) (PLA) (shell) although CS, due to its high molecular weight, high viscosity and polycationic nature, cannot be electrospun on its own, and demonstrated

their antibacterial activity and the high potential of these composite nanofibers for applications in the biomedical field.

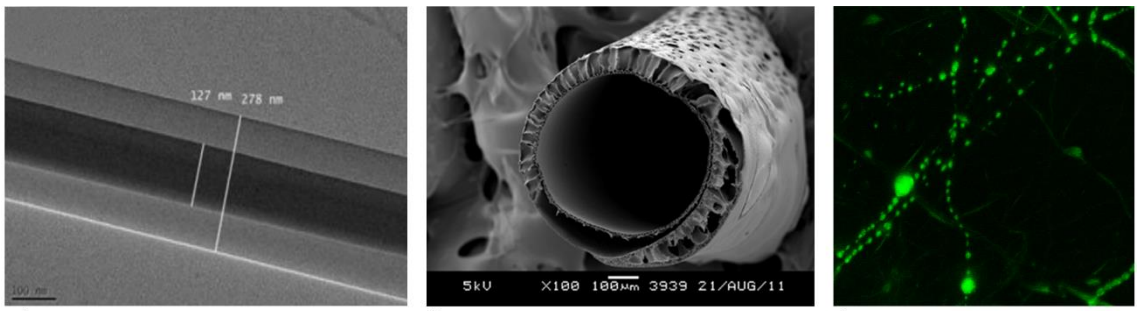

Figure I.5.Core/shell fibers a) Transmission electron microscopy image of: Core/shell chitosan/poly(lactic acid) electrospun composite nanofibers produced using a co-axial approach [121]; b) Scanning electron microscopy image of a cross-section of a polycaprolactone (PCL) hollow fiber in water coagulation bath [122]; c) Confocal microscopy image of a poly(vinyl alcohol) (core)/PCL (shell) nanofiber mesh with encapsulated liposomes (in the core) stained with fluorescein[123].

The combination of fibers with drugs, growth factors and other substances or biomolecules also provides novel functionalities to the produced fibers [120]. The entrapment of substances inside the fibers allows controlling the release rate, which is dependent on the degradation rate of the outer fiber polymer, thus smoothing the sudden release [52]. Several research groups have been showing interesting results from substances encapsulation. Maleki et al. reported an easier control of drug release profile through core/shell fibers compared to monolithic fibers using tetracycline hydrochloride (TCH) as core and poly(lactide-co-glycolide) (PLGA) as shell [124]. Despite their interesting properties the wide application of liposomes in regenerative medicine is difficult due to their short half-life and inefficient retention at the site of application. Mickova and co-workers claim that these disadvantages could be significantly reduced by their combination with nanofibers[123]. They demonstrated the incorporation potential of liposomes into nanofibers by coaxial electrospinning of poly(vinyl alcohol) (PVA) (core) and polycaprolactone (PCL) (shell). The study validated that the enzymes encapsulated on liposomes dispersed into PVA fibers survived intact to the process fabrication. The potential of this system was also proved by the enhancement of mesenchymal stem cell proliferation, indicating its promising characteristics as drug delivery system [123].

Not many studies are available reporting the use of core-shell nanofibers for skin regeneration. Jin et al. demonstrated that nanofibers composed of gelatin (core)/poly(l-

lactid acid)co-poly-(e-caprolactone)(PLLCL) (shell) and epidermal induction medium embedded in the core promoted the desired sustained release of the medium without burst release and further induced the differentiation of adipose-derived stem cells into epidermal lineages [125]. According to Xu et al. an efficient delivery system is critical for the success of cellular therapies. To deliver cells to a dynamic organ, the biomaterial vehicle should mechanically match the non-linear elastic behaviour of the host tissue. In this study, non-linear elastic biomaterials have been fabricated from a chemically crosslinked elastomeric poly(glycerolsebacate) (PGS) (core) and the thermoplastic poly(L-lactic acid) (PLLA)(shell) using the core/shell electrospinning technique. Mechanical tests demonstrated values comparable to skin tissue (Table 3) and *ex vivo* and *in vivo* trials shown that the elastomeric mesh supports and fosters the growth of enteric neural crest (ENC) progenitor cells.

Co-axial electrospinning can also be used to produce hollow fibers without the need of a template to be coated, as in the chemical vapor deposition method [126]. In this strategy the core material is dissolved by a specific solvent, at the end of the process or the core interacts with shell forming a hollow fiber during the processing. Wei et al. showed the potential of hollow fibers to act as a drug delivery system using core/shell fibers of PVA (core) and polyethersulfone (PES) (shell) with the core material containing the drug (curcumin). During the fabrication process the core and shell wall interacted forming a hollow fiber bilayer containing the drug on the fiber inner wall [127].

Core/shell fibers can also be produced using emulsions. This approach does not require a special needle with a physical separation between the core and the shell solutions neither such a careful selection of operation parameters as in the co-axial aproach. In this case the dispersed drop in the emulsion turns into the core and the continuous matrix become the shell [120, 128, 129]. Ma et al. reported the formation of core/shell fibers through the emulsion using sodium alginate as core and poly(ethylene oxide) (PEO) as shell. However, when crosslinking occurs it induces changes on fiber morphology and the electrospun mesh looses the configuration and becomes a film. The water-in-oil (w/o) emulsion is being widely explored to encapsulate hydrophilic drugs or bioactive molecules in the core to avoid burst release and prolong the release time [128]. Zhang et al. prepared bovine serum albumin (BSA) entrapped in a water-in-oil emulsion as the core, encapsulated in the shell polymer (methoxy polyethylene glycol-b-poly(l-lactide-co-e-caprolactone) (PELCL) and poly(l-lactide-co-glycolide)(PLGA)) via emulsion-core (EC) coaxial electrospinning. The fibrous membranes reduced the initial burst release of BSA, which can be tailored by changing the composition to PLGA in the core emulsion. The

results showed that EC electrospinning performed better than conventional co-axial electrospinning with respect to protein delivery for tissue engineering applications[130].

4.4 Hybrid structures

The characteristic small pore size of nanofibrous meshes produced by electrospinning and the lack of specific groups to interact with cells on the commonly used polymers limits the cellular migration into the scaffold and could results in 2D tissue formation becoming a hindrance to the success on 3D tissue regeneration [131, 132]. To overcome these limitations several promising approaches have been developed, either combining different variants of electrospinning or through combination with additive technologies [133, 134].

The combination of different electrospinning set-ups allows the fabrication of hybrid structures. Several research works explored the development of hybrid structures combining different fiber diameters [135-137], different materials to improve the properties of the structure [138-140] or combining aligned/random fibers [141]. For skin regeneration most of the available works only explore the combination of materials and different fiber diameters, building structures without gradients.

The droplet formation phenomena, initially considered an handicap to fiber production, is a consequence of the low viscosity of the polymeric solutions used in electrospinning [50, 142]. However, exploration of particle formation under influence of an electric field, a new technique was developed, called electrospraying, ensuring that with one entanglement per chain it is possible to obtain particles from micro to nano scale [143]. Particle electrospraying is of great interest for tissue engineering applications by providing encapsulation of biomolecules due its high encapsulation efficiency and increase in the surface area [144, 145]. Only a few works are available combining electrospraying with electrospinning, aimed at developing hybrid structures mimicking native tissues. It has been previously demonstrated that combining both techniques it is possible obtain hybrid structures with potential for tissue regeneration due its capacity to promote cell adhesion and proliferation (Fig. I.6a) [146-149] . The combination could be an interesting approach to produced meshes for skin regeneration although it has not been explored in that sense yet. As previously explained nanofiber meshes have unique properties to promote skin regeneration although, especially coupled with controlled delivery of relevant therapeutic molecules. This could be achieved using the electrospraying technique that provides advantages over the more widespread use of nanoparticles prepared through conventional techniques, since no emulsion nor high

temperatures are required, no further drying step is necessary and it provides an enhanced control over particle size distribution [145, 150, 151].

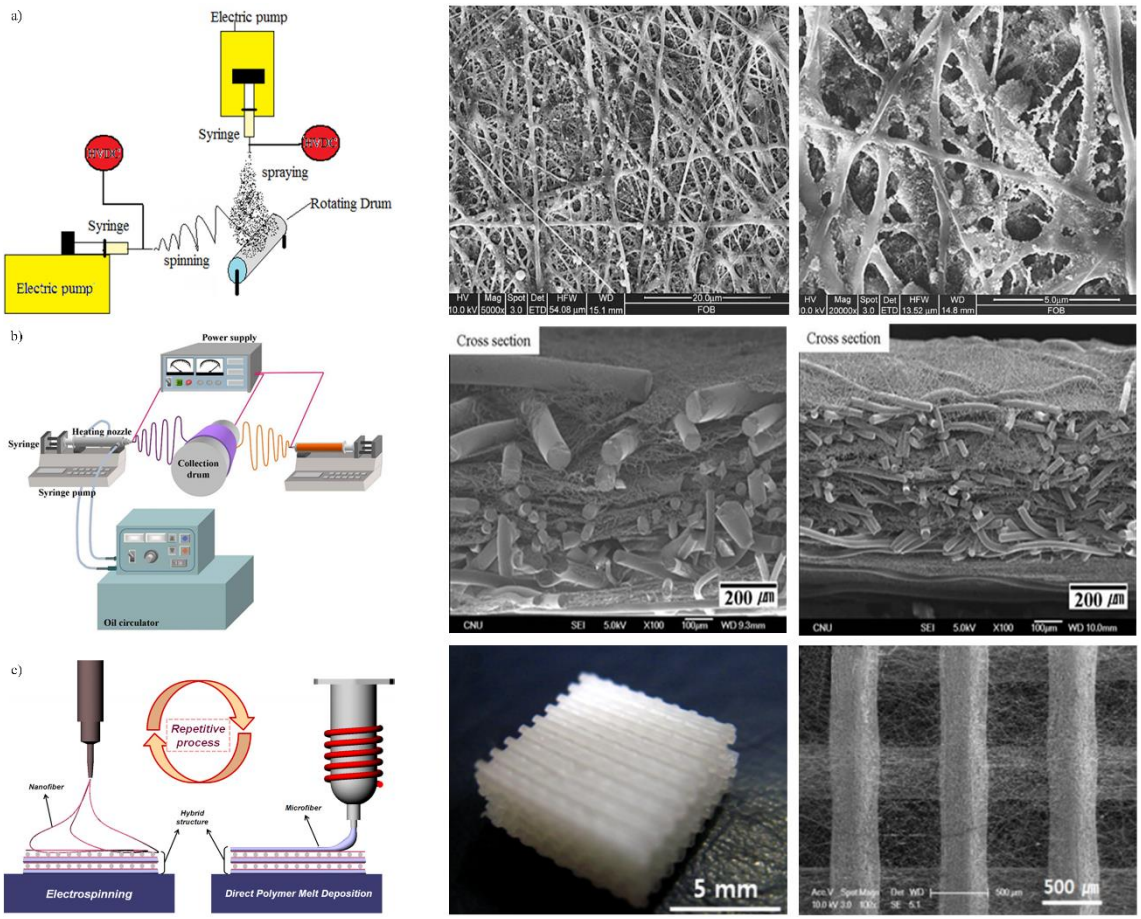

Figure I.6. Hybrid structures produced by combination of: a) Electrospinning and electrospraying [146, 147], b) Solution electrospinning and melt electrospinning [152], c) 3D printing (FDM) and electrospinning [153].

Hybrid structures produced through the combination of solution and melt electrospinning is another interesting emerging approach. The use of a molten polymer with electrostatic field was reported for the first time by Larrondo and Mandley [154-156]. However, only recently the use of melt polymers has received attention again rather than polymers dissolved in organic solvents. Although fibers obtained through melt electrospinning usually present relative high diameters, the technology presents important advantages namely not using organic solvents, thus avoiding solvent accumulation and the need to subsequently eliminating them to decrease sample toxicity [109, 157]. The combination of solution with melt electrospinning also contributes to solve the problems associated with low cellular infiltration as a consequence of high-density packing of nanofibers, with the microfibers increasing the pore size and porosity required for cell infiltration, and

nanofibers contributing to promote cell attachment and growth [145, 158]. However, despite the potential of this kind of combination, only few works are available explored this approach, demonstrating that 3D hybrid structures made from PLGA micro and nanofibers show improved mechanical properties, cell attachment and growth than structures composed only by microfibers, thus representing a greater potential for tissue engineering applications, namely for skin regeneration (Fig. I.6b) [134, 152].

Another strategy to obtain hybrid structures involves additive manufacturing technology combined with electrospinning. Additive manufacturing (AM) techniques have been widely studied for scaffold fabrication due their ability to produce porous structures with high reproducibility, tailored external shape and internal morphology [159-161]. However, the produced scaffolds present lack of nanometer-sized details to mimic the native ECM of tissues. To improve cellular behaviour the combination with electrospun nanofibers is a possibility [131, 160, 162, 163]. The initial works combining both techniques were reported in 2008, demonstrating improved mechanical properties, cell attachment and proliferation of the hybrid structures and their potential for tissue engineering (Fig. I.6c) [153, 164, 165]. Since then, only few additional works have been reported, most of them combining additive techniques based on fused deposition modeling (FDM) with electrospinning, and often using PCL [160, 166-172]. Although no works exploring this approach for skin regeneration are available it would be interesting to integrate the advantages of AM (control of pore size, pore size distribution, interconnectivity and mechanical properties) with electrospun nanofibers. The use of hybrid structures allows combining the advantages of both techniques and reducing or eliminating the disadvantages resulting of the separate use of each technique, as explained in Table I.4.

Table I.4. Critical analysis of the essential characteristics of scaffolds produced by additive manufacturing (AM) in comparison with nanofibers produced by electrospinning and their influence on tissue regeneration.

Type of structure	Characteristics	Influence	References
AM scaffolds	Controlled microstructure	Facilitates oxygen and nutrients transport across the structure by increasing the diffusion efficiency	[161, 164, 173]
	Suitable mechanical properties	Maintains scaffold structural integrity and stability and matches native tissue's mechanical characteristics to expose cells to the correct stress environment	[164, 165, 174, 175]
	Large pore size	Limits cell seeding efficiency	[166, 168, 171, 176]
	Smooth filaments	Inhibits initial cell attachment	[164, 166, 171]
Electrospun nanofibers	High surface area	Mimics the hierarchical structure of ECM that is critical for cell attachment, spreading and proliferation, as well as for nutrient/waste transportation	[52, 79, 82, 168]
	High porosity	Favors cell attachment, differentiation and mimics the native ECM, facilitating nutrient and waste exchange and vascularization	[70, 75, 177-179]
	Fibers with low diameter	Fiber diameters match structural properties of the ECM and confer high surface area to volume specific ratio	[50, 70, 142, 180]
	Low mechanical properties	Limits structural and functional integrity and does not provide the correct stress environment to produce neotissues	[70, 99, 164, 167]
	High packing required to obtain 3D structures	Restricts cellular infiltration across the mesh	[160, 181, 182]

Despite recent advances towards the development of hybrid structures for tissue engineering applications, several challenges still remain. Most of the hybrid structures produced are based on the combination of solution electrospinning together with electrospraying, melt electrospinning or additive manufacturing technologies. Combinations with other techniques, although yet little explored, represent equally exciting potential, even if for specific applications. Pateman and colleagues explored the potential of combining the stereolithography and electrospinning to create channels with oriented fibers supporting the regeneration of injured nerves and guide Schwann cell

growth [183]. This approach could be equally interesting for wound dressing development by, for instance, allowing to produce fibers with photocrosslinkable hydrogels that combine the advantages of wound dressings composed by nanofibers (promoting hemostasis, semipermeability, no scar induction, among others) with photocrosslinkable hydrogels that, beyond the advantages of hydrogels in the wound healing process, allow precise control over the diffusion rate of bioactive substances across the structure [9, 181, 184] .

4.5 Cell electrospinning

Scaffolds are critical to support, promote and guide cell growth, thus making the development of structures mimicking the ECM a subject of intense research. To recreate the complex tissue nano-microstructure, modular structures are required providing precise control over the architecture, biomechanical behaviour, cell density and degradation rate [1, 7, 41]. At present, two main approaches are available to integrate cells into the scaffolds: cell seeding and cell printing/bioprinting, correlated with top-down and bottom-up approaches, respectively. Cell seeding is the most widely used method to integrate cells into 3D structures and consists on seeding cells on scaffolds. However, this approach presents limited control over cell density, localization and spreading, resulting in low seeding efficiency, minimal cell penetration of scaffold walls and not mimicking the cellular organization of native tissues [185-187]. Although different approaches exist for cell seeding, cell printing been attracting great attention due to the possibility of integrating cells directly into the filaments that compose the 3D structure [188, 189]. Different cell printing technologies allow the production of 3D structures, in which cells and biomaterials can be positioned in pre-determined places due to the precise control over the internal/external architecture and layer-by-layer fabrication [161, 186, 189]. The most widely used technologies for cell printing are the inkjet [45, 190-192] extrusion [189, 193, 194], laser [195-197], valve-based [188, 198] and acoustic ones [199, 200] (Fig. I.7).

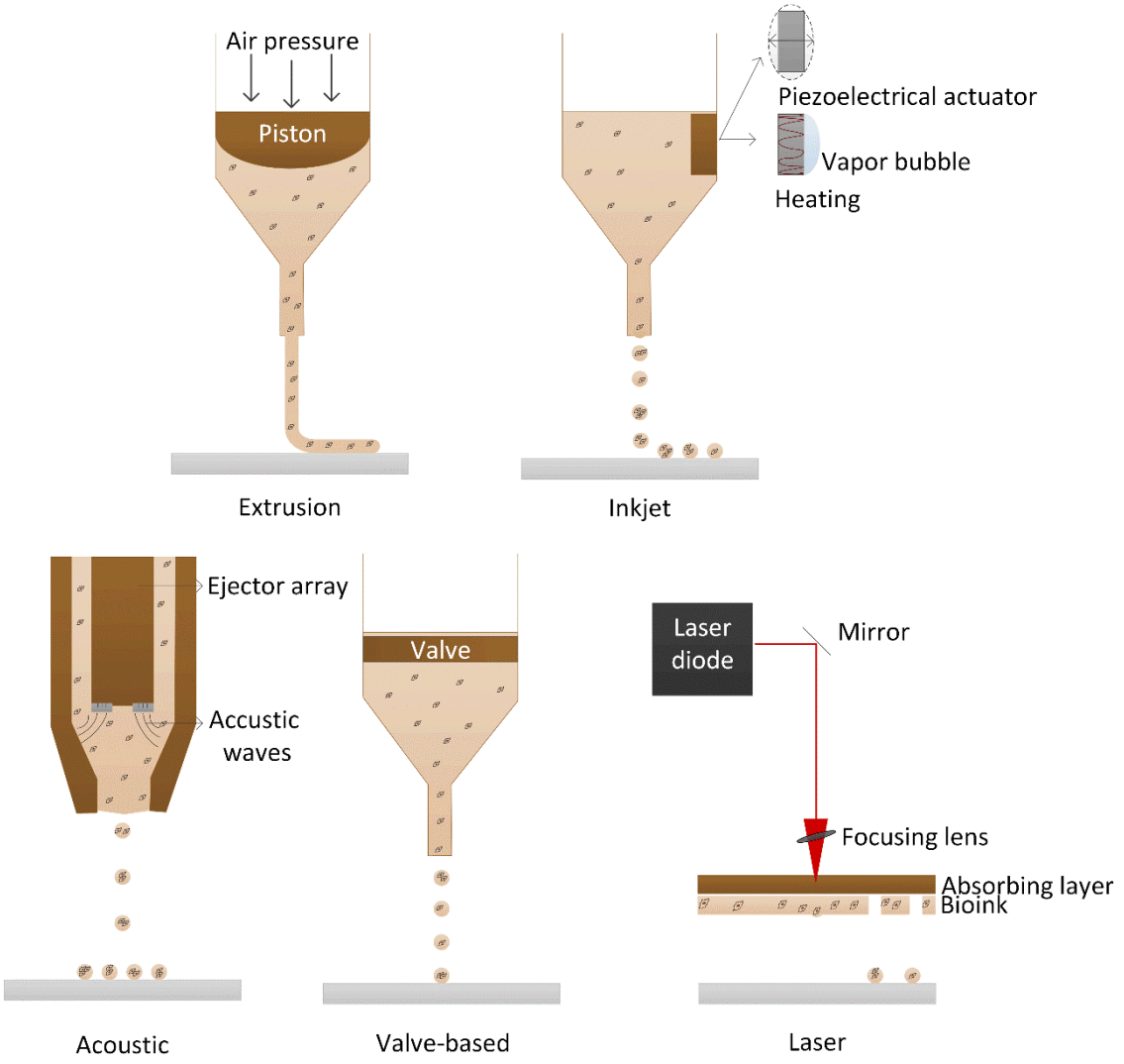

Figure I.7 . Cell printing technologies.

The biological performance of electrospun meshes, similarly to other structures designed for tissue engineering applications, depends on their ability to incorporate the desired cell types and to promote the intended functionality of the incorporated cells [201]. As previously mentioned, the most common procedure relies in incorporating cells after scaffold production, although recent works have been exploring the combination of electrospinning with bioelectrospraying to seed cells during the production of the structure. The earlier incorporation of a high number of cells was reported to improve structural stability and biochemical composition of engineered tissues [202, 203].

Similarly to the previous cell printing technologies mentioned, the cell electrospinning methodology intends to significantly reduce the time needed to generate complex cellularized structures, the non-uniformity in the seeded cells and the time required for cells to fully infiltrate the entire architecture [204]. This concept was pioneered in 2006

by Suwan J. Jayasinghe's research team, when they proposed cell electrospinning with different cell concentrations and using a core-shell set-up and varying flow rates[205]. The cell line used belongs to the neuronal lineage, and hence are more suitable to function under the influence of electric impulses without damage. Since cell suspensions by themselves are not electrospinnable the core-shell approach was used, in which the inner part was composed by a cellular suspension and the outer part by polydimethylsiloxane (PDMS). The outer solution should act as a shield for cells and provide a matrix for cell growth. The cellular viability *in vitro* post electrospinning was evaluated through flow cytometry and showed that cell growth and 100% of confluence in all samples was reached after 3 weeks of culture. *In vivo* tests were performed using real-time bioluminescent imaging in which results showed that the processing did not compromise the ability of the electrospun cells to proliferate [205-207]. However, according to Townsend-Nicholson and colleagues, when the bicomponent filaments (PDMS/cell in suspension) were submerged into the cell growth medium the nanofiber mesh configuration was lost, thus indicating that the cell viability mentioned before corresponded to the cell suspension alone and not to the performance of electrospun meshes incorporating cells. Nevertheless, the study showed the possibility of electrospinning living organisms. The same research team updated the previous work by using the same polymer (PDMS) but increasing the cell concentration from 10^6 to 10^7 cell/mL and using primary porcine vascular smooth muscle cells and rabbit aorta smooth muscle cells [206]. Although cell viability was described as not affected by the electric field and fibers were electrospun containing high cellular concentrations, no evidence of remaining scaffolds after cell culture was provided. Recently, Sampson and co-workers reported *in vitro* and *in vivo* studies using cell electrospun meshes produced with modified matrigel as shell to the cell suspension. According to their results the cells submitted to the electric discharge showed a similar behaviour to the control ones (not submitted to any discharge), although the matrix was dissolved and cells disassociated from the scaffold before analysis[207].

Although a few publications already exist on the topic of cell electrospinning, the issues related to cell behaviour in a high electric field, namely the in depth assessment of cellular damage, has not been reported yet. Jayasinghe and his team reported that cells survive the electrospinning process without any major damage, although enough evidence is still missing showing that the 3D structures encapsulating the cells maintain their architecture over time. Another limitation of this process is related with the fiber size. One major advantage of electrospun nanofibers in wound healing is the relatively small fiber diameters (in the order of nanometers), which mimics the native ECM. In suspension

cells assume a size of around 10-20 μm, which considerably limits the fiber diameter achievable with the cell electrospinning approach to the micrometer size range, thus compromising the natural advantage of electrospinning to mimic the native fibers of ECM (10-300 nm) compared to other competing technologies such as cell printing.
Therefore, additional studies are required to further address the issues described above. However, in the field of skin regeneration this new approach brings enormous potential, with the possibility of incorporating cells into the core of polymer fibers, thus eventually decreasing the problems associated with low cell infiltration as a consequence of small pore size and high packing associated to electrospun 3D meshes.

4.6 *In situ* electrospinning

In situ electrospinning is, a new concept that intends to produce appropriate substitutes for tissue repair and regeneration directly on the patient's lesion [7]. To fabricate the adequate substitutes this approach is associated to real-time imaging techniques and path-planning devices for the digitalization of the damaged area and definition of the path for the deposition of biomaterials with or without cells that can be combined with encapsulated cells [7]. The main goal of this approach is to provide a tool to directly create a customized wound dressing to the wound bed, with easy and quick application, painless to remove and at a low cost [208, 209]. Xu et al. recently patented an easily handled and portable e-spinning battery-operated apparatus for *in situ* electrospinning (Fig. 8a) [210], allowing the deposition of electrospun meshes, with similar characteristics to the ones obtained by the conventional electrospinning technique, directly to the skin and using varied polymeric micro/nanofibers (Fig. 8b) [208]. More recently, the same team explored the effect of *in situ* electrospinning on the wound healing process. They deposited *in situ* mesoporous silica nanoparticles (Ag-MSNs) dispersed in PCL electrospun fibers and evaluated the antimicrobial activity and biological efficacy in wistar rats. The *in vitro* and *in vivo* results confirmed the antimicrobial activity and bioavailability of 5% Ag-MSNs/PCL electrospun fibers (average diameter of 658 nm). The results showed efficient antibacterial properties against predominant pathogenic bacteria (gram negative Escherichia coli) responsible for several burn wound infections. *In vivo* studies clearly showed the improvement of *in situ* deposited nanofibers on wound healing compared to the control groups. After four weeks of post-treatment it was possible to observe significant wound closure and complete re-epithelialization (Fig. I.8c) [209]. This new approach can bring considerable advances in the wound care field, allowing a quick deposition of skin substitutes independently of wound size and depth, although some

issues still remain to addressed, such as the decrease of fiber diameter (from ca. 650 to 10-300 nm, the average diameter of fibers in native ECM), and the matching of mechanical properties between structures developed and native skin.

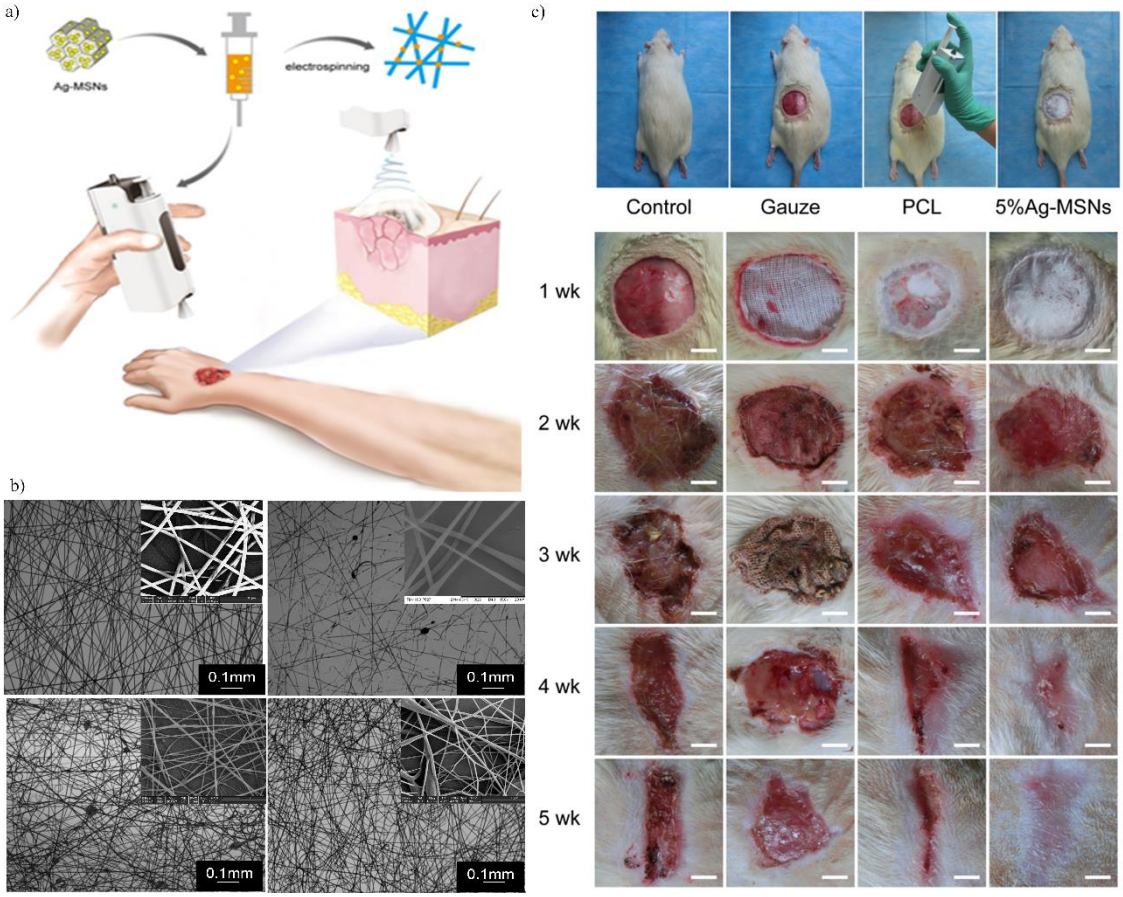

Figure I.8. *In situ* electrospinning concept, a) portable electrospinning system, b) SEM of electrospun meshes obtained with portable system, c) *in vivo* evaluation of in situ electrospun mesh, PCL-polycaprolactone, Ag-MSNs -mesoporous silica nanoparticles[208, 209].

5. Concluding remarks and future trends

Nanoscale constructs, and electrospun meshes in particular, have been receiving great attention from the scientific and medical communities for skin regeneration. In the past few years, important advances have been achieved in terms of nanofiber fabrication strategies, and related material synthesis and functionalization, and *in vitro* cell culture procedures. The developments in the field reported so far have been considerably contributing for a more efficient mimicking of the ECM through the combination of materials, growth factors, proteins and biomolecules which, associated to the novel

advanced processing strategies, making possible the production of wound dressings with a remarkable potential for skin regeneration. However, recent advances in the specific topic of skin regeneration have been mainly focused on materials rather than in sophisticated fabrication strategies to generate biomimetic and complex constructs that resemble the mechanical and structural properties of skin. Research efforts have been focused on both the development of novel material combinations and the improvement of the biochemical properties of existing materials, for instance, through the use of functionalization procedures and surface modification processes. In general, improved skin substitutes need to be developed to avoid the use of animal-derived materials, improve the adhesion of cultured keratinocytes to the wound bed, improve the rate of neovascularization of tissue engineered skin and enhance the scaffolds materials to resist to the wound contraction and fibrosis.

Several advances on the evolving field of electrospinning can be foreseen with specific application in wound healing, namely:

i) Development of combined and functional structures using different deposition strategies, such as the multimaterial approach, where two or more materials are deposited at the same time on a single collector, or create a multilayer structure with sequential production. Other interesting strategy is the use of hybrid structures through the combination of filaments produced using different methodologies, such as using emulsions, copolymers, or the core/shell approach.
ii) Integration of different technologies with electrospinning and different electrospinning approaches to obtain hybrid structures with tunable gradients, properties and functionalities. Combining different materials and fiber compositions, different fiber diameters and nano/microarchitectures to achieve the most suitable mimetic structure to regenerate the skin tissue;
iii) Cell electrospinning of skin cells (keratinocytes and fibroblasts) needs to be explored to evaluate the electric field influence on the cells viability, proliferation and gene expression. The integration of cells into electrospun fibers will bring forward a new generation of skin substitutes and solve problems of cell infiltration associated to electrospun meshes;
iv) The *in situ* electrospinning is a promising technology providing the possibility of direct deposition of electrospun nanofibers on the wound with no restriction due to wound size or depth. This technology open considerable possibilities, especially combined with previously mentioned developments, namely the deposition of

multilayer structures to build hybrid structures or the integration with cell electrospinning.

References

1. Yildirimer L, Thanh NTK, and S. AM, Skin regeneration scaffolds a multimodal bottom-up approach. Trends Biotechnol, 2012. **30**: p. 638-48.
2. Seal BL, Otero TC, and P. A, Polymeric biomaterials for tissue and organ regeneration. Materials Science and Eng R, 2001. **34**: p. 147-230.
3. WHO, The global burden of disease 2004. 2008.
4. WHO, Fact sheet nº365. 2014.
5. Brusselaers, N., et al., Severe burn injury in europe: a systematic review of the incidence, etiology, morbidity, and mortality. Critical Care, 2010. **14:R188**: p. 1-12.
6. Shevchenko RV, James SL, and J. SE, A review of tissue-engineering skin bioconstructs available for skin reconstruction. J. R. Soc. Interface, 2010. **7**: p. 229-58.
7. Pereira RF, et al., Advanced biofabrication strategies for skin regeneration and repair. Nanomedicine, 2013. **8**: p. 603-21.
8. Reddy VJ, et al., Nanofibrous structured biomimetic strategies for skin tissue regeneration. Wound Rep Reg 2013: p. 211-16.
9. Zahedi P, et al., A review on wound dressings with an emphasis on electrospun nanofibrous polymeric bandages. Polym. Adv. Technol 2009. **21**: p. 77-95.
10. Casey G, The physiology of the skin. Nursing Standard 2002. **16**: p. 47-51.
11. MacNeil S, Progress and opportunities for tissue-engineering skin. Nature, 2007. **445**: p. 874-80.
12. Zhou, S., et al., The skin function: a factor of anti-metabolic syndrome. Diabetology & Metab Syndrom, 2012. **4**: p. 1-11.
13. Lai-Cheong JE and M. JA, . Structure and function of skin, hair and nails. Medicine, 2013. **41**: p. 317-20.
14. Timmons J, Skin function and wound healing physiology. Wound Essentials 2006. **1**: p. 9-17.
15. BÖttcher-Haberzeth S, Biedermann T, and R. E, Tissue engineering of skin. Burns 2010. **36** p. 450-60.
16. Scanlon VC and S. T, Essentials of Anatomy and Physiology 5th ed. 2007.
17. Tortora GJ and D. B, Principles of Anatomy and Physiology 13th edition. 2012.

18. Molly MS and J. HG, Exploring and engineering the cell surface interface. Science, 2005(310): p. 1135-1138.
19. Sun T, et al., Development of a 3D Cell Culture System for Investigating Cell Interactions With Electrospun Fibers. Biotechnology and Bioengineering, 2007. **97**(5): p. 1318-1328.
20. Sun T, et al., Self-Organization of Skin Cells in Three-Dimensional Electrospun Polystyrene Scaffolds. Tissue Engineering, 2005. **11**(7/8): p. 1023-1033.
21. Enoch S and L. DJ, Basic science of wound healing. Surgery, 2007. **26**: p. 31-7.
22. Young A and M. CE, The physiology of wound healing. Surgery, 2011. **29**: p. 475-79.
23. Nauta A, Gurtner GC, and L. MT, Wound healing and regenerative strategies. Oral diseases, 2011. **17**: p. 541-49.
24. Monaco, J.L. and W.T. Lawrence, Acute wound healing: An overview. Clin plastic surg, 2003(30): p. 1-12.
25. MacKay D and M. AL, Nutritional Support for wound healing. Alternat. Med. R. , 2003. **8**: p. 359-77.
26. Groeber F, et al., Skin tissue engineering – In vivo and in vitro applications. Advanced Drug Delivery Reviews 2011. **128**: p. 352-66.
27. Pham C, et al., Bioengineered skin substitutes for the management of burns:A systematic review. Burns, 2007. **33**: p. 946-57.
28. Zhong, S., Y. Zhang, and C. and Lim, Tissue scaffolds for skin wound healing and dermal reconstruction. WIREs Nanomedicine and Nanobiotechnology, 2010. **2**: p. 510-25.
29. Vasconcelos A, Gomes AC, and C.-P. A, Novel silk fibroin/ elastin wound dressings. Acta Biomaterialia 2012. **8**: p. 3049-60.
30. Wang T, et al., Hydrogel sheets of chitosan, honey and gelatin as burn wound dressings. Carbohydrate Polymers 2011. **88**: p. 75–83.
31. Weller C and S. G, Wound Dressings Update. Journal of Pharmacy Practice and Research 2006. **36**: p. 318-24.
32. Watson NFS and H. W, Wound dressings. Surgery, 2005. **23**: p. 52-5.
33. Abdelrahman T and N. H, Wound dressings: principles and practice. Surgery, 2011. **29**: p. 491-495.
34. Poinern GEJ, et al., Nanoengineering a Biocompatible Inorganic Scaffold for Skin Wound Healing. Journal of Biomedical Nanotechnology 2010. **6**: p. 497–510.

35. Pramanik S, Pingguan-Murphy B, and O. NAA, Progress if key strategies in development of electrospun scaffolds: bone tissue. Sci. Technol. Adv. Mater., 2012: p. 131-13.
36. Zhang, Z. and M.-K. BB, Tissue Engineered Human Skin Equivalents. Pharmaceutics, 2012. **4**: p. 26-41.
37. Van der Veen VC, et al., Biological background of dermal substitutes. Burns, 2010. **36**: p. 305-21.
38. Harding K, Sumner M, and C. M, A prospective, multicentre, randomised controlled study of human fibroblast-derived dermal substitute (Dermagraft) in patients with venous leg ulcers. International Wound Journal, 2013. **10**: p. 123-37.
39. MacNeil S, Biomaterials for tissue engineering of skin. Materials Today, 2008. **11**: p. 27-35.
40. JN, K., Clinical evaluation of skin substitutes. Burns, 2001. **27**: p. 545-51.
41. Nichol JW and K. A, Modular tissue engineering: engineering biological tissues from the bottom-up. Soft Matter, 2009. **5**: p. 1312-9.
42. Bártolo PJ, et al., Biofabrication strategies for Tissue Engineering, in Advances on modeling in Tissue Engineering, P.J.B. P.R. Fernandes, Editor. 2011, Springer: Berlin. p. 137-76.
43. Nemeno-Guanzon JG, et al., Trends in tissue engineering for blood vessels. J Biomed Biotechnol 2012: p. 956345.
44. Rustad KC, et al., Strategies for organ level tissue engineering. Organogenesis, 2010: p. 61-7.
45. Jakab K, et al., Tissue engineering by self-assembly and bio-printing of living cells. Biofabrication, 2010. **2**: p. 02200.
46. Zamanian B, et al., Self-assembly of Cell-laden Hydrogels on the Liquid-Air Interface, in 3-D Tissue Engineering, J.M. F. Berthiaume, Editor. 2009, Artech House. p. 121-32.
47. Bhardwaj N and K. SC, Electrospinning: a fascinating fiber fabrication technique. Biotechnology Advances, 2010. **28**: p. 325-47.
48. Stanger J, Tucker N, and S. M, Electrospinning. Rapra review reports. Report, 2005. **16**: p. 190.
49. Tucker N, et al., The history of the science and technology of electrospinning from 1600 to 1995. Journal of Engineered fibers and fabrics 2012: p. 63-73.
50. Burger C, Hsiao, and C. B, Nanofibrous materials and their applications. Annu. Rev. Mater. Res. , 2006. **36**: p. 333-68.

51. Teo WE and R. S, A review on electrospinning design and nanofibre assemblies. Nanotechnology, 2006. **17**: p. 89–106.
52. Cui W, Zhou Y, and C. J, Electrospun nanofibrous materials for tissue engineering and drug delivery. Sci. and technol. Adv. Mater., 2010: p. 11014108.
53. JF, C., Apparatus for electrically dispersing fluids. 1902: US.
54. JF, C., Electrical method of dispersing fluids. 1903: US
55. Formhals, A., Process and apparatus for preparing artificial threads. 1934.
56. Formhals, A., Production of artificial fibers. 1937.
57. Formhals, A., Method and apparatus for the production of fibers. 1936.
58. Formhals, A., Artificial fiber construction. 1938.
59. Formhals, A., Method of producing artificial fibers. 1939.
60. Formhals, A., Method and apparatus for the production of artificial fibers. 1939.
61. Formhals, A., Method and apparatus for spinning. 1939.
62. Formhals, A., Artificial thread and method of producing same. 1940.
63. Formhals, A., Production of artificial fibers from fiber forming liquids. 1943.
64. Formhals, A., Method and apparatus for spinning. 1944.
65. Sill TJ and v.R. HA, Electrospinning: Applications in drug delivery and tissue engineering. Biomaterials 2008. **29**: p. 1989-2006.
66. Norton, C., Method of and apparatus for producing fibrous or filamentary material. 1936.
67. Vrieze S, et al., The effect of temperature and humidity on electrospinning. J Mater Sci, 2009. **44**: p. 1357–62.
68. Fang D, et al., Effect of intermolecular interaction on electrospinning of sodium alginate. Carbohydrate Polymers, 2011. **85**: p. 276-79.
69. Nukavarapu SP, et al., Electrospun polymeric nanofibre scaffolds for tissue regeneration, in Nanotechnology and Tissue Engineering: The scaffold, N.L. Laurencin CT., Editor. 2008, Taylor & Francis: London.
70. Shin SH, et al., A short review: Recent advances in electrospinning for bone tissue regeneration. J. Tissue Eng. , 2012. **3**: p. 1-11.
71. Li W J and X. Y, Electrospinning of nanofibres: reivented the wheel? Advanced Materials 2004. **16**: p. 1151-70.
72. Braghirolli DL, Steffens D, and P. P, Electrospinning for regenerative medicine:a review of the main topics. Drug Disc. Today 2014. **19**: p. 743-53.
73. Reneker DH, et al., Electrospinning of Nanofibers from Polymer Solutions and Melts. Adv in Appl Mechan 2007. **41**: p. 43-195.

74. Tiwari SK and V. SS, Importance of viscosity parameters in electrospinning: Of monolithic and core–shell fibers. Materials Science and Engineering C, 2012. **32**(5): p. 1037-42.
75. Bártolo P, et al., Biomedical production of implants by additive electro-chemical and physical processes. CIRP Annals - Manufacturing Technology 2012. **61**(2): p. 635-55.
76. Rogina A, Electrospinning process: Versatile preparation method for biodegradable and natural polymers and biocomposite systems applied in tissue engineering and drug delivery. Applied Surface Science 2014. **296**: p. 221–30.
77. Ramakrishna S, et al., An Introduction to Electrospinning and Nanofibers. Singapore: World Scientific, 2005.
78. Pham QP, Sharma U, and M. AG, Electrospinning of Polymeric Nanofibers for Tissue Engineering Applications: A Review. Tissue Engineering: Part B, 2006. **12**(5): p. 1197-211.
79. Rim NG, Shin CS, and S. H, Current approaches to electrospun nanofibers for tissue engineering. Biomed. Mater, 2013. **8**: p. 1-14.
80. Wiesmann HP and L. L, Scaffold Structure and Fabrication, in Fundamentals of Tissue Engineering and Regenerative Medicine, H.J. Meyer U, Wieamann HP, Meyer T, Editor. 2009, Springer. p. 539-49.
81. Yang F, et al., Tissue Engineering: The therapeutic Strategy of the Twenty-First Century, in Nanotechnolgy and Tissue Engineering: The scaffold C.T.L.a.L.S. Nair, Editor. 2008, CRC. p. 3-32.
82. Liu W, Thomopoulos S, and X. Y., Electrospun nanofibres for regenerative medicine. Adv. Healthcare Mater, 2012. **1**: p. 10-25.
83. Boyer G, et al., Assessment of the in-plane biomechanical properties of human skin using a finite element model updating approach combined with an optical full-field measurement on a new tensile device. Journal of mechanical behavior of biomedical materials, 2013. **27**: p. 273-282.
84. Brown IA, A scanning electron microscope study of the effects of uniaxial tension on human skin. British Journal of Dermatology, 1973. **89**: p. 383–393.
85. Annaidh AN, et al., Characterization of the anisotropic mechanical properties of excised human skin. Journal of Mechanical Behavior of Biomedical Materials, 2012. **5**: p. 139-148.
86. Agache PG, Physiologie de la peau et explorations fonctionnelles cutanées, ed. E.M. Internationales. 2000.

87. Jansen L and Rottier P, Some mechanical properties of human abdominal skin measured on excised strips. Dermatologica, 1985. **117**: p. 65-83.
88. Vogel H, Age dependence of mechanical and biochemical properties of human skin. Bioengineering and the skin, 1987. **3**(67-91).
89. Jacquemoud C, Bruyere-Garnier K, and Coret M, Methodology to determine failure characteristics of planar soft tissues using a dynamic tensile test. Journal of Biomechanics 2007. **40**(2): p. 468-475.
90. Pan J-f, et al., Preparation and Characterization of Electrospun PLCL/Poloxamer Nanofibers and Dextran/Gelatin Hydrogels for Skin Tissue Engineering. PLoS ONE 2014. **9**(11): p. e112885.
91. Gümüşderelioğlu M, et al., A novel dermal substitute based on biofunctionalized electrospun PCL nanofibrous matrix. J Biomed Mater Res Part A 2011. **98**(A): p. 461-472.
92. Atila D, Keskin D, and Tezcaner A, Cellulose acetate based 3-dimensional electrospun scaffolds for skin tissue engineering applications. Carbohydrate Polymers 2015. **133**: p. 251–261.
93. Lee EJ, et al., Hyaluronic Acid/Poly(lactic-co-glycolic acid) Core/Shell Fiber Meshes Loaded with pigallocatechin-3-O-Gallate as Skin Tissue Engineering Scaffolds. J. Nanosci. Nanotechnol, 2014. **14**(11): p. 8458-63.
94. Sigma-Aldrich. [cited 2016 11/02/2016]; Available from: http://www.sigmaaldrich.com/labware/labware-products.html?TablePage=109807607.
95. NanofiberSolutions™. [cited 2016 11/02/2016]; Available from: http://www.nanofibersolutions.com/products.html.
96. Zeus. [cited 2016 11/02/2016]; Available from: http://www.zeusinc.com/.
97. FundaciónCardiovasculardeColombia. Clinical Trial for the Treatment of Diabetic Foot Ulcers Using a Nitric Oxide Releasing Patch: PATHON. 2011 [cited 2016 11/02/2016]; NCT00428727]. Available from: https://clinicaltrials.gov/ct2/show/NCT00428727?term=electrospinning&rank=2.
98. ClinicalTrials.gov. [cited 2016 11/02/2016]; Available from: https://clinicaltrials.gov/ct2/results?term=electrospinning.
99. Agarwal S, Wendorff JH, and G. A, Use of electrospinning technique for biomedical applications. Polymer 2008. **49**: p. 5603-21.
100. Miloh T, Spivak B, and Y. A, Needleless Electrospinning : Electrically Driven Instability and Multiple Jetting from free Surface of a Spherical Liquid Layer. J. Appl. Physics, 2009. **106**: p. 114910-8.

101. Meng ZX, et al., Electrospinning of PLGA/gelatin randomly-oriented and aligned nanofibers as potential scaffold in tissue engineering. Materials Science and Engineering C 2010. **30**: p. 1204–10.
102. Schneider T, et al., Influence of fiber orientation in electrospun polymer scaffolds on viability, adhesion and differentiation of articular chondrocytes. Clinical Hemorheology and Microcirculation, 2012. **52**: p. 325–36.
103. Jahani H, et al., The Effect of aligned and random electrospun fibrous scaffolds on rat mesenchymal stem cell proliferation. Cell Journal 2012. **14**: p. 31-8.
104. Shang S, et al., The effect of electrospun fibre alignment on the behavior of rat periodontal ligament cells. Europ. Cells and Mat 2010. **19**: p. 180-92.
105. Jha BS, et al., Electrospun Collagen: A Tissue Engineering Scaffold with Unique Functional Properties in a wide Variety of Applications. J of Nanomat 2011: p. 1-15.
106. Said SS, et al., Antimicrobial PLGA ultrafine fibers: Interaction with wound bacteria. Europ J of Pharm and Biopharm 2011. **79**: p. 108–18.
107. Said SS, et al., Bioburden-responsive antimicrobial PLGA ultrafine fibers for wound healing. Europ J of Pharm and Biopharm 2012. **80**: p. 85–94.
108. Coşkun G, et al., Histological evaluation of wound healing performance of electrospun poly(vinyl alcohol)/sodium alginate as wound dressing in vivo. Bio-Medical Materials and Engineering 2014. **24** p. 1527–1536.
109. Hutmacher DW and D. PD, Melt Electrospinning. Chem Asian J 2011. **6**: p. 44–56.
110. Sun D, et al., Near-Field Electrospinning. Nano Lett., 2006. **6**(4): p. 839-42.
111. Chang, C., K. Limkrailassiri, and L. and Lin, Continuous near-field electrospinning for large area deposition of orderly nanofiber patterns. Appl Phys Lett 2008. **93**(12): p. 123111.
112. Kim HN, et al., Nanotopography-guided tissue engineering and regenerative medicine. Advanced Drug Delivery Reviews 2013. **65**: p. 536–58.
113. Cooper A , Bhattarai N, and Z. M, Fabrication and cellular compatibility of aligned chitosan–PCL fibers for nerve tissue regeneration. Carbohydrate Polymers 2011. **85**: p. 149–56.
114. Kenar H, et al., A 3D aligned microfibrous myocardial tissue construct cultured under transient perfusion. Biomaterials 2011. **32**: p. 5320-9.
115. Wang C-Y, et al., Aligned natural–synthetic polyblend nanofibers for peripheral nerve regeneration. Acta Biomaterialia 2011. **7**: p. 634–43.

116. Cox H, The cleavage lines of the skin. British Journal of Surgery, 1941. **29**(114): p. 234-240.
117. Stark HL, Directional variations in the extensibility of human skin. British Journal of Plastic Surgery, 1977. **30**(2): p. 105-114.
118. Patel S, et al., Bioactive Nanofibers: Synergistic Effects of Nanotopography and Chemical Signaling on Cell Guidance. Nano Lett., 2007. **7**(7): p. 2122-28.
119. Kurpinski K, et al., The Effect of Fiber Alignment and Heparin Coating on Cell Infiltration into Nanofibrous PLLA Scaffolds. Biomaterials, 2010. **31**(3): p. 3536–42.
120. Elahi MF, et al., Core/shell Fibers for Biomedical Applications-A Review. J Bioengineer & Biomedical Sci 2013. **3**: p. 1-14.
121. Nguyen TTT, Chung OH, and P. JS., Coaxial electrospun poly(lactic acid)/chitosan (core/shell) composite nanofibres and their antibacterial activity. Carbohydrate Polymers 2011. **86**: p. 1799– 806.
122. Diban N, et al., Development and characterization of poly(εcaprolactone) hollow fiber membranes for vascular tissue engineering. Journal of Membrane Science, 2013. **438**(2013): p. 29-37.
123. Mickova A, et al., Core/Shell Nanofibers with Embedded Liposomes as a Drug Delivery System. Biomacromol, 2012. **13**: p. 952−62.
124. Maleki M, et al., Electrospun Core–Shell Nanofibers for Drug Encapsulation and Sustained Release. Polymer Engineering and Science 2013: p. 1770-9.
125. Jin G, et al., Controlled release of multiple epidermal induction factors through core-shell nanofibres for skin regeneration. Europ. J. of Pharmac. And Biopharmac 2013. **85**: p. 689-98.
126. Khajavi R and A. M, Electrospinning as a versatile method for fabricating coreshell, hollow and porous nanofibres. Scientia Iranica F, 2012. **19**: p. 2029–34.
127. Wei Z, et al., Preparation and drug delivery study of electrospun hollow PES ultrafine fibers with a multilayer wall. Colloid and Polymer Science, 2014. **292**: p. 1339–45.
128. Zhang, H., et al., Electrospinning of ultrafine core/shell fibers for biomedical applications. Sci China Chem 2010. **53**: p. 1246–54.
129. Ma G, et al., Electrospun sodium alginate/poly(ethylene oxide) core–shell nanofibres scaffolds potential for tissue engineering applications. Carbohydrate Polym 2012. **87**: p. 737– 43.

130. Zhang, H., et al., Controlled release of bovine serum albumin from electrospun fibrous membranes via an improved emulsion-core technique. Abstracts / Journal of Controlled Release 2011. **152**((2011)): p. e133–e191.
131. Wang N, et al., Electrospun fibro-porous polyurethane coatings for implantable glucose Biosensors. Biomaterials 2013a. **34**: p. 888-901.
132. Sun B, et al., Advances in three-dimensional nanofibrous macrostructures via electrospinning. Progr Poly Sci 2014. **39**: p. 862-90.
133. Dalton PD, et al., Electrospinning and additive manufacturing: converging technologies. Biomater. Sci, 2013. **1**: p. 171-85.
134. Yoon YI, et al., Fabrication of Microfibrous and Nano-/Microfibrous Scaffolds: Melt and Hybrid Electrospinning and Surface Modification of Poly(L-lactic acid) with Plasticizer. BioMed Research Intern 2013: p. 1-10.
135. Grey CP, et al., Gradient fiber electrospinning of layered scaffolds using controlled transitions in fiber diameter. Biomaterials 2013. **34**(2013): p. 4993-5006.
136. Sundararaghavan HG and B. JA, Gradients with Depth in Electrospun Fibrous Scaffolds for Directed Cell Behavior. Biomacromolecules, 2011. **12**(2344-50).
137. Abrigo M, Kingshott P, and M. SL, Electrospun Polystyrene Fiber Diameter Influences Bacterial Attachment, Proliferation and Growth. Appl. Mater. Interfaces, 2015. **7**(14): p. 7644-52.
138. Tijing LD, et al., One-step fabrication of antibacterial (silver nanoparticles/poly(ethylene oxide)) e Polyurethane bicomponent hybrid nanofibrous mat by dual-spinneret electrospinning. Materials Chemistry and Physics 2012. **137**(2012): p. 557-61.
139. Jin G, Prabhakaran MP, and R. S, Stem cell differentiation to epidermal lineages on electrospun nanofibrous substrates for skin tissue engineering. Acta Biomaterialia, 2011. **7**(2011): p. 3113-22.
140. Har-el Y-e, et al., Electrospun soy protein scaffolds as wound dressings: Enhanced reepithelialization in a porcine model of wound healing. Wound Medicine, 2014. **5**(2014): p. 9-15.
141. Park SH, et al., Creation of a hybrid scaffold with dual configuration of aligned and random electrospun fibers. Appl. Mater. Interfaces,, 2016: p. 1-27.
142. Garg K and B. GL, Electrospinning jets and nanofibrous structures. Biomicrofluid 2011. **5**: p. 013403-19.

143. Shenoy SL, et al., Role of chain entanglements on fiber formation during electrospinning of polymer solutions: good solvent, non-specific polymer-polymer interaction limit. Polymers, 2005. **43**: p. 3372-84.
144. Jaworek A, et al., Electrospinning and electrospraying techniques for nanocomposites non-woven fabric production. Fibres&Textiles in Eastern Europe, 2009. **17**: p. 77-81.
145. Bock N, Dargaville TR, and W. MA, Electrospraying of polymers with therapeutic molecules: state of art. Prog Poly Sci 2012. **37**: p. 1510-51.
146. Gupta D, et al., Nanostructured biocomposite substrates y electrospinning and electrospraying for the mineralization of osteoblasts. Biomat 2009. **30**: p. 2085–94.
147. Francis L, et al., Simultaneous electrospin–electrosprayed biocomposite nanofibrous scaffolds for bone tissue regeneration. Acta Biomaterialia, 2010. **6**: p. 4100–9.
148. Li W, et al., Nanofibrous mats layer-by-layer assembled via electrospun cellulose acetate and electrosprayed chitosan for cell culture. Europ Poly J 2012. **48**: p. 1846–53.
149. Zhu, W., et al., Highly aligned nanocomposite scaffolds by electrospinning and electrospraying for neural tissue regeneration. Nanomedicine: Nanotechnology, Biology, and Medicine, 2015. **11**(2015): p. 693-704.
150. Sokolsky-Papkov M, et al., Polymer carriers for drug delivery in tissue engineering. Adv Drug Deliv Rev 2007. **59**: p. 187-206.
151. Freiberg S and Z. X, Polymer microspheres for controlled drug release. Int J Pharm, 2004. **282**: p. 1-18.
152. Kim SJ, et al., Fabrication and characterization of 3-dimensional PLGA nanofiber/microfiber composite scaffolds. Polym, 2010. **51**: p. 1320–7.
153. Park SH, et al., Development of dual scale scaffolds via direct polymer melt deposition and electrospinning for applications in tissue regeneration. Acta Biomat, 2008. **4**: p. 1198-207.
154. Larrondo L and M. JRS, Electrostatic fiber spinning from polymer melts: Experimental observations on fiber formation and properties. J Poly Sci Part B 1981a. **19**: p. 909–20.
155. Larrondo L and M. JRS, Electrostatic fiber spinning from polymer melts: examination of the flow field in an electrically driven jet. J Poly Sci Part B 1981b. **19**: p. 921–32.

156. Larrondo L and M. JRS, Electrostatic fiber spinning from polymer melts; electro static deformation of pendent drop of polymer melt. J Poly Sci Part B 1981c. **19**: p. 933–40.
157. Dalton PD, Klee D, and M. M, Electrospinning with dual collection rings. Polymer, 2005. **46**: p. 611–14.
158. Ekaputra AK, et al., The three-dimensional vascularization of growth factor-releasing hybrid scaffolds of poly(e-caprolactone)/collagen fibers and hyaluronic acid hydrogel. Biomat 2011. **32**: p. 8108–17.
159. Bártolo PJ, et al., Advanced Processes to Fabricate Scaffolds for Tissue Engineering, in Virtual Prototyping & Bio Manufacturing in Medical Applications, B.P. Bidanda B, Editor. 2008, Springer: , New York. p. 149-70.
160. Mota C, et al., Dual-Scale Polymeric Constructs as Scaffolds for Tissue Engineering. Materials 2011. **4**: p. 527-42.
161. Mota C, et al., Additive manufacturing techniques for the production of tissue engineering constructs. J Tissue Eng Regen Med 2012.
162. Mitchell GR, Ahn K-h, and D. FJ, The potential of electrospinning in rapid manufacturing processes. Virt and Phy Prot, 2011. **6**: p. 63-77.
163. Wang X, Ding B, and L. B, Biomimetic electrospun nanofibrous structures for tissue engineering. Materials Today, 2013. **16**: p. 229-41.
164. Kim GH, et al., Hybrid process for fabricating 3D hierarchical scaffolds scaffolds combining rapid prototyping and electrospinning. Macrom. Rapid Commun, 2008. **29**: p. 1577-81.
165. Giannitelli SM, et al., Combined additive manufacturing approaches in tissue engineering. Acta Biomaterialia 2015. **24**(2015): p. 1-11.
166. Ahn SH, Koh YH, and K. GH, A three-dimensional hierarchical collagen scaffold fabricated by combined solid freeform fabrication (SFF) and electrospinning process to enhance mesenchymal stem cell (MSC) proliferation. J. Micromech. Microeng, 2010. **20**: p. 1-7.
167. Centola M, et al., Combining electrospinning and fused deposition modeling for the fabrication of hybrid vascular graft. Biofabricat, 2010. **2**: p. 1-11.
168. Martins A, et al., Hierarchical starch-based fibrous scaffold for boné tissue engineering applications. J. Tissue Eng. Regen. Med., 2009. **3**: p. 37-42.
169. Vaquette C, et al., A biphasic scaffold design combined with cell sheet technology for simultaneous regeneration of alveolar bone/periodontal ligament complex. Biomat., 2012. **33**: p. 5560-73.

170. Yan F, et al., A multi-scale controlled tissue engineering scaffold prepared by 3D printing and NFES technology. AIP Adv, 2014. **4**: p. 031321-1.
171. Yu YZ, et al., Fabrication of hierarchical polycaprolactone/gel scaffolds via combined 3D bioprinting and electrospinning for tissue engineering. Adv. Manuf., 2014.
172. Canha-Gouveia A, et al., Hierarchical scaffolds enhance osteogenic differentiation of human Wharton's jelly derived stem cells. Biofabrication 2015. **7**(2015): p. 1-13.
173. Rogers, C., et al., A novel technique for the production of electrospun scaffolds with tailored three-dimensional micro-patterns employing additive manufacturing. Biofabrication, 2014. **6**(3): p. 035003.
174. Sahoo, N., et al., Nanocomposites for Bone Tissue Regeneration. Nanomedicine, 2013. **8**(4): p. 639-53.
175. Pon-On, W., et al., Mechanical properties, biological activity and protein controlled release by poly(vinyl alcohol)–bioglass/chitosan–collagen composite scaffolds: A bone tissue engineering applications. Materials Science and Engineering C, 2014. **38**(2014): p. 63-72.
176. Pfister A, et al., Biofunctional Rapid Prototyping for Tissue-Engineering Applications: 3D Bioplotting versus 3D Printing. Journal of Polymer Science: Part A: Polymer Chemistry, 2004. **42**: p. 624-38.
177. Khadka, D. and D. Haynie, Protein- and peptide-based electrospun nanofibers in medical biomaterials. Nanomedicine, 2012. **8**(8): p. 1242-62.
178. Cipitria, A., et al., Design, fabrication and characterization of PCL electrospun scaffolds—a review. J. Mater. Chem., 2011, 21, 9419, 2011. **21**: p. 9419.
179. Bártolo, P., et al., Biomanufacturing for tissue engineering: Present and future trends. Virtual and Physical Prototyping, 2009. **4**(4): p. 203-16.
180. Ji, W., et al., Bioactive Electrospun Scaffolds Delivering Growth Factors and Genes for Tissue Engineering Applications. Pharm Res 2011. **28**: p. 1259-72.
181. Leong, M., et al., Fabrication and in vitro and in vivo cell infiltration study of a bilayered cryogenic electrospun poly(D,L-lactide) scaffold. JOURNAL OF BIOMEDICAL MATERIALS RESEARCH A 2010. **94A**(4): p. 1141-49.
182. Goh, K., A. Listrat, and D. and Béchet, Hierarchical Mechanics of Connective Tissues: Integrating Insights from Nano to Macroscopic Studies. Journal of Biomedical Nanotechnology, 2014. **10**(10): p. 2264-507.
183. Pateman, C., et al., 3D Micro-Printing of Nerve Guides for Peripheral Nerve Repair. European Cells and Materials 2013. **26**(Suppl.7): p. 78.

184. Stephens-Altus JS, et al., Development of bioactive photocrosslinkable fibrous hydrogels. Journal of Biomedical Materials Research A 2011. **A**: p. 1-10.
185. Melchels FPW, et al., Effects of the architecture of tissue engineering scaffolds on cell seeding and culturing. Acta Biomat, 2010. **6**: p. 4208–17.
186. Melchels FPW, et al., Additive manufacturing of tissues and organs. Progress in Polymer Science 2012. **37**: p. 1079– 104.
187. Villalona GA, et al., Cell-Seeding Techniques in Vascular Tissue Engineering. Tissue Engineering: Part B, 2010. **16**(3): p. 341-50.
188. Tasoglu S and D. U, Bioprinting for stem cell research. Trends in Biotechnology 2013. **31**(1): p. 10-9.
189. Ferris CJ, et al., Biofabrication: an overview of the approaches used for printing of living cells. Appl Microbiol Biotechnol 2013. **97**: p. 4243–58.
190. Boland T, et al., Application of inkjet printing to tissue engineering. Biotechnol, 2006. **1**: p. 910–17.
191. Nakamura M, et al., Biocompatible Inkjet Printing Technique for Designed Seeding of Individual Living Cells. Tissue Eng, 2005. **11**(11-12): p. 1658-66.
192. Smith CM, et al., Three dimensional bioassembly tool for generating viable tissue engineered constructs. Tissue Eng A 2004. **10**: p. 1566–76.
193. Chung JHY, et al., Bio-ink properties and printability for extrusion printing living cells. Biomater. Sci, 2013. **1**: p. 763–773.
194. Wang X, et al., Generation of three-dimensional hepatocyte/gelatin structures with rapid prototyping system. Tissue Eng A 2006. **12**(83–90).
195. Odde DJ and R. MJ, Laser-guided direct writing for applications in biotechnology. Biotechnol, 1999. **17**: p. 385–89.
196. Ma Z, et al., Laser-guidance-based cell deposition microscope for heterotypic single-cell micropatterning. Biofab, 2011. **3**: p. 034107.
197. Gaebel R, et al., Patterning human stem cells and endothelial cells with laser printing for cardiac regeneration. Biomaterials, 2011. **32**: p. 9218–30.
198. Moon SJ, et al., Layer by layer three-dimensional tissue epitaxy by cell-laden hydrogel droplets. Tissue Eng. Part C, 2010. **16**(1): p. 157-66.
199. Demirci U and M. G, Cell encapsulating droplet vitrification. Lab Chip 2007. **7**: p. 1428–33.
200. Fang Y, et al., Rapid generation of multiplexed cell cocultures using acoustic droplet ejection followed by aqueous two-phase exclusion patterning. Tissue Eng. Part C 2012. **18**(9): p. 647–57.

201. Beachleya V and W. X, Polymer nanofibrous structures: Fabrication, biofunctionalization, and cell interactions. Progress in Polymer Science 2010. **35**: p. 868–92.
202. Vunjak-Novakovic G, et al., Dynamic cell seeding of polymer scaffolds for cartilage tissue engineering. Biotechnology Progr 1998. **14**: p. 193-202.
203. Carrier RL, et al., Cardiac tissue engineering: Cell seeding, cultivation parameters, and tissue construct characterization. Biotechnol Bioeng, 1999. **64**: p. 580-589.
204. Jayasinghe SN, Cell electrospinning: a novel tool for functionalising fibres, scaffolds and membranes with living cells and other advanced materials for regenerative biology and medicine. Analyst, 2013. **138**: p. 2215–23.
205. Townsend-Nicholson A and J. SN, Cell Electrospinning: a Unique Biotechnique for Encapsulating Living Organisms for Generating Active Biological Microthreads/Scaffolds. Biomacromolecules, 2006. **7**: p. 3364-9.
206. Jayasinghe SN, Irvine S, and M. JR, Cell electrospinning highly concentrated cellular suspensions containing primary living organisms into cell-bearing threads and scaffolds. Nanomedicine, 2007. **2**(4): p. 555-67.
207. Sampson SL, S.L., Gustafsson K, Jayasinghe SN,. Robertson BD, Cell Electrospinning: An In Vitro and In Vivo Study. Small, 2014. **10**(1): p. 78–82.
208. Xu, S.-C., et al., A battery-operated portable handheld electrospinning apparatus. Nanoscale, 2015. **7**: p. 12351–55.
209. Dong, R.-H., et al., In-situ deposition of personalized nanofibrous dressing via a handy electrospinning device for skin wound care. Nanoscale, 2016: p. 1-6.
210. Xu, S.-C., et al., A battery-operated portable handheld e-spinning apparatus (BOEA) 2012: China.

Chapter II

Aims

To develop a tissue-engineered structure is important to keep in mind that 3D microenvironments guide cellular behavior. Based on this, it is a key challenge to develop biocomplex scaffolds to better mimic the native ECM. Structurally, electrospun meshes mimic the skin ECM perfectly, for that reason to explore different materials and processing strategies to achieve the better microenvironment is needed.

The main aim of this thesis is to investigate the electrospinning technique to develop a hybrid structure that has the capability to promote skin regeneration. For this purpose Polycaprolactone and Gelatin were explored to produce hybrid electrospun meshes evaluating three distinct methodologies (Multilayer, Coated and Blend). Both polymers are widely used in TE field and its properties well known. PCL is an aliphatic polyester that presents good mechanical properties is biocompatible and biodegradable. On the other hand, gelatin, a protein derived from collagen, displays many integrin-binding sites for cells and is biocompatible, biodegradable and presents excellent non-antigenicity.

To reach an optimal wound dressing it is necessary to obtain a structure that mimics the mechanical and biological properties of native skin tissue and comprise several key features of wound dressings (adequate water vapour permeability, easy conformability to the wound, promote haemostasis and capability to absorb wound exudate). To achieve it several tasks were performed, briefly, the electrospinning process was optimized exploring different solvent systems and processing parameters. After selection of optimized parameters the PCL structures were evaluated in terms of degradation and in a parallel work the crosslinking of gelatin was also studied. The next step was the development of hybrid structures and characterized them to choose the structure that better mimic the properties of native skin ECM.

The project highlights how it is possible to combine the same materials in different ways and to tailor the properties based on the final application. Therefore, useful knowledge for future adaptation is provided for tissue engineering field. The development of this project provided a further insight on wound dressings offering a new point of view of hybrid structures development using the same technique. By combining different processing strategies, it was possible to obtain structures with different characteristics that can be tailored based on the final application.

Part 2

Chapter III

Development of a new assembled electrospinning system and electrospun meshes production optimization

Development of a new assembled electrospinning system and electrospun meshes production optimization|Chapter III

Contents

1. Introduction

Electrospinning is an electrostatic fibre fabrication technique that has been attracting increasing interest due to its versatility and potential for applications in different fields [1]. In the biomedical field, electrospinning has been used to produce biosensors, filtration devices, scaffolds for tissue engineering, including wound dressing, drug delivery and enzyme immobilization systems [2, 3]. In tissue engineering, electrospun meshes have a great potential due to their high surface area and interconnectivity, beneficial for tissue ingrowth and cell migration, coupled with controlled delivery of incorporated biomolecules [4-6].

The conventional setup of a solution electrospinning system consists of three major components: a high voltage power supply, a spinneret and a collector that can be used in a horizontal or vertical arrangement [5, 7, 8]. The syringe contains a polymeric solution, pumped at a constant and controlled rate. The polymer jet is initiated when the voltage

is turned on and the opposing electrostatic forces overcome the surface tension of the polymer. Just before the jet formation, the polymer droplet under the influence of the electric field assumes a cone shape with convex sides and a rounded tip, known as the Taylor cone [2, 9, 10]. During the jet's travel, the solvent gradually evaporates, and charged polymer fibers are deposited in the collector [10].

Several laboratory-type and industrial scale electrospinning systems are commercially available [11-13]. However, laboratory-type systems are still relatively expensive, and, due to its low complexity, most research laboratories assembled their own systems [14-16].

The solution electrospinning process is influenced by several parameters, such as: solution parameters (e.g. viscosity, polymer concentration, solvent type), processing parameters (e.g. flow rate, distance between needle and collector, voltage, type of collector) and ambient conditions (e.g. temperature and humidity) [17]. For tissue engineering applications, where hydrogels are commonly used, it is fundamental to control the fabrication environment. However, this is not possible with most commercial available laboratory-type systems that present several limitations such as:

- metallic parts in contact with the electric field and thus affecting it, inducing the formation of secondary jets and, consequently, the deposition of fibers not only on the collector surface but also over all metallic components. Moreover, non-stable jets can induce solvent drop deposition over the electrospun meshes making them toxic;
- flow rate control exerted by a step motor that limits the accurate control of flow rate compared to the use of a syringe pump;
- fiber production mostly limited to horizontal mode strategies.

These drawbacks limit the versatility and reproducibility of this technique by compromising the stability of the electric field. To solve some of these limitations a new design of an electrospinning system is presented and evaluated.

2. Materials and Methods

2.1. New design of an electrospinning system

The digital representation of the new design of a solution electrospinning system is presented in Fig. III.1. In this new system a significant number of nonconductive components were introduced. The box of the equipment (1) is made in acrylic, with a main hole to allow solvent evaporation. This structure incorporates a door to access to the equipment inner part and some additional entry spot to allow the entrance of the infusion tubes supplying the polymeric solution. The base of the equipment (3) is made in cork (Corecork TB40, Amorim, Portugal) due to its adequate mechanical resistance

and machinability properties, insulate characteristics and eco-friendly nature. An acrylic part (2) is used to support the rod (4) made of teflon. The collector (5) is a grounded copper plate. The needle support (6) is made of acrylonitrile butadiene styrene (ABS) and slides on to adjust the distance between the needle (single or core/shell) and the collector. The collector (5), is static but its fixation system allows its easy replacement by other type of collectors. Items (1), (2), (4) and (5) were purchased and items (3) and (6) produced using a computer numeric control machine (CNC, from INAUTOM, Portugal) and an additive manufacturing system (Dimension machine from Stratasys). Additionally, the new system includes a syringe pump (model Pump 11Elite, Harvard apparatus) to supply the polymeric solution, a polymeric tube connecting the syringe and the needle, a Liquid Crystal Display (LCD) to control the voltage, an emergency button and a high voltage source (model PS/MJ30P0400-11, Glassman High Voltage, Inc).

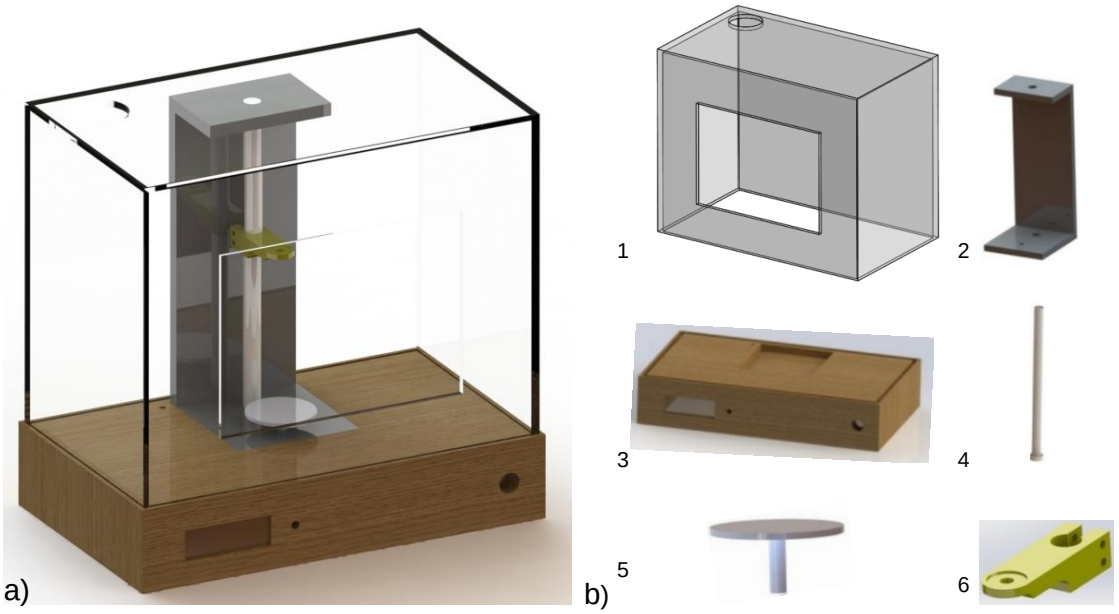

Figure III.1. New design of electrospinning system. a) Computer aided design (CAD) model of electrospinning system proposed; b) Main components:1 - acrylic box, 2 - acrylic support, 3 - cork base, 4 - teflon rod, 5 - collector, 6 - needle support. Technical draws are available in appendix A, section 1.

The assembled electrospinning, which corresponds to a more versatile, flexible and user friendly system, is shown in Fig. III.2. Key features of this system are:

- Allows the preparation of samples using vertical or horizontal configurations;
- Due to the selection of non-conductive materials the jet is kept stable, not presenting secondary jets;
- Provides accurate regulation of voltage due to the addition of a controller to the high voltage source.

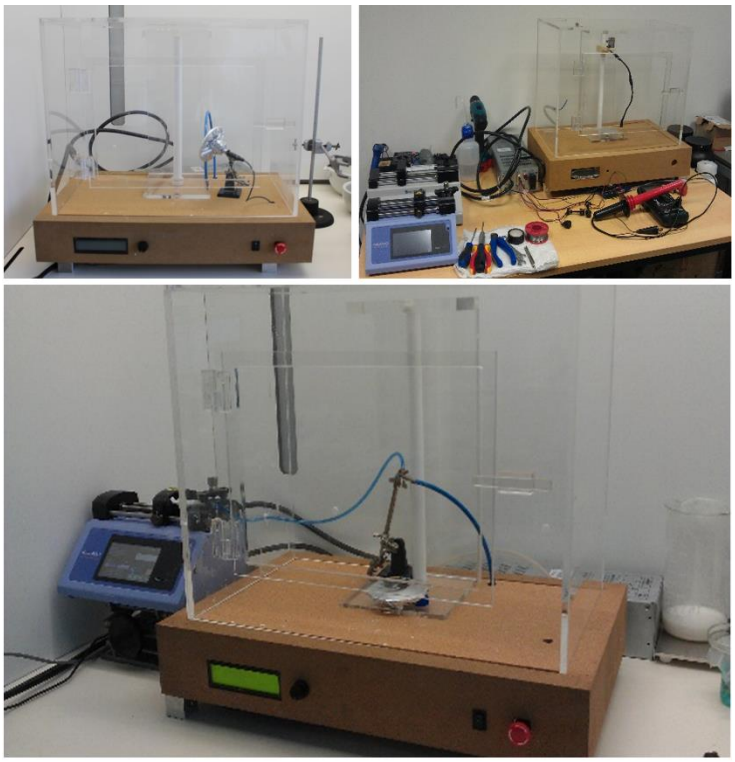

Figure III.2. Assembled electrospinning apparatus.

2.2. Materials

Poly (ε-caprolactone) (PCL) (Mw 50000 (g/mol), bulk density: 1.1g.cm-3) was kindly supplied by Perstorp (UK) and dissolved in dimethyl Ketone (DMK) (Sigma-Aldrich), and acetic acid (AA) (PanReac AppliChem). Gelatin powder from pig skin (type A, 300 bloom, 60 mesh) were kindly supplied by Italgelatine (Italy). For polymers dissolution, different solvents were explored as indicated in Table 1. In order to increase the conductivity of the solutions prepared with acetic acid, 2% v/v of triethylamine (TEA, Sigma Aldrich) was added. After optimization, 1,4-butanediol diglycidyl ether (BDDGE, Alpha Aesar, Germany) was used as the gelatin crosslinker.

2.3. Electrospinning of nanofiber meshes

Polymeric meshes were processed using a single jet approach. Table III.1 presents the processing parameters used to produce the meshes. Non-woven electrospun meshes were obtained at room temperature and relative humidity of 40-50 %. Crosslinking of electrospun gelatin fibers were produced through the incorporation of BDDGE on the gelatin solution immediately before fiber electrospinning to avoid the loss of configuration that is induced through a crosslinking bath after fiber production.

Table III.1. Parameters tested to optimize the electrospun mesh production.

Polymer	Solution parameters		Processing parameters		
	Solvent system	Polymer concentration (wt%)	Distance between collector and needle (cm)	Voltage (kV)	Flow rate (mL/h)
PCL	AA/TEA (2% v/v)	6, 11, 17	7, 10, 12	7, 10, 12	0.72, 3.17
	DMK				
Gelatin	AA/TEA (2% v/v)	5, 10, 15			0.4, 0.72

2.4. Physico-chemical characterization

2.4.1. Morphology and fiber diameter

The morphology of the produced meshes was examined by scanning electron microscopy (SEM) using a Quanta 400 FEG ESEM/EDAX Genesis X4M (FEI Company, USA). Prior to examination samples were coated with a gold/palladium (Au/Pd) thin film, by sputtering, using the SPI module sputter coater equipment. SEM images were also used to measure the fiber diameter using Image J software. For each condition, three individual samples were analyzed and fifty measurements per image were carried out.

2.4.2. Structure

Fourier transform infrared (FTIR) spectroscopy with attenuated total reflectance (ATR) was used to evaluate the chemical composition of the materials and to detect possible structural changes. FTIR analyses were carried out using an Alpha-P Brucker FTIR-ATR spectrometer, in the range of 4000–500 cm^{-1}, at a 4 cm^{-1} resolution with 64 scans.

2.5. *In vitro* studies

Human dermal neonatal fibroblasts (hDNF) isolated from the foreskin of healthy male newborns (ZenBio, US) were cultured, expanded, and maintained in Dulbecco's modified eagle medium (DMEM) (Gibco, US), at 37ºC in a humidified atmosphere of 5% CO_2. The culture medium was changed twice a week and cells were trypsinized (0.25% trypsin/0.05% ethylenediamine tetraacetic acid (EDTA)/0.1% glucose in PBS (pH 7.5)) when they reached 70-80% of confluence. Cells from passages between 8 and 11 were used in this study. To assess cytotoxicity, electrospun meshes were tested in direct (samples) and indirect (leachables) contact with different pre-conditions (washed and non-washed in ultrapure water). Samples were sterilized with UV light followed by washing during 24 hours. hDNF cells were seeded in culture wells for 24 hours at a density of $2x10^4$ cells/well. 24 hours later, samples (direct contact) and culture medium in contact with samples (indirect contact) were incubated with cells for another 24 hours.

The culture medium was then removed from the wells and fresh basal medium with 20% v/v resazurin (Sigma) was added. Cells were incubated (37ºC, 5% v/v CO_2) for an additional period of 2 hours, after which 300 µL per well were transferred to a black 96-well plate and measured (Ex at 530 nm, Em at 590 nm) using a micro-plate reader (Synergy MX, BioTek, US). The control consisted in cells alone. For the quantification of the total double-stranded DNA (dsDNA) content, the cell pellets were recovered from the wells and washed with phosphate buffered saline (PBS). The suspension was then centrifuged (10 000 rpm, 5 min) and then stored at -20ºC until further analysis. The dsDNA quantification was performed using the Quant-iT PicoGreen dsDNA kit (Molecular Probes, Invitrogen, US), according to the manufacturer's protocol. Briefly, the samples were thawed and lysed in 1% v/v Triton X-100 (in PBS) for 1 hour at 250 rpm at 4ºC. Then, they were transferred to a black 96-well plate with clear bottom (Greiner) and diluted in Tris-EDTA (TE) buffer (200 mM Tris–HCl, 20 mM EDTA, pH 7.5). Finaly, samples were incubated for 5 min at room temperature in the dark, and fluorescence was measured using a microplate reader (Ex at 480, Em at 520 nm).

2.6. Statistical analyses

All data points were expressed as mean ± standard deviation (SD). Statistical analysis (Levene's and T test) was carried out using IBM SPSS Statistics 20.0 with 99% confidence level for cytotoxicity assays. The results were considered statistically significant when $p \leq 0.05$ (*).

3. Results and discussion

3.1. Microscopic and macroscopic characterization of electrospun meshes

SEM images of the different produced meshes are presented in Figs. III.3 and III.4. For simplicity, only the tested conditions that resulted in fibers without beads or drops are presented in these figures. The SEM microscopies related to the other conditions are available at appendix A, section 2. Results show that a stronger electric field increased the amount of produced fibers per time, which is correlated to the higher amount of charges into the solution, thereby increasing the jet velocity and, consequently, supplying more solution to the collector. The distance between the needle tip and the collector also determines the fiber diameter. By Increasing this distance, the flight time is longer, allowing the solvent to evaporate, resulting in higher polymer chain stretching, which leads to a decrease in fiber diameter. These results show that the designed electrospinning is able to process proper meshes, being particularly relevant the production of gelatin meshes, which is strongly affected by ambient parameters, namely

the relative humidity. Concerning the PCL and gelatin meshes, according to the parameters tested significant differences were observed in terms of fiber diameter or morphology. Thus, for further analyses, the following requirements were selected, providing (i) longer distance to promote solvent evaporation and high chain stretching, (ii) high density of fibers per area requiring less production time and (iii) continuous and uniform fiber production enhancing mechanical performance. Therefore, the following fiber production parameters were selected: 17 wt% of PCL dissolved in DMK, produced with a flow rate of 3.17 mL/h, 12 cm distance between needle and collector and 10 kV of voltage; 15 wt% of Gelatin dissolved in AA and 2% v/v of TEA, produced with a flow rate of 0.4 mL/h, a 12 cm distance between needle and collector and 12 kV of voltage. Moreover as gelatin is a water-soluble protein, a crosslinking is needed to improve its mechanical properties and to increase its stability in aqueous medium [19]. Gelatin fibers were *in situ* crosslinked with BDDGE, according a protocol previously established [20]. The morphology of selected meshes is shown in Fig. III.5a-c. The fiber diameter measurements, the reduced standard deviation observed and the homogeneity of the obtained fibers demonstrates the stability of samples produced with the developed apparatus. From Fig. III:5 e) it is also possible to observe that the developed system improves fiber deposition in the collector.

FTIR-ATR spectra, used to evaluate possible structural changes in the electrospun meshes, are shown in Fig. III.5d. The spectrum of PCL meshes presents a 1720.7 cm^{-1} peak, corresponding to the C=O bond, characteristic to esters, and additional peaks between 750 and 1500 cm^{-1}, corresponding to the CH_2 groups of PCL chain. Two other peaks at 2863.69 cm^{-1} and 2941.57 cm^{-1} can also be observed, corresponding to the CH bonds. The FTIR spectrum of gelatin shows prominent peaks in four different amide regions, namely at 1600-1700 cm^{-1}, corresponding to amide I, 1520-1565 cm^{-1}, corresponding to amide II, 670-1240 cm^{-1}, corresponding to amide III, and 3000–3500 cm^{-1}, corresponding to amide A. The absorption of amide I contains contributions from the C=O stretching vibration of amide group and a minor contribution from the C-N stretching vibration. Amide II absorption is related to N-H bending and C-N stretching vibrations. Amide III presents vibrations from C-N stretching attached to N-H in-bending with weak contributions from C-C stretching and C=O in-plane bending. At 2930 and 2890 cm^{-1}, it is possible to observe two peaks associated to the contribution of aliphatic moieties from BDDGE, confirming the incorporation of BDDGE into the gelatin matrix (Fig. III.5d)). For both samples, no solvent residues were detected and no structural changes were observed.

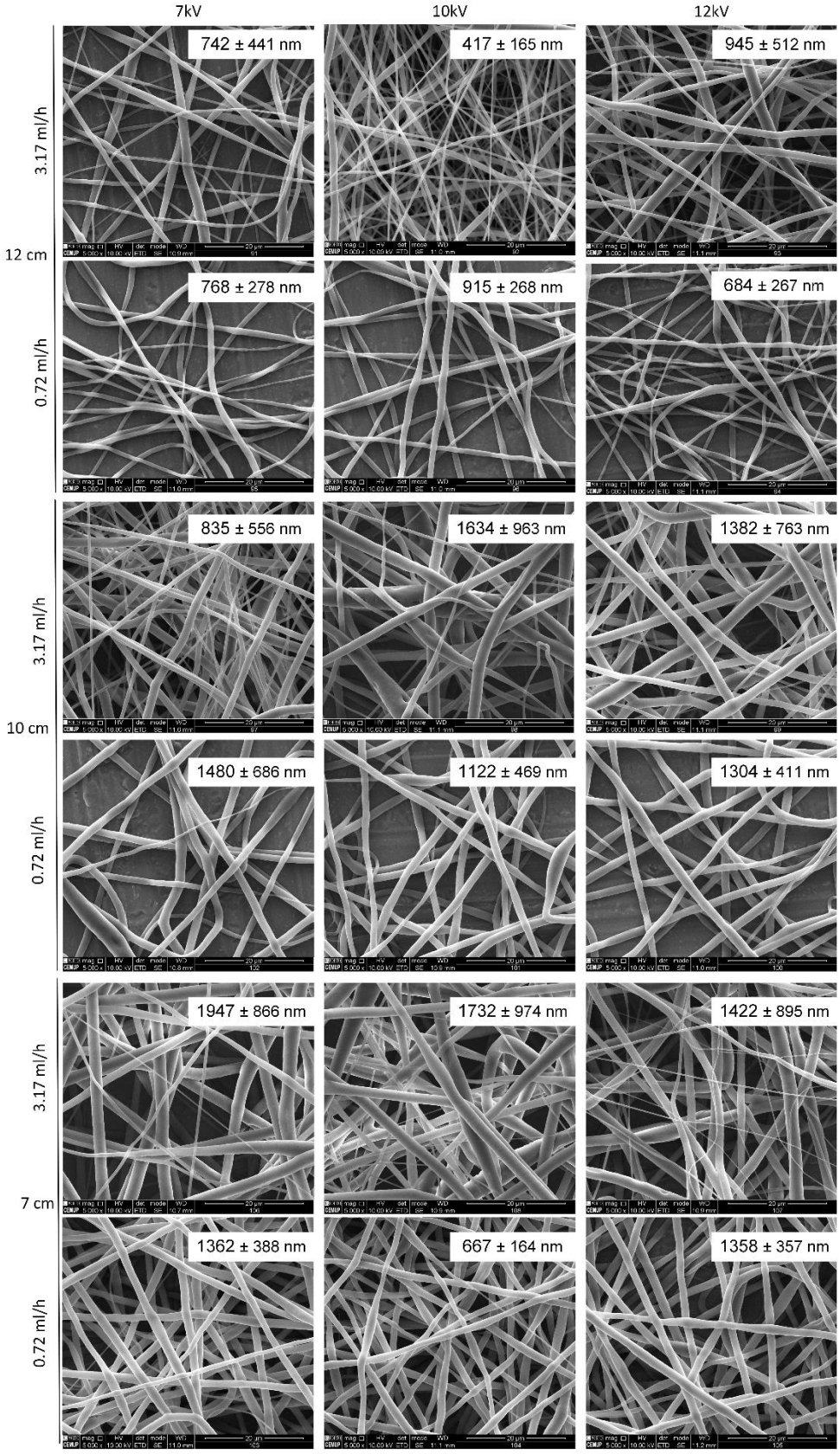

Figure. III.3. Electrospun PCL meshes (17 wt%, dissolved in DMK) obtained using different flow rates, distances between needle and collector and voltage. For each mesh it is presented the average fiber diameter. Scale bars: 20 μm.

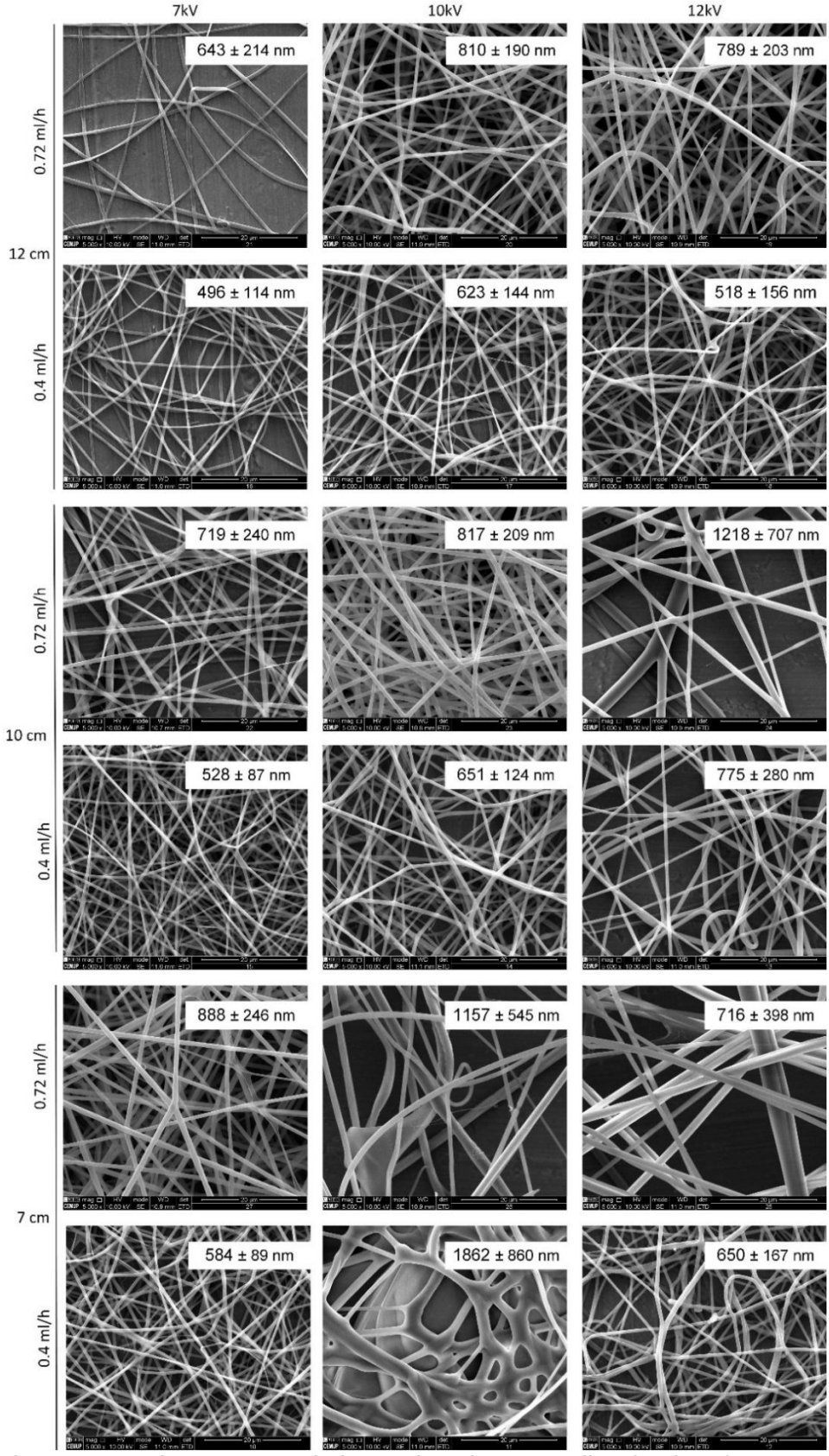

Figure. III.4. Electrospun gelatin meshes (15 wt%, dissolved AA/TEA 2% v/v) obtained using different flow rates, distances between needle and collector and voltage. For each mesh it is presented the average fiber diameter. Scale bars: 20 µm.

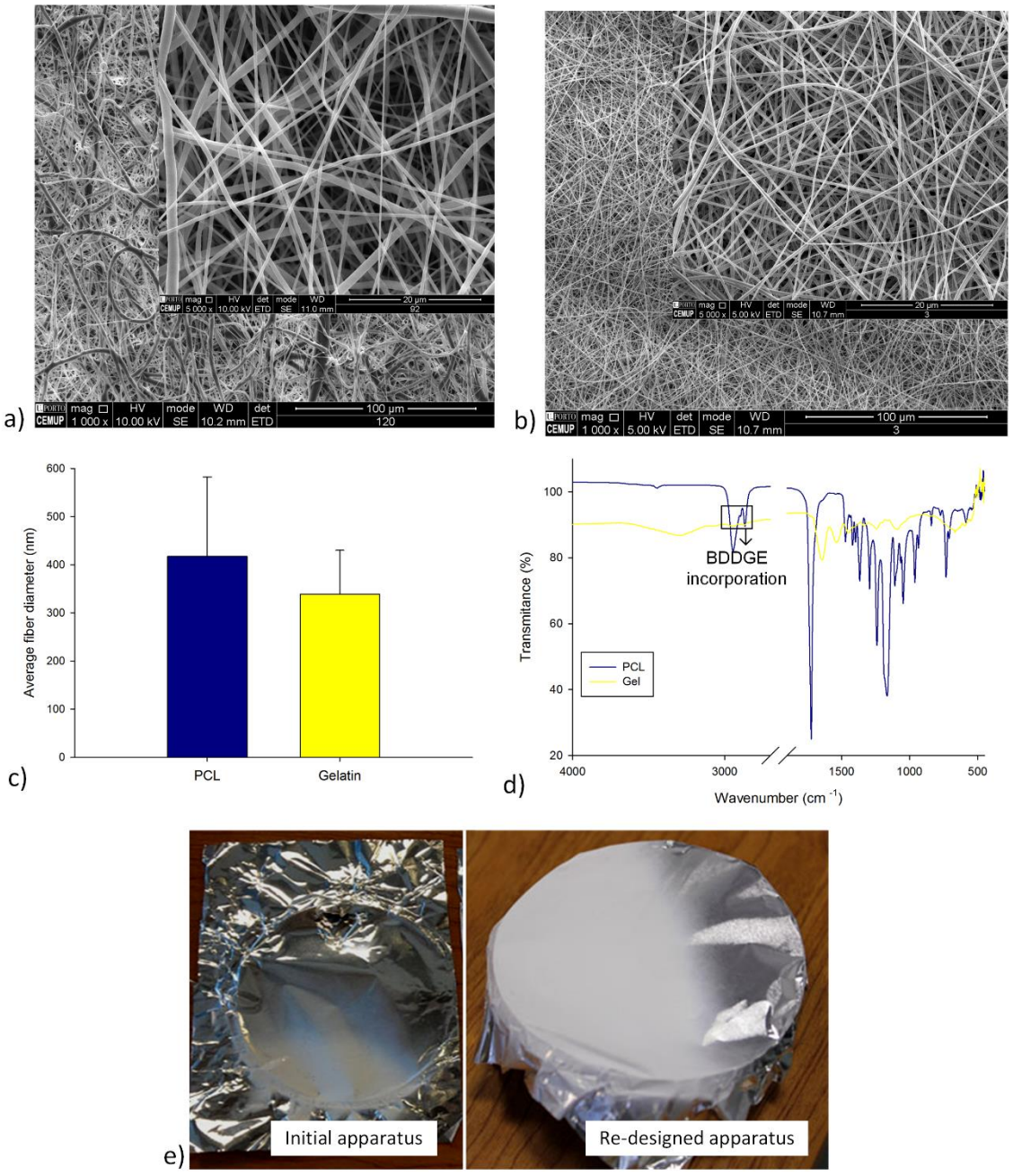

Figure III.5. Characterization of PCL and gelatin electrospun meshes selected for further analysis. a) Fiber morphology with 1000 and 5000 magnifications of PCL meshes; b) Fiber morphology with 1000 and 5000 magnifications of gelatin meshes crosslinked with BDDGE; c) Comparison between PCL and gelatin average fiber diameter; d) FTIR spectra of PCL and crosslinked gelatin and e) Influence of the purpose electrospinning system on fiber deposition over the collector in comparison with initial one comprising significant metallic components.

3.2. Cytotoxicity of nanofibers produced

Cytotoxicity of the produced electrospun meshes system was assessed to demonstrate the process stability, as a stable jet allows to produce electrospun meshes without solvent deposition. According to the obtained results (Fig. III.6), fibroblasts cultured in contact with electrospun meshes remained metabolically active for both PCL and gelatin meshes. After 24h no cytotoxicity was observed either in direct or indirect contact assays. In direct contact assays, no statistical significance was observed between control and samples, meaning that the structures, when in contact with cells, does not induce any toxicity. Regarding indirect contact assay, no leachables delivered from the samples to the medium presented toxicity.

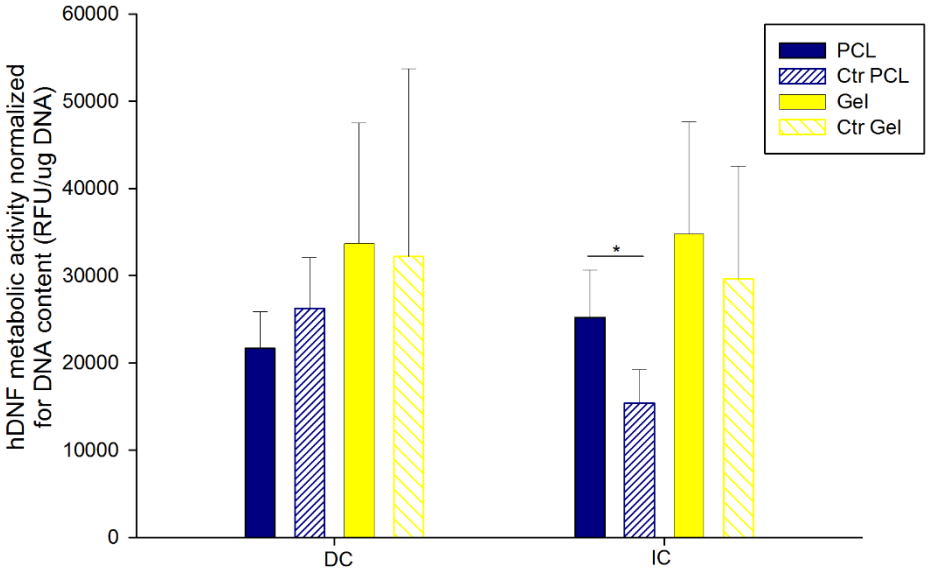

Figure III.6. Cytotoxicity assay of PCL and gelatin electrospun meshes in direct contact (DC) and indirect contact (IC) with fibroblasts (hDNF cells), using as control cells seeded on the well. Statistical significance for p≤0.05 (*).

4. Conclusions

This paper introduces a solution electrospinning system developed to produce electrospun meshes for applications in tissue engineering and more specifically for wound dressing applications. For the fabrication of the electrospinning system non-conductive materials (cork and polymers) were used to replace metallic ones, allowing to obtain a feasible and versatile laboratory-scale apparatus with ability to produce reproducible nanofiber meshes from materials with distinct characteristics. The system was used to produce nanofibers from two distinct polymers, using two different solvents, demonstrating its versatility of the new re-assembled apparatus. The fabrication of gelatin meshes is particularly relevant, as like other natural polymers, it is a material very

sensitive to the environmental conditions, in particular the relative humidity. Keeping the processing parameters stable is key to obtain high quality and reproducible meshes, i.e., with no beads, resulting in filaments with constant diameter and in meshes with high porosity between pores. Meshes did not show any presence of remaining solvents, which can be correlated to the lack of toxicity detected through the biological assays.

The two selected materials are particularly relevant for skin applications. PCL presents high mechanical properties but, due to its hydrophobic nature presents low interaction with cells. Contrary, gelatin displays many integrin-binding sites for cell adhesion, migration, proliferation, and differentiation due to the abundant Arg–Gly–Asp (RGD) amino acid sequences in its protein chain, which has been claimed to favor cell behavior. The combination of both materials may allow to produce meshes with improved properties.

References

1. Bártolo P, et al., Biomedical production of implants by additive electro-chemical and physical processes. CIRP Annals - Manufacturing Technology 2012. **61**(2): p. 635–655.
2. Teo WE and Ramakkrishna S, A review on electrospinning design and nanofibre assemblies. Nanotechnology, 2006. **17**: p. 89–106.
3. Ramakrishna S, et al., An Introduction to Electrospinning and Nanofibers. Singapore: World Scientific, 2005.
4. Rim NG, Shin CS, and Shin H, Current approaches to electrospun nanofibers for tissue engineering. Biomed. Mater, 2013. **8**: p. 1-14.
5. Bhardwaj N and Kundu SC, Electrospinning: a fascinating fiber fabrication technique. Biotechnology Advances, 2010. **28**: p. 325-47.
6. Niu H and Lin T, Fiber Generators in Needleless Electrospinning. Journal of Nanomaterials, 2012: p. 1-13.
7. Sill TJ and von Recum HA, Electrospinning: Applications in drug delivery and tissue engineering. Biomaterials 2008. **29**: p. 1989-2006.
8. Shin SH, et al., A short review: Recent advances in electrospinning for bone tissue regeneration. J. Tissue Eng. , 2012. **3**: p. 1-11.
9. Nukavarapu SP, et al., Electrospun polymeric nanofibre scaffolds for tissue regeneration, in Nanotechnology and Tissue Engineering: The scaffold, N.L. Laurencin CT., Editor. 2008, Taylor & Francis: London.
10. Li W J and Xia Y, Electrospinning of nanofibres: reivented the wheel? Advanced Materials 2004. **16**: p. 1151-70.

11. Innovative Mechanical Engineering Technologies B.V. IME Technologies. 2016; Available from: http://www.imetechnologies.nl/.
12. Co, I. Inovenso. 06/12/2016]; Available from: http://inovenso.com/about/.
13. ElMarco. NanoSpider. 06/12/2016]; Available from: http://www.elmarco.com/electrospinning/electrospinning-technology/.
14. Har-el Y-e, et al., Electrospun soy protein scaffolds as wound dressings: Enhanced reepithelialization in a porcine model of wound healing. Wound Medicine, 2014. **5**(2014): p. 9-15.
15. Liu S-J, et al., Electrospun PLGA/collagen nanofibrous membrane as early-stage wound dressing. Journal of Membrane Science, 2010. **355**: p. 53–59.
16. Gümüşderelioğlu M, et al., A novel dermal substitute based on biofunctionalized electrospun PCL nanofibrous matrix. J Biomed Mater Res Part A 2011. **98**(A): p. 461-472.
17. Dias, J.R., P.L. Granja, and P.J. Bártolo, Advances in electrospun skin substitutes. Progress in Materials Science, 2016. **84**: p. 314-334.
18. Ward, A.G. and A. Courts, The science and technology of gelatin. London:Academic Press, Inc.,, 1977.
19. Dias JR, Granja PL, and Bártolo PJS. Internal crosslinking evaluation of gelatin electrospinning fibers with 1,4 - butanediol Diglycidyl ether (Bddge) for skin regeneration in 10th World Biomaterials Congress. 2016. Montréal, Canada.

Part 3

Chapter IV

In vitro and in vivo PCL electrospun meshes degradation

In vitro and in vivo PCL electrospun meshes degradation|Chapter IV

Contents

1. Introduction

When skin damage occurs the standard proceeding is applying a wound dressing due to their efficiency, low cost and availability [1]. The dressing has as main functions to promote a moist environment in the wound, protect the wound against mechanical injury and microbial contamination especially during inflammatory stage [2]. Electrospun

wound dressing present exceptional properties compared to the conventional dressing such as promotion of haemostasis phase, wound exudates absorption, semi-permeability, easy conformability to the wound, functional ability and no scar induction [3]. Ideally, the dressing should be able to fit to the wound shape, absorb wound fluid without increasing bacterial proliferation or causing excessive dehydration, provide pressure for hemostasis, and prevent leakage from the bandage [4]. The dressing should also support the wound and surrounding tissues, eliminate pain, promote reepithelialisation during the reparative phase, and be easily applied and removed with minimal injury to the wound [5]. According to tissue engineering principles, a tissue-engineered device should be able to promote the tissue regeneration with a proportional rate to its degradation. [6]. Based on this the materials used and their degradation rates are a concerning topic. One of the most used synthetic polymer in tissue engineering field is the Polycaprolactone due its biodegradability, biocompatibility, structural stability and mechanical properties [7, 8]. However, as a result of semi-crystalline and hydrophobic nature of PCL, this shows a slow degradation rate (2-4 years) that limit its application as wound dressing for skin regeneration [6]. The degradation rates of PCL electrospun fibres show some changes compared to the bulk PCL as consequence of larger surface area-to-volume ratio and crystallinity changes induced by the electrospinning process [9]. In this work will be performed the evaluation of degradation kinetics of PCL electrospun meshes *in vitro* and *in vivo*. For the first time will be addressed the comparison of hydrolytic and enzymatic *in vitro* degradation with *in vivo* assays. PCL is a biodegradable aliphatic polyester and, for that reason, was selected as enzyme the lipase that hydrolyses the esters bonds [9, 10]. There are different source of lipase in the human body as leukocytes, presents on the wound healing process, being the lipase concentration on healthy adults in the range 30-190U/L [11, 12]. *In vitro* assay, were monitored PCL electrospun fibers degradation in PBS and PBS/lipase medium. The degradation kinetics were evaluated through the quantification of weight lost, swelling degree, thermal behavior, molecular weight changes and mechanical properties. According to *in vivo* assay, the degradation was assessed by histology and hematoxylin and eosin staining.

2. Material and Methods

2.1 Electrospun meshes preparation

Poly (ε-caprolactone) (PCL) (Mw 50000 (g/mol), bulk density: 1.1g.cm-3) was kindly supplied by Perstorp and dissolved in acetone that was purchased to Sigma-Aldrich. A PCL/DMK (17wt-%) solution was prepared by dissolving the polymer and stirred it at

37ºC overnight. The samples were produced by home-made electrospinning at room temperature with a constant flow rate of 3.17 mL/h (SP11Elite, Harvard Apparatus), 12 cm of distance between syringe and collector and 10kV of voltage.

2.2 Degradation Profile

2.2.1 In vitro

The samples were prepared with 10x40mm of dimensions with an average thickness of 166 ± 40µm and 10.164 ± 2.515µg of average weight. Two different sets were prepared, for the first set each specimen was immersed into a capped bottle containing 10 ml of phosphate buffer solution (PBS) (8 g NaCl, 0.2 g KCl, 1.44 g $Na_2HPO_4.12H_2O$, 0.2 g KH_2PO_4 in 1L ddH_2O, pH 7.4) and 0.02% (wt/v) of sodium azide, as the bacteriostatic agent. The second set each specimen was immersed into a capped bottle containing 10 ml of phosphate buffer solution (PBS) with 150U/L lipase concentration (amano lipase, from Burkholderia cepacia; Sigma Aldrich), and 0.02% (wt/v) of sodium azide. The bottles were incubated at 37 ºC with a constant shaking of 100 r.p.m during 91 days. For each condition (PBS and PBS/lipase) 15 samples were tested at each time-point. Except to the samples in PBS/Lipase medium that, after day 28, only 6 samples per each time-point were tested due to the total degradation of some samples. All solution in PBS were changed weekly and in PBS/Lipase was changed twice a week to guarantee the enzymatic activity.

2.2.1.1 Morphology, porosity and surface area

Electrospun meshes morphology were examined by scanning electron microscopy (SEM) using a Quanta 400 FEG ESEM/EDAX Genesis X4M (FEI Company, USA) in CEMUP, University of Porto. Prior to examination samples were coated with a gold/palladium (Au/Pd) thin film, by sputtering, using the SPI Module Sputter Coater equipment. SEM images were also used to evaluate the fiber diameter distribution using Image J software. To each condition three individual samples were analyzed and fifty measurements per image were carried out. The apparent density and porosity of electrospun meshes were calculated using the following equations (1)(2) [13], where the meshes thickness was measured by a micrometer.

$$\text{Apparent density}\ (\text{g.cm}^{-3}) = \frac{\text{mesh mass(g)}}{\text{mesh thickness (cm)} \times \text{mesh area (cm}^2\text{)}} \quad (1)$$

$$\text{Mesh porosity} = \left(1 - \frac{\text{Mesh apparent density}(\text{g.cm}^{-3})}{\text{Bulk density of PCL}(\text{g.cm}^{-3}}\right).100\% \quad (2)$$

The surface area to volume ratios (SA:Vol) for electrospun PCL meshes was, also, calculated.

2.2.1.2 Weight loss and water uptake

At each time-point (7, 14, 28, 42, 63, 77 and 91 days) the samples were removed from the buffer solution, washed with distilled water and weight to evaluate the swelling degree (3). After that, the samples were incubated during 24h at 37ºC and the dry weight was evaluated to quantify the weight loss (4).

$$\text{Degree of sweeling}\ (\%) = \frac{W_w - W_d}{W_d}.100 \quad (3)$$

Where W_w is the wet weight and W_d is the dry weight.

$$\text{Weight loss}\ (\%) = \frac{W_0 - W_d}{W_0}.100 \quad (4)$$

Where W_0 is the initial weight and W_d is the dry weight.

2.2.1.3 Simultaneous Thermal Analysis (STA)

Thermal properties and stability were determined using the Simultaneous Thermal Analyzer, STA 6000 system (PerkinElmer, USA). Samples with 1.5-2.5mg were placed into ceramic pans and the tests were performed under dry nitrogen purge (flow rate of 20mL min^{-1}). Samples were submitted to a heating from 30ºC to 450ºC at 10ºC/min. Melting temperatures (Tm) were obtained at the peak of the melting endotherms. The enthalpies of fusion (ΔH_m) were obtained from the areas under the peaks. Indium and silver samples were used as calibration standards. The crystallinity degree ($X_c(\%)$) was determined according to the following equation [14] :

$$X_c\ (\%) = \left(\frac{\Delta H_m}{w\Delta H_m^0}\right).100 \quad (5)$$

where, ΔH_m is the experimental melting enthalpy and w is the weight fraction of material. Additionally, it was assumed for ΔH_m^0 , the enthalpy of melting of 100% crystalline PCL the value of 139 J/g [15, 16].

2.2.1.4 Gel Permeation Chromatography (GPC)

The samples molecular weight distribution were determined using Gel Permeation/Size Exclusion Chromatographer system, with triple detection (GPC/SEC) (Malvern / Viscotek Instruments Ltd) composed of a Viscotek GPC Max pump and autosampler, with a viscotek T60A dual detector and a refractive index detector from Knauer, model K2301. Samples were individually dissolved in tetrahydrofuran (THF) (HiperSolv Chromanorm, VWR) (99.7% purity). After that 100 µL of solution was injected into the GPC, which had been previously calibrated with polymethlylmethacrylate (PMMA) standards (Polycal) in THF with known molecular weights of 64898 and 95081 Da. Distilled THF with flow rate 1ml.min^{-1} was used as the mobile phase. The PL gel 10 µm mixed-B columns were composed of polystyrene diniylbenzene copolymer 7.5 mm, with spherical sizes from 2-100 µm. For each scaffold type, three samples were collected, each of which was analysed in triplicate. The average molecular mass distributions were determined using Omnisec Viscotek software, version 4,6,2,359.

2.2.1.5 Contact angle (CA)

To perform the evaluation of hydrophilicity character was used a static contact angle through optic tensiometer of Paralab Company with model: Theta. The water contact angle is measured through the droplet spreads on the surface and recording its height and width.

2.2.1.6 Mechanical tests

The elongation at break and Young's modulus of PCL electrospun samples were determined using a texturometer (TA.XT Plus model, Stable Micro System SMD, England) with a 5N load cell. Testing was carried out in a controlled environment at RT and relative air humidity of 45%. The gauge length was 15 mm and the test speed was 1 mm.s^{-1}. At least five individual samples were tested from each group and measurements were reported as mean ± standard deviation.

2.2.2 *In vivo*

2.2.2.1 Subcutaneous implantation

The electrospun meshes were prepared in circular shape with 0.8 mm of diameter and sterilized with UV light prior to implantation. All animal experiments were conducted

following protocols approved by the Ethics Committee of the Portuguese Official Authority on Animal Welfare and Experimentation (DGAV) and were performed at FMUP-Faculdade de Medicina da Universidade do Porto. CD1 male mice were housed at 22 ºC with a 12 h light/dark cycle, and had ad libitum access to water and food. For each experimental group (7 days, 60 days and 90 days) 6 animals were used and 4 electrospun meshes were subcutaneously implanted in the back of the subcutaneous pockets created in each animal. The animals were anesthetized by Ketamine/xylazine (0.1mL/20g mouse at final dosage of 87.5 mg/kg Ketamine/12.5 mg/kg Xylazine) and anesthesia was maintained over the course of surgery by continuous isofluorane delivery. The dorsal surgical sites were shaved and sterilized. Four subcutaneous pockets were created per mouse for the insertion of the electrospun membranes. After implantation, incisions were closed with sutures and analgesics were administrated (Tramadol). The animals were routinely monitored for general appearance, activity, and healing of the implant sites, and were euthanized after 7, 60 and 90 days for retrieval of implants. No animals were lost during the study.

2.2.2.2 Histology and Hematoxylin and Eosin staining

For histological evaluation, implantation sites were harvested, which included the entire electrospun mesh and some surrounding tissue and fixed in 4% paraformaldehyde overnight. Samples were dried through a series of graded alcohol baths and in xylene, embedded in paraffin and sectioned in 5 mm thick slices. Sections were stained with Hematoxylin and Eosin (H&E) (Beyotime, China).

2.3. Statistical analyses

All data points were expressed as mean ± standard deviation (SD). Statistical analysis (Levene's and T test) was carried out using IBM SPSS Statistics 20.0 with 95% confidence level. The results were considered statistically significant when $p \leq 0.05$ (*).

3. Results and Discussion

3.1 In vitro

The electrospun PCL *in vitro* degradation rate was monitored in different mediums (PBS and PBS/lipase) and characterized with different techniques.

3.1.1 Morphology, porosity and Surface area

The microscopy images shows the morphology of non-degraded and degraded electrospun meshes according different periods of time for medium with or without

enzyme. As demonstrated in the Fig. IV.1a) the enzymatic degradation occurs at the material surface increasing the fibres surface roughness with time and, consequently, a massive decrease of fibres diameters. For tissue engineering applications is appropriate that the fibres suffer gradual degradation leaving enough space for new tissue ingrowth. Comparing the Fig. IV.1a) with the Fig. IV.2b) is notorious that the enzyme accelerates the degradation process as expected.

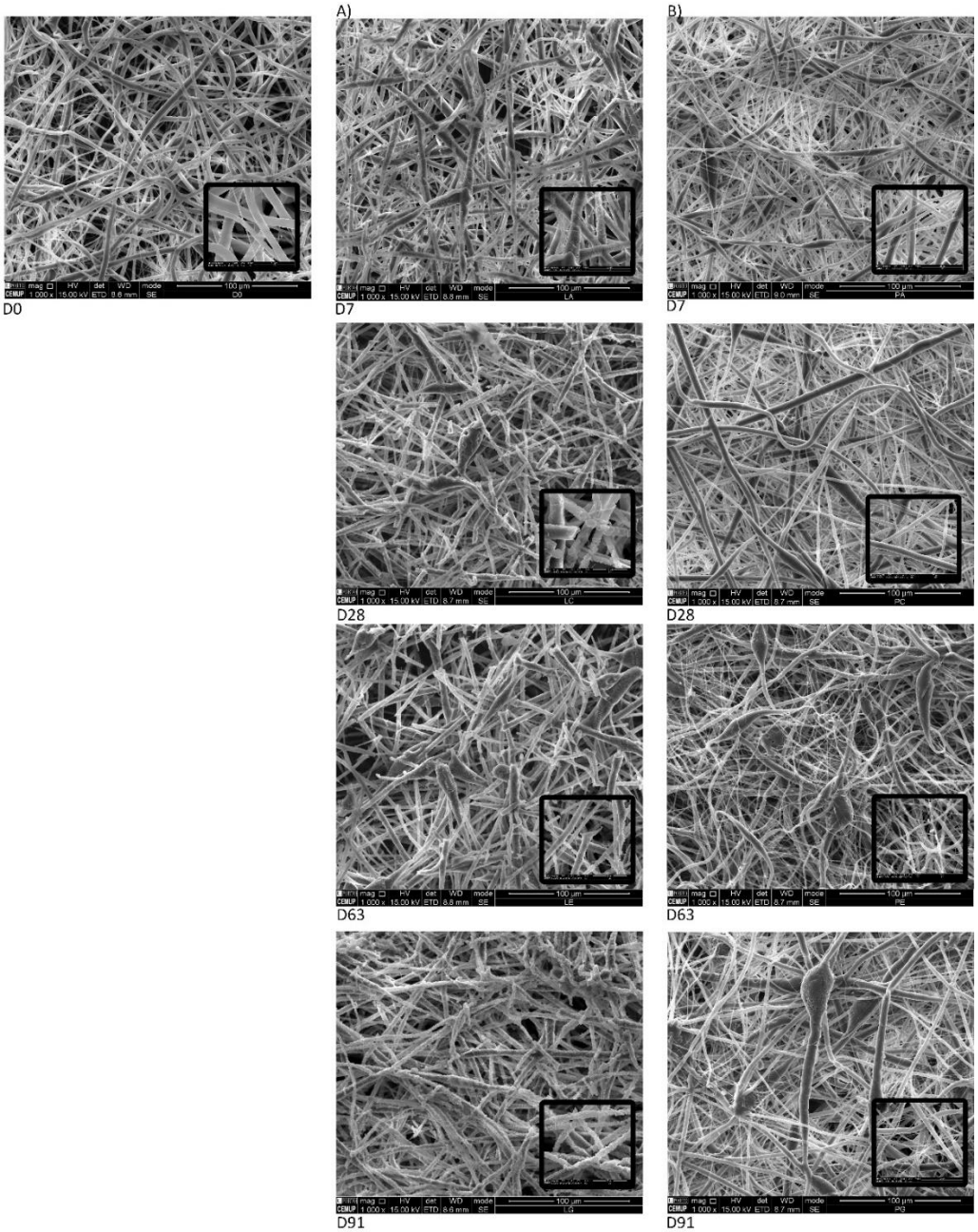

Figure IV.1. SEM images for different periods of time (Day 0, 7, 28, 63 and 91); a) enzymatic degradation, b) hydrolytic degradation. Scale bars corresponding to 100 µm.

Scaffolds must comprise a highly porous structure fully interconnected to provide large surface area to allow cell ingrowth, uniform cell distribution, and facilitate the neovascularization of the structure [17-19].

An ideal scaffold has to an open and interconnected pore network and a high degree of porosity (>60-90%) to interact and integrate with the host tissue [20]. According to the previous equations the theoretical values for the porosity of electrospun meshes produced is 98.11 ± 0.24 %.

Most part of cells used in tissue engineering are anchorages dependent therefore the scaffold should facilitate their attachment. Thus, scaffolds with a large and reachable surface area are favourable in order to hold the number of cells required to replace or restore tissue or organ functions [21]. Approximate ratio of the electrospun mesh were determined (Table IV.1) and results demonstrated that the electrospun mesh provide higher surface area-to-volume ratio (SA:Vol = 14.3 mm^{-1}) compared to other structures from the same material as a solvent cast film of PCL that show 10.26 mm^{-1} of SA:Vol [6].

Table IV.1. Meshes dimensions and approximated surface-area-to-volume ratio for electrospun PCL meshes. The shape of the scaffold was assumed as a rectangular prism.

Structure	Lenght (mm)	Width (mm)	Thickness (mm)	Surface area (mm^2)	Volume (mm^3)	SA:Vol (mm^{-1})
Electrospun mesh	40	10	0.17	97	6.8	14.3

3.1.2 Physico and thermal characterization

Weight loss is a direct measurement to quantify the polymer degradation. When the long polymer chains are cleaved to shorter ones the weight of the original fibre is reduced [22]. According to the weight lost results, the enzymatic degradation resulted in a massive samples degradation, as showed in Fig.IV.2. In PBS medium, the weight loss was slight, reaching only 1.44% after 91 days. On the other hand, the degradation on PBS/lipase medium showed a fast degradation until the 42 day reaching 84.42% of weight loss after that the degradation become slower but reached, at the end of the degradation time, 97.11% of weight loss.

Upon implantation, the biomaterials interact with the surrounding fluids, initially by uptaking them, which starts the degradation process [23]. The water uptake makes the materials more flexible and promotes changes in the dimensions of the implant material.

Simultaneously, a higher water uptake enhances the hydrolysis process [23]. In the Fig.IV.3 it is possible to observe the water uptake in both mediums, their profile is very unstable as result of the constant degradation of samples that does not allow the evaluation with constant weight. The meshes swelling degree profile showed that even though the PCL has a hydrophobic character the meshes with high porosity have a massive capability to retain water. The average values for both medium was above 200% of water uptake over all degradation period.

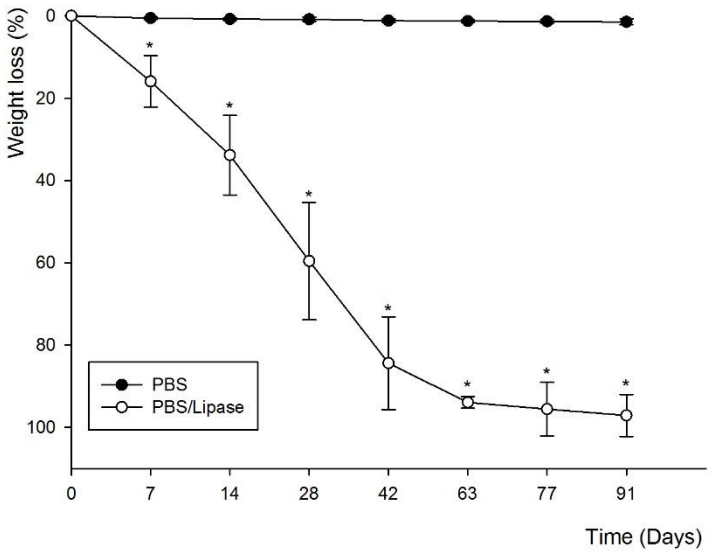

Figure IV.2. Weight loss profile of PBS and PBS/lipase medium. Statistical significance ($p \leq 0.05$).

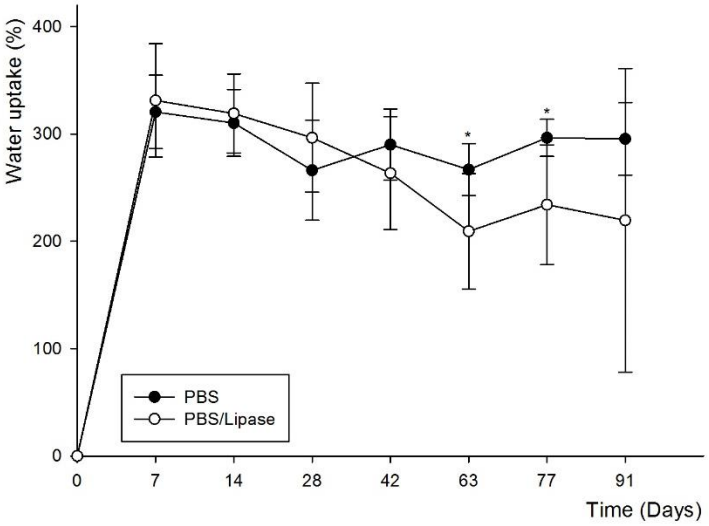

Figure IV.3. Water uptake profile of PBS and PBS/lipase medium. Statistical significance ($p \leq 0.05$).

Using STA equipment was possible obtain curves corresponding to TG and DTA/DSC measurements of non-processed and processed PCL and PCL meshes degraded in different mediums. The values of melting temperature (T_m), degradation temperature (T_{deg}), enthalpy and crystallinity level for all samples are presented in Table IV.2.

The PCL grain results showed a Tm of 63.21 ± 0.41 ºC and a crystallinity degree of 31.6 ± 2.29 %. On the other hand, the processed PCL by electrospinning presents lower values of Tm (62.74 ± 0.73 ºC) and crystallinity (26.49 ± 2.60 %) than the raw material. According to the literature, several authors correlate the fast solvent evaporation with the low molecular arrangement into the polymer leading to a crystallinity decrease of electrospun fibres [24, 25]. The Tm is determined by the energy state of the sample that is often affected by the processing. The reduction of Tm in electrospun sample compared to the raw material might be due to the polymer chain orientations that change during the electrospinning process [26].The meshes degraded on PBS/lipase presents a turning point at the day 42, up it the crystallinity and the melting temperature increased due to the degradation of the amorphous part that occurred rapidly as the weight loss demonstrated. After that the velocity of weight loss decrease as the crystallinity and melting temperature correlated to the degradation of the crystalline part of the polymer. The samples degraded in PBS medium showed a slightly weight loss that corresponding only to the degradation of amorphous part thus the crystallinity increase as Tm.

Table IV.2. Thermal properties of meshes during degradation period. Tm – Melting temperature; ΔH – Enthalpy; %Xc – Cristallinity degree; Tdeg. – Degradation temperature.

Sample Type	Degradation time (days)	Tm (ºC)	ΔH (J/g)	%Xc	Tdeg. (ºC)
PCL grain	-	63.21 ± 0.41	43.92 ± 3.18	31.6 ± 2.29	386.82 ± 0.75
PCL mesh	-	62.74 ± 0.73	35.16 ± 3.61	26.49 ± 2.6	376.86 ± 1.55
PBS	7	63.49 ± 0.95	37.99 ± 0.86	27.33 ± 0.62	379.13 ± 2.97
	14	64.27 ± 1.37	39.50 ± 0.29	24.42 ± 0.31	377.81 ± 1.94
	28	64.34 ± 0.38	47.65 ± 1.31	34.28 ± 0.94	376.9 ± 1.51
	42	64.59 ± 1.11	49.78 ± 3.51	35.81 ± 2.53	380.95 ± 1.26
	63	64.48 ± 0.78	51.36 ± 3.2	36.95 ± 2.3	380.22 ± 0.22
	77	64.93 ± 0.58	53.7 ± 3.82	38.64 ± 2.75	379.13 ± 0.39
	91	65.82 ± 0.10	53.96 ± 1.02	38.82 ± 0.74	380.98 ± 0.32
Enzymatic	7	64.36 ± 0.49	40.24 ± 1.06	28.95 ± 0.77	380.69 ± 1.25
	14	63.88 ± 0.28	47.29 ± 1.68	34.02 ± 1.21	377.76 ± 3.63
	28	64.67 ± 0.32	53.65 ± 0.89	36.60 ± 0.64	378.95 ± 2.86

	42	65.68 ± 0.75	53.61 ± 3.34	38.57 ± 2.4	375.78 ± 2.20
	63	64.52 ± 0.77	43.83 ± 4.25	31.53 ± 3.06	369.98 ± 4.40
	77	65.42 ± 0.6	43.78 ± 1.72	31.5 ± 1.24	375.09 ± 2.86
	91	64.52 ± 0.86	33.74 ± 2.98	24.27 ± 2.15	374.32 ± 1.25

During the degradation period, the molecular weights (Mw) of electrospun meshes were measured (Table IV.3.). In spite of the PCL theoretical molecular weight is 50kDa according GPC test this value is slightly low. The degradation can occur through two different mechanisms: surface erosion or bulk degradation, consequently the changes of Mw and weight during the degradation period allows to distinguish the two mechanisms [27]. Hydrolytic degradation is characterized by the bulk degradation for that reason despite the slight weight loss was observed a decrease of Mw. On the other hand, the enzymatic degradation reached 97.11 % of weight loss although the Mw remained closed to the initial value due to the surface erosion mechanism. In terms of Polydispersity index all samples shows values above 1 meaning that all samples present a very broad size distribution [28].

Table IV.3. Electrospun meshes characterization according to the degradation mediums.[a] Samples without enough dimension to perform mechanical tests; [1] statistical significance ($p \leq 0.05$) compared to Day 0; [2] statistical significance ($p \leq 0.05$) compared to the homologous time-point of enzymatic degradation.

Medium	Degradation time (Days)	Mn (Da)	Mw(Da)	PDI	Contact Angle (°)	E (MPa)	EB (%)
n.a.	0	32.7 ± 9.7	45.5 ± 6.6	1.7	121.09 ± 1.18	8.16 ± 3.56	221.22 ± 65.75
PBS	7	41.5 ± 4.2	57.8 ± 11.6	1.4	124.05 ± 1.04	6.17 ± 4.7	99.84 ± 44.47 [1]
	14	46.7 ± 3.4	60 ± 1.5	1.3	131.41 ± 2.53	4.45 ± 2.66	157.04 ± 98.38
	28	47.5 ± 10.3	64.6 ± 15.8	1.4	116.29 ± 3.05	5.07 ± 0.64 [2]	120.87 ± 58.46 [2]
	42	28.1 ± 6.2	50.1 ± 10.3	1.8	113.48 ± 0.3	13.37 ± 5.5 [2]	187.96 ± 73.3 [2]
	63	39 ± 12.7	59.4 ± 18.2	1.5	105.4 ± 1.21	5.12 ± 2.6	181.60 ± 102.89
	77	25.5 ± 6.5	42.6 ± 3.1	1.7	97.33 ± 4.77	10.91 ± 1.99	138.90 ± 28.16
	91	35.3 ± 12.5	48.2 ± 9.9	1.4	124.75 ± 1.9	7.78 ± 0.60	81.09 ± 21.59 [1]
Enzymatic	7	43.7 ± 3.7	59.7 ± 3.6	1.4	122.41 ± 0.93	13.39 ± 7.55	52.17 ± 21.48 [1]
	14	31.6 ± 11.8	48 ± 9.7	1.5	111.78 ± 1.34	49.12 ± 74.68	34.27 ± 39.98 [1]
	28	35.6	45.9	1.3	102.54 ± 1.18	69.78 ± 22.42 [1]	7.84 ± 2.0 [1]
	42	21.1 ± 5.8	33.3 ± 4.1	1.6	101.12 ± 4.75	139.65 ± 60.09 [1]	6.59 ± 0.83 [1]
	63	33 ± 7.8	45.9 ± 1.1	1.4	96.29 ± 6.63	- [a]	- [a]
	77	26.6 ± 9	51 ± 11.8	1.9	0		

	91	38.5 ± 24.9	57.7 ± 2.9	1.5	0		

The water uptake of biodegradable polymers indicates its hydrophilic/hydrophobic character and consequently, their susceptibility to degradation by hydrolysis processes [29]. To evaluate the hydrophilic character of the electrospun meshes, the contact angle between the mats and the water droplet was measured. As known the PCL has a hydrophobic character and the nanofibres meshes produced through electrospinning process showed an angle of 121.09 ± 1.18 (Table IV.3.) meaning that electrospun meshes has, also, a hydrophobic behaviour. With the enzymatic degradation meshes became more permeable with bigger pores allowing the integration of the water droplet into de sample increasing the mesh hydrophilicity over the degradation period.

3.1.3 Mechanical tests

To evaluate the mechanical properties of electrospun meshes degraded, stress-strain tests were performed. For each degradation time, three consecutive tensile tests were measured for three different samples. The Young's modulus (E) and the elongation at maximum strain at break (EB) are summarized in Table IV.3. According to the literature, several studies were performed to evaluate the skin Young's modulus and elongation at break for tensile tests, being the average value between 2.9-150MPa and 17-207%, respectively [30-33]. The results obtained for electrospun samples meshes without degradation was 8.16 ± 3.56 MPa for Young's modulus and 221.22 ± 65.75% for elongation at break, these values are in good agreement with the literature. The samples degraded in enzymatic medium showed a progressive increase of Young's Modulus until day 28, after that, it suffer a slight decrease until day 42. This trend is correlated with the increase of crystallinity, observed by thermal analysis, showing that increasing the crystallinity the Young's modulus increases too, due to the decrease of elasticity caused by the sharp degradation. According to the elongation at break was observed a decrease with time of degradation consequence of the huge degradation observed. The E and EB values of the samples in PBS medium showed a non-consistent trend, consequence of a slightly degradation during all degradation period.

3.2 In vivo biocompatibility and degradation of electrospun meshes

The main goal of the *in vivo* studies performed in this work was to assess the in vivo degradation profile of the electrospun meshes produced as described in the previous

sections. After the implantation and retrieval of the PCL electrospun meshes, specimens were routinely processed for histology and transversal sections were analyzed by standard H&E staining.

After 7 days of subcutaneous implantation (Fig.IV.4), the membranes were clearly visualized and presented a macroscopic aspect similar to the hydrated membranes prior to implantation. Few adhesion sites were observed and no major alterations were detected. Image reconstruction of the full membrane (Fig. IV.4A) showed that the membranes remained parallel to the skin of the animal below the muscular layer. H&E staining images at higher magnifications revealed that low foreign body response was observed at the surface of the membranes (Fig. IV.4B) and in the interior part of the membrane we could already observe some cells (Fig. IV.4B and C dark pink) though the majority of the area is still occupied by the PCL nanofibers (Fig. IV.4C, light pink). The same can be observed throughout the membrane, even where the exposed membrane area was higher (at the end-limits of the meshes (Fig. IV:4D and E).

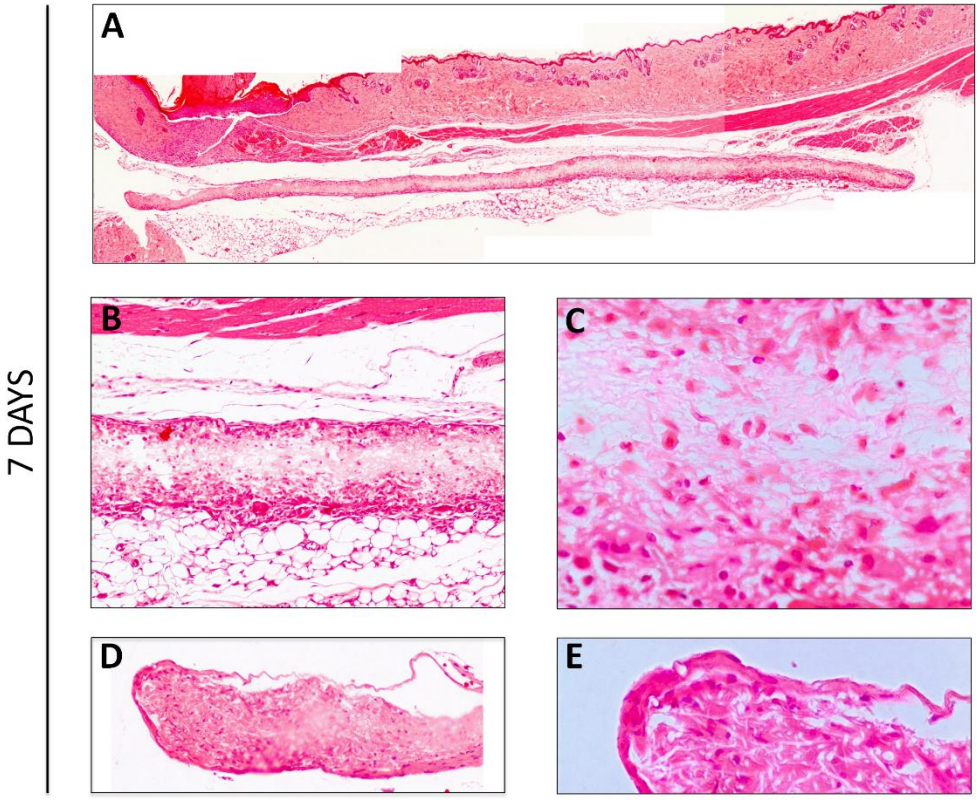

Figure IV.4. H& E staining for PCL electrospun meshes implanted after 7 days. A) reconstruction of the full membrane; B –C) Interior membrane section; D-E) end-limits of the meshes.

At later timepoints (60 and 90 days, Fig. IV.5 and IV.6 respectively) higher cell infiltration was clearly present through the interior/ non-exposed area of the meshes. After 60 days of implantation, the retrieval was harder to achieve since the macroscopic observation of the membranes revealed translucent meshes but still presenting the circular format. When analysing histological sections (Fig. IV.5), one can clearly observe the increased cell number in the interior of the membranes and blood vessels can also be distinguished within the membrane (Fig. IV.5 B-E) (erythrocytes in bright red) demonstrating that the electrospun PCL membranes are in fact being integrated in host tissue. Furthermore, hollow spaces can also be observed indicating that the material is being degraded.

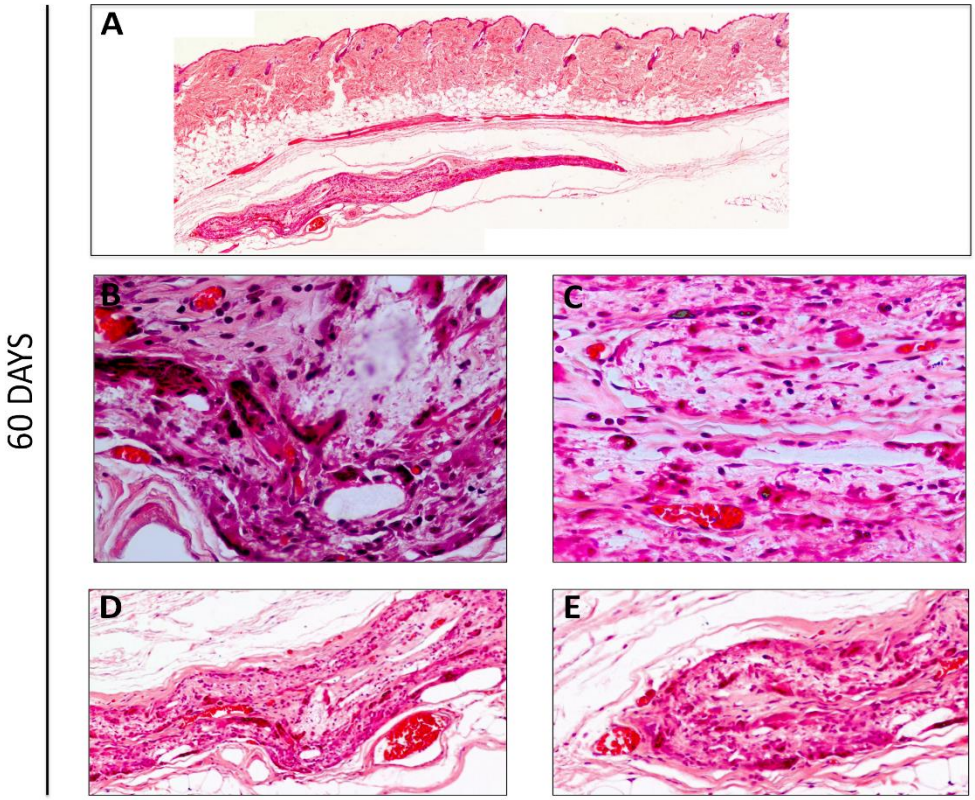

Figure IV.5. H& E staining for PCL electrospun meshes implanted after 60 days. A) reconstruction of the full membrane; B –C) Interior membrane section; D-E) end-limits of the meshes.

A very similar pattern can be observed on the 90 days post-implantation H&E sections (Fig. IV.6), where larger blood vessels containing red blood cells can be identified and stronger collagen staining (pink) is present (Fig. IV.6 B-D).

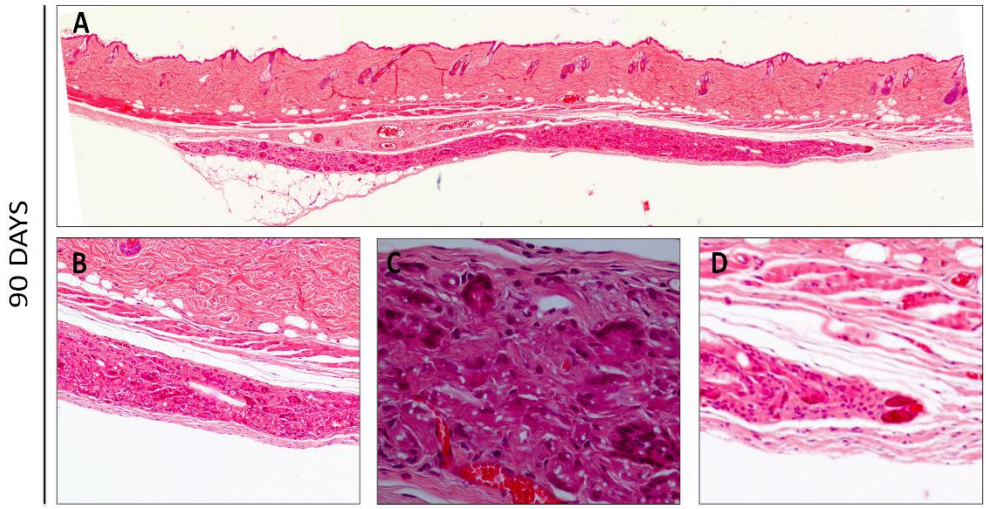

Figure IV.6. H& E staining for PCL electrospun meshes implanted after 90 days. A) reconstruction of the full membrane; B –C) Interior membrane section; D) end-limits of the meshes.

When analysing the images along the time (Fig. IV.7) one can state that at the initial timepoints, host organism is in fact reacting to the electrospun meshes but after 7 days the inflammation processes are already lessened; the cells attach to the surface of the material and posterior timepoints (60 and 90 days) analysis revealed that the cells are in fact able to infiltrate the meshes and colonize the interior part. After 90 days, the cells that infiltrate the meshes are already producing extracelular matrix components (such as collagens displayed in pink) that are probably occupying the place of the degraded PCL nanofibers. Hollow spaces can be observed and the presence of blood vessels penetrating the matrices with larger diameters (with the increase of the time of permanence inside the host organism) show the biointegration of the PCL electrospun meshes.

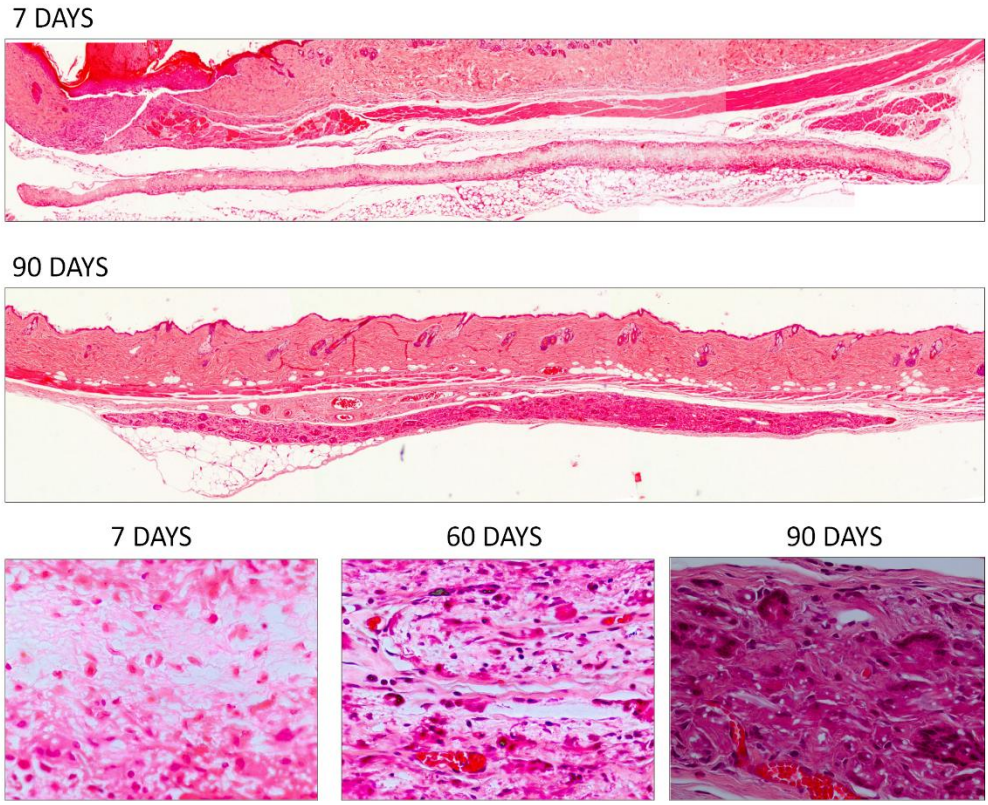

Figure IV.7. Comparison of PCL electrospun meshes H&E staining implanted during 7, 60 or 90 days.

Surface and bulk erosion can describe how a degrading polymer erodes, in surface erosion, the polymer degrades from the exterior surface. The inside of the material does not degrade until all the surrounding material around it has been degraded [34]. In bulk erosion, degradation occurs throughout the whole material equally. Both the surface and the inside of the material degrade [34]. Surface erosion and bulk erosion are not exclusive, many materials undergo a combination of surface and bulk erosion [35]. In the electrospun PCL meshes a bulk erosion phenomena seam to take place though further studies are needed.

PCL degradation rate depends on its structural organisation though in this field there is a controversy in the evaluation of electrospun degradation *in vitro* and/or *in vivo*. Several works have been explore *in vitro* degradation of PCL electrospun meshes either hydrolytic or enzymatic degradation. A study performed by Natu where evaluated the long term hydrolytic degradation for PCL in fibres, sponges, films and discs shapes, their results demonstrated that the processing does not affect significantly the degradation rate during the advanced stage [36]. In terms of weight loss Castilla-Cortázar study demonstrated that PCL network in degradation with lipase only lost 18% of weight after

14 weeks and according Peng the PCL electrospun fibres only 5% of weight was lose in 18 days [16].

There are, also, some *in vivo* studies to evaluate the electrospun meshes degradation where PCL is combined with other materials, in all studies was created subcutaneous pockets to implant the electrospun meshes. According Jiang study, the histological and immunofluorescence evaluation showed that the continuous degradation of PCL/PTMC scaffolds induced a macrophagemediated foreign body reaction [37]. This study evaluated the samples after 1 month of implantation, from histology degradation was observed and correlated, by the authors, to the PTMC part [37]. Other study performed by Shi et al., evaluated the degradation during 24 weeks of PCL/Gel membranes with different ratios. The study demonstrated the incorporation of gelatin increases the biocompatibility and the biodegradation rate of the membranes [38]. The work developed by Xue et al., evaluated the PCL and Gelatin electrospun meshes *in vivo* during 6 months [39]. Results demonstrated that after 12 weeks the PCL samples were degraded, although the samples with 70% of PCL with 30% of gelatin takes only 1 week to degrade [39]. Only Bölgen work evaluated *in vitro* and *in vivo* degradation of PCL electrospun meshes during 6 months for hydrolytic degradation and 90 days for *in vivo* degradation. In this study was demonstrated that the main reason for the different degradation behaviour was attributed to the different surface/volume ratio of the fibres. Authors, demonstrated, also, that *in vivo* degradation was faster than hydrolytic one due to the enzymes presence [40].

The present study evaluated, for the first time, the hydrolytic and enzymatic degradation and correlate with *in vivo* results, both performed during 90 days. Initially a slightly reaction to the PCL electrospun meshes was observed but at day 7 the inflammation process is residual. Posterior time-points (60 and 90 days) showed the cellular infiltration throughout of mesh and after 90 days the PCL electrospun meshes were replaced by collagen.

4. Conclusions

In vitro degradation of electrospun meshes were monitored during 91 days in different mediums (hydrolytic and enzymatic) in order to evaluate its degradation rate for short-term applications, namely skin tissue regeneration. After the degradation period the samples in enzymatic medium reached 97.11% of weight loss, demonstrating the direct influence of enzyme in degradation velocity. Characteristic of enzymatic degradation was possible verify trough SEM microscopies the erosion of fibers surface throughout

degradation time. Consequently, YM increase and Eb decrease due to the transition to a brittle structure. From our results the degradation after 90 days was evident in both situations (in vitro and in vivo), demonstrating the use of PCL electrospun meshes for short-term applications suitable.

References

1. Vasconcelos, A., A.C. Gomes, and A. Cavaco-Paulo, Novel silk fibroin/ elastin wound dressings. Acta Biomaterialia 2012. **8**: p. 3049-60.
2. Pereira, R.F., et al., Advanced biofabrication strategies for skin regeneration and repair. Nanomedicine, 2013. **8**: p. 603-21.
3. Zahedi, P., et al., A review on wound dressings with an emphasis on electrospun nanofibrous polymeric bandages. Polym. Adv. Technol 2009. **21**: p. 77-95.
4. Dias, J.R., P.L. Granja, and P.J. Bártolo, Advances in electrospun skin substitutes. Progress in Materials Science, 2016. **84**: p. 314-334.
5. Wang T, et al., Hydrogel sheets of chitosan, honey and gelatin as burn wound dressings. Carbohydrate Polymers 2011. **88**: p. 75–83.
6. Bosworth, L.A. and S. Downes, Physicochemical characterisation of degrading polycaprolactone scaffolds. Polymer Degradation and Stability 2010. **95**: p. 2269-2276.
7. Okamoto M and John B, Synthetic biopolymer nanocomposites for tissue engineering scaffolds. Prog Polym Sci 2013. **38**(10-11): p. 1487-1503.
8. Dash TK and Konkimalla VB, Poly- e-caprolactone based formulations for drug delivery and Tissue engineering. J. Control. Release 2012. **158**: p. 15-33.
9. Cipitria, A., et al., Design, fabrication and characterization of PCL electrospun scaffolds—a review. J. Mater. Chem., 2011, 21, 9419, 2011. **21**: p. 9419.
10. Patricio T, et al., Characterisation of PCL and PCL/PLA scaffolds for tissue engineering. Procedia CIRP, 2013. **5**: p. 110-114.
11. Tietz, N.W. and D.F. Shuey, Lipase in serum – the elusive enzyme – an overview. Clin Chem, 1993. **39**(5): p. 746-756.
12. Gomes, M.E., et al., Starch-poly(e-caprolactone) and starch-poly(lactic acid) fibre-mesh scaffolds for bone tissue engineering applications:structure, mechanical properties and degradation behaviour. J Tissue Eng Regen Med, 2008. **2**: p. 243-252.
13. He, W., et al., Fabrication of collagen-coated biodegradable polymer nanofiber mesh and its potential for endothelial cells growth. Biomaterials 2005(26): p. 7606–761.

14. López-Rodríguez, N., et al., Crystallization, morphology, and mechanical behavior of polylactide/poly(ε-caprolactone) blends. Polym. Eng. Sci. , 2006. **46** p. 1299-1308.
15. Crescenz, V., et al., Thermodynamics of fusion of polybeta-propiolactone and poly-epsilon-caprolactone e comparative analysis of melting of aliphatic polylactone and polyester chains. Eur Polym J

1972. **8**: p. 449-463.
16. Castilla-Cortázar, I., et al., Hydrolytic and enzymatic degradation of a poly(ε-caprolactone) network. Polymer Degradation and Stability, 2012. **97**: p. 1241-1248.
17. O'Brien, F.J., Biomaterials & scaffolds for tissue engineering. MaterialsToday, 2011. **14**(3): p. 88-95.
18. Léon y Léon, C.A., New perspectives in mercury porosimetry. Advances in Colloid and Interface Science, 1998. **76-77**: p. 341–372,.
19. Garg, T., et al., Scaffold: A Novel Carrier for Cell and Drug Delivery, . Critical Reviews™ in Therapeutic Drug Carrier Systems, 2012. **29**(1): p. 1-63.
20. Freyman, T.M., I.V. Yannas, and L.J. Gibson, Cellular materials as porous scaffolds for tissue engineering. Prog Mater Sci. , 2001. **46**: p. 273–82.
21. Dhandayuthapani, B., et al., Polymeric Scaffolds in Tissue Engineering Application: A Review. International Journal of Polymer Science, 2011: p. 1-19.
22. Liu S-J, et al., Electrospun PLGA/collagen nanofibrous membrane as early-stage wound dressing. Journal of Membrane Science, 2010. **355**: p. 53–59.
23. Azevedo, H.S., M.G. Francisco, and R.L. Reis, In Vitro Assessment of the Enzymatic Degradation of Several Starch Based Biomaterials. Biomacromolecules, 2003. **4** p. 1703-1712.
24. Huang, Z.-M., et al., A review on polymer nanofibers by electrospinning and their applications in nanocomposites. Composites Science and Technology 2003. **63**: p. 2223-2253.
25. Greiner, A. and J.H. Wendorff, Electrospinning: a fascinating method for the preparation of ultrathin fibers. Angew Chem Int Ed Engl., 2007. **46**(30): p. 5670-5703.
26. Picciani, P.H.S., et al., Structural, Electrical, Mechanical, and Thermal Properties of Electrospun Poly(lactic acid)/ Polyaniline Blend Fibersa. Macromol. Mater. Eng., 2010. **295**: p. 618-627.

27. Peng, H., et al., Controlled enzymatic degradation of poly(3-caprolactone)-based copolymers in the presence of porcine pancreatic lipase. Polymer Degradation and Stability, 2010. **95**: p. 643-650.
28. Chanda, M. and S.K. Roy, Plastics Technology Handbook. 2007: CRC Press.
29. Azevedo HS and Reis RL, Understanding the enzymatic degradation of biodegradable polymers and strategies to control their degradation rate, in iodegradable Systems in Tissue Engineering and Regenerative Medicine, Reis RL and San Roman J, Editors. 2005, CRC Press: Boca Raton, FL. p. 177-201.
30. Vogel, H., Age dependence of mechanical and biochemical properties of human skin. Bioengineering and the skin, 1987. **3**(67-91).
31. Jansen, L. and P. Rottier, Some mechanical properties of human abdominal skin measured on excised strips. Dermatologica, 1985. **117**: p. 65-83.
32. Jacquemoud, C., K. Bruyere-Garnier, and M. Coret, Methodology to determine failure characteristics of planar soft tissues using a dynamic tensile test. Journal of Biomechanics 2007. **40**(2): p. 468-475.
33. Pan, J.-f., et al., Preparation and Characterization of Electrospun PLCL/Poloxamer Nanofibers and Dextran/Gelatin Hydrogels for Skin Tissue Engineering. PLoS ONE 2014. **9**(11): p. e112885.
34. Ulery, B.D., L.S. Nair, and C.T. Laurencin, Biomedical Applications of Biodegradable Polymers. Journal of polymer science, 2011. **49**: p. 832-864.
35. Uhrich, K.E., et al., Polymeric Systems for Controlled Drug Release. Chem Rev, 1999. **99**: p. 3181-3198.
36. Natu, M.V., H.C. de Sousa, and M.H. Gil, Influence of polymer processing technique on long term degradation of poly(ε-caprolactone) constructs. Polymer Degradation and Stability 2013. **98**: p. 44-51.
37. Jiang, T., et al., The Tissue Response and Degradation of Electrospun Poly(e-caprolactone)/Poly(trimethylene-carbonate) Scaffold in Subcutaneous Space of Mice. Journal of Nanomaterials, 2014. **2014**: p. 1-7.
38. Shi, R., et al., Fabrication and evaluation of a homogeneous electrospun PCL–gelatin hybrid membrane as an anti-adhesion barrier for craniectomy. J. Mater. Chem. B, 2015. **3**(4063-4073).
39. Xue, J., et al., Fabrication and evaluation of electrospun PCL–gelatin micro-/nanofiber membranes for antiinfective GTR implants. J. Mater. Chem. B, 2014. **2**: p. 6867.

40. Bolgen, N., et al., In vitro and in vivo degradation of non-woven materials made of poly(ε-caprolactone) nanofibers prepared by electrospinning under different conditions. J. Biomater. Sci. Polymer Edn, 2005. **16**(12): p. 1537-1555.

Chapter V

Evaluation of gelatin electrospun fibers crosslinking with BDDGE (1,4 – butanediol Diglycidyl ether) for skin regeneration

Evaluation of gelatin electrospun fibers crosslinking with BDDGE (1,4 – butanediol Diglycidyl ether) for skin regeneration |Chapter V

Contents

1. Introduction

Skin is the largest vital organ in the body, protecting it against the external environment [1-5]. Although skin has a self-regeneration ability, this capacity is strongly reduced in the case of full-thickness lesions, making necessary the use of grafts or dressings [1]. The usual procedure when skin damage occurs consists in the application of a wound dressing due their efficiency, low cost and availability [6, 7]. Wound dressings made from electrospun nanofibers present advantageous properties compared to conventional dressings such as the potential to promote the hemostasis phase, wound exudate absorption, semi-permeability, easy conformability to the wound, functional ability and no scar induction [8].

Gelatin, derived from collagen, is a natural mimic of the extracellular matrix (ECM) of human tissues and organs and is widely used in the tissue engineering field due to of its excellent biological origin, biocompatibility, biodegradability non-immunogenicity, cell-interactivity and commercial availability [9, 10]. However, gelatin is a water-soluble protein derived from partial hydrolysis of collagen and crosslinking is usually needed to improve its mechanical properties and stability, making gelatin scaffolds insoluble in biological environments [10]. Several gelatin crosslinking methods are available, such as enzymatic using transglutaminase [11, 12], or chemical using fructose [13], dextran dialdehyde [14], diepoxy [15], formaldehyde [16], glutaraldehyde [13, 16, 17], genipin [15, 18, 19], diisocyanates [20], or carbodiimides [21]. The widely used aldehyde-based crosslinking strategy has provided a powerful tool to tailor the physical properties of gelatin films [22-24] although the assumed toxicity of such chemicals makes their use uncertain [22]. Epoxy compounds are preferred as a stabilizing agent of collagen-based materials for biomedical applications due to their lower toxicity compared to commonly used dialdehydes [25-27].

The search for alternative crosslinkers presenting low toxicity and good stability is the main objective of this research work. Amongst water-soluble polyepoxides, 1,4-butanediol diglycidyl ether (BDDGE) is commercially available as a crosslinking agent in dermal filler formulations [26]. Although un-reacted BDDGE should be considered from slightly to moderately toxic [27], residual BDDGE might undergo hydrolysis yielding a diol-ether (3,3′(butane-1,4-diylbis(oxy)) bis propane-1,2-diol), which has been proven non-toxic, thus limiting safety risks [26]. This study evaluates the ability of BDDGE to crosslink electrospun gelatin nanofibers and provides the first insights on the physicochemical and in vitro biological performance of produced scaffolds in the context of skin tissue engineering applications.

2. Materials and Methods

2.1. Materials

Gelatin powder of pig skin (type A, 300 bloom, 60 mesh) was kindly supplied by Italgelatine (Italy). Acetic acid (AA) glacial was purchased from PanReac AppliChem, triethylamine (TEA) from Sigma Aldrich, and 1,4-butanediol diglycidyl ether (BDDGE) from Alpha Aesar. All materials used were of reagent grade and used without any further purification.

2.2. Electrospinning of crosslinked gelatin nanofiber meshes

A gelatin/AA/TEA solution was prepared by dissolving gelatin (15 wt-%) in AA and then adding 2 wt-% of TEA to the solution and stirring at 37ºC overnight. TEA was added to increase the solution's conductivity. Crosslinking of electrospun gelatin fibers was carried out through the incorporation of BDDGE on the gelatin solution immediately before fiber electrospinning to avoid the loss of configuration that is induced through a crosslinking bath after fiber production. The effect of different BDDGE concentrations (2, 4 and 6 wt-%) at varied time-points (24, 48 and 72h) was tested.

Gelatin nanofibrous meshes were processed using a home-made electrospinning apparatus. Non-woven gelatin electrospun meshes were obtained at room temperature (RT) and relative humidity of 40-50% with a constant flow rate of 0.4 mL/h (SP11Elite, Harvard Apparatus) and 12 kV of voltage. A grounded copper plate was used as collector and it was positioned 12 cm away from the needle tip.

2.3. Physico-chemical characterization

2.3.1. Apparent density and porosity

The apparent density and porosity of gelatin electrospun meshes were calculated using equations (1) and (2) [28], respectively, and the mesh thickness was measured using a micrometer.

$$\text{Apparent density } \left(g \cdot cm^{-3}\right) = \frac{\text{mesh mass(g)}}{\text{mesh thickness (cm)} \cdot \text{mesh area (cm}^2\text{)}} \quad (1)$$

$$\text{Mesh porosity} = \left(1 - \frac{\text{Mesh apparent density(g} \cdot \text{ cm}^{-3}\text{)}}{\text{Bulk density of gelatin(g} \cdot \text{ cm}^{-3}\text{)}}\right) \cdot 100\% \quad (2)$$

2.3.2. Morphology and fiber diameter

The morphology of each electrospun fibrous mesh was examined by scanning electron microscopy (SEM) using a Quanta 400 FEG ESEM/EDAX Genesis X4M (FEI Company, USA) in CEMUP, University of Porto. Prior to examination samples were coated with a gold/palladium (Au/Pd) thin film, by sputtering, using the SPI Module Sputter Coater equipment. SEM images were also used to evaluate the fiber diameter distribution using Image J software. To each condition three individual samples were analyzed and fifty measurements per image were carried out.

2.3.3. Mesh Structure

Fourier transform infrared (FTIR) spectroscopy with attenuated total reflectance (ATR) was used to evaluate the chemical composition of the materials and to detect possible structural changes. FTIR analyses were carried out using an Alpha-P Brucker FTIR-ATR spectrometer, in the range of 4000–500 cm^{-1}, at a 4 cm^{-1} resolution with 64 scans.

2.3.4. Crosslinking extent

The ninhydrin (NHN) assay was used to quantify the number of amino groups involved in the crosslinking reaction through UV-vis spectrometry. Crosslinked gelatin electrospun meshes with different crosslinker percentages and dried after different periods of time were tested. A precise amount of sample (10.5±0.5 mg) was heated with ninhydrin solution (200 mg/100 mL) for 10 min in a water bath at 90ºC. Afterwards, 5 mL of ethanol was added to 100 µL of each sample and the absorbance recorded on a spectrophotometer (lambda 35 from Perkin Elmer, USA) at a wavelength of 570 nm with glycine as standard. Linear regression was performed with a correlation of 0.9976. The extent of crosslinking was defined according to eq. 3:

$$\text{Crosslinking degree } (\%) = \left(1 - \frac{NH_t}{NH_0}\right) \cdot 100 \quad (3)$$

where, NH_0 is the amount of free amino groups in the gelatin before crosslinking and NH_t is the amount of free amino groups after crosslinking [29].

2.3.5. Dissolvability and water uptake

To assess the dissolvability, samples were dried for 24h before weight determination, followed by incubation in distilled water and sodium azide (0.02%) as bacteriostatic agent. After 24h of incubation samples were removed from the distilled water solution and weighted again to evaluate the swelling degree (eq. 4). Then, the samples were dried for an additional 24h period at 37ºC and weighted to evaluate their dissolvability (eq. 5).

$$\text{Degree of sweeling } (\%) = \frac{W_w - W_d}{W_d} \cdot 100 \ , \quad (4)$$

where W_w is the wet weight and W_d is the dry weight.

$$\text{Dissolvability } (\%) = \frac{W_0 - W_d}{W_0} \cdot 100, \quad (5)$$

where W_0 is the initial weight and W_d is the dry weight.

2.3.6. Water vapor permeability

To evaluate the water permeation rate of electrospun meshes, glass bottles with the same size and type were filled with PBS solution and the electrospun meshes were fixed on their openings. The area available for vapor permeation was 2.39 cm^2. Evaporation of water through the mesh was monitored by the measurement of weight loss according to standard test methods for water vapor transmission [30]. Briefly, each set was weighted and kept at 32°C during 24h, after which the weight of each set was recorded again to quantify the amount of water evaporated.

2.3.7 Mechanical properties

The tensile strength and modulus of crosslinked electrospun gelatin samples were determined both in the dry and wet state using a texturometer (TA.XT Plus model, Stable Micro System SMD, England) with a 5N load cell. Mechanical tests were carried out in a controlled environment at RT and relative air humidity of 45%. The gauge length was 15 mm and the test speed was 1 $mm \cdot s^{-1}$. At least five individual samples were tested from each group and measurements were reported as mean ± standard deviation according the statistical method used (mixed effect model).

2.4. *In vitro* studies

Human dermal neonatal fibroblasts (hDNF) isolated from the foreskin of healthy male newborns (ZenBio, US) were cultured, expanded, and maintained in Dulbecco's modified eagle medium (DMEM) (Gibco, US), at 37ºC in a humidified atmosphere of 5% CO_2. The culture medium was changed twice a week and cells were trypsinized (0.25% trypsin/0.05% ethylenediamine tetraacetic acid (EDTA)/0.1% glucose in PBS (pH 7.5)) when they reached 70-80% of confluence. Cells from passages between 8 and 11 were used in this study.

2.4.1. Cytotoxicity

To assess cytotoxicity, electrospun meshes were tested in direct (samples) and indirect (leachables) contact under different pre-conditions (washed and non-washed in ultrapure water). Samples were sterilized with UV light followed by washing during 24h. hDNF cells were seeded in culture wells for 24h at a density of $2x10^4$ cells/well. 24h later, samples (direct contact) and culture medium having been in contact with samples (indirect contact) were incubated with the cells for another 24h. The culture medium was then removed from the wells and fresh basal medium with 20% v/v resazurin (Sigma) was added. Cells were incubated (37ºC, 5% v/v CO_2) for an additional 2h period, after which 300 µL per well were transferred to a black 96-well plate and measured (Ex at 530 nm, Em at 590 nm) using a micro-plate reader (Synergy MX, BioTek, US). The control consisted in cells alone.

For the quantification of the total double-stranded DNA (dsDNA) content, the cell pellets were recovered from wells and washed with phosphate buffered saline (PBS). The suspension was then centrifuged (10 000 rpm, 5 min) and then stored at -20ºC until further analysis. The dsDNA quantification was performed using the Quant-iT PicoGreen dsDNA kit (Molecular Probes, Invitrogen, US), according to the manufacturer's protocol. Briefly, the samples were thawed and lysed in 1% v/v Triton X-100 (in PBS) for 1h at 250 rpm at 4ºC. Then, they were transferred to a black 96-well plate with clear bottom (Greiner) and diluted in Tris-EDTA buffer (200 mM Tris–HCl, 20 mM EDTA, pH 7.5). After adding the Quant-iT PicoGreen dsDNA reagent, samples were incubated for 5 min at RT in the dark, and fluorescence was measured using a microplate reader (Ex at 480, Em at 520 nm).

2.4.2. Cell metabolic activity and proliferation

Cell metabolic activity and proliferation assays were performed using hDNF cells seeded on electrospun meshes at a cell density of $1x10^4$ cells per sample. To promote an efficient cell penetration into the mesh the seeding was performed with only 10 µL. After 2h medium up to 500 µL was added and cultured during 7 days. Metabolic activity was estimated using the resazurin-based assay, using electrospun meshes without cells as control. For the proliferation assay samples were tested in direct contact with hDNF cells and pre-washed with ultrapure water. Afterwards, they were cultured for 7 days, and their metabolic activity was measured at days 1, 3 and 7.

2.4.3. Cell morphology and fibronectin deposition

For the same time-points as for the cell metabolic activity (1, 3 and 7 days), cells seeded in electrospun meshes were stained for filamentous actin (F-actin), nuclei (Dapi) and fibronectin (FN) deposition. Briefly, samples were washed with PBS, fixed for 20 min in 4 wt-% paraformaldehyde (PFA, Sigma), and permeabilized with 0.2% Triton X-100 (Sigma) for 7 min. Samples were then incubated for 1h with 1 wt-% bovine serum albumin (BSA, Merck) in PBS. For FN staining, electrospun meshes were incubated overnight at 4ºC with rabbit anti-fibronectin (f3648, Sigma, 1: 300) and then with the goat anti-rabbit secondary antibody Alexa Fluor® 488 $F(ab')_2$ fragment (Molecular Probes-Invitrogen, 1:2000, 2h at RT). Subsequently, samples were incubated with the conjugated probe phalloidin/Alexa Fluor® 594 (Molecular Probes-Invitrogen, 1:40, 1h at RT) for F-actin staining. Samples were then washed three times with the PBS solution and nuclei were counterstained with 40,6-diamidino-2-phenylindole dihydrochloride (DAPI, Sigma, 0.1 $mg{\cdot}mL^{-1}$) in vectashield (vector), just before confocal visualization (CLSM, Leica SP2AOBS, Leica Microsystems) using LCS software (Leica Microsystems). The scanned Z-series were projected onto a single plane and pseudo-colored using ImageJ. The cells cultured in electrospun meshes were also visualized trough SEM to evaluate their morphology. Briefly, samples were washed with PBS, fixed for 30 min in 2.5 wt-% glutaraldehyde (GA, Fluka), and dehydrated with a successive graded ethanol series (40, 50, 70, 90 and 100%) for 15 min each. After that, critical point drying (CPD7501, Polaron Range) was performed to ensure the complete dehydration of samples.

2.5. Statistical analyses

All data points were expressed as mean ± standard deviation (SD). Statistical analysis (Levene's and T test) was carried out using IBM SPSS Statistics 20.0 with 99% confidence level for extent of crosslinking and cytotoxicity assays. Linear mixed model (LMM) was used to test differences between the effects of concentration, time and environment (wet and dry) in Young's Modulus, tensile strength at break and elongation at break. Concentration, time and environment were treated as a fixed factor and replication experiment was treated as a random factor to take into account possible heterogeneity of the samples in each set. Parameters estimation were performed by lme package and multiple comparison adjustment were performed by mulcomp package from the R statistical software [31]. The results were considered statistically significant when $p \leq 0.05$ (*).

3. Results and discussion

3.1. Macroscopic and morphological characterization

An optimal scaffold requires a highly porous (>60-90%) and fully interconnected structure to provide a large surface area for cell ingrowth, uniform cell distribution, easy access to oxygen and nutrients by the cells, facilitating vascularisation [32-35]. The porosity of electrosopun meshes can be influenced by several parameters such as the fiber diameter and fibers density per area. The theoretical values calculated for the porosity of electrospun meshes produced (Table V.1) range between 97.37 (2% v/v BDDGE, 72h) and 98.76% (4% v/v BDDGE, 24h). The results showed that higher diameters yield slightly high mesh porosity values as a consequence of less fibers packing, leaving larger spaces between fibers. However, all sample demonstrated a high degree of porosity.
SEM morphological analyses of electrospun gelatin meshes with and without BDDGE are presented in Fig. V.1. The results show that the obtained electrospun meshes present an uniform random deposition, with well-defined filaments and without beads. The *in situ* crosslinked fibers keep their morphology after incorporating BDDGE in the polymeric solution prior to fiber spinning. Fiber diameters strongly depend on both the amount of crosslinker and the incubation time (Table V.1). For all samples, the fiber diameter generally decreased with increasing the crosslinking reaction time in BDDGE as a consequence of new bonds formation, bringing the molecular chains closer and thereby decreasing the fiber diameter. Using 2% of BDDGE the diameter decreased from 346 ± 158 nm at 24h to 284 ± 120 nm at 72h of incubation. With 4% of BDDGE the diameter decreased from 378 ± 137 nm at 24h to 339 ± 91 nm at 72h of incubation and with 6%

of BDDGE there is a reduction from 341 ± 134 nm at 24h to 276 ± 88 nm at 72h. At 48h of crosslinking reaction a non-agreement with the general trend was observed, which can be correlated with the instability associated to an incomplete reaction.

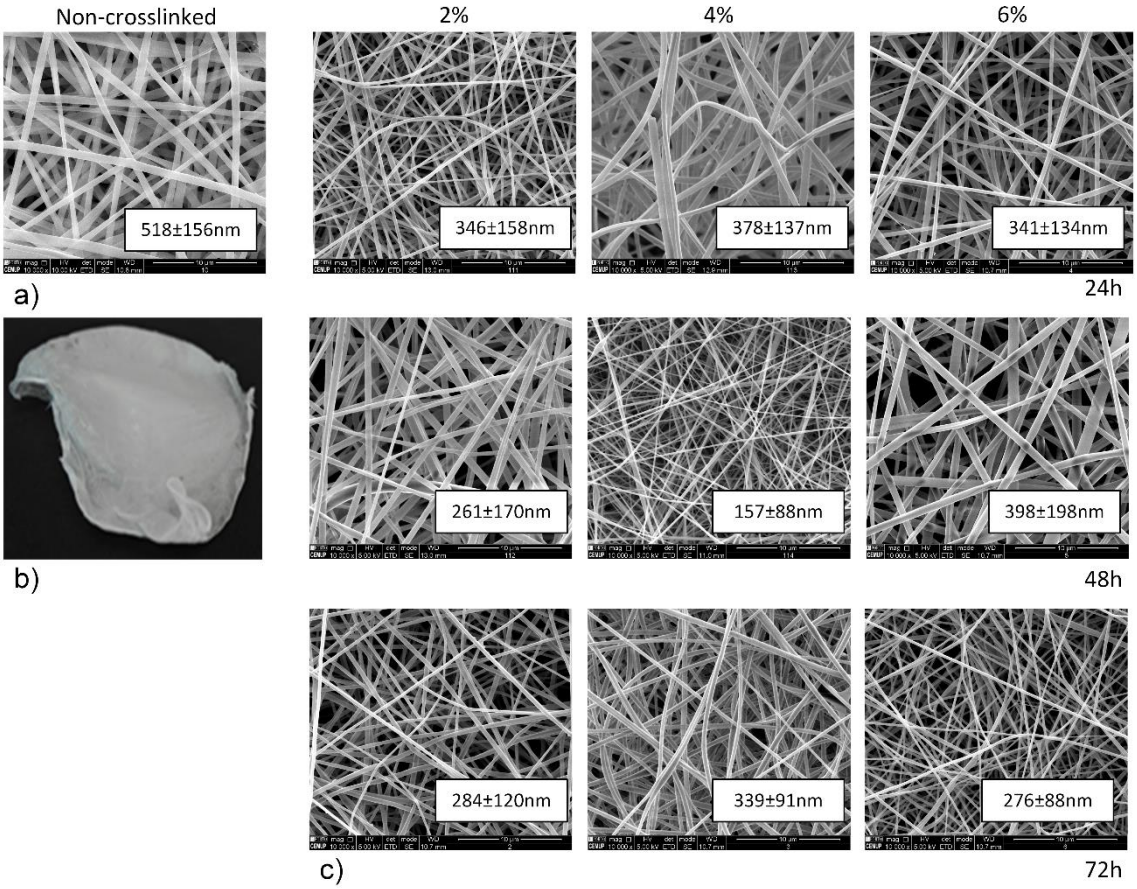

Figure V.1. Morphological evaluation of gelatin electrospun meshes. a) Uncrosslinked sample, b) Electrospun mesh at macroscale. c) Electrospun gelatin nanofibrous meshes crosslinked with different concentrations of BDDGE at different time-points. Average fiber diameter is indicated in white background. Scale bars correspond to 10 µm.

Table V.1. Characterization of gelatin electrospun meshes produced. Mechanical properties correspond to tests performed on wet samples only. Statistical significance for $p<0.05$, (a) compared to 6% of BDDGE at the same incubation time, (b) compared to 4% of BDDGE at the same incubation time and (c) compared to 2% of BDDGE at the same incubation time.

BDDGE (%)	Crosslinking duration (h)	Crosslinking degree (%)	Apparent density	Porosity (%)	Average fiber diameter (nm)	Swelling degree (%)	Dissolvability (%)	Water vapor permeability (g/m^2/day)	Elastic modulus (MPa)	Tensile strength (MPa)	Elongation at break (%)
2	24	9.55 ± 1.31[a]	0.01222	98.30	346 ± 158	460.01 ± 317.36	53.60 ± 18.58	2425.49 ± 137.71	0.77 ± 0.45	0.26 ± 0.15	35.45 ± 5.88
	48	25.49 ± 0.59[a,b]	0.01250	98.26	261 ± 170	380.65 ± 84.28	15.27 ± 6.23	2359.52 ± 91.13	0.42 ± 0.23	0.05 ± 0.02	23.80 ± 10.81
	72	43.45 ± 0.52 [a,b]	0.01893	97.37	284 ± 120	615.68 ± 31.34	30.68 ± 10.67	2462.43 ± 100.52	0.31 ± 0.11	0.08 ± 0.06	25.20 ± 8.99
4	24	35.19 ± 0.61[a]	0.00893	98.76	378 ± 137	644.40 ± 158.78	24.83 ± 1.56	2582.86 ± 46.80	0.67 ± 0.45	0.16 ± 0.15	45.01 ± 9.46
	48	42.75 ± 0.60 [b,c]	0.01471	97.96	157 ± 88	468.48 ± 227.89	23.91 ± 5.33	2647.62 ± 54.22	0.60 ± 0.26	0.12 ± 0.10	33.23 ± 19.67
	72	65.94 ± 0.23 [b]	0.01579	97.81	339 ± 91	567.22 ± 124.63	17.21 ± 10.19	2292.69 ± 147.36	0.30 ± 0.15	0.04 ± 0.03	29.10 ± 11.60
6	24	59.53 ± 0.97 [b,c]	0.01339	98.14	341 ± 134	2375.48 ± 274.11	52.65 ± 4.61	2111.36 ± 115.50	0.16 ± 0.19	0.03 ± 0.02	15.04 ± 8.32
	48	67.57 ± 2.04 [b,c]	0.01676	97.67	398 ± 198	1291.11 ± 142.93	38.06 ± 4.72	2160.13 ± 141.19	0.33 ± 0.15	0.04 ± 0.02	26.12 ± 7.76
	72	72.81 ± 1.70 [c]	0.01798	97.50	276 ± 88	820.79 ± 90.90	28.43 ± 7.99	2299.82 ± 101.10	0.43 ± 0.24	0.02 ± 0.01	35.67 ± 15.35

This seems to be confirmed by the fact that samples are more stable when incubated during 72h with 4% or 6% of BDDGE, corresponding to 65.94% and 72.81% of crosslinking degree and a decrease of fiber diameter of 34.56% and 46.72%, respectively, compared to the non-crosslinked gelatin mesh (518 ± 165 nm) (Table V.1 and Fig. V.1a). Effectively, the decrease of standard deviation at the end of 72h suggests the stabilization of the reaction.

3.2. Physico-chemical and structural characterization

Fourier transform infrared spectroscopy with attenuated total reflection (FTIR-ATR) analyses were performed to evaluate the interaction between gelatin and BDDGE on electrospun meshes using uncrosslinked gelatin as control. The different spectra obtained are shown in Fig. V.2. The FTIR spectrum of gelatin (uncrosslinked) is characterized by strong and sharp bands that include prominent absorption bands directly associated with the protein's secondary structure [36]. The FTIR spectra of crosslinked gelatin samples shows prominent bands in four different amide regions, namely at 1700-1600 cm^{-1} corresponding to amide I, at 1565-1520 cm^{-1}, corresponding to amide II, at 1240-670 cm^{-1} corresponding to amide III, and at 3500–3000 cm^{-1} corresponding to amide A [36-40]. The absorption of amide I contains contributions from the C=O stretching vibration of amide group and a minor contribution from the C-N stretching vibration [36]. Amide II absorption is related to N-H bending and C-N stretching vibrations. Amide III presents vibrations from C-N stretching attached to N-H in-bending with weak contributions from C-C stretching and C=O in-plane bending [41]. In samples crosslinked with BDDGE, at 2930 and 2890 cm^{-1}, it is possible to observe intensity changes compared to the uncrosslinked gelatin spectrum, which are associated to the contribution of aliphatic moieties from BDDGE, confirming the incorporation of BDDGE into the gelatin matrix (Fig. V.2 and Table V.2) [39].

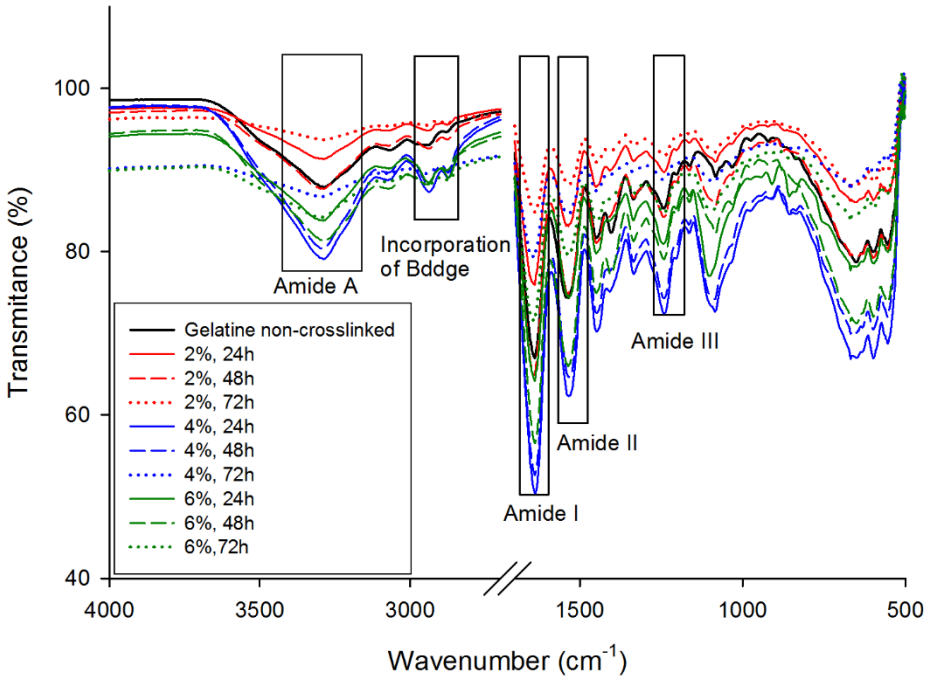

Figure V.2. FTIR spectra of uncrosslinked and gelatin crosslinked with BDDGE at different crosslinking degrees.

Table V.2. Ratio between non-crosslinked and crosslinked samples at 2930 and 2890 cm^{-1}, ratio ≥1 means presence of BDDGE.

BDDGE (%)	Crosslinking duration (h)	Ratio between intensity of non-crosslinked and crosslinked samples (a.u.)	
		2930 cm^{-1}	2890 cm^{-1}
2	24	1.41	2.34
	48	0.99	2.47
	72	1.01	2.08
4	24	1.02	2.23
	48	1.01	2.34
	72	1.01	1.70
6	24	0.99	1.63
	48	0.98	2.49
	72	1.02	2.35

The extension of crosslinking reaction was also assessed through UV/Vis used to quantify the crosslinking degree as a function of the amount of crosslinker and incubation time at different time-points. As expected, higher crosslinker amount and longer incubation times resulted in higher crosslinking degrees, showing that the crosslinking

degree, and thus the properties of the obtained meshes can be easily tuned by simply varying the amount of crosslinker and the incubation time. For instance, using 2% of BDDGE incubated for 72h resulted in a crosslinking degree of 43.45%, although using 4% of BDDGE incubated for only 48h resulted in a similar crosslinking degree (42.75%). It is important to highlight that the maximum crosslinking degree reached was 72.81%, corresponding to samples crosslinked in 6% of BDDGE and incubated for 72h. The reaction between BDDGE and gelatin occurs in acidic conditions due to the AA/TEA solution used to dissolve the gelatin, which results in protonation of the carboxylic acid groups (Fig. V.3), and thereby limiting the achievement of 100% of crosslinking degree [39, 42, 43].

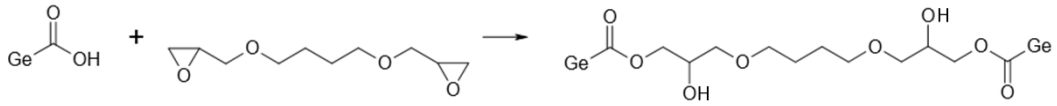

Figure V.3. Characteristic reaction between BDDGE and gelatin under acidic pH.

3.3 Water uptake, swelling, dissolvability and water vapor permeability

The water uptake of biodegradable polymers is an important indicator of their hydrophilic/hydrophobic character and, therefore, their susceptibility to degrade by hydrolysis [44]. The water uptake makes the materials more flexible and promotes changes in the dimensions of the implant material [45]. Table V.1 shows the correlation between the water uptake and the crosslinker concentration and incubation time. The uncrosslinked samples were not evaluated due to their high dissolvability in aqueous medium. The capability to absorb water is known to decrease with the increase of crosslinking degree as the polymer chains become closer due to the new bond formation, making the mesh more dense, with higher retraction forces [39, 46]. This trend was also observed in this work, using gelatin crosslinked with BDDGE (4 and 6% v/v) for different reaction times.

Concerning the swelling degree, a less predictable behavior was observed, especially using 2% v/v of BDDGE, where an instability associated to incomplete reaction was observed. The results obtained for 4% and 6% of BDDGE clearly show that the swelling degree is influenced by the hydrophilic character of BDDGE, significantly increasing (for 6%, comparing to 2 and 4%) with the increase of crosslinker content. This is probably due to an increase in pH, leaving less protons available, increasing anion-anion repulsive forces and allowing the absorption of an increasing water volume [47, 48].

The dissolvability assay represents the amount of uncrosslinked material immediately dissolved by the medium. Similarly, to the swelling degree the dissolvability decreased

with the increase of crosslinking degree due the presence of less unreacted components. Samples with the lowest crosslinking degree (9.55 ± 1.30%), corresponding to 2% of BDDGE at 24h, present 53.60 ± 18.58% of dissolved matter. Samples with the highest crosslinking degree (72.81± 1.70%) present only 28.43 ± 7.99% of dissolved material. Results show a clear evolution of swelling degree with the dissolution of samples with 4% and 6% of BDDGE.

An ideal wound dressing should control the water loss evaporation at an optimal rate. It should be permeable to maintain a moist environment avoiding wound dehydration. Therefore, the water vapor permeability (WVP) is one of the most important characteristics of wound dressings [49]. A wound with a dry environment causes tissue desiccation and consequently the tissue matrix becomes dehydrated, the cells die and a hard scab is formed [50]. Subsequently the keratinocytes have to pass beneath this scab to reach viable tissue, which consumes energy and time, and delays the wound healing process [49]. However, it is important to underline that a moist wound environment is not a wet wound environment, since excess of exudates will lead the patient to hypergranulation tissue formation in the wound bed and macerated periwound skin [49, 50]. Therefore, an important objective in providing topical wound care relies in selecting a dressing which can maintain a moist wound surface and, at same time, remove exudates [49-51]. The common permeation rate for healthy skin is 204 g/m^2/day, while for injured skin can range from 279 g/m^2/day, for a first-degree burn, to 5138 g/m^2/day, for a granulating wound [52, 53]. For an ideal wound dressing a rate of 2500 g/m^2/day is recommended to provide an adequate level of moisture without risking wound dehydration [49, 52, 54]. The water vapor permeability through the gelatin electrospun meshes ranges between 2111.36 ± 115.5 and 2647.62 ± 54.22 g/m^2/day, which is in the range of recommended values. The WVP of dressings is influenced by the pore size and interconnectivity between pores, with meshes with small pores and packed fibers resulting in low permeability to water vapor [55]. From Table V.1 it is possible to observe that there's a general tendency for a decrease in WVP values with the increase in crosslinking degree from 2 to 6% of BDDGE, which can be correlated with both the reduction in the fiber diameter and the increase in packing of the fibers.

3.4. Mechanical characterization

The mechanical properties of crosslinked electrospun gelatin meshes were also investigated as a function of amount of crosslinker and incubation time. Representative stress-strain curves for samples tested in the dry and wet state are shown in the Fig. V.4a. From those curves, it was possible to obtain the Young's modulus, the tensile

strength and the elongation at break. As expected, in the dry state gelatin electrospun meshes show the distinctive behaviour of brittle and rigid materials, having high values of Young's modulus and low values of elongation at break, as a consequence of a rigid protein network [39]. In the dry state, the Young's modulus of all samples (Fig. V.4b) decrease by increasing the incubation time in BDDGE from 24 to 72h. The same trend was observed for samples in the wet state (Fig. V.4b), except for samples crosslinked with 6% of BDDGE, which showed a slight increment from 24 to 72h although not statistically significant. This decrease of the Young's modulus is related to the new bonds formed between polymer chains upon crosslinking, which increases the elasticity of the structure. It is worthwhile mentioning that samples in the wet state exhibited Young's modulus values between 0.16 ± 0.19 and 0.77 ± 0.45 MPa, in comparison to 25.61 ± 9.71 to 113.09 ± 63.85 MPa in the dry state, clearly demonstrating that an hydrogel was formed after crosslinking with BDDGE, directly improving the elasticity of the produced meshes. Samples in the dry state present low elongation at break values due their rigid nature without water (Fig. V.4c). According to independent works of van Wachem and Zeeman, crosslinking of collagen with BDDGE at acidic pH promoted higher tensile strength and elongation at break values than the crosslinking reaction under alkaline conditions [56, 57]. In the wet state, the elongation at break, up to 4% of crosslinker, decreased with the incubation time, while an increase was observed when 6% of BDDGE was used, as a consequence of the higher crosslinking degree achieved, leading to a denser and more compact structure. However for incomplete reactions (24h and 48h), at lower concentrations (2% and 4% v/v of BDDGE), the elongation and tensile strength was higher due to the plasticizing provided by the secondary hydroxyl groups and hydroxyl-terminated pendant groups from hydrolyzed un-reacted epoxides of BDDGE [39].

The tensile strength at break (TSB) is characterized by the maximum tensile stress supported before sample break. In both states (dry and wet) the TBS values decreased with the incubation time for each set and from the lower crosslinker concentration to the higher concentration. These variations can be attributed to the hydroxyl compounds from hydrolyzed un-reacted epoxides of BDDGE that may be attached to gelatin and can take part in weakening the interactions between protein chains, consequently enhancing the mobility of the macromolecules, reducing the Young's modulus and tensile strength and enhancing the elongation of electrospun meshes crosslinked with BDDGE [39].

For the human skin values of 2.9-150 MPa for Young's Modulus, 1-32 MPa for Tensile Strength and 17-207% for elongation at break can be considered as reference [58-61]. Several works have been demonstrating the similarity between the mechanical properties of skin tissue and electrospun meshes made by different materials and

production strategies [62-64]. In terms of mechanical properties, the gelatin electrospun meshes developed here exhibit values generally lower than natural skin, although this behavior can be easily improved by developing hybrid structures to mimic the mechanical properties of the skin.

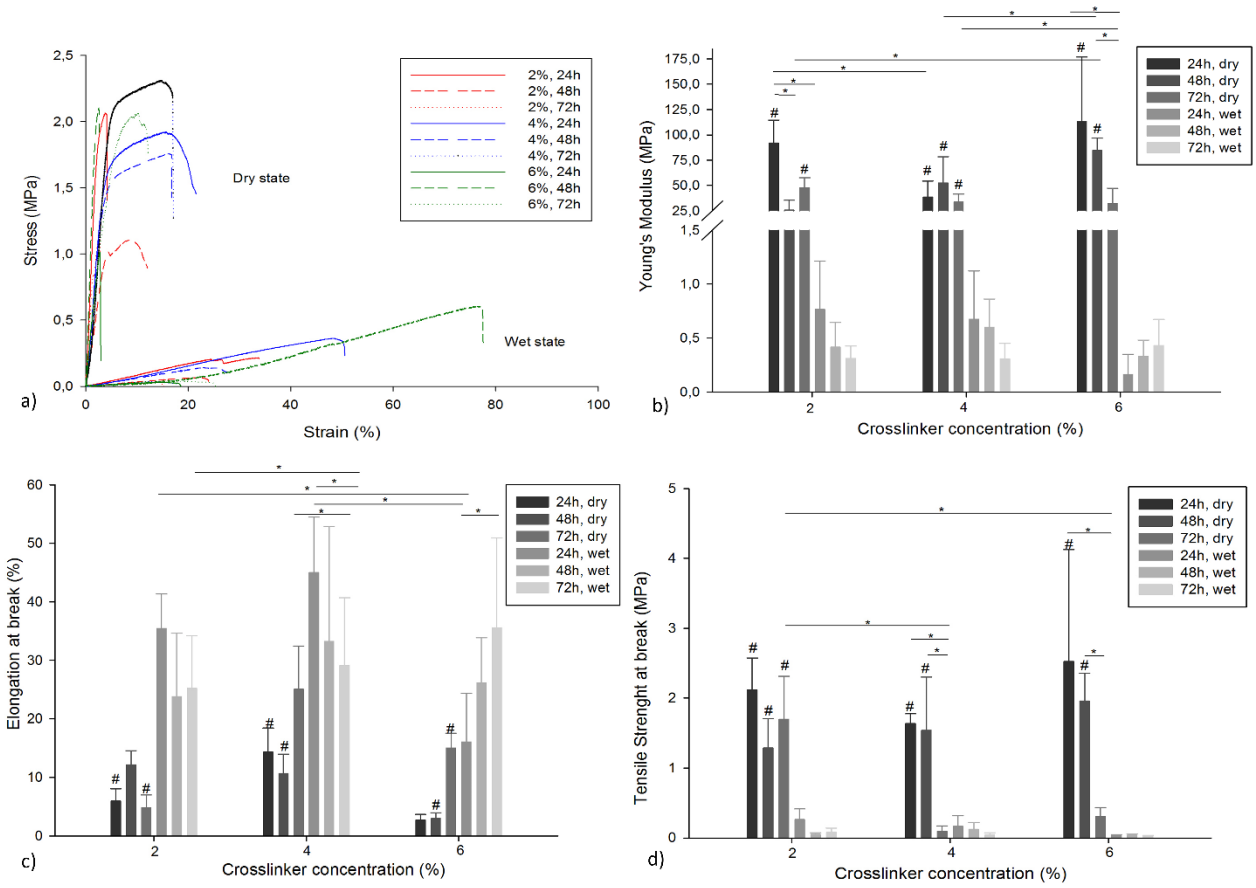

Figure V.4. Mechanical behaviour of electrospun gelatin meshes in the wet and dry state. a) Stress-strain representative curves. b) Young's Modulus. c) Elongation at break. d) Tensile strength at break. Statistical significance for p≤0.05 (*) and statistical significance for p≤0.05 compared to the same condition in wet state (#).

3.5. Biological behavior

The cytotoxicity of the electrospun meshes was assessed using samples crosslinked in BDDGE at different concentrations (2, 4 and 6%) during only 48h which, according to the previous results, are representative of low, medium and high crosslinking degrees (35.18%, 42.75% and 65.94%, respectively).

The results presented in Fig. V.5 show that fibroblasts remained metabolically active in all considered cases. After 24h no cytotoxicity was observed even for samples with high amount of crosslinker and the additional washing step did not influence the toxicity, either

in direct or indirect contact assays. In direct contact assays differences between samples with 2 and 6% of BDDGE exhibited statistical significance to the control (pre-washed or not). In indirect contact assays, statistically significant differences were observed between samples with 2% BDDGE (control and washed) and between samples with 6% BDDGE (control and non-washed samples). In indirect contact assays results show an increased metabolic activity of cells in indirect contact with samples compared to the control, which can eventually be explained by the release of uncrosslinked gelatin to the medium. Gelatin displays many integrin-binding sites for cell adhesion, migration, proliferation, and differentiation due to the abundant Arg–Gly–Asp (RGD) amino acid sequences in its protein chain, which may enhance the metabolic activity of cells [65].

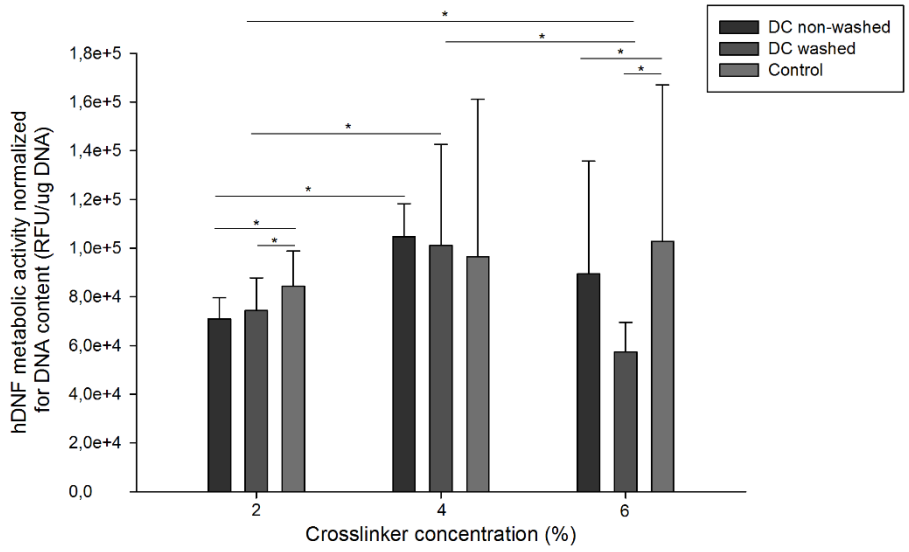

a)

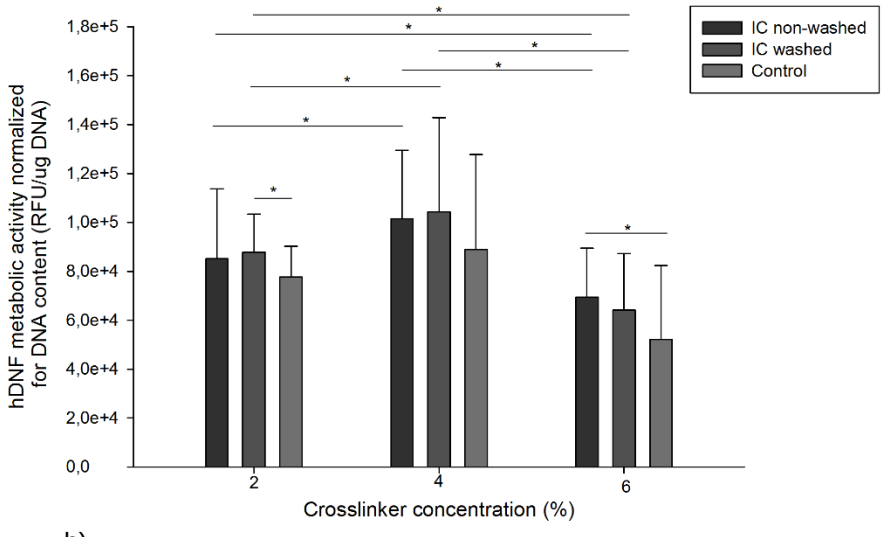

b)

Figure V.5. Cytotoxicity assessment of electrospun gelatin meshes crosslinked with 2, 4 and 6% of BDDGE for 48h. a) Direct contact (DC) and b) Indirect contact (IC) with hDNF cells, using as cells alone as control. Statistical significance for $p \leq 0.05$ (*).

The proliferation of fibroblasts seeded on the electrospun gelatin meshes crosslinked with 4% of BDDGE (72h) during 7 days was accessed using the metabolic activity assay and cell morphology was further observed by SEM and confocal microscopy. Samples with 4% BDDGE (72h crosslinking) were selected according to the previous results. Since no samples showed cytotoxic effects the selection was based on the combination of adequate crosslinking degree, stability and mechanical properties but providing the lower amount of crosslinker possible. As shown in Fig. V.6a fibroblasts cultured on the crosslinked gelatin electrospun meshes proliferated throughout the 7 days of culture. SEM images (Fig. V.6b) show the intimate interaction between the cells and the nanofibrous structures. From day 1 to day 7, in agreement with metabolic activity assessment, it is possible to observe an increase in cell number, as well as the integration and spreading of cells in the filamentous electrospun mesh. According to Jin and co-authors (2014) the integrin-binding sites available on gelatin promote cell adhesion and proliferation, and the nano-sized fibers encourage better cell proliferation and signaling [65].

Electrospinning presents a unique ability to fabricate nanofiber-based scaffolds that best mimic the nanometer scale of the native ECM of skin [66]. Consequently, electrospun skin substitutes have been claimed to have increased potential to promote better cellular attachment, growth and differentiation due the high surface area, high aspect ratio and high microporosity provided by the low fiber diameter structure [67-69], which seems to be confirmed in the present work. Confocal microscopy images (Fig. V.6b) of cells cultured on the electrospun meshes show the capability of fibroblasts to adhere and proliferate across the 7 days of culture and that they exhibit a proper phenotype, with a typical fibroblastic morphology. Additionally, after 7 days of culture, the production of fibronectin by the fibroblasts is clearly observed, sowing their ability to synthesize new ECM. Fibronectin is a large glycoprotein which plays an essential role in development, wound healing and angiogenesis [70].

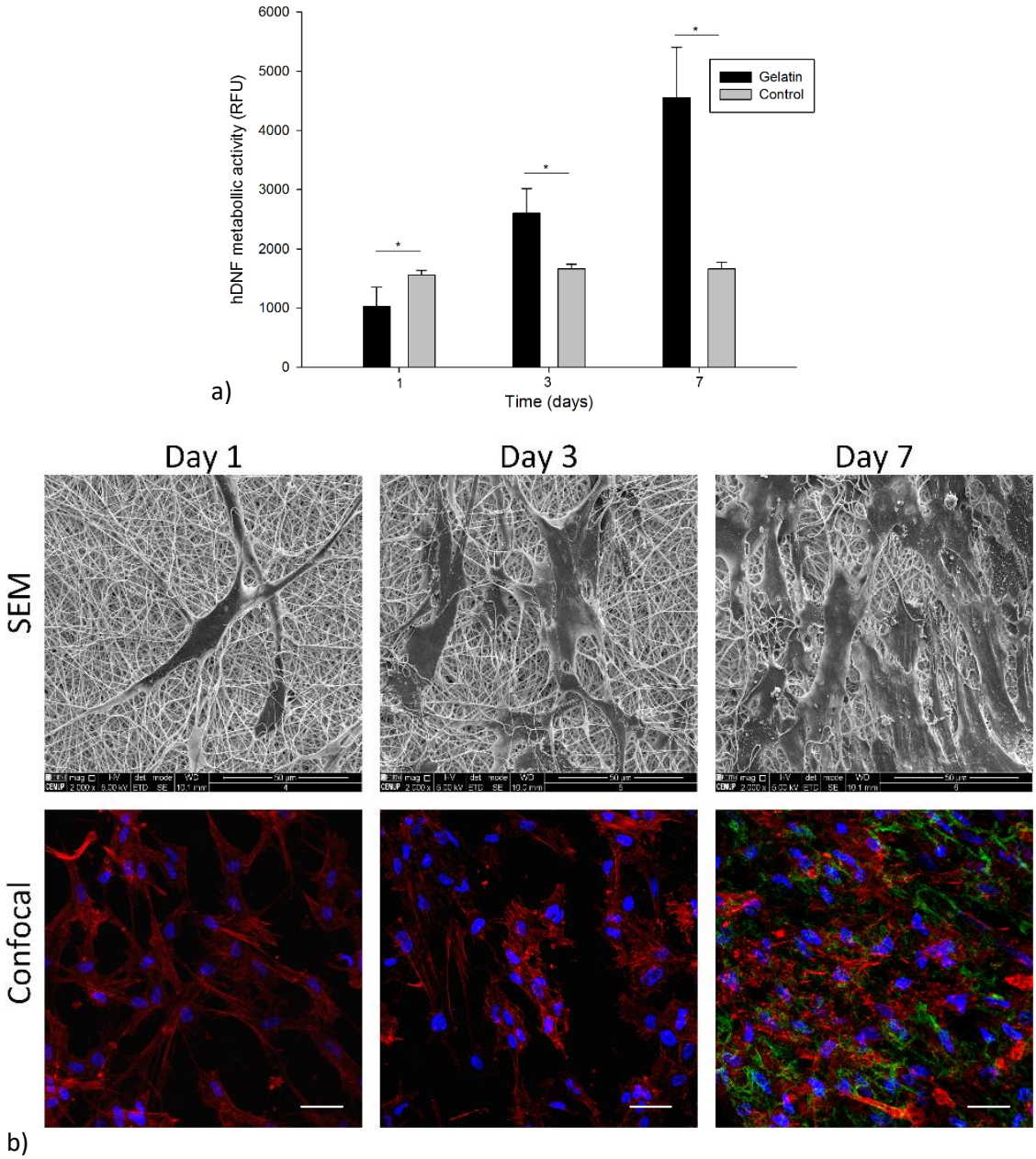

Figure V.6. Proliferation of hDNF cells on electrospun gelatin meshes. a) Metabolic activity, using electrospun meshes without cells as control. Statistical significance for p≤0.05 (*). Scale bars correspond to 50 μm; b) SEM and confocal microscopy images of cells cultured on electrospun meshes (blue: nuclei; red: actin; green: fibronectin). Scale bars correspond to 50 μm.

Gelatin is a cost-effective, biocompatible, biodegradable and cell-interactive material, known for not causing any adverse immune response [65]. However, its fast degradation in aqueous media, associated to usually low mechanical properties, considerably limit its application [71]. Hence, new non-toxic gelatin crosslinkers are fundamental to improve the potential application of this biomaterial for tissue engineering applications. BDDGE

is a widely used crosslinker in hyaluronic fillers already available in the market for several years. FDA determined that the use of unreacted BDDGE below 2 parts per million is safe since those trace amounts are prone to hydrolysis ultimately yielding CO_2 and water [26]. Martucci and colleagues (2015) described for the first time the use of BDDGE as crosslinker of gelatin for preparing biodegradable films for food packaging. According to this study, the films produced by casting with different percentages of BDDGE (0.5, 1 and 3%), revealed a great potential for food packing due to their non-toxicity and enhanced mechanical properties [39]. However, this paper reports for the first time the use of BDDGE as *in situ* crosslinker of electrospun gelatin nanofibers for biomedical applications. Due to its similarity with the native ECM, gelatin electrospun meshes have been previously investigated as dressings for wound healing and drug release, revealing promising properties [9]. However, most of the crosslinkers used are toxic and/or non-stable, inducing changes in the fiber morphology due to the crosslinking bath/vapor used after fibers production [9, 72]. The *in situ* crosslinking method used here represents a more effective crosslinking strategy than the traditional vapor crosslinking due to the homogenous mixing between polymer and crosslinker at the syringe prior to fiber formation [73]. The current study further demonstrates the possibility of modulating fiber diameter by controlling the *in situ* crosslinking parameters. Furthermore, the obtained electrospun meshes kept their morphology after the crosslinking process. Ultimately, gelatin electrospun meshes crosslinked with BDDGE shows great potential as wound dressings due to their ideal water vapor permeability rate, stability on aqueous medium, adequate swelling degree, non-toxicity and capability to promote fibroblasts attachment, proliferation and production of ECM proteins.

4. Conclusions

The main purpose of this research work was to explore, for the first time, the potential of crosslinking gelatin fibers with BDDGE, improving its stability in aqueous media and mechanical properties. BDDGE-crosslinked gelatin meshes were synthesized, characterized and tested regarding their toxicity and potential as wound dressing. Electrospun gelatin fibers crosslinked with BDDGE were successfully produced, allowing to obtain meshes with a well-defined morphology and random deposition. The crosslinking degree could be tuned changing the amount of crosslinker and the incubation time, which allowed the control of both fiber diameter and mechanical properties. 4% and 6% BDDGE (both incubated for 72h) provided gelatin fibers with high crosslinking degree and stable diameters of 339 ± 91 and 276 ± 88 nm, respectively, although 4% BDDGE resulted in the best combination of mechanical properties. Cytotoxicity assays revealed no toxicity and proliferation assays showed that fibroblasts

were able to attach and proliferate, producing new extracellular matrix within the electrospun meshes. Overall, this study demonstrated the potential of BDDGE as an alternative gelatin crosslinker due its non-toxicity and capability to tailor gelatin's mechanical and physical properties.

References

1. S. MacNeil, Progress and opportunities for tissue-engineering skin, Nature.445 **(**2007)874-80.
2. G. Casey, The physiology of the skin, Nursing Standard. 16 **(**2002)47-51.
3. S.S. Zhou,D. Li,Y.M. Zhou,J.M. Cao, The skin function: a factor of anti-metabolic syndrome, Diabetology & Metab Syndrom.4 **(**2012)1-11.
4. L. Yildirimer,N.T.K. Thanh,A.M. Seifalian, Skin regeneration scaffolds a multimodal bottom-up approach, Trends Biotechnol.30 **(**2012)638-48.
5. V.J. Reddy,S. Radhakrishnan,R. Ravichandran,S. Mukherjee,R. Balamurugan,S. Sundarrajan,S. Ramakrishna, Nanofibrous structured biomimetic strategies for skin tissue regeneration, Wound Rep Reg. **(**2013)211-16.
6. P. Zahedi,I. Rezaeian,S.O. Ranaei-Sidat,S.H. Jafari,P. Supaphol, A review on wound dressings with an emphasis on electrospun nanofibrous polymeric bandages, Polym. Adv. Technol. 21 **(**2009)77-95.
7. A. Vasconcelos,A.C. Gomes,A. Cavaco-Paulo, Novel silk fibroin/ elastin wound dressings, Acta Biomaterialia. 8 **(**2012)3049-60.
8. R.F. Pereira,C.C. Barrias,P.L. Granja,P.J. Bártolo, Advanced biofabrication strategies for skin regeneration and repair, Nanomedicine.8 **(**2013)603-21.
9. Y.Z. Zhang,J. Venugopal,Z.M. Huang,C.T. Lim,S. Ramakrishna, Crosslinking of the electrospun gelatin nanofibers, Polymer. 47 **(**2006)2911–2917.
10. A.G. Ward,A. Courts, The science and technology of gelatin, London:Academic Press, Inc.,**(**1977).
11. E.P. Broderick,D.M. O'Halloran,Y.A. Rochev,M. Griffin,R.J. Collighan,A.S. Pandit, Enzymatic stabilization of gelatin-based scaffolds, J Biomed Mater Res B Appl Biomater.72 **(**2005)37-42.
12. C.W. Yung,L.Q. Wu,J.A. Tullman,G.F. Payne,W.E. Bentley,T.A. Barbari, Transglutaminase crosslinked gelatin as a tissue engineering scaffold, J Biomed Mater Res Part A. 83 **(**2007)1039-1046.

13. K. Ulubayram,E. Aksu,S.I.D. Gurhan,K. Serbetci,N. Hasirci, Cytotoxicity evaluation of gelatin sponges prepared with different cross-linking agents, J. Biomater. Sci. Polym. **(**2002)1203–1219.
14. J.P. Draye,B. Delaey,A. Van de Voorde,A. Van Den Bulcke,B. De Reu,E. Schacht, In vitro and in vivo biocompatibility of dextran dialdehyde cross-linked gelatin hydrogel films. , Biomaterials. **(**1998)1677-1687.
15. H.W. Sung ,D.M. Huang,W.H. Chang,R.N. Huang,J.C. Hsu, Evaluation of gelatin hydrogel crosslinked with various crosslinking agents as bioadhesives: In vitro study., J. Biomed. Mater. Res. **(**1999)520–530.
16. R.R. Ray,S.C. Jana,G. Nanda, Immobilization of β-amylase from Bacillus megaterium B6 into gelatin film by cross-linking, J of applied bacterial. **(**1995)157-162.
17. S. Matsuda,H. Iwata,N. Se,Y. Ikada, Bioadhesion of gelatin films crosslinked with glutaraldehyde. , J Biomed Mater Res. **(**1999)20-7.
18. S.M. Lien,W.T. Li,T.J. Huang, Genipin-crosslinked gelatin scaffolds for articular cartilage tissue engineering with a novel crosslinking method, Mater. Sci. Eng. Biomim. Mater. Sens. Syst. **(**2008)36–43.
19. C.H. Yao,B.S. Liu,C.J. Chang,S.H. Hsu,Y.S. Chen, Preparation of networks of gelatin and genipin as degradable biomaterials, Mater Chem Phys. **(**2004)204-8.
20. A.A. Apostolov,D. Boneva,E. Vassileva,J.E. Mark,S. Fakirov, Mechanical properties of native and crosslinked gelatins in a bending deformation., J. Appl. Polym. Sci. **(**2000)2041-8.
21. Y. Ming-Kung,L. Yan-Ming,C. Kuang-Ming,D. Niann-Tzyy,L. Cheng-Che,Y. Jenn-Jong, A novel cell support membrane for skin tissue engineering: Gelatin film cross-linked with 2-chloro-1-methylpyridinium iodide., Polymer. **(**2011)996-1003;.
22. A. Bigi,G. Cojazzi,S. Panzavolta,K. Rubini,N. Roveri, Mechanical and thermal properties of gelatine films at different degrees of glutaraldehyde crosslinking, Biomaterials.**(**2001)763-768.
23. J.F. Martucci,A. Accareddu,R.A. Ruseckaite, Preparation and characterization of plasticized gelatin films cross-linked with low concentrations of glutaraldehyde, J.. Materials Sci.**(**2012)2382–3292.
24. J. Guo,L. Ge,X. Li,C. Mu,D. Li, Periodate oxidation of xanthan gum and its crosslinking effects on gelatin-based edible films, Food Hydrocolloids.**(**2014)243–250.
25. D. Enea,F. Henson,S. Kew,J. Wardale,A. Getgood,R. Brooks,N. Rushton, Extruded collagen fibres for tissue engineering applications: effect of crosslinking

method on mechanical and biological properties, Journal of Material Science: Materials in Medicine.**(**2011)1569–1578.

26. K. De Boulle,R. Glogau,T. Kono,M. Nathan,A. Tezel,J.-X. Roca- Martinez,S. Paliwal,D. Stroumpoulis, A review of the metabolism of 1,4-butanediol diglycidyl ether–crosslinked hyaluronic acid dermal fillers, Dermatologic Surg. **(**2013)1758–1766.
27. J. Zhang,X. Ma,D. Fan,C. Zhu,J. Deng,J. Hui,P. Ma, Synthesis and characterization of hyaluronic acid/human-like collagen hydrogels, Materials Science and Engineering: C.**(**2014)547–554.
28. W. He,Z. Ma,T. Yong,W.E. Teo,S. Ramakrishna, Fabrication of collagen-coated biodegradable polymer nanofiber mesh and its potential for endothelial cells growth, Biomaterials. **(**2005)7606–761.
29. M.-K. Yeh,Y.-M. Liang,K.-M. Cheng,N.-T. Dai,C.-C. Liu,J.-J. Young, A novel cell support membrane for skin tissue engineering: Gelatin film cross-linked with 2-chloro-1-methylpyridinium iodide, Polymer. **(**2011)996-1003.
30. I. ASTM, Standard test methods for water vapor transmission of materials, in E96/E96M-10.
31. R.C. Team, R: A language and environment for statistical computing., ed. R.F.f.S. Computing. 2014, Vienna, Austria.
32. F.J. O'Brien, Biomaterials & scaffolds for tissue engineering, MaterialsToday. 14 **(**2011)88-95.
33. C.A. Léon y Léon, New perspectives in mercury porosimetry, Advances in Colloid and Interface Science.76-77 **(** 1998)341–372,.
34. T. Garg,O. Singh,S. Arora,R.S.R. Murthy, Scaffold: A Novel Carrier for Cell and Drug Delivery, , Critical Reviews™ in Therapeutic Drug Carrier Systems.29 **(**2012)1-63.
35. T.M. Freyman,I.V. Yannas,L.J. Gibson, Cellular materials as porous scaffolds for tissue engineering, Prog Mater Sci. .46 **(**2001)273–82.
36. N. Cebi,M.Z. Durak,O.S. Toker,O. Sagdic,M. Arici, An evaluation of Fourier transforms infrared spectroscopy method for the classification and discrimination of bovine, porcine and fish gelatins, Food Chemistry. 190 **(**2016)1109–1115.
37. M. Nagarajan,S. Benjakul,T. Prodpran,P. Songtipya,H. Kishimura, Characteristics and functional properties of gelatin from splendid squid (Loligoformosana) skin as affected by extraction temperatures, Food Hydrocolloids.29 **(**2012)389–397.

38. D. Hashim,M.Y. Che,R. Norakasha,M. Shuhaimi,Y. Salmah,Z. Syahariza, Potential use of Fourier transform infrared spectroscopy for differentiation of bovine and porcine gelatins, Food Chemistry.118 **(**2010)856–860.
39. J.F. Martucci,J.P. Espinosa,R.A. Ruseckaite, Physicochemical properties of films based on bovine gelatin cross-linked with 1,4-butanediol diglycidyl ether, Food Bioprocess Technol. **(**2015)1645-1656.
40. R. Núñez-Flores,B. Giménez,F. Fernández-Martín,M.E. López-Caballero,M.P. Montero,M.C. Gómez-Guillén, Physical and functional characterization of active fish gelatin films incorporated with lignin, Food Hydrocolloids.39 **(**2013)243–250.
41. J. Bandekar, Amide modes and protein conformation, Biochimica et Biophysica Acta: Protein Structure and Molecular Enzymology.1120 **(**1992)123–143.
42. L. Shecter,J. Wynstra,R.P. Kurkjy, Glycidyl ether reactions with amines, Ind. Eng. Chem. .48 **(**1956).
43. R.G. Paul,A.J. Bailey, Chemical Stabilisation of Collagen as a Biomimetic, The Scientific World Journal.3 **(**2003)138–155.
44. M.M. Hohmann,M. Shin,G. Rutledge,M.P. Brenner, Electrospinning and electrically forced jets I stability theory, Phys. Fluid. **(**2001)2201–2220.
45. H.S. Azevedo,M.G. Francisco,R.L. Reis, In Vitro Assessment of the Enzymatic Degradation of Several Starch Based Biomaterials, Biomacromolecules.4 **(**2003)1703-1712.
46. G. Vargas,J.L. Acevedo,J. López,J. Romero, Study of cross-linking of gelatin by ethylene glycol diglycidyl ether, Materials Letters. 62 **(**2008)3656–3658.
47. N.V. Gupta,H.G. Shivakumar, Investigation of Swelling Behavior and Mechanical Properties of a pH-Sensitive Superporous Hydrogel Composite, Iranian Journal of Pharmaceutical Research.11 **(**2012)481-493.
48. H.K. Ju,S.Y. Kim,Y.M. Lee, pH/temperature-responsive behaviors of semi-IPN and comb-type graft hydrogels composed of alginate and poly(N-isopropylacrylamide), Polymer.42 **(**2001)6851- 6857.
49. S.-Y. Gu,Z.-M. Wang,J. Ren,S.-Y. Zhang, Electrospinning of gelatin and gelatin/poly(L-lactide) blend and its characteristics for wound dressing Materials Science and Engineering C. 29 **(**2009)1822–1828.
50. C.K. Field,M.D. Kerstein, Overview of wound healing in a moist environment, The American Journal of Surgery.16 **(**1994)2-6.
51. M. Abrigo,S.L. McArthur,P. Kingshott, Electrospun Nanofibers as Dressings for Chronic Wound Care: Advances, Challenges, and Future Prospects, Macromol. Biosci. .14 **(**2014)772-792.

52. L.O. Lamke,G.E. Nilsson,H.L. Reithner, The evaporative water loss from burns and the water-vapour permeability of grafts and artificial membranes used in the treatment of burns, Burns.3 **(**1977)159-165.
53. R. Dave,H.M. Joshi,V.P. Venugopalan, Biomedical evaluation of a novel nitrogen oxides releasing wound dressing, J Mater Sci: Mater Med.23 **(**2012)3097–3106.
54. S. Gustaitea,J. Kazlauskea,J. Bobokalonova,S. Perni,V. Dutschkc,J. Liesienea,P. Prokopovich, Characterization of cellulose based sponges for wound dressings, Colloids and Surfaces A: Physicochem. Eng. Aspects. 480 **(**2015)336–342.
55. P.I. Morgado,A.A. Ricardo,I.J. Correia, Asymmetric membranes as ideal wound dressings: An overview on production methods, structure, properties and performance relationship, Journal ofMembrane Science.490 **(**2015)139–151.
56. P.B. van Wachem,R. Zeeman,P.J. Dijkstra,J. Feijen,M. Hendriks,P.T. Cahalan,M.J.A. van Luyn, Characterization and biocompatibility of epoxy-crosslinked dermal sheep collagens, J. Biomed.Mater. Res.47 **(**1999)270-277.
57. R. Zeeman,P.J. Dijkstra,P.B. van Wachem,M.J.A. van Luyn,M. Hendriks,P.T. Cahalan,J. Feijen, Crosslinking and modification of dermal sheep collagen using 1,4-butanediol diglycidyl ether, J.Biomed. Mater. Res. .46 **(**1999)424-433.
58. H. Vogel, Age dependence of mechanical and biochemical properties of human skin, Bioengineering and the skin.3 **(**1987).
59. L. Jansen,P. Rottier, Some mechanical properties of human abdominal skin measured on excised strips, Dermatologica.117 **(**1985)65-83.
60. C. Jacquemoud,K. Bruyere-Garnier,M. Coret, Methodology to determine failure characteristics of planar soft tissues using a dynamic tensile test, Journal of Biomechanics. 40 **(**2007)468-475.
61. J.-f. Pan,N.-H. Liu,H. Sun,F. Xu, Preparation and Characterization of Electrospun PLCL/Poloxamer Nanofibers and Dextran/Gelatin Hydrogels for Skin Tissue Engineering, PLoS ONE. 9 **(**2014) e112885.
62. M. Gümüşderelioğlu,S. Dalkıranoğlu,R.S.T. Aydın,S. Çakmak, A novel dermal substitute based on biofunctionalized electrospun PCL nanofibrous matrix, J Biomed Mater Res Part A. 98 **(**2011)461-472.
63. D. Atila,D. Keskin,A. Tezcaner, Cellulose acetate based 3-dimensional electrospun scaffolds for skin tissue engineering applications, Carbohydrate Polymers. 133 **(**2015)251–261.
64. E.J. Lee,J.H. Lee,L. Jin,O.S. Jin,Y.C. Shin,S.J. Oh,J. Lee,S.-H. Hyon,D.-W. Han, Hyaluronic Acid/Poly(lactic-co-glycolic acid) Core/Shell Fiber Meshes Loaded

with pigallocatechin-3-O-Gallate as Skin Tissue Engineering Scaffolds, J. Nanosci. Nanotechnol.14 **(**2014)8458-63.

65. G. Jin,Y. Li,M.P. Prabhakaran,W. Tian,S. Ramakrishna, In vitro and in vivo evaluation of the wound healing capability of electrospun gelatin/PLLCL nanofibers, Journal of Bioactive and Compatible Polymers.29 **(**2014)628–645.
66. J.R. Dias,P.L. Granja,P.J. Bártolo, Advances in electrospun skin substitutes, Progress in Materials Science.84 **(**2016)314-334.
67. W. Cui,Y. Zhou,J. Chang, Electrospun nanofibrous materials for tissue engineering and drug delivery, Sci. and technol. Adv. Mater.**(**2010)11014108.
68. S. Pramanik,B. Pingguan-Murphy,N.A.A. Osman, Progress if key strategies in development of electrospun scaffolds: bone tissue, Sci. Technol. Adv. Mater.**(**2012)131-13.
69. W. Liu,S. Thomopoulos,Y. Xia, Electrospun nanofibres for regenerative medicine, Adv. Healthcare Mater.1 **(**2012)10-25.
70. A. Hielscher,K. Ellis,C. Qiu,J. Porterfield,S. Gerecht, Fibronectin Deposition Participates in Extracellular Matrix Assembly and Vascular Morphogenesis, PLoS ONE.11 **(**2016)e0147600.
71. A. Kasuya,S. Sobajima,M. Kinoshita, In vivo degradation and new bone formation of calcium phosphate cement–gelatin powder composite related to macroporosity after in situ gelatin degradation, J Orthop Res. 30 **(**2012)103-1111.
72. S.R. Gomes,G. Rodrigues,G.G. Martins,M.A. Roberto,M. Mafra,C.M.R. Henriques,J.C. Silva, In vitro and in vivo evaluation of electrospun nanofibers of PCL, chitosan and gelatin: A comparative study., Materials Science and Engineering C.46 348-358.
73. A.P. Kishan,R.M. Nezarati,C.M. Radzicki,A.L. Renfro,J.L. Robinson,M.E. Whitely,E.M. Cosgriff-Hernandez, In situ crosslinking of electrospun gelatin for improved fiber morphology retention and tunable degradation, J. Mater. Chem. B. 3 **(**2015)7930.

Part 4

Chapter VI

Hybrid Electrospun structures to promote skin regeneration

Hybrid Electrospun structures to promote skin regeneration|Chapter VI

Contents

1. Introduction

The largest vital organ in the body is the skin. It represents 7% of its total weight, being its main function to protect the human being against the external environment [1-5]. This layered tissue plays other important functions such as the control of the body

temperature, sense of touch or the synthesis of vitamin D [1, 6]. When skin damage occurs a consecutive cascade of events takes place to restore the skin structure and function [7, 8].This is known as wound healing, a process that consists, mainly in five different phases: hemostasis, inflammation, migration, proliferation and maturation, occurring sequentially after damage [7, 9]. Through this elaborate process the skin presents self-regeneration ability, although this capacity is strongly reduced in the case of full-thickness lesions, requiring for the use of a graft or dressing [4]. Despite the encouraging recent developments of new wound dressings and tissue engineering-based products, there is plenty of room for innovative strategies to promote skin tissue regeneration [10, 11]. Important advances have been made clinically with the use of PermaDerm® (Regenicin Inc., USA) and Apligraf® (Novartis, USA) [12], but a skin equivalent, able to fully replicate the important aspects of its functionality is yet to be developed. Over the last years electrospun meshes are have gained increasing attention through the combination of materials and processing strategies, which present great potential for skin regeneration [3].This year was certified the first company (Bioinincia, Spain) with the capability to scale up electrospinning technique for biomedical applications representing a great advance to materialise the research developed in this field [13]. Wound dressings prepared from electrospun nanofibers have been claimed to present exceptional properties compared to conventional dressings, such as improved promotion of haemostasis, absorption of wound exudates, adequate permeability, conformability to the wound, and avoidance of scar induction [9, 14-16]. The skin multilayer structure, with a mesh-like organization, can be mimicked by electrospinning technology [17]. New electrospinning processing strategies are thus being explored in which natural and synthetic materials are combined with new design approaches allowing the production of hybrid structures [17]. Several research works explored the development of hybrid structures combining different fiber diameters [18-20], different materials to improve the properties of the structure [21-23] or combining aligned/random fibers [24]. For skin regeneration most of the available works only explore the combination of materials and different fiber diameters, building structures without gradients[17].

In this work, we propose to combine the advantages of natural (gelatin) and synthetic (polycaprolactone) polymers into electrospinned nanofibers through different approaches to investigate the most suitable structure to promote skin regeneration. Polycaprolactone (PCL) is a well-known aliphatic linear polyester that has been extensively used in tissue engineering applications due to its biodegradability, biocompatibility, structural stability and mechanical properties [25, 26]. PCL presents semi-crystalline structure, hydrophobic nature and low bioactivity which reduces the cell

affinity and small tissue regeneration rates [27, 28]. To overcome these drawbacks we introduced into the structure gelatin, which is obtained through the collagen denaturation and is typically derived from bovine or porcine skin [29, 30]. Due to its biological origin, gelatin is similar to collagen and apparently is able to retain signals information such as the arginine–glycine–aspartic acid (RGD) sequence [12]. It also promotes differentiation and proliferation, which makes it an attractive polymer for tissue engineering [31-33]. Despite the similarity of gelatin with collagen, it presents better tensile modulus and possess excellent biodegradability, non-antigenicity, and cost efficiency as collagen [29, 34]. One of the major drawbacks of gelatin is that it dissolves as a colloidal solution at temperatures at 37 °C or above, and gels near room temperature [31, 35]. As such, gelatin electrospun meshes are often cross-linked or combined with synthetic polymers in order to maintain a fibrous structure [36, 37]

Here we explore three different processing strategies, multilayer, coating and blending to combine both materials into hybrid wound dressing structures capable of promoting skin regeneration. The main goal is to better mimic the skin ECM not only at the morphological point of view but, also, its mechanical and biological properties.

2. Materials and Methods

2.1 Materials & Methods

Poly (ε-caprolactone) (PCL) (Mw 50000 (g/mol), bulk density: 1.1g.cm-3) was kindly supplied by Perstorp and dissolved in acetone that was purchased to Sigma-Aldrich. Gelatin (Ge) powder of pig skin (type A, 300 bloom, 60 mesh) were kindly supplied by Italgelatine, and the acetic acid glacial was purchased from PanReac AppliChem. To increase the gel/AA solution conductivity was added, to the solution, 2% v/v of Triethylamine (TEA) purchased from Sigma Aldrich. BDDGE was provided from Alpha Aesar and used as crosslinking agent of gelatin without any further purification. A gelatin/AA/TEA solution (15 wt-%) and PCL/DMK (17wt-%) was prepared for electrospinning by dissolving the polymers and stirred it at 37ºC overnight. The crosslinker was added and stirred immediately before the electrospun fibers' production. To the preparation of the blend solution PCL and Ge were dissolved in acetic acid and TEA (2 % v/v), (17 wt-% and 15 wt-%, respectively) and was stirred together during 2h before the production of the meshes. No crosslinker agent was added due the hydrogen bonds formed between materials which stabilized gelatin in aqueous solution [38].

Pure PCL and gelatin meshes have been used as controls. Gelatin was crosslinked with 1,4-butanediol diglycidyl ether (BDDGE) according to our previous chapter.

2.2 Electrospun meshes preparation

Polymeric nanofibre meshes were processed by using a specially designed electrospinning machine using a single jet approach. Control samples were produced with pure PCL and Ge while the hybrid structures resulted from a combination of both polymers using three distinct methodologies (Fig.VI.1). The multilayer structure was composed by 5 layers combining the materials (Ge/PCL/Ge/PCL/Ge). The 5 layers was defined in order to obtain a compact structure (with no physical separation between layers). The second reason was to guarantee that, independently of side (top or bottom), the first contact between the multilayer structure and cells occurs always with the same material. The blended mesh was produced after mixing both polymers in solution followed by spinning into one single fibre to obtain a filament that combined both materials and consequently obtain combined properties. Finally, we have used coating methodology which consisted in the electrospinning of a PCL fibre mesh production followed by immersion in a gelatin solution (5 w/v-% with 1 v/v-% of BDDGE) and drying at 37 ºC. The details regarding the different processing parameters are available in Table VI.1. The optimal processing parameters of PCL and Gelatin electrospun mesh were defined in previous work. Blend processing otimization is available on appendix A, section 3.

All the non-woven electrospun meshes were obtained at room temperature and relative humidity of 40-50 % using a syringe pump (SP11Elite, Harvard Apparatus) combined with a high voltage source (HV power supply, Gamma High Voltage Research, US) and a grounded copper plate as collector. Crosslinking of electrospun gelatin fibers was carried out through the incorporation of BDDGE on gelatin solution to avoid the loss of configuration that is usually induced by immersion in the crosslinking solution [39].

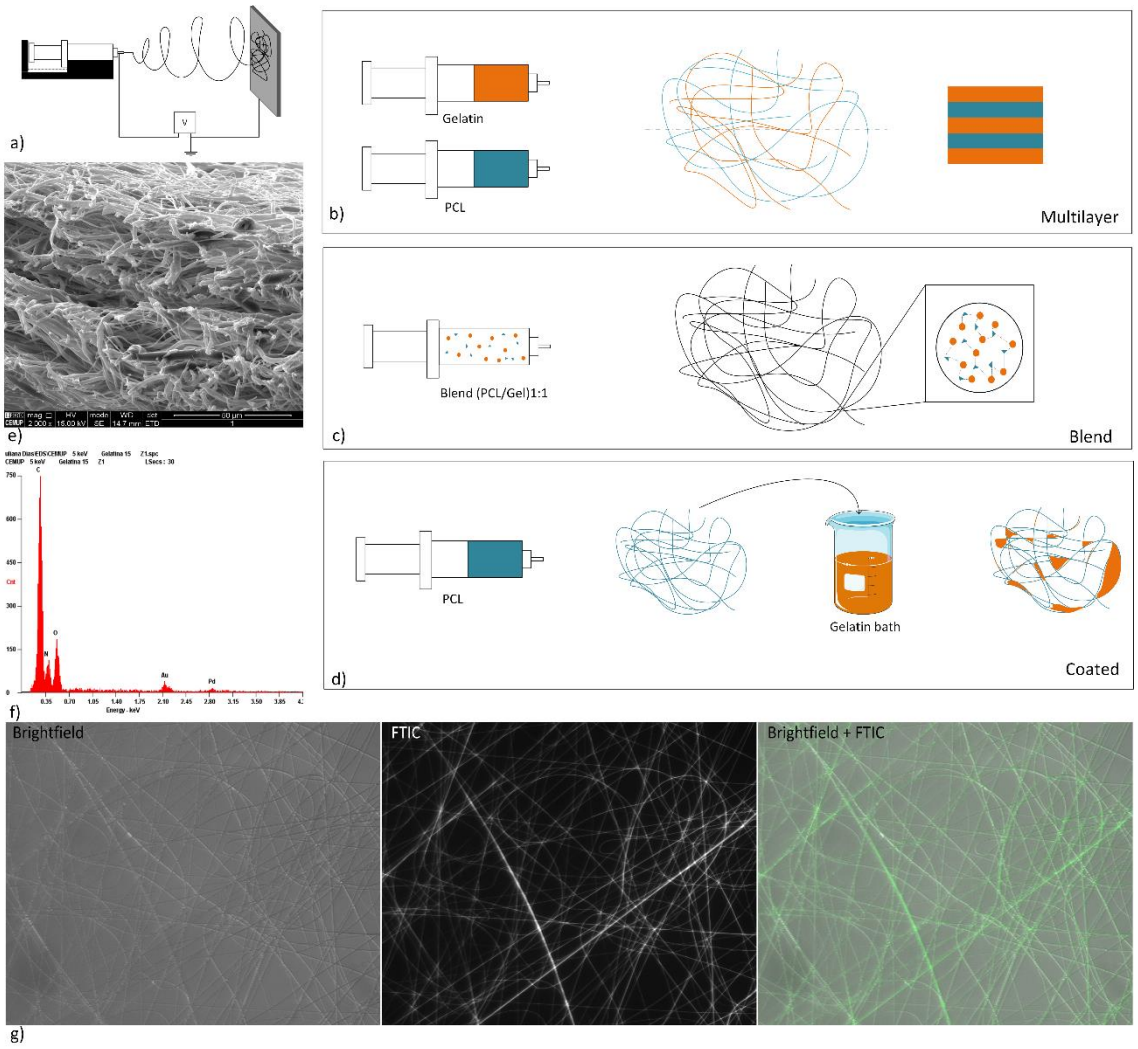

Figure VI.1. Representative scheme of methodologies used to prepare hybrid structures, a) electrospinning scheme, b) Multilayer methodology, c) Blend methodology, d) Coated methodology, e) SEM cross-section of multilayer mesh, f) EDS of coated mesh to demonstrate the presence of gelatin and PCL, g) Fluorescence microscopy image, gelatin was marked with FTIC to demonstrate the presence of PCL and Ge in the same filament.

Table VI.1. Processing parameters and after processing.

Electrospun mesh	Flow rate (mL/h)	Distance between collector and needle tip (cm)	Voltage (kV)	After processing
PCL	3.17	12	10	none
Gelatin	0.4	12	12	Incubation at 37ºC, during 72h
Multilayer	5 layers structure (Ge-PCL-Ge-PCL-Ge)			Incubation at 37ºC, during 72h
Coated	3.17	12	10	Immersion in a gelatin solution during 30 min followed by incubation at 37ºC, during 72h
Blend	0.3	12	12	None

2.3. Physicochemical characterization

2.3.1. Apparent density and porosity

The apparent density and porosity of electrospun meshes were calculated using equations (1) and (2) [40], respectively, where the mesh thickness was measured using a micrometer.

$$\text{Apparent density } \left(g \cdot cm^{-3}\right) = \frac{\text{mesh mass(g)}}{\text{mesh thickness (cm)} \cdot \text{mesh area (cm}^2\text{)}} \qquad (1)$$

$$\text{Mesh porosity} = \left(1 - \frac{\text{Mesh apparent density}(g \cdot cm^{-3})}{\text{Bulk density of PCL/gelatin}(g \cdot cm^{-3})}\right) \cdot 100\% \qquad (2)$$

2.3.2. Morphology and fiber diameter

The morphology of each electrospun fibrous mesh was examined by scanning electron microscopy (SEM) using a Quanta 400 FEG ESEM/EDAX Genesis X4M (FEI Company, USA) in CEMUP, University of Porto. Prior to examination samples were coated with a gold/palladium (Au/Pd) thin film, by sputtering, using the SPI Module Sputter Coater equipment. SEM images were also used to evaluate the fiber diameter distribution using Image J software. To each condition three individual samples were analyzed and fifty measurements per image were carried out.

2.3.3. Structure

Fourier transform infrared (FTIR) spectroscopy with attenuated total reflectance (ATR) was used to evaluate the chemical composition of the materials and to detect possible

structural changes. FTIR analyses were carried out using an Alpha-P Brucker FTIR-ATR spectrometer (Brucker, Belgium), in the range of 4000–500 cm^{-1}, at a 4 cm^{-1} resolution with 64 scans.

2.3.4. Water uptake

To assess the swelling degree samples were dried for 24h before weight determination, after which they were incubated in distilled water and sodium azide (0.02%) as bacteriostatic agent. After 24h of incubation samples were removed from the distilled water solution and weighted again to evaluate the swelling degree (eq. 4).

$$\text{Degree of sweeling } (\%) = \frac{W_w - W_d}{W_d} \cdot 100, \qquad (4)$$

where W_w is the wet weight and W_d is the dry weight.

2.3.5. Water vapor permeability

The water permeation rate of electrospun meshes was estimated. Glass bottles with the same size and type were filled with PBS solution and the electrospun meshes were fixed on their openings. The area available for vapor permeation was 2.39 cm^2. Evaporation of water through the mesh was monitored by the measurement of weight loss according to standard test methods for water vapor transmission [41]. Briefly, each set was weighted and kept at 32°C during 24h, after which the weight of each set was recorded again to quantify the amount of water evaporated.

2.3.6. Contact Angle

To assess the hydrophilicity of electrospun samples a static contact angle through optical contact angle was used (Data Physics, model: OCA 15 plus, Germany). The water contact angle was measured through the spread of droplets on the surface and recording its height and width. Each experiment was recorded during 1 minute.

2.3.7 Mechanical properties

The tensile strength and modulus of electrospun samples were determined in wet state using a texturometer (TA.XT Plus model, Stable Micro System SMD, England) with a 5N load cell. Testing was carried out in a controlled environment at RT and relative air humidity of 45%. The gauge length was 15 mm and the test speed was 1 $mm.s^{-1}$. At

least five individual samples were tested from each group and measurements were reported as mean ± standard deviation according the statistical method used (mixed effect model). All experiments were performed with samples thickness prior perform the tensile tests.

2.4. *In vitro* studies

Human dermal neonatal fibroblasts (hDNF) isolated from the foreskin of healthy male newborns (ZenBio, US) were cultured, expanded, and maintained in Dulbecco's modified eagle medium (DMEM) (Gibco, US), at 37ºC in a humidified atmosphere of 5% CO_2. The culture medium was changed twice a week and cells were trypsinized (0.25% trypsin/0.05% ethylenediamine tetraacetic acid (EDTA)/0.1% glucose in PBS (pH 7.5)) when they reached 70-80% of confluence. Cells from passages between 8 and 11 were used in this study.

2.4.1. Cytotoxicity

To evaluate their cytotoxicity electrospun meshes were tested in direct (samples) and indirect (leachables) contact under pre-washed in ultrapure water. Samples were sterilized with UV light followed by washing during 24h. hDNF cells were seeded in culture wells for 24h at a density of $2x10^4$ cells/well. 24h later, samples (direct contact) and culture medium having been in contact with samples (indirect contact) were incubated with the cells for another 24h. The culture medium was then removed from the wells and fresh basal medium with 20% v/v resazurin (Sigma) was added. Cells were incubated (37ºC, 5% v/v CO_2) for an additional 2h period, after which 300 µL per well were transferred to a black 96-well plate and measured (Ex at 530 nm, Em at 590 nm) using a micro-plate reader (Synergy MX, BioTek, US). The control consisted in cells alone.

For the quantification of the total double-stranded DNA (dsDNA) content, the cell pellets were recovered from wells and washed with phosphate buffered saline (PBS). The suspension was then centrifuged (10 000 rpm, 5 min) and then stored at -20ºC until further analysis. The dsDNA quantification was performed using the Quant-iT PicoGreen dsDNA kit (Molecular Probes, Invitrogen, US), according to the manufacturer's protocol. Briefly, the samples were thawed and lysed in 1% v/v Triton X-100 (in PBS) for 1h at 250 rpm at 4ºC. Then, they were transferred to a black 96-well plate with clear bottom (Greiner, AUT) and diluted in Tris-EDTA buffer (200 mM Tris–HCl, 20 mM EDTA, pH 7.5). After adding the Quant-iT PicoGreen dsDNA reagent, samples were incubated for

5 min at RT in the dark, and fluorescence was measured using a microplate reader (Ex at 480, Em at 520 nm).

2.4.2. Cell metabolic activity and proliferation

Cell metabolic activity and proliferation assays were performed using hDNF cells seeded on electrospun meshes at a cell density of $1x10^4$ cells per sample. To promote an efficient cell penetration into the mesh the seeding was performed with only 10 µL and incubated for 2 hours. 500 µL was then added and cultured during 14 days, changing the medium every 3 days. Metabolic activity was estimated using the resazurin-based assay and using electrospun meshes without cells as control. For the proliferation assay samples direct contact assay was performed with hDNF cells and pre-washed with ultrapure water. Afterwards, they were cultured for 14 days, and their metabolic activity was measured at days 1, 3, 7 and 14.

2.4.3 Cell morphology, fibronectin deposition and Ki-67 expression

For the studied time-points (1, 3, 7 and 14 days) cells seeded in electrospun meshes were stained for filamentous actin (F-actin), nuclei (Dapi), fibronectin (FN) deposition and ki-67 protein expression (ki67). Briefly, samples were washed with PBS, fixed for 20 min in 4 wt-% paraformaldehyde (PFA, Sigma), and permeabilized with 0.2% Triton X-100 (Sigma) for 7 min. Samples were then incubated for 1h with 1 wt-% bovine serum albumin (BSA, Merck) in PBS. For FN staining, electrospun meshes were incubated overnight at 4ºC with rabbit anti-fibronectin (f3648, Sigma, 1: 300) and then with the goat anti-rabbit secondary antibody Alexa Fluor® 488 $F(ab')_2$ fragment (Molecular Probes-Invitrogen, 1 : 2000, 2 h at RT). After this, samples were incubated with the conjugated probe phalloidin/Alexa Fluor® 594 (Molecular Probes-Invitrogen, 1: 40, 1 h at RT) for F-actin staining. For ki67 staining, electrospun meshes were incubated overnight at 4ºC with rabbit anti-ki67 (Ab15580, Abcam, 1: 200) and then with the goat anti-rabbit secondary antibody Alexa Fluor® 488 $F(ab')_2$ fragment (Molecular Probes-Invitrogen, 1: 1000, 2 h at RT). In both staining samples were subsequently washed three times with the PBS solution and nuclei were counterstained with 40,6-diamidino-2-phenylindole dihydrochloride (DAPI, Sigma, 0.1 $mg \cdot mL^{-1}$) in vectashield (vector), just before confocal visualization (CLSM, Leica SP2AOBS, Leica Microsystems) using LCS software (Leica Microsystems). The scanned Z-series were projected onto a single plane and pseudo-colored using ImageJ. The cells cultured in electrospun meshes were also visualized trough SEM to evaluate their morphology. Briefly, samples were washed with PBS, fixed for 30 min in 2.5 wt% glutaraldehyde (GA, Fluka), and dehydrated with a successive

graded ethanol series (40, 50, 70, 90 and 100%) for 15 min each. After that, critical point drying (CPD7501, Polaron Range) was performed to ensure the complete dehydration of samples.

2.5. Statistical analyses

All data points were expressed as mean ± standard deviation (SD). Statistical analysis (Levene's and T test) was carried out using IBM SPSS Statistics 20.0 with 99% confidence level for cytotoxicity assays. Linear mixed model (LMM) was used to test differences between the effects of composition in Young's Modulus, tensile strength at break and elongation at break. Composition was treated as a fixed factor and replication experiment was treated as a random factor to take into account possible heterogeneity of the samples in each set. Parameters' estimation was performed by lme package and multiple comparison adjustment was performed by mulcomp package from the R statistical software [42]. The results were considered statistically significant when $p \leq 0.05$ (*).

3. Results and discussion

3.1 Macroscopic and morphological characterization

Electrospun skin substitutes are demonstrating an increased potential to promote cellular attachment, growth and differentiation due the high surface area, high aspect ratio and high microporosity provided by the low fiber diameter structure [11, 43-45].

SEM morphological images of electrospun meshes for different methodologies and controls are shown in Fig. VI.2 (a-d). According to the SEM images, electrospun meshes obtained show uniform random deposition with continuous filaments well defined without presence of beads. Depending on the methodology there are distinct average diameters that can be visualized in table VI.2. For multilayer samples the average fiber diameter are 490 ±330 nm, in which the standard deviation is high as consequence of the average diameters corresponding to fibers from PCL and Gelatin and consequently the range of diameters is high. The coated methodology presents the fibers with highest diameters (2050 ± 700 nm) of methodologies as consequence of coating. After PCL electrospun preparation the gelatin bath make gelatin cover some filaments make it larger and fill some pores. With the blend methodology was possible to obtain the smallest fibers diameters (199 ± 107 nm) even compared to the control meshes, 417 ± 165 and 339 ±91 corresponding to PCL and Gel, respectively.

The skin ECM fibers, composed of collagen, elastin and fibrillin fibers , are reported to exhibit diameters between 10 and 300 nm, and the minimum fiber diameter required for fibroblast adhesion and migration, and maximum interfiber distance that fibroblasts are able to bridge, have been described as approximately 10 and 200 nm [11, 46, 47].

According to the above mentioned equations (Equations 1 and 2) the theoretical values for the porosity of the electrospun produced meshes range between 97.32 ± 0.83 (coated) and 98.78 ± 0.33 % (Gelatin) (Table VI.2). In the case of the coated methodology the value is below of 98% since the fibres were coated with the gelatin. Comparing gelatin and the other electrospun meshes (PCL, Multilayer and Blend) the porosity is similar between them (~98.5%).

Table VI.2. Properties of electrospun mesh structures.

Sample	Apparent density (g.cm $^{-3}$)	Porosity (%)	WVP (g/m^2/day)	Swelling degree (%)	Average fiber diameter (nm)	Contact angle (º) t=2s	Mechanical properties		
							Elastic Modulus (MPa)	Tensile Strength (MPa)	Elongation at break (%)
PCL	0.021 ± 0.003	98.11 ± 0.24	2365.50 ± 121.22	341.19 ± 68.34	417 ± 165	135.98 ± 6.62	5.41 ± 2.45	0.87 ± 0.37	219.97 ± 76.08
Gelatin	0.009 ± 0.002	98.78 ± 0.33	2292.69 ± 147.36	568.92 ± 67.28	339 ± 91	36.62 ± 15.83	0.31 ±0.15	0.04 ± 0.03	29.1 ± 11.60
Multilayer	0.017 ± 0.001	98.61 ± 0.04	2470.75 ± 171.34	354.87 ± 13.05	n.a.	101.58 ± 17.82	2.51 ± 0.71	0.34 ± 0.11	83.20 ± 14.84
Coated	0.033 ± 0.010	97.32 ± 0.83	1862.13 ± 182.58	149.29 ± 46.51	2050 ± 700	91.86 ± 5.25	7.47 ± 1.85	1.09 ± 0.13	64.13 ± 10.57
Blend	0.015 ± 0.003	98.80 ± 0.24	2466.57 ± 76.84	198.06 ± 33.05	199 ± 107	37.74 ± 17.82	4.61 ± 4.14	1.29 ± 1.24	69.40 ± 33.25

3.2 Physico-chemical and structural characterization

Fourier transform infrared spectrometry with attenuated total reflection (FTIR-ATR) analysis was performed to evaluate any interaction between synthetic and natural polymer in the hybrid structures developed, using the “raw” meshes as control. The different spectra obtained are shown in Figure VI.2 g). PCL spectrum is characterized by the presence of several bands being the most common at 1720.7 cm^{-1}, corresponding to the C=O bond characteristic in esters. Between 750 and 1500 cm^{-1} we can observe some bands corresponding to a CH_2 groups of PCL chain. Lastly, it can be observed two bands with 2863.69 cm^{-1} and 2941.57 cm^{-1}, corresponding to the CH bond. The FTIR spectra of gelatin shows pronounced bands in four different amide regions, specifically at 1700-1600 cm^{-1} corresponding to amide I, at 1565-1520 cm^{-1}, to amide II, at 1240-670 cm^{-1} to amide III, and at 3500–3000 cm^{-1} corresponding to amide A [48-52]. The absorption of amide I contains contributions from the C=O stretching vibration of amide group and a minor contribution from the C-N stretching vibration [48]. Amide II absorption is related to N-H bending and C-N stretching vibrations. Amide III presents vibrations from C-N stretching attached to N-H in-bending with weak contributions from C-C stretching and C=O in-plane bending [53]. In our FTIR results, corresponding to the hybrid electrospun meshes no chemical change was observed, being possible to detect the presence of both polymers in the same structure.

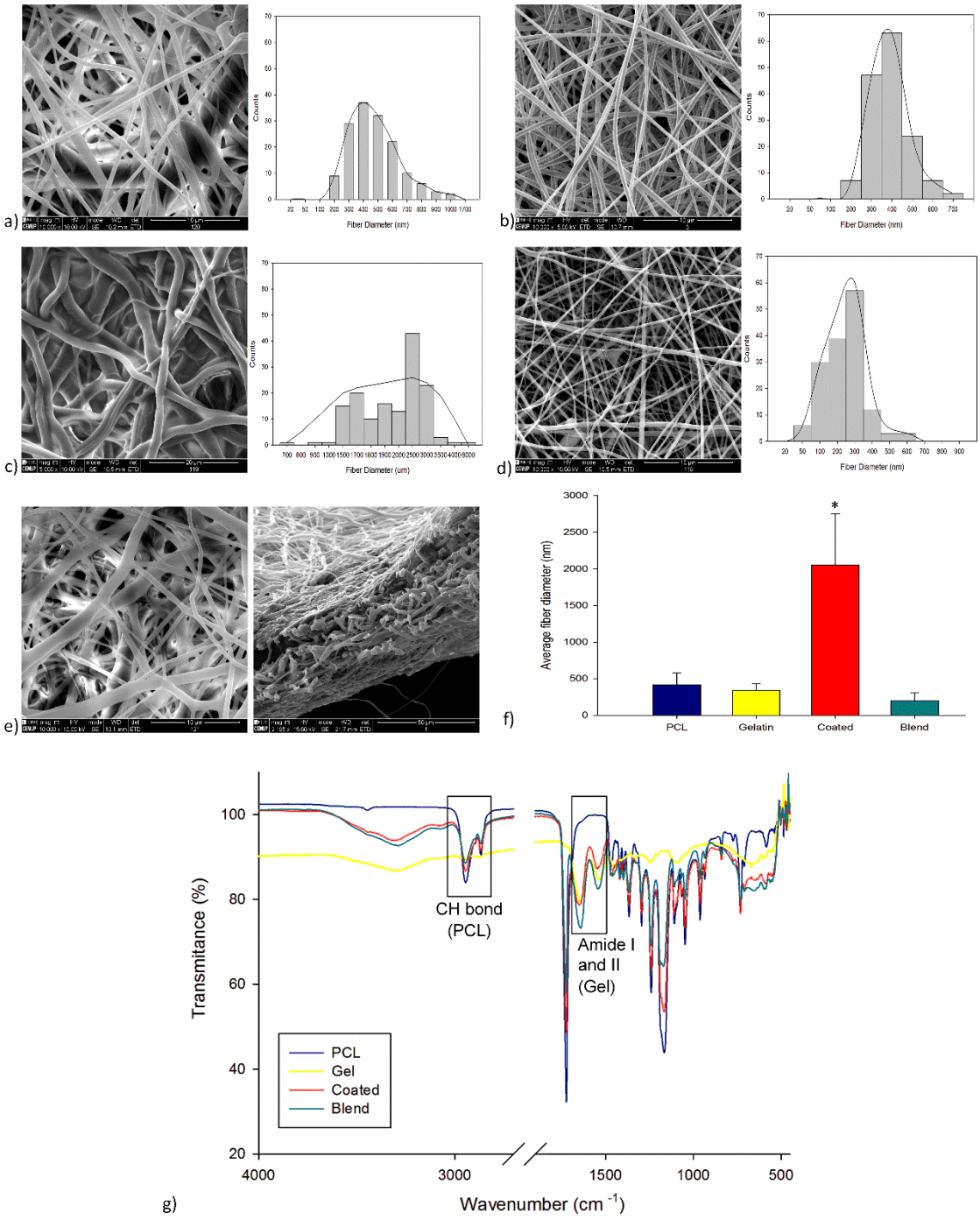

Figure VI.2. Scanning electron microscopy of hybrid structures and controls, a) PCL, b) Gel, c) Coated, d) Blend, e) Multilayer top and cross-section, f) comparative fiber average diameters, g) FTIR spectrums of electrospun meshes. Statistical significance for p≤0.05 (*). Scale bars: 10 µm, except c) that is 20 µm and e) cross-section that is 50 µm.

The water uptake of biodegradable polymers indicates the hydrophilic/hydrophobic character of the materials and therefore, their susceptibility to degradation by hydrolysis processes [54]. To evaluate the hydrophilic character of the electrospun meshes, the contact angle between the meshes was measured by the sessile drop technique. As known, PCL has a hydrophobic character [55]. In agreement, nanofiber meshes produced through electrospinning process presented an angle of 135.98 ± 6.62º (Table VI. 2). On the other hand, gelatin is characterized by its hydrophilic behaviour [56] and presented an angle of 36.62 ± 15.83º. The hybrid structures were, also, tested demonstrating a decrease of contact angle that are directly associated to the increase of hydrophilic character of sample through the incorporation of gelatin. Due to the intrinsic characteristics of electrospun meshes after 30 seconds all sample absorbed the water droplet, being the values above corresponding to the two seconds of test. In fact, the high porosity allows for the penetration of water throughout the meshes even when is made by hydrophobic material.

One of the most important feature of a wound dressing is to control the water loss evaporation at an optimal rate. The dressing should be permeable to keep a moist environment and prevent wound dehydration [57]. However, it is important to emphasize that a moist wound environment is not a wet wound environment, since excess of exudates will lead the patient to hypergranulation tissue formation in the wound bed and macerated periwound skin [57, 58]. Therefore, an important objective in providing topical wound care is selecting a dressing which can maintain a moist wound surface while being able to remove the produced exudate [57-59]. A healthy skin presents a permeation of 204 g/m2/day, while for injured skin, a first-degree burn, can range to 279 g/m2/day and for a granulating wound to 5138 g/m2/day [60, 61]. An ideal wound dressing must have a rate of 2500 g/m2/day to provide an adequate level of moisture without compromising wound dehydration [57, 60, 62]. The permeability of water vapor through the electrospun meshes produced ranges from 1862.13 ± 182.58 (Coated) to 2470.75 ± 171.34 g/m2/day (Multilayer). WVP is influenced by the pore size and interconnectivity between pores, small pores and packed fibers into the mesh decrease the permeability to the water vapor. The PCL mesh presents higher WVP than Gelatin. Despite the porosity of Gelatin being slightly higher the packing of fibers can be bigger due to lower diameter as compared to PCL fibers and for that reason the WVP is less than the PCL mesh. Looking to the hybrid structures, the Multilayer and Blend methodologies presents values in the range of the ideal permeation rate, 2470.75 ± 171.34 and 2466.57 ± 76.84 g/m2/day, respectively. However, the coated structure presents a WVP rate far from the ideal rate that is related to the lower porosity as

compared to the other methodologies, consequence of coating with gelatin that fill some pores.

The swelling degree of biodegradable polymers is correlated with its hydrophilic/hydrophobic character and, therefore, their susceptibility to degradation by hydrolysis processes [63]. The swelling increase the materials' flexibility and promotes changes in the dimensions of the implant material [64]. The processing methodologies have generated fiber meshes with distinct capabilities to uptake water. According to the swelling degree values shown in Table VI.2, Gelatin presents the higher swelling degree, consequence of its hydrophilic character. In spite of the hydrophobic character of PCL, the PCL structure demonstrated a great capability to retain water consequence of mesh high porosity. Coated structures have a swelling degree of 149.29 ± 46.51% which is the lowest value from all the processed fiber meshes, which is correlated with the fact that some pores were filled with gelatin limiting the water uptake. Regarding the Blend fiber meshes the swelling degree is also low compared to the other structures which can be related to the high packing of fibers due its low fiber diameter. The Multilayer structure presented the highest value of the hybrid meshes (354.87 ± 13.05%) because it combines, in the same structure, both materials in different layers which allows to keep the main characteristics of raw materials. In the same structure it was possible to increase the hydrophilicity and avoid the fiber packing due to the combination of fibers with a different range of diameters.

3.3 Mechanical properties

Electrospun meshes were investigated according different structures composition. Representative stress-strain curves are shown in the Figure VI.3a). From that was possible obtain the Young's Modulus (MPa), Elongation at break (%) and Tensile Strenght at break (MPa). Besides improving the adequate environment for cells to adhere and proliferate, one of the most important reasons to combine PCL with gelatin is to improve the poor mechanical properties of gelatin [56], which is possible to observe in Figure VI.3. An important objective of this study is to evaluate which hybrid structure matches closely skin mechanical properties. Pure PCL and Gelatin meshes where used as controls, corresponding to the best and the worst mechanical properties, respectively. The main idea behind developing hybrid structures is to achieve intermediate properties and according to the results (Fig. VI.3b), c) and d) and Table VI.2) it is notorious that the hybrid structures present improved properties (Young's modulus, Tensile strength at break and elongation at break) compared to pure Gelatin. The Young's Modulus of hybrid structures have not statistical significance when compared to the PCL, where PCL

presents 5.41 ± 2.45 MPa, Multilayer 2.51 ± 0.71 MPa, Coated 7.47 ± 1.85 MPa and Blend 4.61 ±4.14 MPa. Comparing the hybrid structures, the Multilayer and Coated show statistical significance, the last one presenting the higher elastic modulus even when compared to the PCL probably due to the lower porosity degree presenting a behavior more similar to a film than an electrospun mesh.

The tensile strength at break (TSB) is based on the maximum tensile stress supported by the sample before break. The Coated and Blend samples show the high values of TSB, followed by PCL, Multilayer and Gelatin. Only the Blend structure presents statistical significance when compared to Multilayer and Gelatin electrospun meshes.

Regarding to the elongation at break the PCL presents the highest value (219.97 ± 76.08) with statistical significance from other samples. Overall hybrid structures presented a better mechanical performance as compared to pure Gelatin.

Due to the heterogeneity of human skin, its mechanical properties presents a wide range of values [17]. Can be considered as reference values: 2.9-150 MPa for Young's Modulus, 1-32 MPa for Tensile Strength and 17-207 % for Elongation at break [65-68]. According to the results, in terms of mechanical properties, all hybrid structures show improved properties as compared to the gelatin electrospun mesh. There is no statistical significance between the studied mechanical parameters of Coated and Blend structures which are both stiffer then the Multilayer structure, closely mimicking the native skin mechanical properties. However, the standard deviation associated to the Blend structure can be related to the lack of fiber diameter homogeneity.

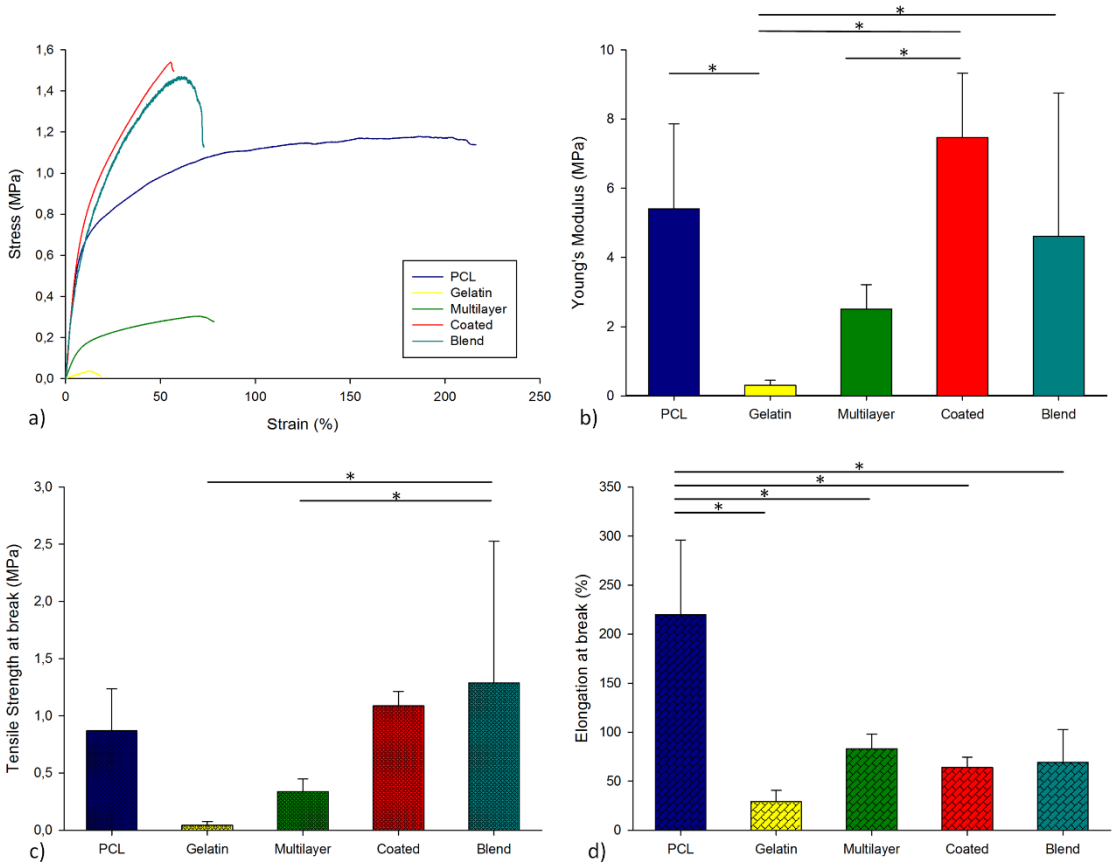

Figure VI.3. Mechanical behaviour at wet state, a) stress-strain representative curves; b) Young's Modulus, c) Tensile strength at break and d) Elongation at break. Statistical significance for p≤0.05 (*).

3.4 Cytotoxicity

The cytotoxicity of the produced electrospun meshes was performed to the hybrid structures and single structures. According to the results obtained (Fig. VI.4), fibroblasts remained metabolically active in all conditions tested. In the direct contact assay, after 24h, no cytotoxicity was observed for Gelatin, Multilayer and Coated samples. However, a slight decrease in the metabolic activity of PCL and Blend samples can be correlated with the presence of a small amount of solvent residues into the electrospun mesh. In the indirect assay no sample has present any toxicity.

From all the tested samples, the multilayer structures presented the higher metabolic activity in direct contact and PCL in the indirect contact assay.

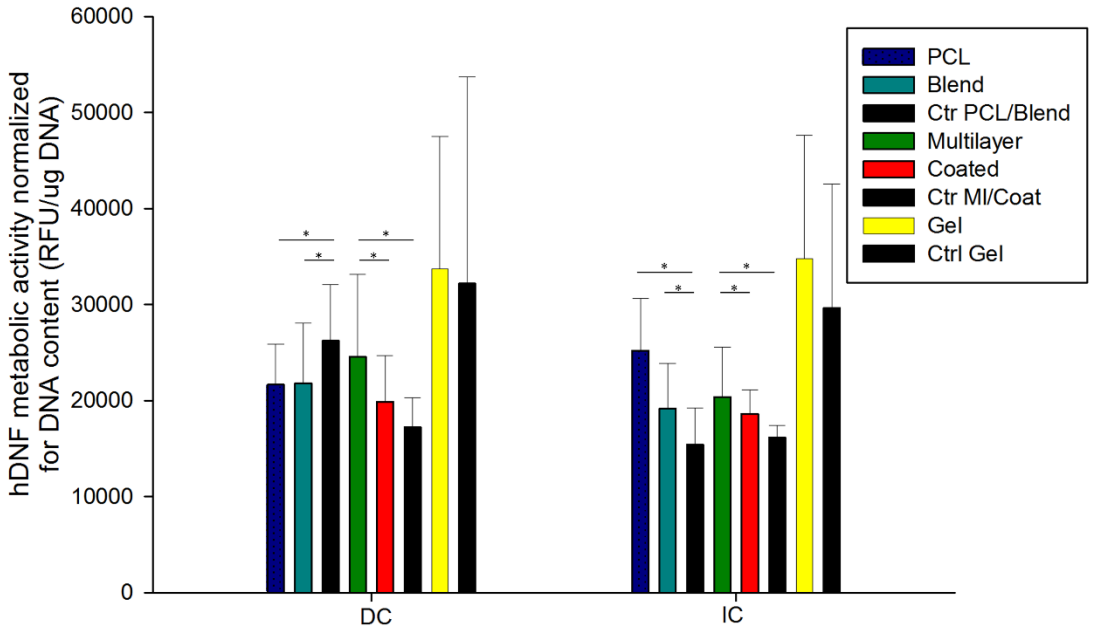

Figure VI.4. hDNF Metabollic activity normalized for DNA content of different methodologies. Statistical significance (*) p≤0.05.

3.5 Cell metabolic activity and proliferation

The proliferation of hDNF during 14 days seeded on electrospun meshes was accessed using the metabolic activity assay (Fig. VI.5) and cells morphology were further observed by SEM (Fig. VI.6) and confocal microscopy (Fig. VI.7 and VI.8). Throughout of 14 days the cells remaining metabolic active and increasing its activity between time-points.

According literature PCL does not have affinity to the cells due to its hydrophobic character [55]and on the other hand gelatin has many integrin-binding sites and thus can enhance the metabolic activity of cells. So is expected that the hybrid structures present better biologic activity than PCL electrospun meshes due the addition of gelatin. At day 1 the metabolic activity is low, probably due to the release of any residue of solvent, or cells are still adhering and adapting to the surface of the fibres, or some of them lost during the seeding. Though after it the hDNF activity increases consistently over the 14 days with statistical significance as compared with the control. Looking to the results at day 3, PCL presents the lowest activity and Blend the highest, additionally both are statistical different from the other samples. The other approaches presents similar results without statistical significance. At day 7 the PCL and Blend presents the same behavior that in the previous time-point. Its notorious that after 7 days of culture the hybrid structures present higher metabolic activity than Ge and this trend is kept up to 14 days. At the end of proliferation assay the hybrid structure with higher activity was the Coated followed by Multilayer and Blend structure. This important result clearly demonstrates that to promote the cell activity is necessary, not only, the adequate biological

environment but, also, the appropriate mechanical properties. According to Wells substrate stiffness affect in different ways the cell function, from the most simple point of view stiffness can regulate cell growth, viability and resistance to apoptosis [69]. Moreover, enough scaffold stiffness is crucial for anchorage-dependent cells helping it bonding to the matrix and proliferate [70]. However, the cell migration is commonly associated to an intermediate stiffness level [71]. The coated structure is stiffer than the other hybrid structures and the cells metabolic activity is higher up day 14, corroborate the literature.

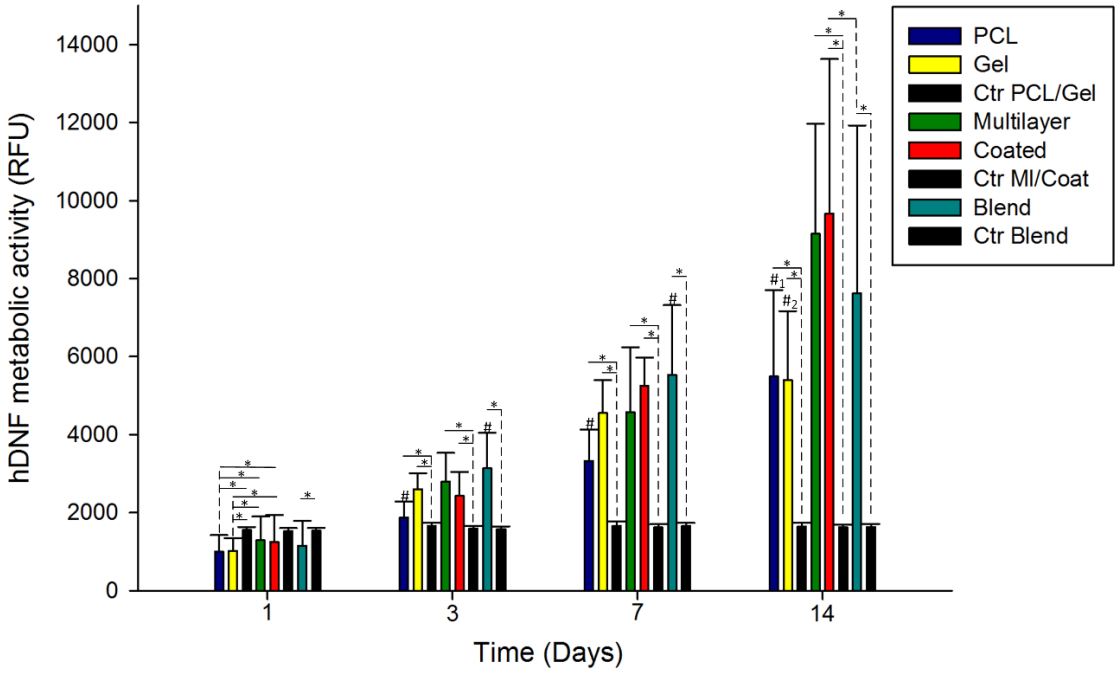

Figure VI.5. hDNF metabolic activity assay. The control were used electrospun meshes without cells seeded. Statistical significance for p≤0.05 (*) and '#' for statistical significance compared with all other samples, '$\#_1$'except gelatin, '$\#_2$' except PCL.

3.6 Cell morphology, fibronectin deposition and Ki-67 expression

Regarding SEM, after 24h it is possible to observe cells adhered to the nanofibers presenting the typical spindle-like fibroblast morphology, showing a higher degree of spreading with some extended lamellipodia over the surface of all the electrospun structures. Depending on the type of sample it is possible observe different amount of cells there are directly related to the hydrophilic/hydrophobic character of the structure. The seeding was made on the center of the structure but in the hydrophilic structures the seeding is automatically absorbed and the cells are spread around all structure. In the case of hydrophobic surface the cells take more time to spread across the structure and for that reason the cells density is higher in the center of sample. With time, cells spread

across all structures, although, at day 14 the PCL, Multilayer and Coated samples present an uniform film formed with cells at the structure' surface.

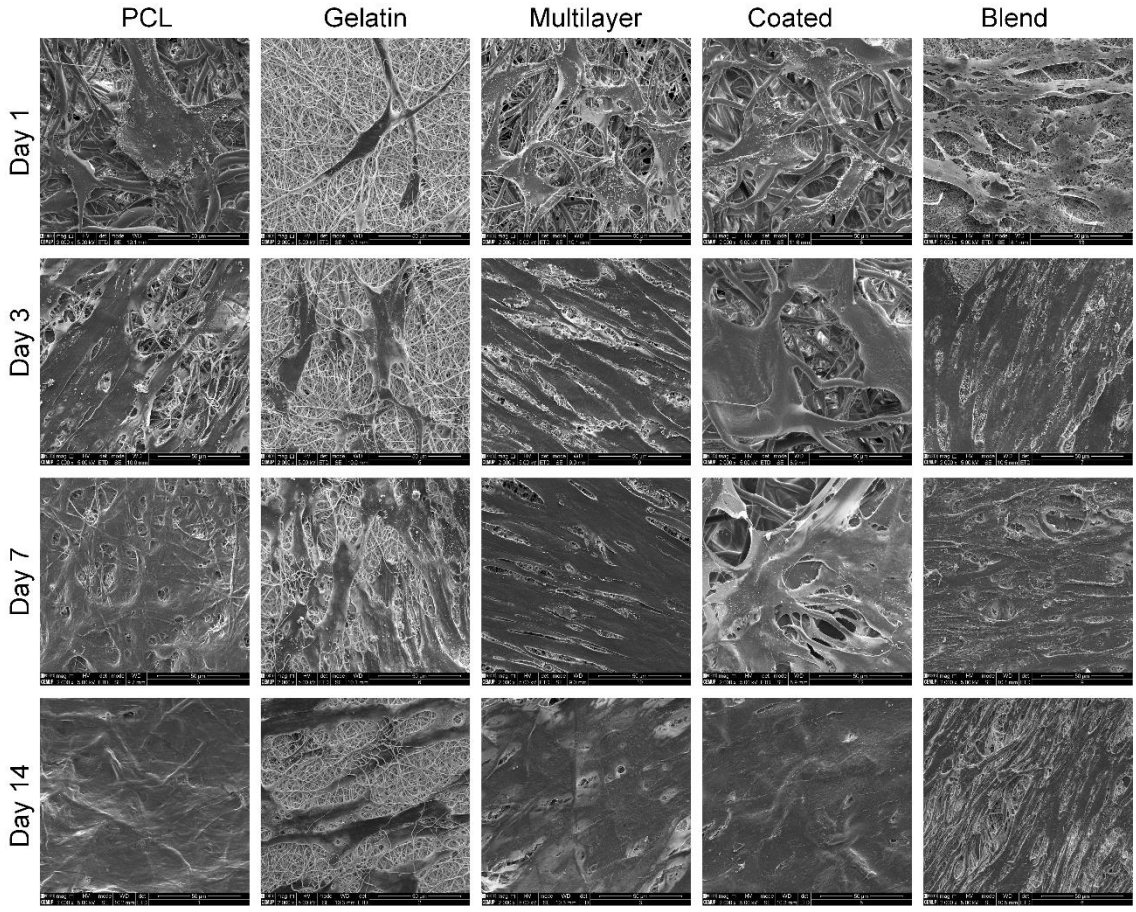

Figure VI.6. Scanning electron microscopy images representative of hDNF proliferation in different structures over 14 days (Scale bars: 50 µm).

Confocal microscopy was performed at day 1, 3, 7 and 14 of culture. Time-points of 1st and 14th day are represented in Figures VI.7 and VI.8, respectively. The time-points corresponding to day 3 and 7 can be found in appendix A, section 4. According to the images obtained, all structures present the typical fibroblastic morphology, increasing the number of cells with the culture time, correlating well with SEM observation. Fibronectin deposition was explored due to its importance in the wound healing process and the Ki-67 expression was evaluated due to its association to cell proliferation [72, 73]. Regarding to the images at Day 1, it is possible observe in PCL, Gelatin and Coated structures the interaction between cells. However, only in PCL, Coated and Blend samples have fibronectin deposition in a fibrillary form. In terms of cell proliferation all structures present Ki-67 protein but with highest expression in Gelatin, Multilayer and Blend structures. After 14 days of culture the presence of cytoskeleton, which provides a structural framework, facilitates intracellular transport, supports cell junctions and

transmits signals about cell contact, adhesion and motility, is lower in the Gelatin electrospun mesh, probably due to the poor structure stiffness. In the other electrospun meshes a complex cytoskeleton was observed with several cell junctions, forming a network exhibiting cell alignment, mostly in case of the Coated and Blend structures that is common occurs with aligned fibres.

In all structures the fibronectin has been deposited by the cells in a fibrillar form and comparing with the actin cytoskeleton location indicates that its distribution followed cellular organization. After 14 days the cells on PCL, Gelatin, Multilayer, Coated and Blend structures continues proliferating, although with higher expression of Ki67 marker in Multilayer structure.

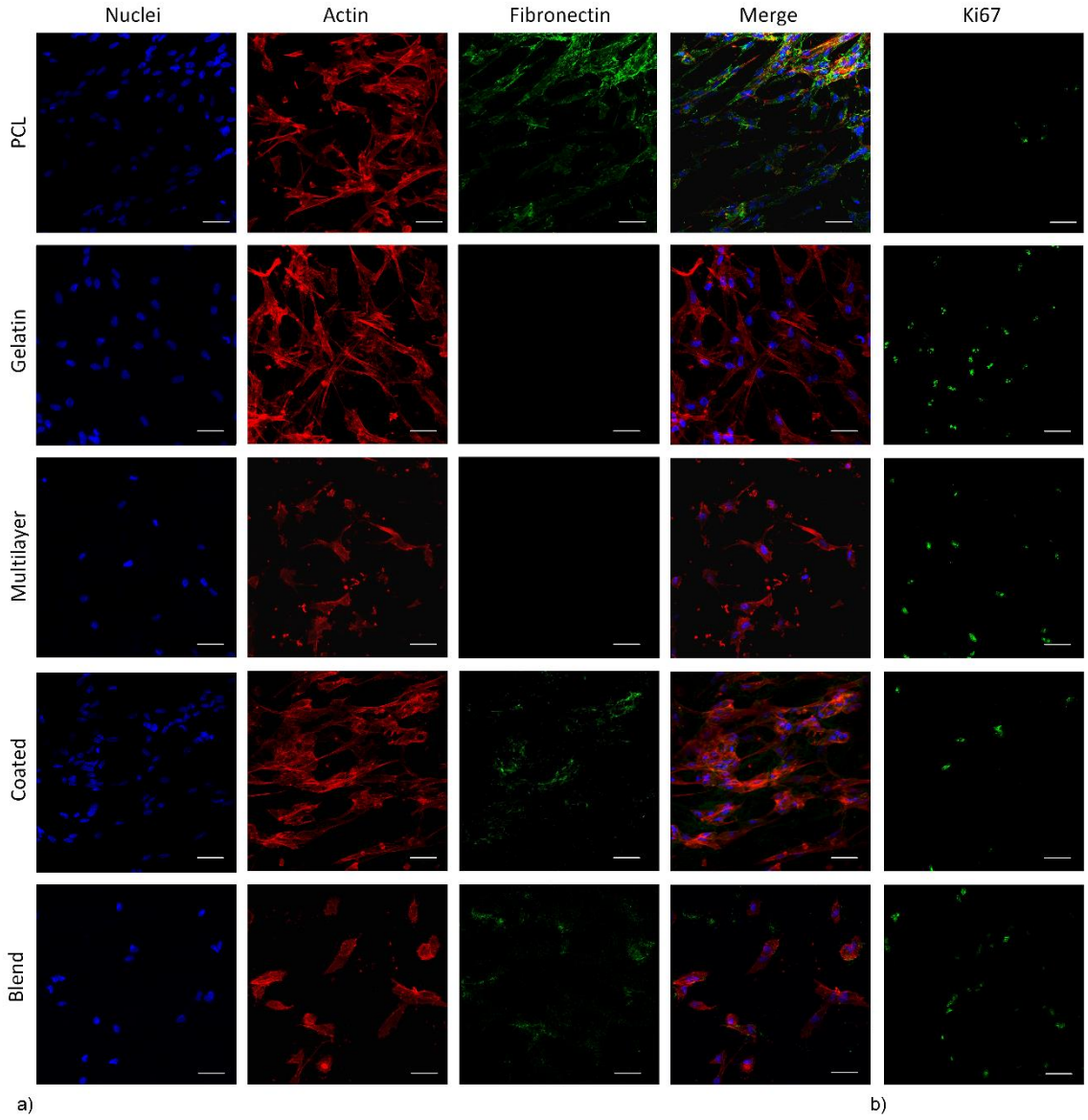

Figure VI.7. Confocal representative images after 1 day of hDNF culture, a) stained for nuclei (blue), F-actin (red), Fibronectin (green) and b) stained for Ki67 (green) (scale bars: 50µm).

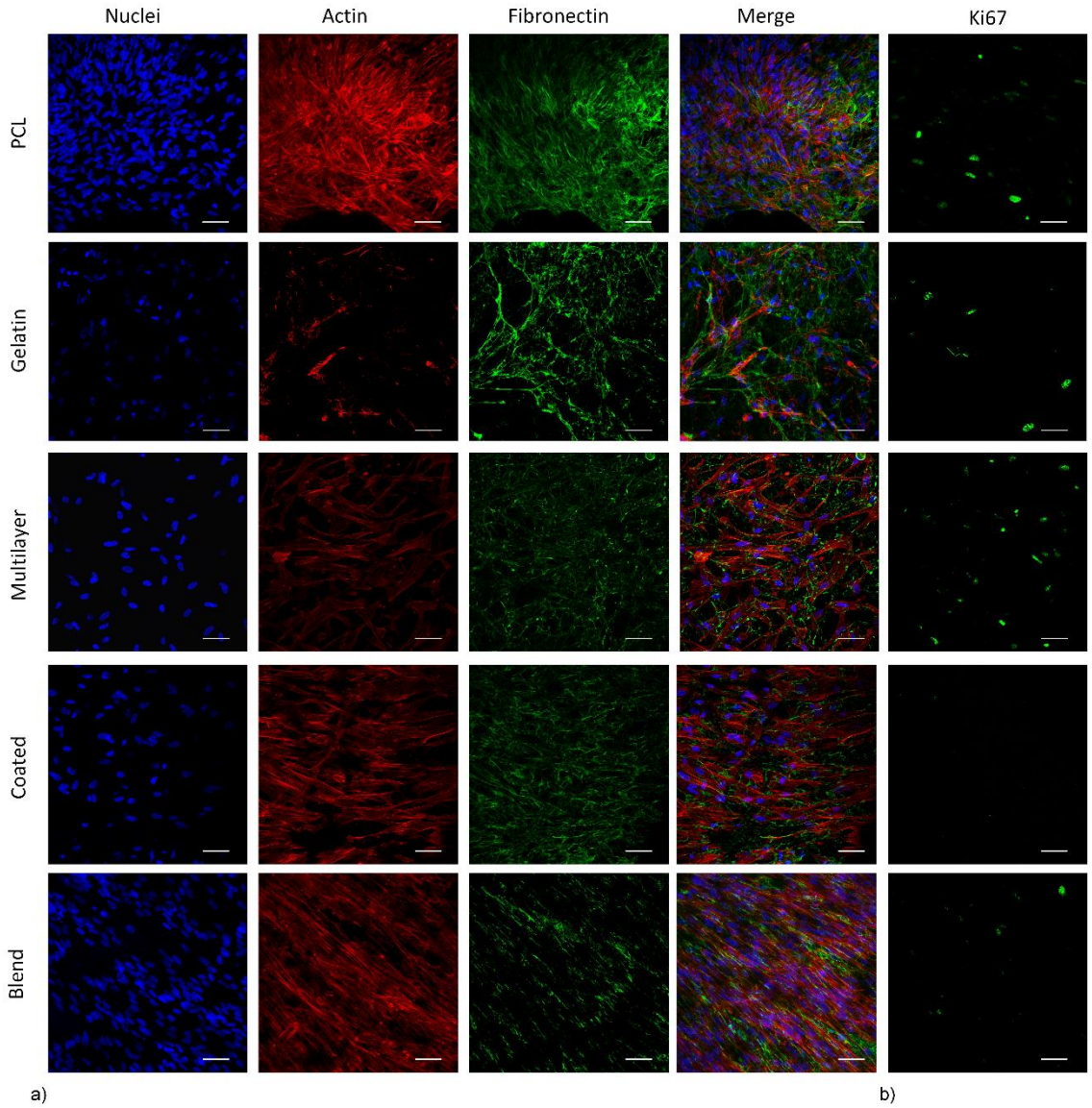

Figure VI.8. Confocal representative images after 14 day of hDNF culture, a) stained for nuclei (blue), F-actin (red), Fibronectin (green) and b) stained for Ki67 (green) (scale bars: 50µm).

PCL is a well-known biomaterial widely used in tissue engineering applications mostly due to its mechanical properties, although its hydrophobic nature limits its application in biomechanical systems [55]. On the other hand, gelatin presents many integrin bindings that are essentials to promote cell adhesion, differentiation and proliferation although presents poor mechanical properties [74]. The development of combined and functional structures has been highlighted as the most promisor strategy to overcome the limitations of each of the materials alone [17]. Most of the published works in the literature explore the combination of PCL with gelatin as a blend using different ratios and have evaluated the best performing formulation for a specific application [33, 38, 75, 76].

However, most of these studies evaluate the mechanical properties in dry state when final application is in moist environment.

Few works [77, 78] have been exploring the core/shell approach with PCL/Ge or vice-versa. Those studies described that is possible make fibers with well-defined core and shell demonstrating its potential for drug delivery systems and the possibility to tailor the fibers properties according materials concentration.

Planz et al., work evaluated two different approaches (Blend and Multimaterial) and demonstrated that fabricated a structure that mimic the biomechanical characteristics of native ECM in human skin [70]. However, gelatin fibers were used as sacrifice material to create a bio-adaptive hybrid structure, degrading into the cell culture medium and increasing the mesh porosity over time [70]. In our work are addressed and compared, for the first time, three different strategies to produce hybrid structures where PCL and Gelatin are combined according to different processing approaches (Blend, Multilayer and Coated). The current study demonstrates the impact of using different strategies to combine two widely studied materials into hybrid structures on several properties. This will affect the materials' properties and stability and ultimately the biological performance towards a wound dressing application. The compromise between the physical environments *vs* biochemical cues (adhesion points) is a key factor to favors the cell-matrix interactions.

Furthermore, the hybrid electrospun meshes obtained show different properties and performances being the most promisors the Multilayer and Blend structures. Both have shown to have a great potential as wound dressings due to their ideal water vapor permeability rate, adequate water uptake, hydrophilicity, non-toxicity and capability to promote fibroblasts attachment, proliferation and ECM production (fibronectin). The multilayer structure has the particularity of being easier to handle due to its multiscale fibers and, therefore, ideal to be used as wound dressing.

4. Conclusions

A correlation between the different electrospun hybrid structures using PCL and Gelatin was addressed in this work, targeting wound dressing applications. Hybrid structures were successfully developed combining the major advantages from individual PCL and Gelatin electrospun meshes make possible to obtain constructs with good mechanical and biological performance, fitting the requirements to promote an optimal wound healing process. According to the biological assays the use of toxic solvents and crosslinker does not induce any toxicity to the final structures and the hDNF cells can proliferate during 14 days. From the hybrid structures and according all characterization performed the

multilayer structure demonstrated to be the most promising strategy to be used as a combined processing route for wound dressing.

References

1. Casey, G., The physiology of the skin. Nursing Standard 2002. **16**: p. 47-51.
2. Yildirimer, L., N.T.K. Thanh, and A.M. Seifalian, Skin regeneration scaffolds a multimodal bottom-up approach. Trends Biotechnol, 2012. **30**: p. 638-48.
3. Reddy, V.J., et al., Nanofibrous structured biomimetic strategies for skin tissue regeneration. Wound Rep Reg 2013: p. 211-16.
4. MacNeil, S., Progress and opportunities for tissue-engineering skin. Nature, 2007. **445**: p. 874-80.
5. Zhou, S.S., et al., The skin function: a factor of anti-metabolic syndrome. Diabetology & Metab Syndrom, 2012. **4**: p. 1-11.
6. Lai-Cheong JE and McGrath JA, . Structure and function of skin, hair and nails. Medicine, 2013. **41**: p. 317-20.
7. Enoch S and Leaper DJ, Basic science of wound healing. Surgery, 2007. **26**: p. 31-7.
8. Tortora GJ and Derrickson B, Principles of Anatomy and Physiology 13th edition. 2012.
9. Zahedi, P., et al., A review on wound dressings with an emphasis on electrospun nanofibrous polymeric bandages. Polym. Adv. Technol 2009. **21**: p. 77-95.
10. Pereira, R.F., et al., Advanced biofabrication strategies for skin regeneration and repair. Nanomedicine, 2013. **8**: p. 603-21.
11. Dias JR, Granja PL, and Bártolo PJ, Advances in electrospun skin substitutes. Progress in Materials Science, 2016.
12. Pereira, I.H.L., et al., Elaboration and Characterization of Coaxial Electrospun Poly(ε-Caprolactone)/Gelatin Nanofibers for Biomedical Applications. Advances in Polymer Technology, 2014. **33**(1).
13. Climent, M., La primera fábrica del mundo de nanofibras 'bio', in El Mundo. 2017.
14. Rieger, K.A., N.P. Birch, and J.D. Schiffman, Designing electrospun nanofiber mats to promote wound healing – a review J. Mater. Chem. B, 2013. **1**: p. 4531.
15. Abrigo, M., S.L. McArthur, and P. Kingshott, Electrospun Nanofibers as Dressings for Chronic Wound Care: Advances, Challenges, and Future Prospects. Macromol. Biosci., 2014. **14**: p. 772-792.

16. Augustine, R., N. Kalarikkal, and S. Thomas, Advancement of wound care from grafts to bioengineered smart skin substitutes. Prog Biomater 2014. **3**: p. 103-113.
17. Dias, J.R., P.L. Granja, and P.J. Bártolo, Advances in electrospun skin substitutes. Progress in Materials Science, 2016. **84**: p. 314-334.
18. Grey CP, et al., Gradient fiber electrospinning of layered scaffolds using controlled transitions in fiber diameter. Biomaterials 2013. **34**(2013): p. 4993-5006.
19. Sundararaghavan HG and Burdick JA, Gradients with Depth in Electrospun Fibrous Scaffolds for Directed Cell Behavior. Biomacromolecules, 2011. **12**(2344-50).
20. Abrigo M, Kingshott P, and McArthur SL, Electrospun Polystyrene Fiber Diameter Influences Bacterial Attachment, Proliferation and Growth. Appl. Mater. Interfaces, 2015. **7**(14): p. 7644-52.
21. Tijing LD, et al., One-step fabrication of antibacterial (silver nanoparticles/poly(ethylene oxide)) e Polyurethane bicomponent hybrid nanofibrous mat by dual-spinneret electrospinning. Materials Chemistry and Physics 2012. **137**(2012): p. 557-61.
22. Jin G, Prabhakaran MP, and Ramakrishna S, Stem cell differentiation to epidermal lineages on electrospun nanofibrous substrates for skin tissue engineering. Acta Biomaterialia, 2011. **7**(2011): p. 3113-22.
23. Har-el Y-e, et al., Electrospun soy protein scaffolds as wound dressings: Enhanced reepithelialization in a porcine model of wound healing. Wound Medicine, 2014. **5**(2014): p. 9-15.
24. Park SH, et al., Creation of a hybrid scaffold with dual configuration of aligned and random electrospun fibers. Appl. Mater. Interfaces,, 2016: p. 1-27.
25. Okamoto M and John B, Synthetic biopolymer nanocomposites for tissue engineering scaffolds. Prog Polym Sci 2013. **38**(10-11): p. 1487-1503.
26. Dash TK and Konkimalla VB, Poly- e-caprolactone based formulations for drug delivery and Tissue engineering. J. Control. Release 2012. **158**: p. 15-33.
27. Patricio T, et al., Characterisation of PCL and PCL/PLA scaffolds for tissue engineering. Procedia CIRP, 2013. **5**: p. 110-114.
28. Gümüşderelioğlu M, et al., A novel dermal substitute based on biofunctionalized electrospun PCL nanofibrous matrix. J Biomed Mater Res Part A 2011. **98**(A): p. 461-472.
29. Joshi JR and Patel RP, Role of Biodegradable Polymers in Drug Delivery. International Journal of Current Pharmaceutical Research, 2002. **4**: p. 74-81.

30. Ige OO, Umoru LE, and Aribo S, Natural Products: A Minefield of Biomaterials. International Scholarly Research Network 2012(1-20).
31. Sell SA, et al., The Use of Natural Polymers in Tissue Engineering: A Focus on Electrospun Extracellular Matrix Analogues. Polymers, 2010. **2**: p. 522-553.
32. Khan MN, Islam JMM, and Khan MA, Fabrication and characterization of gelatin-based biocompatible porous composite scaffold for bone tissue engineering. Biomed Mater Res Part A, 2012. **100**: p. 3020-3028.
33. Gautam S, Dinda AK, and Mishra NC, Fabrication and characterization of PCL/gelatin composite nanofibrous scaffold for tissue engineering applications by electrospinning method. Materials Science and Engineering C 2013. **33**(1228-1235).
34. Nagiah N, et al., Development and characterization of coaxially electrospun gelatine coated poly (3-hydroxybutyric acid) thin films as potential scaffolds for skin regeneration. Materials Science and Engineering C 2013. **33**: p. 4444-4452.
35. Zhan J and Lan P, The Review on Electrospun Gelatin Fiber Scaffold. Journal of Research Updates in Polymer Science, 2012. **1**: p. 59-71.
36. Panzavolta S, et al., Electrospun gelatin nanofibers: Optimization of genipin cross-linking to preserve fiber morphology after exposure to water. Acta Biomaterialia, 2011. **7**: p. 1702-1709.
37. Yeh, M.-K., et al., A novel cell support membrane for skin tissue engineering: Gelatin film cross-linked with 2-chloro-1-methylpyridinium iodide. Polymer 2011(52): p. 996-1003.
38. Zhang, Y., et al., Electrospinning of Gelatin Fibers and Gelatin/PCL Composite Fibrous Scaffolds. Journal of Biomedical Materials Research Part B Applied Biomaterials 2005: p. 156-165.
39. Zhang, Y.Z., et al., Crosslinking of the electrospun gelatin nanofibers. Polymer 2006. **47** p. 2911–2917.
40. He, W., et al., Fabrication of collagen-coated biodegradable polymer nanofiber mesh and its potential for endothelial cells growth. Biomaterials 2005(26): p. 7606–761.
41. ASTM, I., Standard test methods for water vapor transmission of materials, in E96/E96M-10.
42. Team, R.C., R: A language and environment for statistical computing., ed. R.F.f.S. Computing. 2014, Vienna, Austria.
43. Cui, W., Y. Zhou, and J. Chang, Electrospun nanofibrous materials for tissue engineering and drug delivery. Sci. and technol. Adv. Mater., 2010: p. 11014108.

44. Pramanik, S., B. Pingguan-Murphy, and N.A.A. Osman, Progress if key strategies in development of electrospun scaffolds: bone tissue. Sci. Technol. Adv. Mater., 2012: p. 131-13.
45. Liu, W., S. Thomopoulos, and Y. Xia, Electrospun nanofibres for regenerative medicine. Adv. Healthcare Mater, 2012. **1**: p. 10-25.
46. Molly MS and Juliana HG, Exploring and engineering the cell surface interface. Science, 2005(310): p. 1135-1138.
47. Sun T, et al., Development of a 3D Cell Culture System for Investigating Cell Interactions With Electrospun Fibers. Biotechnology and Bioengineering, 2007. **97**(5): p. 1318-1328.
48. Cebi, N., et al., An evaluation of Fourier transforms infrared spectroscopy method for the classification and discrimination of bovine, porcine and fish gelatins. Food Chemistry 2016. **190**: p. 1109–1115.
49. Nagarajan, M., et al., Characteristics and functional properties of gelatin from splendid squid (Loligoformosana) skin as affected by extraction temperatures. Food Hydrocolloids, 2012. **29**: p. 389–397.
50. Hashim, D., et al., Potential use of Fourier transform infrared spectroscopy for differentiation of bovine and porcine gelatins. Food Chemistry, 2010 **118** p. 856–860.
51. Martucci, J.F., J.P. Espinosa, and R.A. Ruseckaite, Physicochemical properties of films based on bovine gelatin cross-linked with 1,4-butanediol diglycidyl ether. Food Bioprocess Technol, 2015(8): p. 1645-1656.
52. Núñez-Flores, R., et al., Physical and functional characterization of active fish gelatin films incorporated with lignin. Food Hydrocolloids, 2013. **39**: p. 243–250.
53. Bandekar, J., Amide modes and protein conformation. Biochimica et Biophysica Acta: Protein Structure and Molecular Enzymology, 1992. **1120**: p. 123–143.
54. Azevedo HS and Reis RL, Understanding the enzymatic degradation of biodegradable polymers and strategies to control their degradation rate, in iodegradable Systems in Tissue Engineering and Regenerative Medicine, Reis RL and San Roman J, Editors. 2005, CRC Press: Boca Raton, FL. p. 177-201.
55. Cipitria, A., et al., Design, fabrication and characterization of PCL electrospun scaffolds—a review. J. Mater. Chem., 2011, 21, 9419, 2011. **21**: p. 9419.
56. Xing, Q., et al., Increasing Mechanical Strength of Gelatin Hydrogels by Divalent Metal Ion Removal. Sci Rep., 2014. **4**: p. 4706.
57. Gu, S.-Y., et al., Electrospinning of gelatin and gelatin/poly(L-lactide) blend and its characteristics for wound dressing Materials Science and Engineering C 2009. **29** p. 1822–1828.

58. Field, C.K. and M.D. Kerstein, Overview of wound healing in a moist environment. The American Journal of Surgery, 1994. **16**(1A (SUPPL)): p. 2-6.
59. Abrigo, M., S.L. McArthur, and P. Kingshott, Electrospun Nanofibers as Dressings for Chronic Wound Care: Advances, Challenges, and Future Prospects. Macromol. Biosci. , 2014. **14**: p. 772-792.
60. Lamke, L.O., G.E. Nilsson, and H.L. Reithner, The evaporative water loss from burns and the water-vapour permeability of grafts and artificial membranes used in the treatment of burns. Burns, 1977. **3**(3): p. 159-165.
61. Dave, R., H.M. Joshi, and V.P. Venugopalan, Biomedical evaluation of a novel nitrogen oxides releasing wound dressing. J Mater Sci: Mater Med, 2012. **23**: p. 3097–3106.
62. Gustaitea, S., et al., Characterization of cellulose based sponges for wound dressings. Colloids and Surfaces A: Physicochem. Eng. Aspects 2015. **480** p. 336–342.
63. Hohmann, M.M., et al., Electrospinning and electrically forced jets I stability theory. Phys. Fluid. , 2001(13): p. 2201–2220.
64. Azevedo, H.S., M.G. Francisco, and R.L. Reis, In Vitro Assessment of the Enzymatic Degradation of Several Starch Based Biomaterials. Biomacromolecules, 2003. **4** p. 1703-1712.
65. Vogel, H., Age dependence of mechanical and biochemical properties of human skin. Bioengineering and the skin, 1987. **3**(67-91).
66. Jansen, L. and P. Rottier, Some mechanical properties of human abdominal skin measured on excised strips. Dermatologica, 1985. **117**: p. 65-83.
67. Jacquemoud, C., K. Bruyere-Garnier, and M. Coret, Methodology to determine failure characteristics of planar soft tissues using a dynamic tensile test. Journal of Biomechanics 2007. **40**(2): p. 468-475.
68. Pan, J.-f., et al., Preparation and Characterization of Electrospun PLCL/Poloxamer Nanofibers and Dextran/Gelatin Hydrogels for Skin Tissue Engineering. PLoS ONE 2014. **9**(11): p. e112885.
69. Wells, R.G., The Role of Matrix Stiffness in Regulating: Cell Behavior. Hepatology, 2008. **47**(4): p. 1394-1399.
70. Planz, V., et al., Three-dimensional hierarchical cultivation of human skin cells on bio-adaptive hybrid fibers. Integr. Biol., 2016. **8**: p. 775-784.
71. Discher, D.E., P. Janmey, and Y.-l. Wang, Tissue Cells Feel and Respond to the Stiffness of Their Substrate. Science, 2005. **310**: p. 1139-1143.
72. Hielscher, A., et al., Fibronectin Deposition Participates in Extracellular Matrix Assembly and Vascular Morphogenesis. . PLoS ONE, 2016. **11**(1): p. e0147600.

73. Scholzen, T. and J. Gerdes, The Ki-67 Protein: From the Known and the Unknown. Journal of Cellular Physiology, 2000. **182**: p. 311–322
74. Jin, G., et al., In vitro and in vivo evaluation of the wound healing capability of electrospun gelatin/PLLCL nanofibers. Journal of Bioactive and Compatible Polymers, 2014. **29**(6): p. 628–645.
75. Zheng, R., et al., The influence of Gelatin/PCL ratio and 3-D construct shape of electrospun membranes on cartilage regeneration. Biomaterials 2014. **35**: p. 152-164.
76. Yao, R., et al., Electrospun PCL/Gelatin composite fibrous scaffolds: mechanical properties and cellular responses. Journal of Biomaterials Science, Polymer Edition, 2016. **27**(9): p. 824-838.
77. He, M., et al., Fibrous guided tissue regeneration membrane loaded with anti-inflammatory agent prepared by coaxial electrospinning for the purpose of controlled release. Surface Science, 2015.
78. Gulfam, M., et al., Highly Porous CoreShell Polymeric Fiber Network. Langmuir, 2011. **27**: p. 10993–10999.

Part 5

Chapter VII

Concluding Remarks and Future Prospects

Concluding Remarks and Future Prospects |Chapter VII

In this work, a bold attempt was made to achieve a new wound dressing composed of electrospun fibers to promote wound healing. For this purpose, hybrid structures were developed to better mimic the skin 3D microenvironment.

The re-design of electrospinning apparatus was made successfully increasing the home-made system reproducibility through the replacement of most metallic parts by non-conductive components. The validation was made aided by SEM images obtained ranging the solution and processing parameters. From all samples prepared, the optimal conditions were defined as 17 wt-% of PCL dissolved in DMK and 15 wt-% of Ge dissolved in AA/TEA (2v/v-%). PCL meshes were produced with 10kV of voltage, a distance between needle and collector of 12 cm and a flow rate of 3.17mL/h. Ge electrospun meshes were prepared with 12kV, a distance between needle and collector of 12 cm and a flow rate of 0.4mL/h.

In vitro enzymatic degradation showed a weight loss of 97.1% after 90 days demonstrating the increase of degradation rate compared to the bulk material consequence of high surface area and porosity degree. *In vivo* results evidence that the pores size does not limit the cell infiltration, after 60 days a complete integration of electrospun meshes with surrounding tissues were verified. And, after 90 day of implantation a dense extracellular matrix components were produced indicating the possible degradation of electrospun meshes. *In vitro* and *in vivo* results demonstrated that PCL electrospun meshes are suitable for short-term applications.

A new methodology was explored successfully to induce an internal gelatin crosslinking to overcome its solubility in aqueous medium and keep the fiber morphology after crosslinking reaction. Moreover, ranging the reaction time and crosslinker amount was possible to tailor the fiber diameters and consequently the electrospun mesh properties.

Hybrid structures were design to mimic the skin ECM in terms of morphology and biomechanical properties. The hybrid structures obtained demonstrated that by exploring different processing strategies it is possible obtain structures with distinct properties. Biological assays proved that more than biological cues the mechanical structures properties had an important role to support the cell adhesion and proliferation.

Mechanical tests showed that hybrid structures provide similar properties to the native tissue. From the methodologies, the Coated approach demonstrated some limitations in terms of WVP rate and lower porosity degree consequence of the coating after electrospun fibers production. On the other hand, the Blend and Multilayer approaches fit most of the requirements to be an ideal wound dressing, although the thickness of Blend structure is a concern topic due to its weakness. Multilayer structure demonstrated be the most robust structure according the characterizations performed.

Concluding, the attained results suggest that hybrid structures show a huge potential to be used as wound dressing. Combining biological and mechanical properties in a wound dressing has an important role to the wound healing process. This study casts light on the improvement on electrospun structures preparation, exploring different processing approaches to achieve desirable properties. The development of these hybrid structures provided a further insight on wound dressing applications, benefiting from the advantage of the electrospun fibers similarity to the native skin ECM conjugated with the good polymer properties. At least, it should be underlined that no subject was completely explored and there is always room for improvement.

For future work, regarding the hybrid structures development, other approaches should be considered, optimized and characterized. Encapsulate drugs, growth factors or antibacterial agents into the fibers should be explored and optimized followed by a deep physical-chemical characterization.

The cellular adhesion and proliferation observed in all hybrid structures must be addressed to the poor cellular infiltration, commonly associated to the electrospun meshes. Additionally, a more comprehensive study should be directed to the *in vitro* and *in vivo* degradation kinetics of hybrid structures.

Related to the multilayer structure the integrity of the structure should be evaluated to guarantee its behavior as a complete structure avoiding layers' separation. The co-culture of fibroblasts and keratinocytes must be performed to evaluate the potential of the hybrid fiber mats for the hierarchical three-dimensional co-cultivation of different human skin cells.

Study the healing effect of hybrid structures after cutaneous application *in vivo* by evaluating it microbiologically, morphologically, and histologically.

Part 6

Appendix A – Supplementary data

Section 1 - Technical drawing

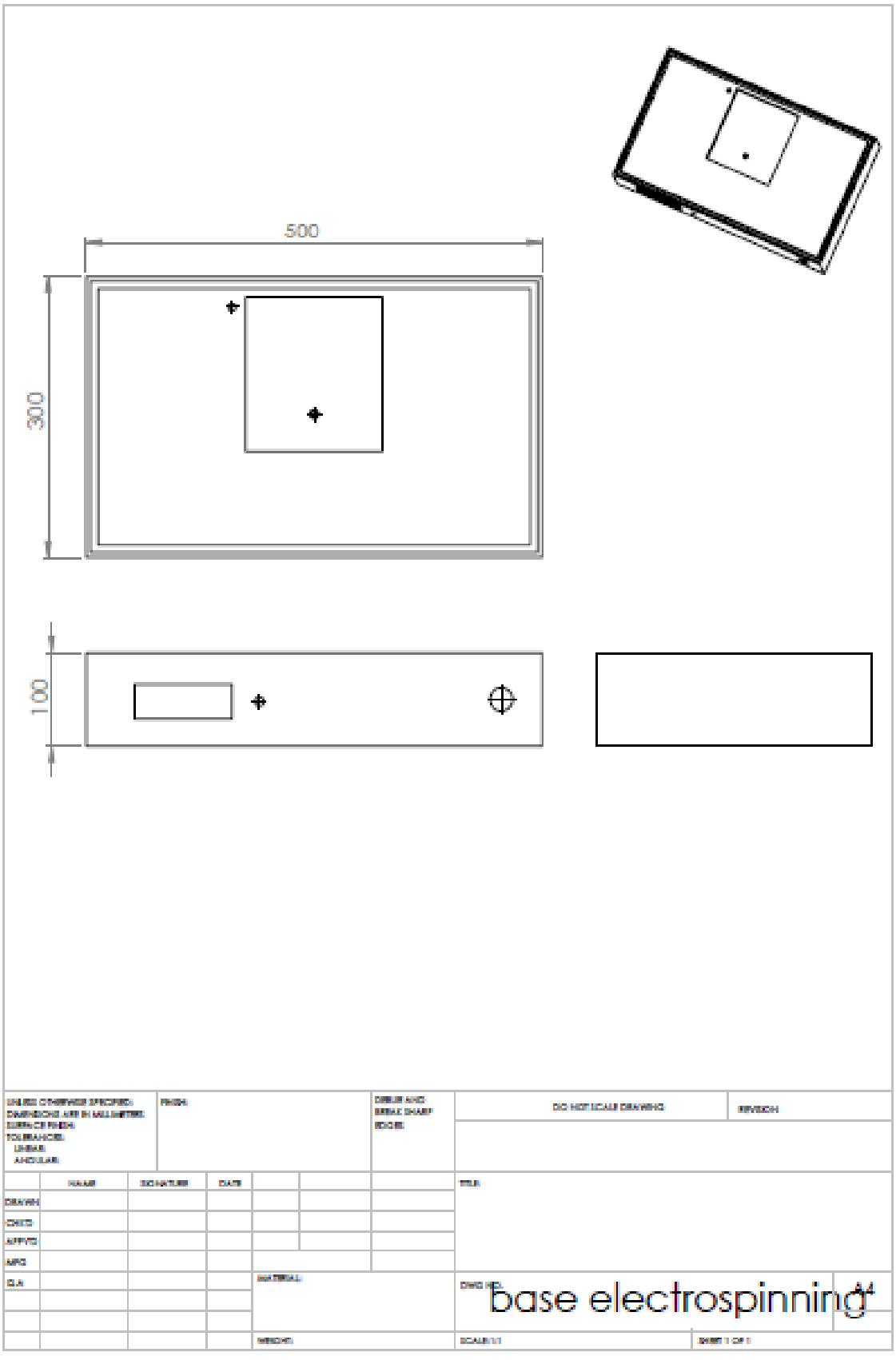

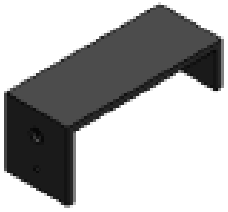

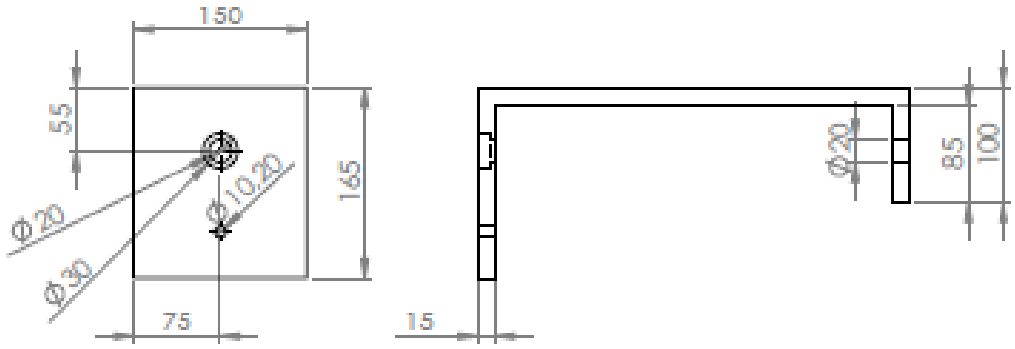

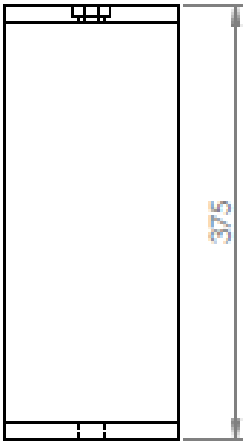

UNLESS OTHERWISE SPECIFIED: DIMENSIONS ARE IN MILLIMETERS SURFACE FINISH: TOLERANCES: LINEAR: ANGULAR:		FINISH:				BREAK SHARP EDGES:	DO NOT SCALE DRAWING
	NAME	SIGNATURE	DATE				TITLE:
DRAWN							
CHK'D							
APP'D							
MFG							
Q.A				MATERIAL:			DWG NO. Suporte
				WEIGHT:			SCALE:1:1

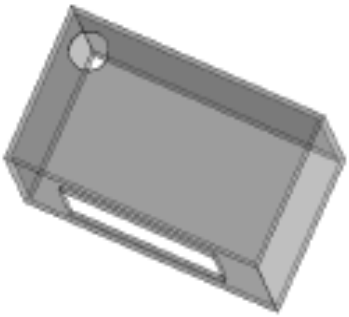

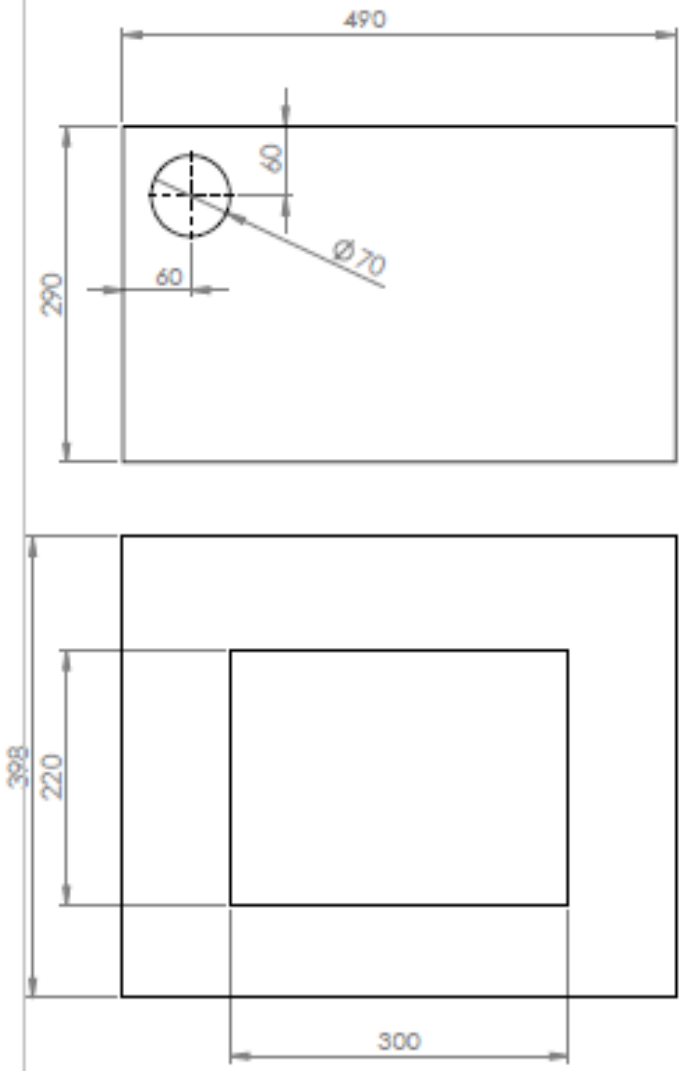

UNLESS OTHERWISE SPECIFIED: DIMENSIONS ARE IN MILLIMETERS SURFACE FINISH: TOLERANCES: LINEAR: ANGULAR:		FINISH:		BREAK SHARP EDGES	DO NOT SCALE DRAWING		REVISION
	NAME	SIGNATURE	DATE				TITLE:
DRAWN							
CHKD							
APPVD							
MFG							
Q.A				MATERIAL:		DWG NO.	A4
					acrilico		
				WEIGHT:		SCALE:1:1	SHEET 1 OF 1

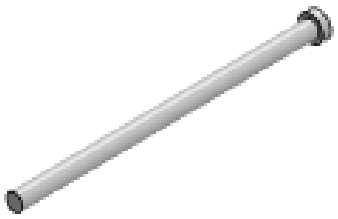

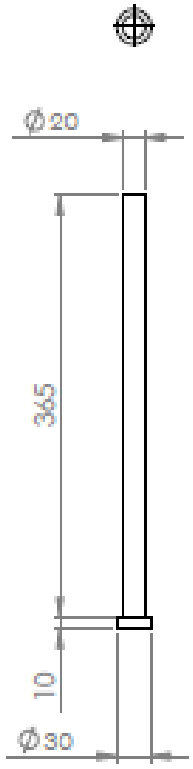

UNLESS OTHERWISE SPECIFIED: DIMENSIONS ARE IN MILLIMETRES SURFACE FINISH: TOLERANCES: LINEAR: ANGULAR:		FINISH:		DEBUR AND BREAK SHARP EDGES	DO NOT SCALE DRAWING		REVISION
	NAME	SIGNATURE	DATE				TITLE:
DRAWN							
CHK'D							
APP'D							
MFG							
Q.A.				MATERIAL:		DWG NO. varão	A4
				WEIGHT:		SCALE: 1:1	SHEET 1 OF 1

Section 2 – SEM images

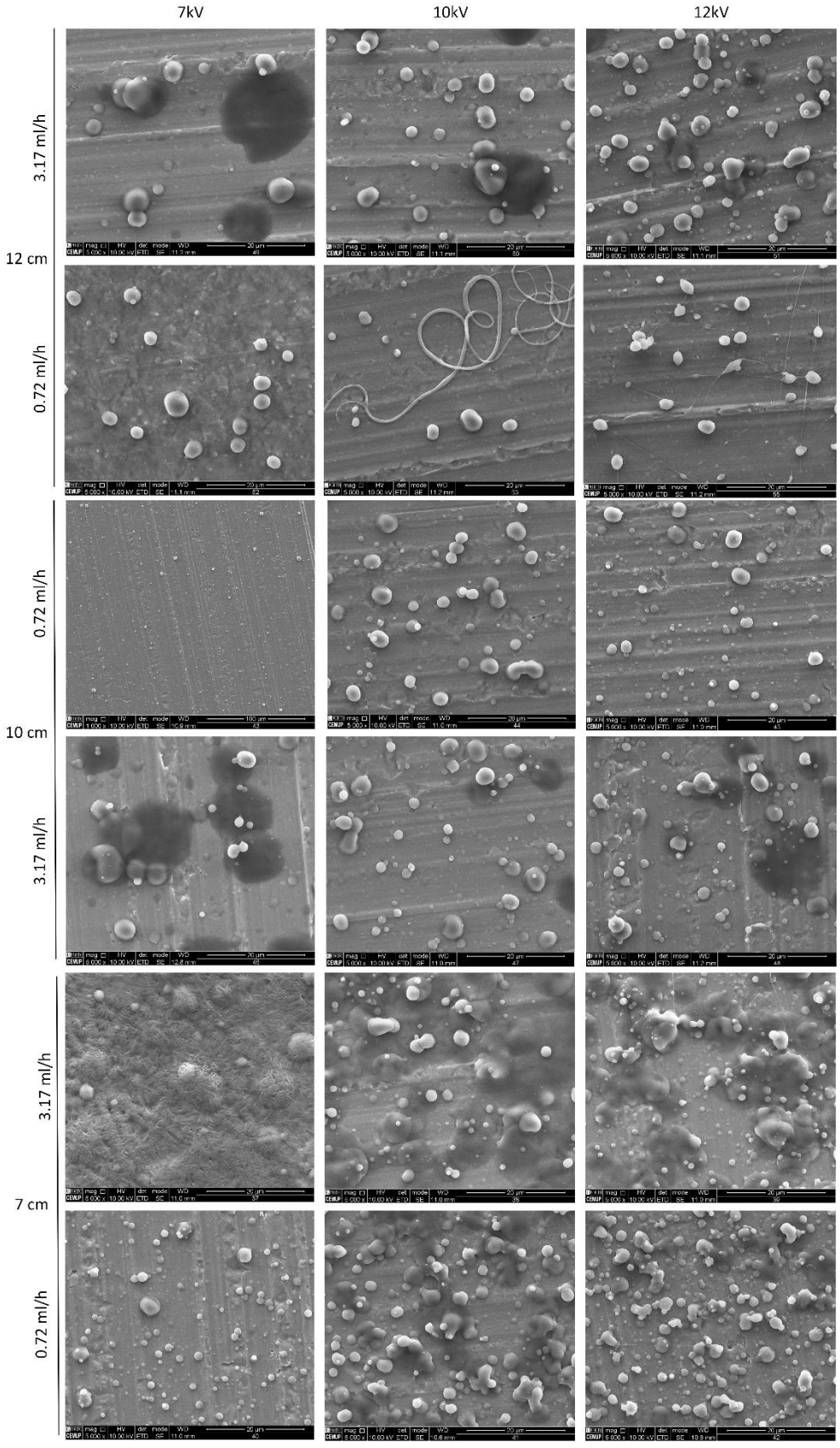

Figure SA.II.1. SEM of 6wt% of PCL in AA/TEA (2% v/v), scale bars: 20µm.

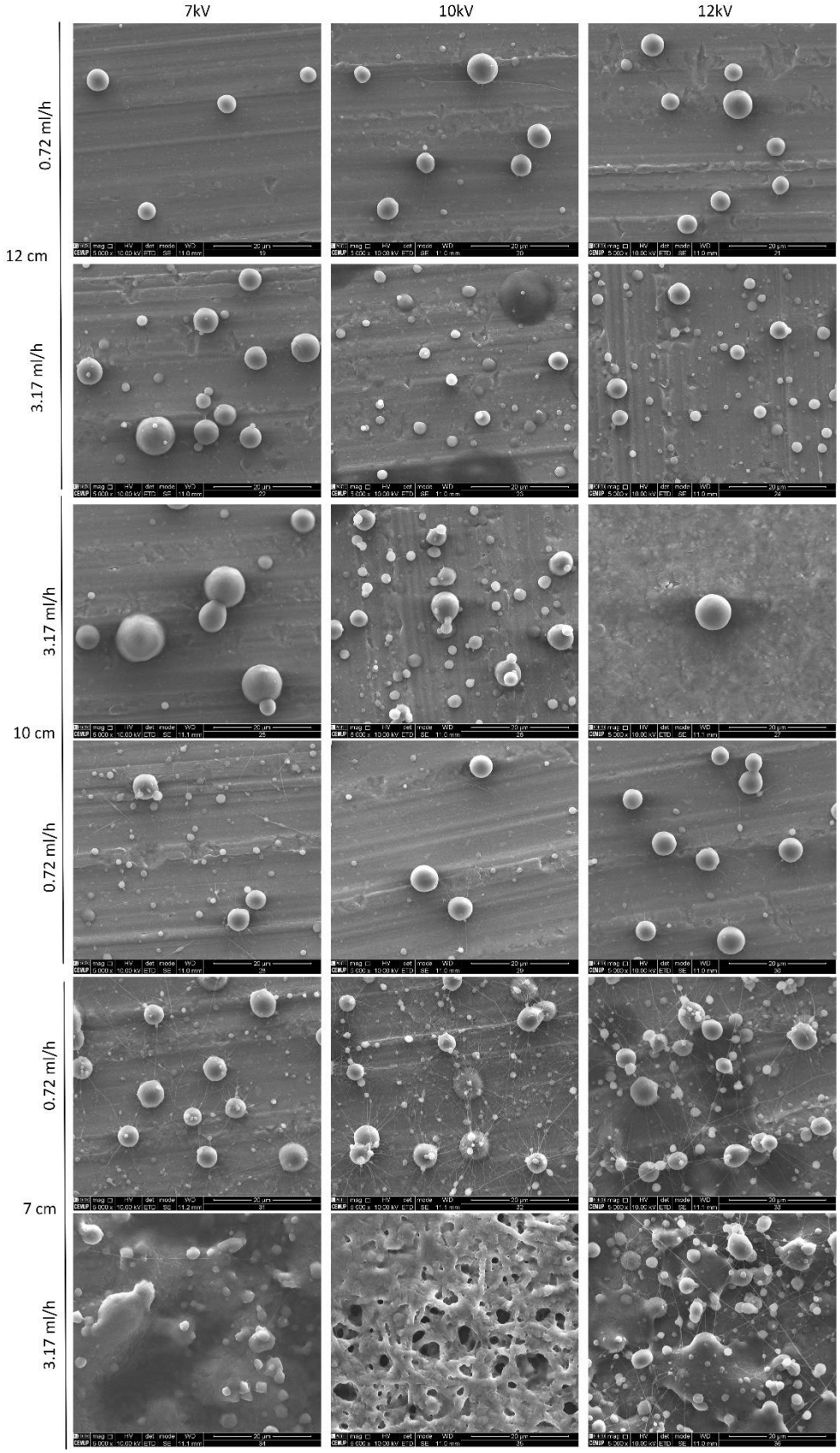

Figure SA.II.2. SEM of 11 wt% of PCL in AA/TEA (2% v/v), scale bars: 20µm.

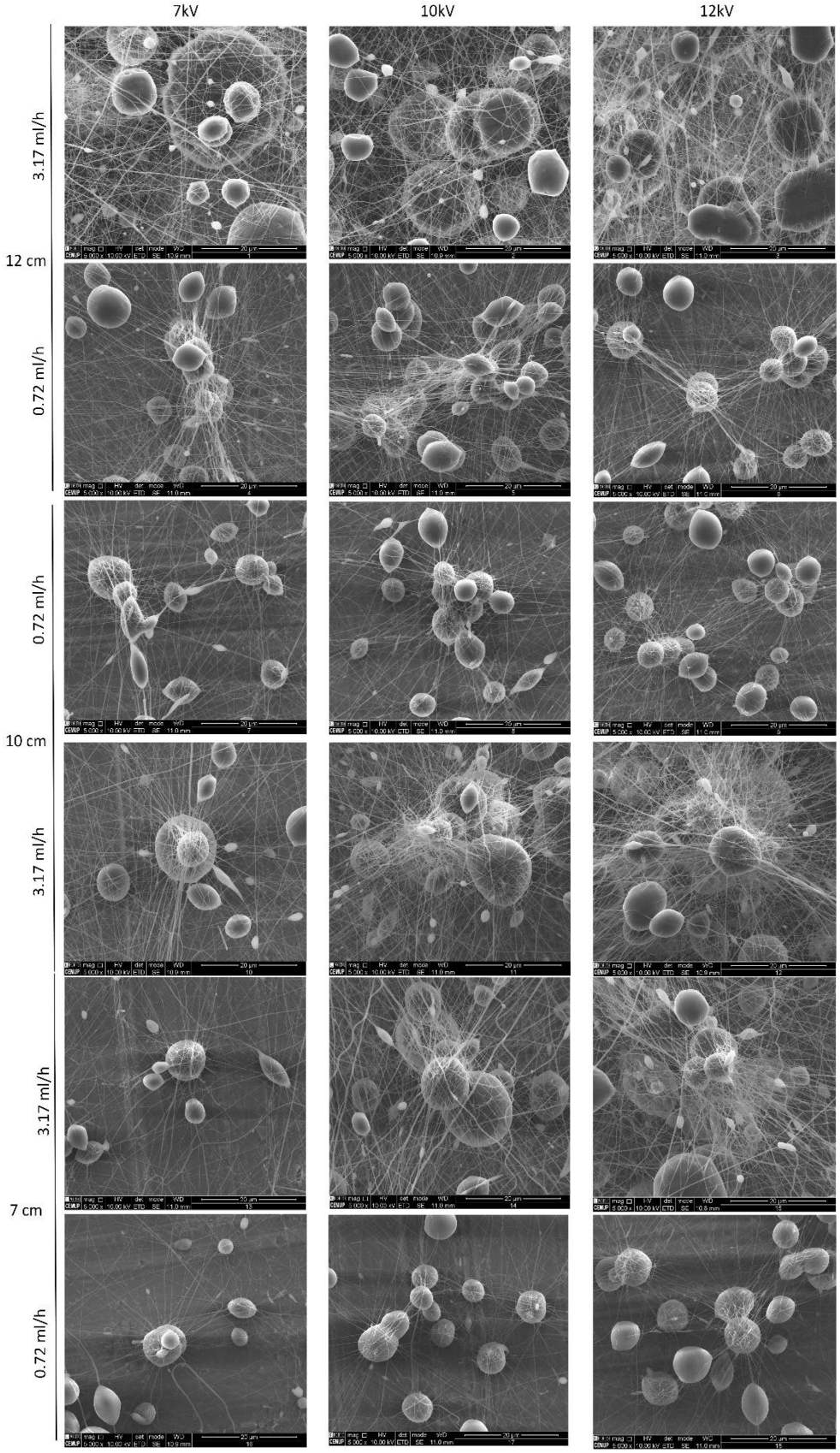

Figure SA.II.3. SEM of 17 wt% of PCL in AA/TEA (2% v/v), scale bars: 20µm.

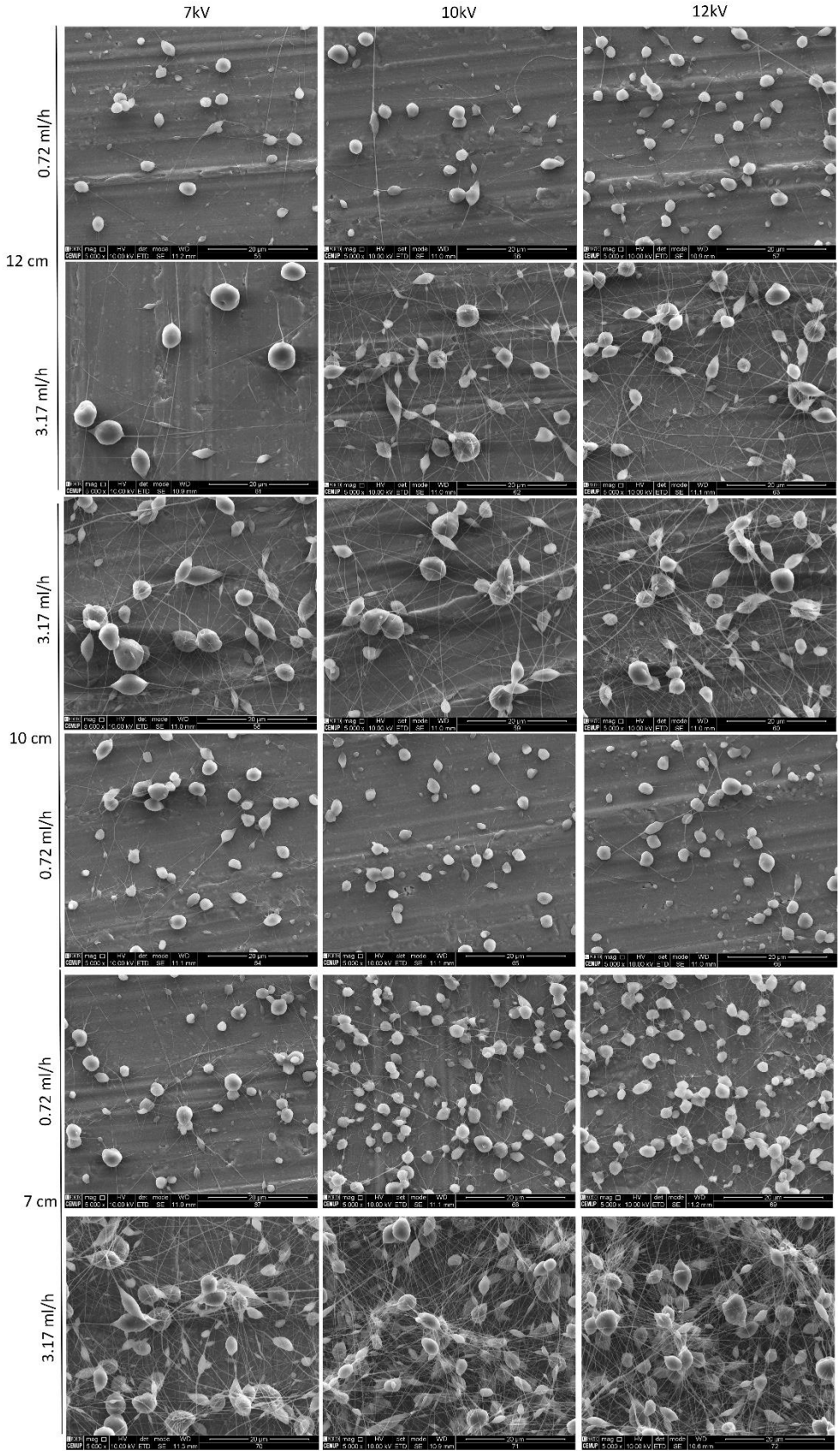

Figure SA.II.4. SEM of 6 wt% of PCL in DMK, scale bars: 20µm.

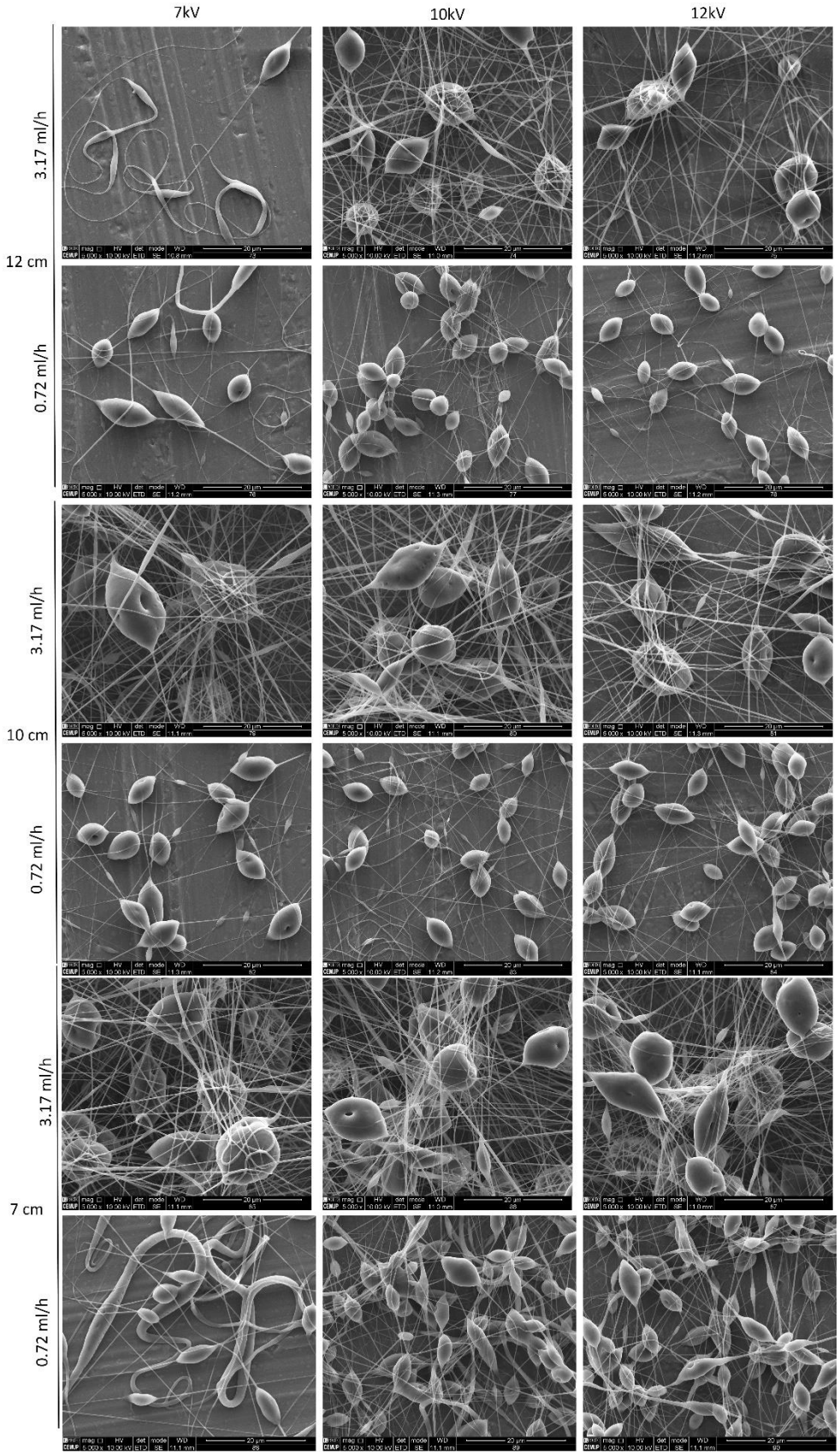

Figure SA.II.5. SEM of 11 wt% of PCL in DMK, scale bars: 20µm.

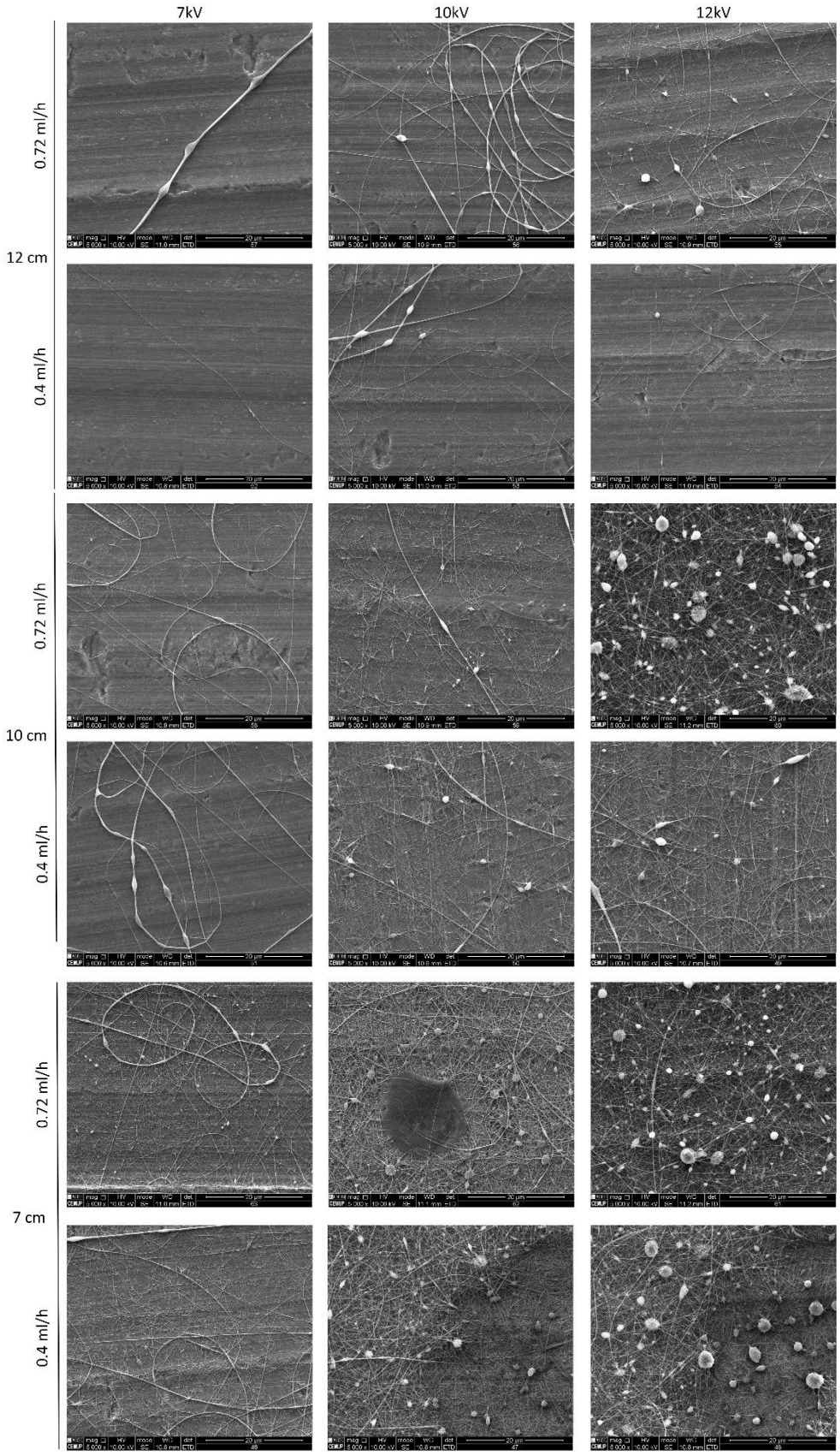

Figure SA.II.6. SEM of 5 wt% of Ge in AA/TEA (2% v/v), scale bars: 20µm.

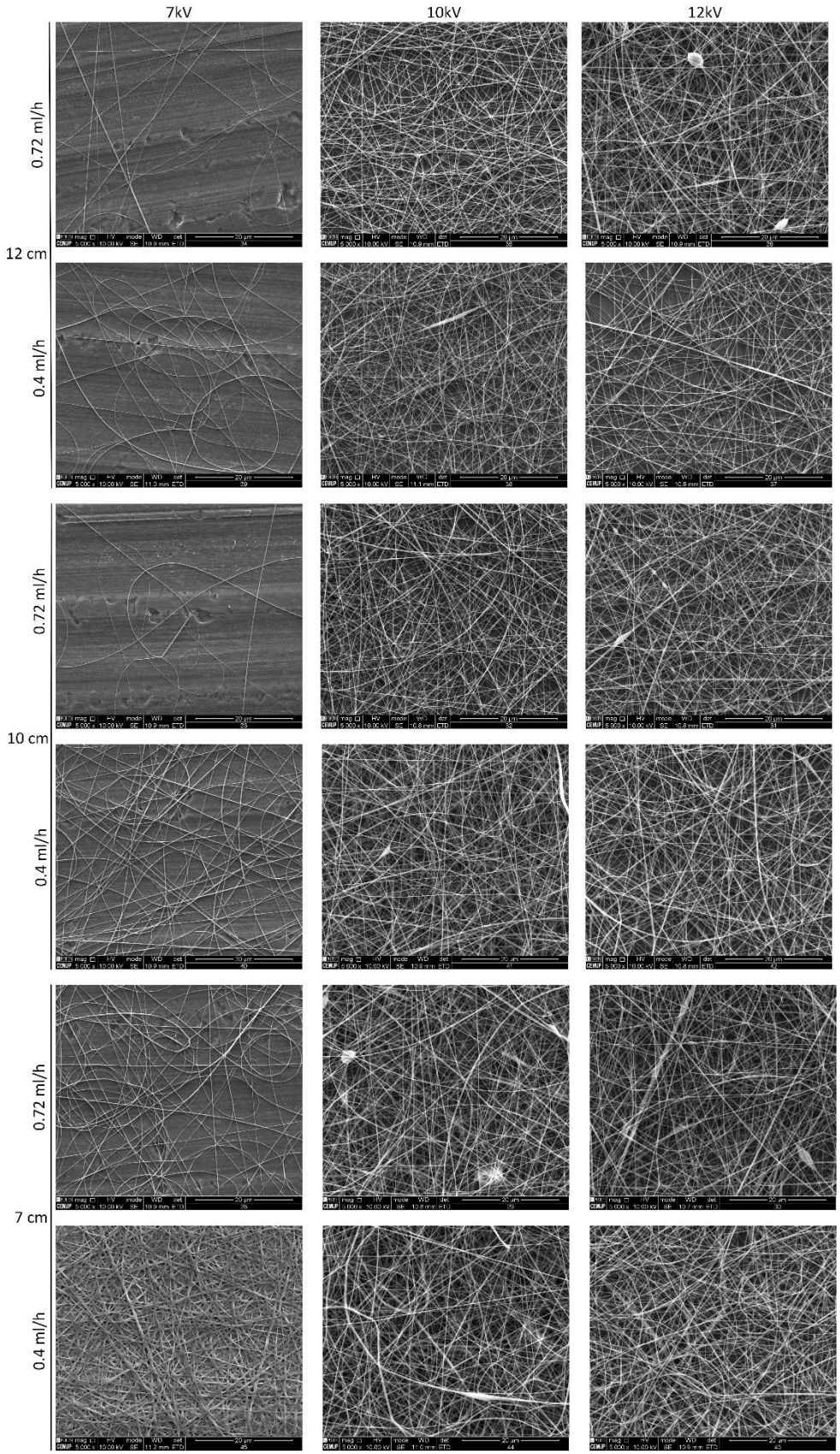

Figure SA.II.7. SEM of 10 wt% of Ge in AA/TEA (2% v/v), scale bars: 20µm.

Section 3 – SEM images

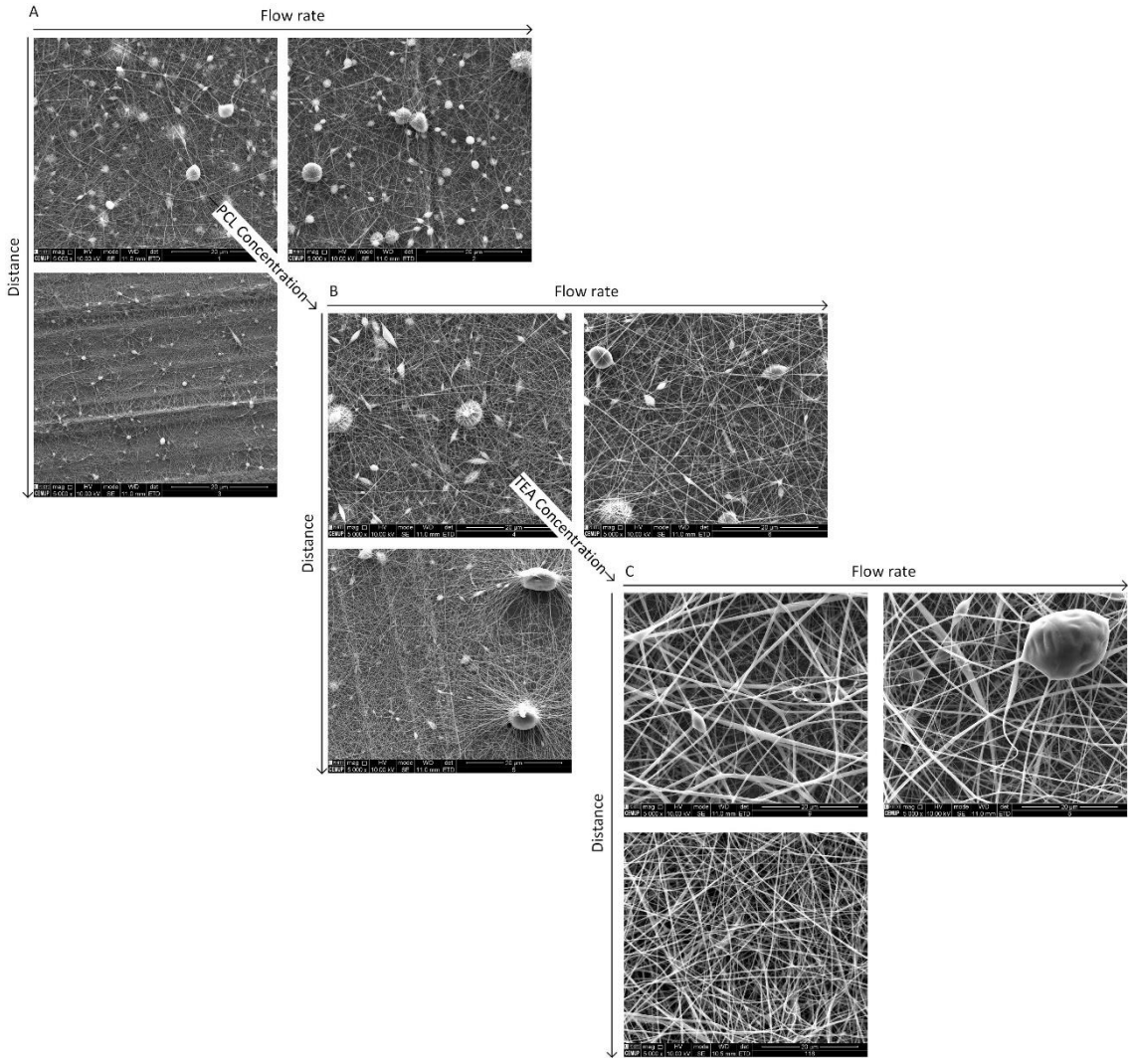

Figure SA.III.1 . Blend production optimization. A) 1:1 (11 wt-% PCL: 15 wt-% Ge (AA/ 1% TEA)) 12kV, flow rate 0.3-0.4 mL/h and distance 10-12cm; B) 1:1 (17 wt-% PCL: 15 wt-% Ge (AA/ 1% TEA)) 12kV, flow rate 0.3-0.4 mL/h and distance 10-12cm; C) 1:1 (17 wt-% PCL: 15 wt-% Ge (AA/ 2% TEA)) 12kV, flow rate 0.3-0.4 mL/h and distance 10-12cm. Scale bars: 20µm.

Section 4 – Confocal images

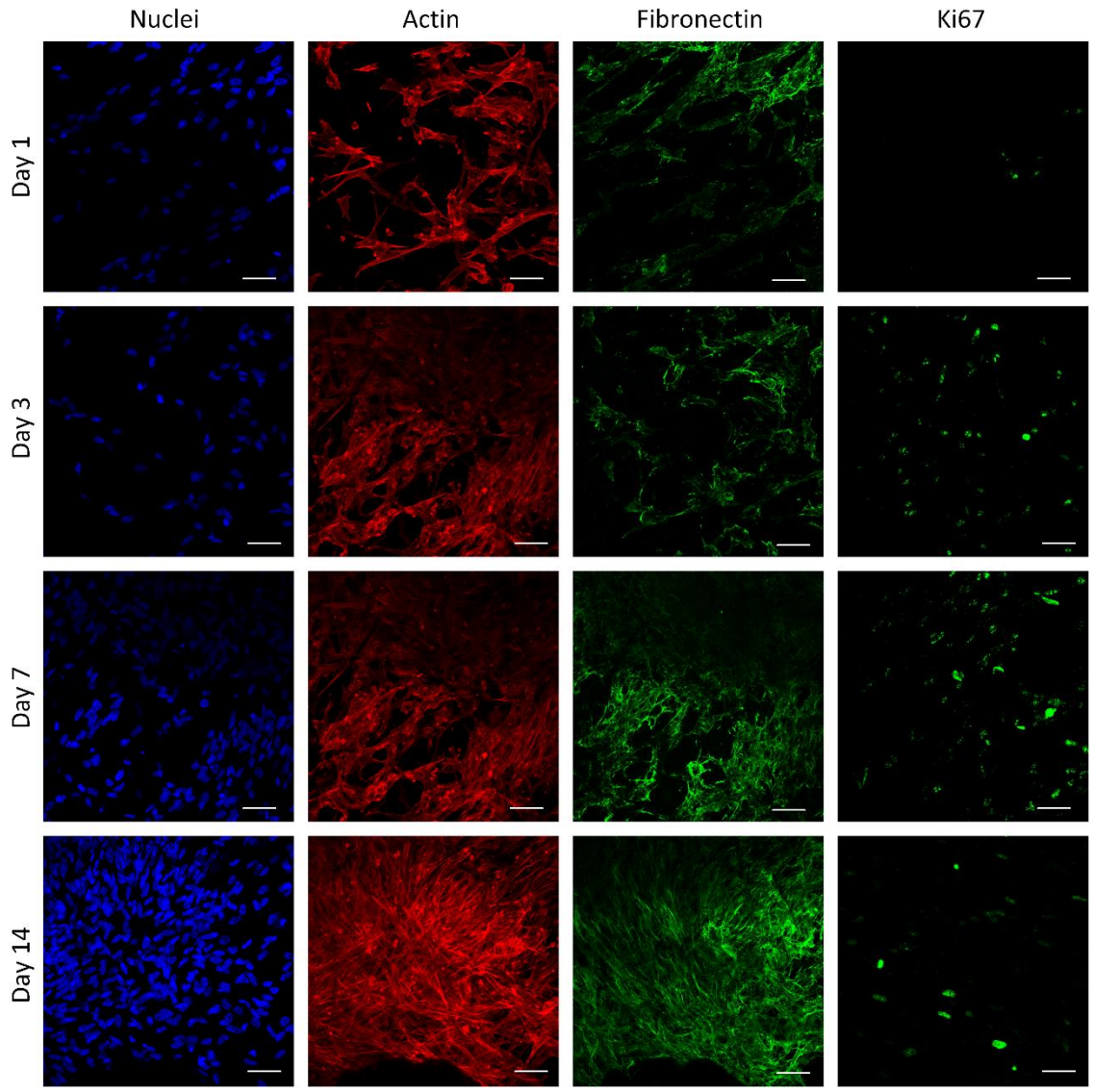

Figure SA.IV.1 . PCL confocal images for each time-point, scale bars: 50µm.

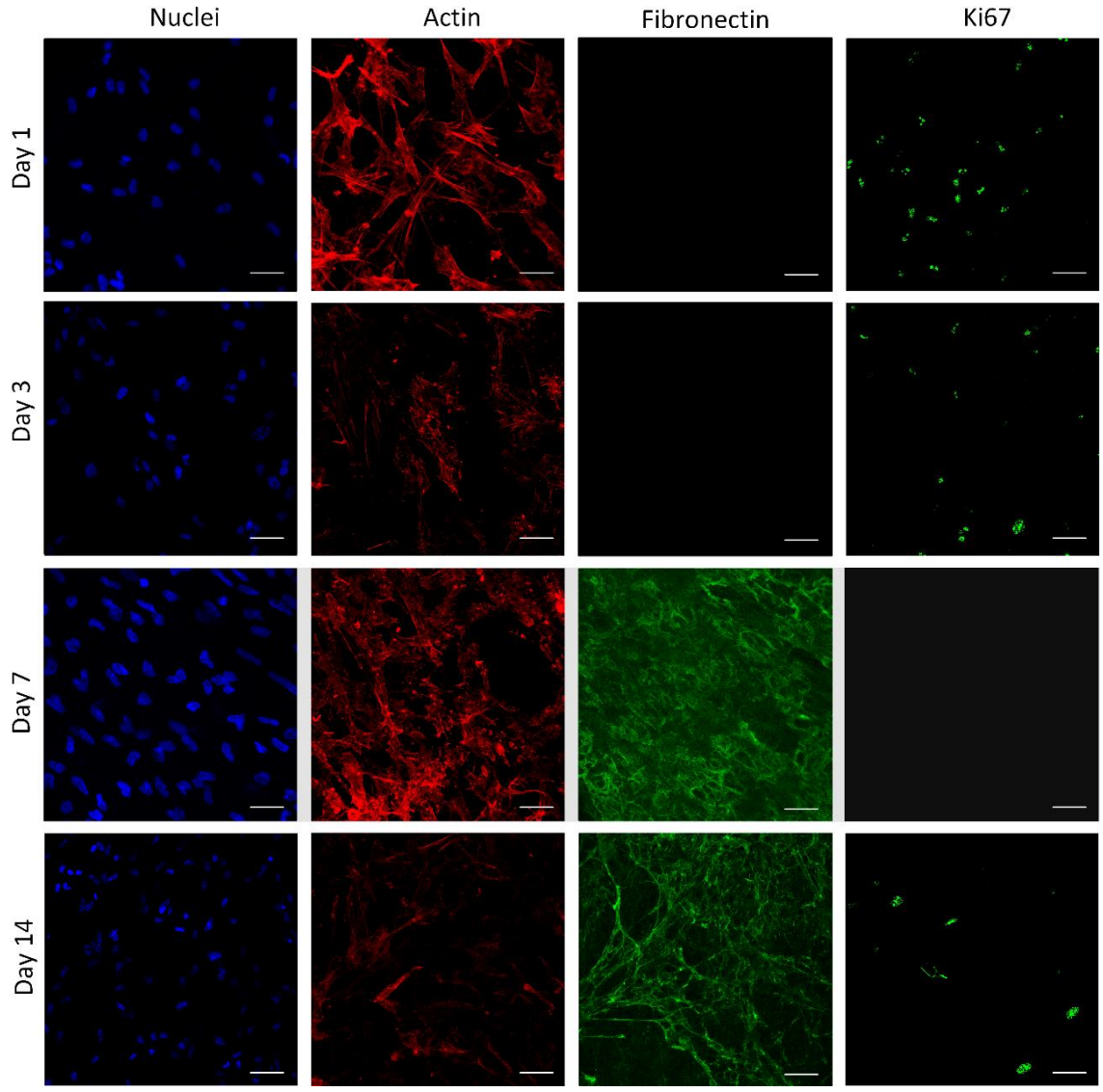

Figure SA.IV.2. Ge confocal images for each time-point, scale bars: 50µm.

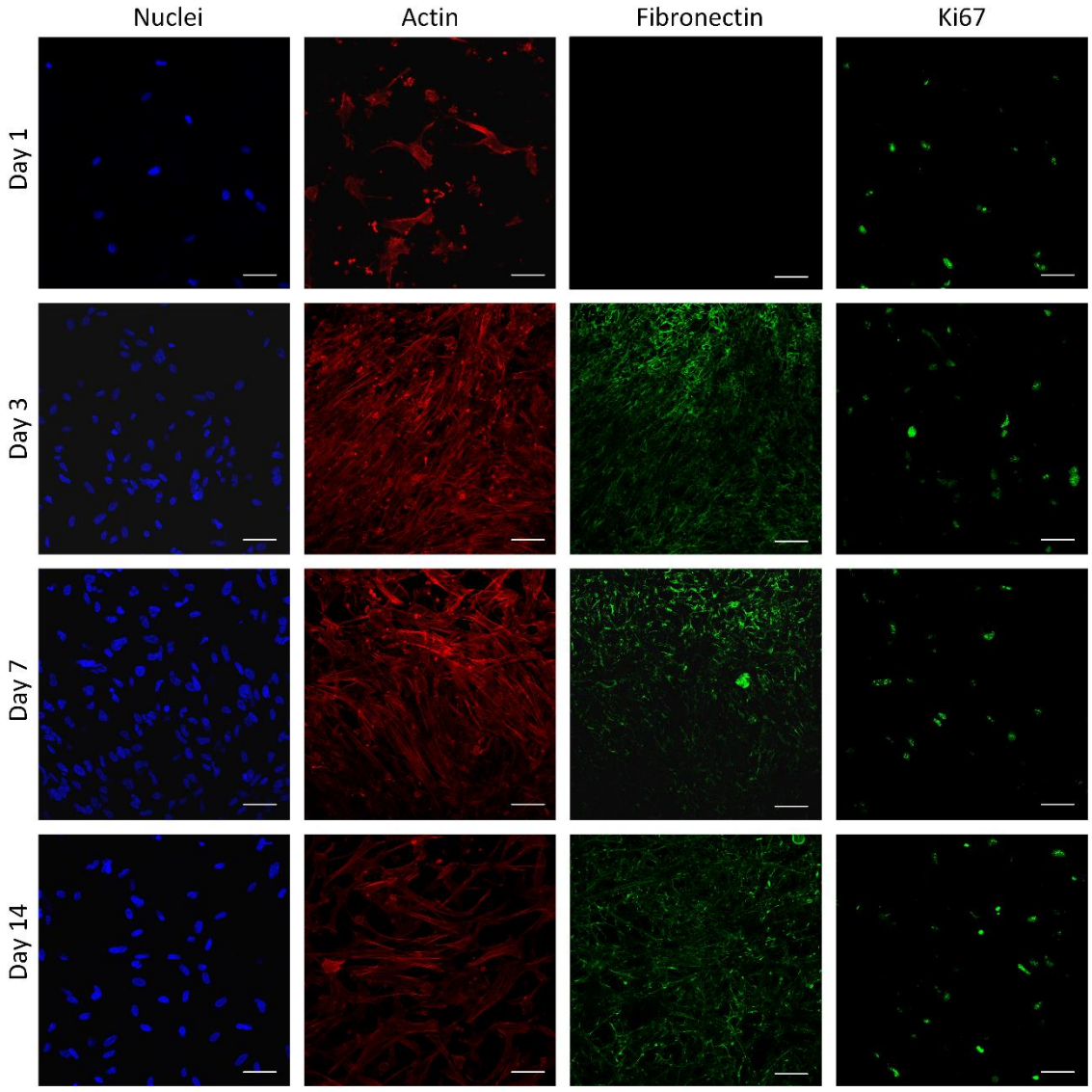

Figure SA.IV.3. Multilayer confocal images for each time-point, scale bars: 50µm.

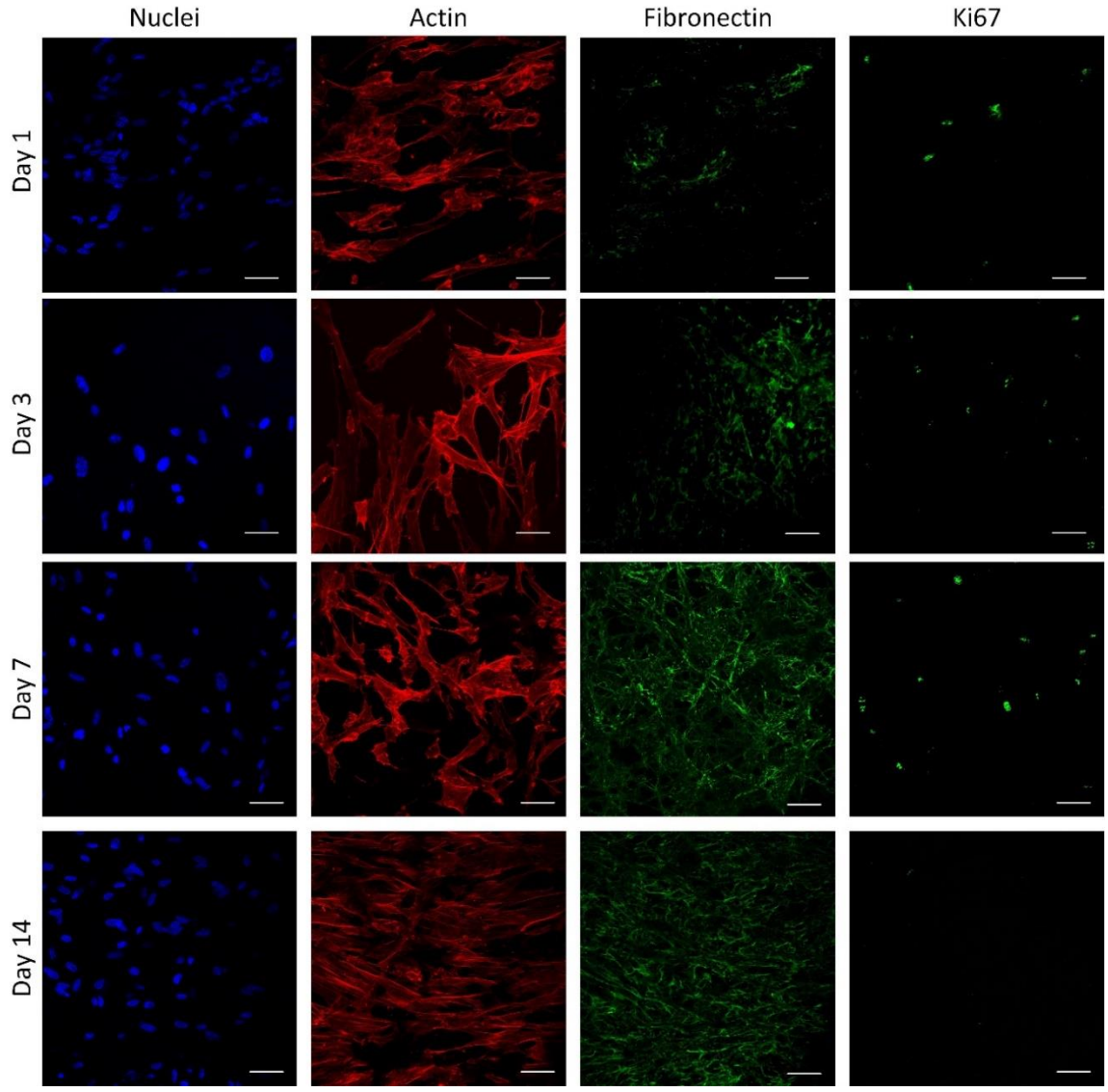

Figure SA.IV.4. Coated confocal images for each time-point, scale bars: 50µm.

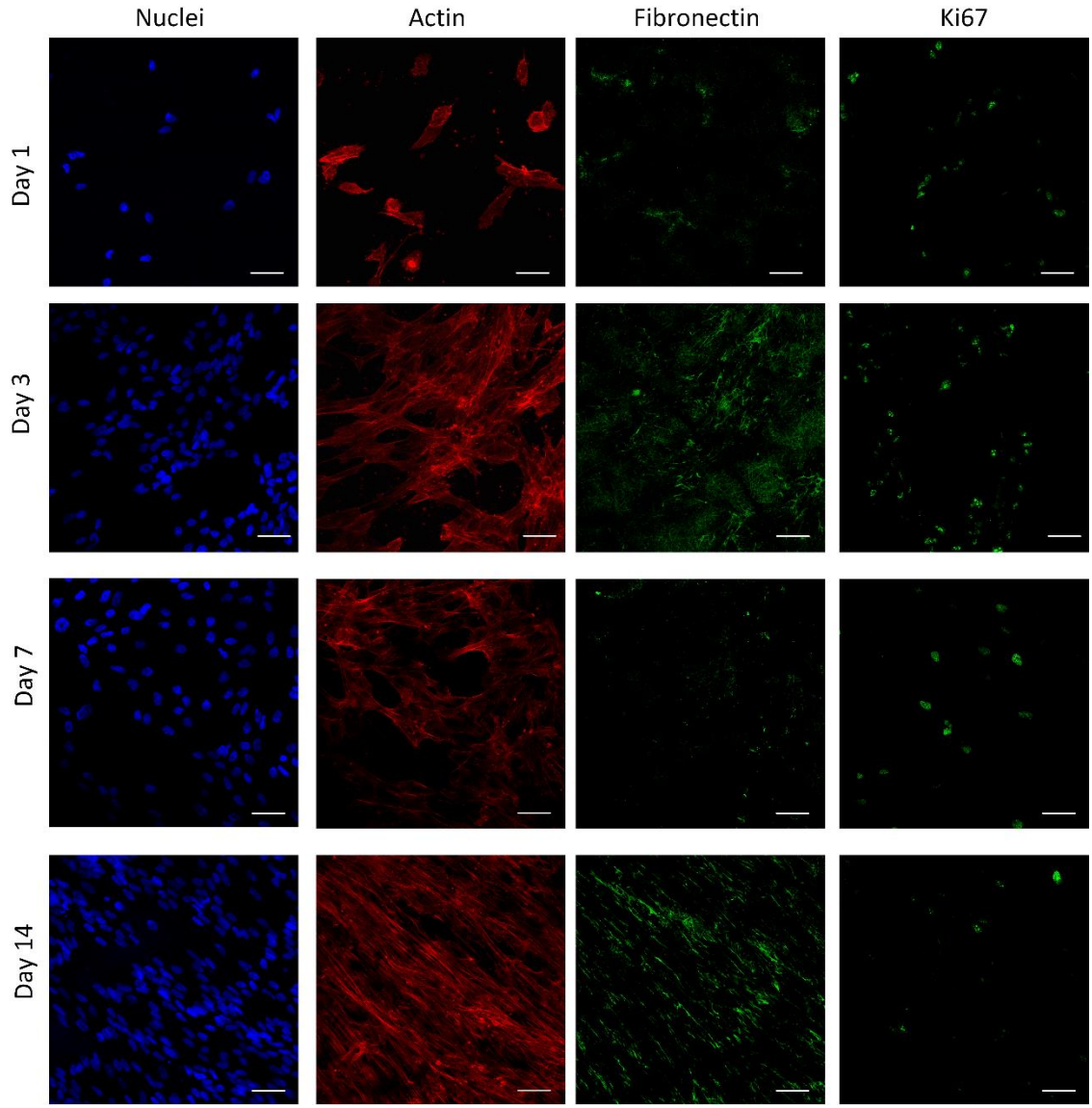

Figure SA.IV.5. Blend confocal images for each time-point, scale bars: 50µm.

Appendix B – Published papers

Progress in Materials Science 84 (2016) 314–334

Contents lists available at ScienceDirect

Progress in Materials Science

journal homepage: www.elsevier.com/locate/pmatsci

Advances in electrospun skin substitutes

J.R. Dias [a,b,c,d,*], P.L. Granja [b,c,d,e,1], P.J. Bártolo [f,1]

[a] Centre for Rapid and Sustainable Product Development (CDRsp), Polytechnic Institute of Leiria, Leiria, Portugal
[b] I3S - Instituto de Investigação e Inovação em Saúde, Universidade do Porto, Porto, Portugal
[c] INEB - Instituto de Engenharia Biomédica, Universidade do Porto, Porto, Portugal
[d] ICBAS - Instituto de Ciências Biomédicas Abel Salazar, Universidade do Porto, Porto, Portugal
[e] Faculdade de Engenharia da Universidade do Porto (FEUP), Departamento de Engenharia Metalúrgica e Materiais, Porto, Portugal
[f] School of Mechanical, Aerospace and Civil Engineering & Manchester Institute of Biotechnology, University of Manchester, Manchester, UK

ARTICLE INFO

Article history:
Received 15 April 2016
Received in revised form 9 September 2016
Accepted 18 September 2016
Available online 20 September 2016

Keywords:
Electrospinning
Skin
Wound healing
Electrospun nanofibers
Polymeric materials

ABSTRACT

In recent years, nanotechnology has received much attention in regenerative medicine, partly owing to the production of nanoscale structures that mimic the collagen fibrils of the native extracellular matrix. Electrospinning is a widely used technique to produce micro-nanofibers due its versatility, low cost and easy use that has been assuming an increasingly prominent position in the tissue engineering field. Electrospun systems have been especially investigated for wound dressings in skin regeneration given the intrinsic suitability of fibrous structures for that purpose. Several efforts have been made to combine distinct design strategies, synthetic and/or natural materials, fiber orientations and incorporation of substances (e.g. drugs, peptides, growth factors or other biomolecules) to develop an optimized electrospun wound dressing mimicking the native skin. This paper presents a comprehensive review on current and advanced electrospinning strategies for skin regeneration. Recent advances have been mainly focused on the materials used rather than on sophisticated fabrication strategies to generate biomimetic and complex constructs that resemble the mechanical and structural properties of the skin. The technological limitations of conventional strategies, such as random, aligned and core-shell technologies, and their poor mimicking of the native tissue are discussed. Advanced strategies, such as hybrid structures, cell and *in situ* electrospinning, are highlighted in the way they may contribute to circumvent the limitations of conventional strategies, through the combination of different technologies and approaches. The main research challenges and future trends of electrospinning for skin regeneration are discussed in the light of *in vitro* but mainly *in vivo* evidence.

Contents

* Corresponding author at: Biomaterials for Multistage Drug & Cell Delivery Group, Instituto de Investigação e Inovação em Saúde, Universidade do Porto, Rua Alfredo Allen, 208 4200-135 Porto, Portugal.
E-mail address: juliana.dias@ineb.up.pt (J.R. Dias).
[1] These authors contributed equally to this work.

http://dx.doi.org/10.1016/j.pmatsci.2016.09.006
0079-6425/

1. Introduction

The first shield between the external environment and the human body is the skin. This tissue plays a crucial role in body protection and, when damaged at full-size, the human life could be in risk [1,2]. According to the World Health Organization (WHO) it is estimated that every year 265,000 deaths occurs caused by burns and, annually about 6 million people were burned requiring medical attention [3–6]. The average length of stay in the hospital is 8.4 days, thus resulting in a considerable social and economic burden for the health care systems worldwide. Therefore, innovative strategies are required to promote skin tissue regeneration, despite the encouraging recent developments in wound dressings and tissue engineering-based products [7]. Electrospun meshes have been gaining increasing attention through the combination of materials and processing strategies of great potential for skin regeneration [8]. Wound dressings prepared from electrospun nanofibers have been claimed to present exceptional properties compared to conventional dressings, such as similarity to architecture of the natural extracellular matrix (ECM), improved promotion of hemostasis, absorption of wound exudates, permeability, conformability to the wound, and avoidance of scar induction [9]. New processing strategies are thus being explored in which natural and synthetic materials are combined with new design approaches allowing the incorporation of substances that turn not electrospinnable materials into electrospinnable ones. In this review skin regeneration strategies will be revised with a focus on electrospinning methodologies and materials.

2. Skin tissue and wound healing process

The human body comprises several organs each one with specific functions, dimensions and shapes. The largest vital organ in the body is the skin that represents 7% of the total body weight and has the main function of protecting the human being against the external environment. It also helps protecting the body against excessive water loss, against attacks from chemicals and other harmful substances, and ultraviolet radiation [1,8,10–12]. In spite of the protective function of the skin, this tissue plays other important functions namely: (i) control of body temperature, by secreting sweat through the sweat glands, thereby lowering the temperature; (ii) sensory, through different receptors able to detect touch, pain, pressure and temperature; and (iii) synthesis of vitamin D (after exposure to sunlight), a precursor of calcitriol hormone that is converted in the liver and kidneys and plays an important role in the calcium absorption in the small intestine [10,13]. Although the skin works as a barrier it is not totally impermeable: some substances are transferred across the skin, such as sweat, drugs and biomolecules [10,14].

Skin functions are carried out by specialized cells and structures found in the two main skin layers, epidermis and dermis (Fig. 1). Besides these two layers, beneath the dermis there is the hypodermis that provides support to the dermis [10,15]. The epidermis, the outermost skin layer, is around 120 μm thick and is composed by numerous cells closely linked in different stages of differentiation, which form the stratified squamous epithelium [10]. The epidermis is avascular (nourished through diffusion from the dermis), consists of 4 different types of cells (keratinocytes, melanocytes, Langerhans cells and merkels cells) and presents 5 distinct cell layers (stratum basale, spinosum, granolosum, lucidum and corneum) [16,17]. The dermis layer is composed by a complex mesh of ECM material that provides structure and resilience to the skin. The thickness of this layer varies according to the body region but is in average of 2 mm [10,17]. The dermis is composed by a nanometer-sized network of structural proteins (collagen, which provides strength and flexibility, and elastin, which provides elasticity), blood and lymph vessels, and specialized cells (mast cells that help in the healing process and protect against pathogenic organisms, and fibroblasts that produce collagen and elastin). This ECM network is engaged in a ground substance that is mostly composed by glycosaminoglycans and plays an important role in hydration and in maintaining moisture levels in the skin [10,14]. The ECM is also highly dynamic, being constantly synthesized and re-organized by the cellular components, but in turn also having a prominent role in directing cellular behaviour through direct and indirect signaling. For instance, ECM molecules control cell adhesion through specific cell binding sites, cell migration through

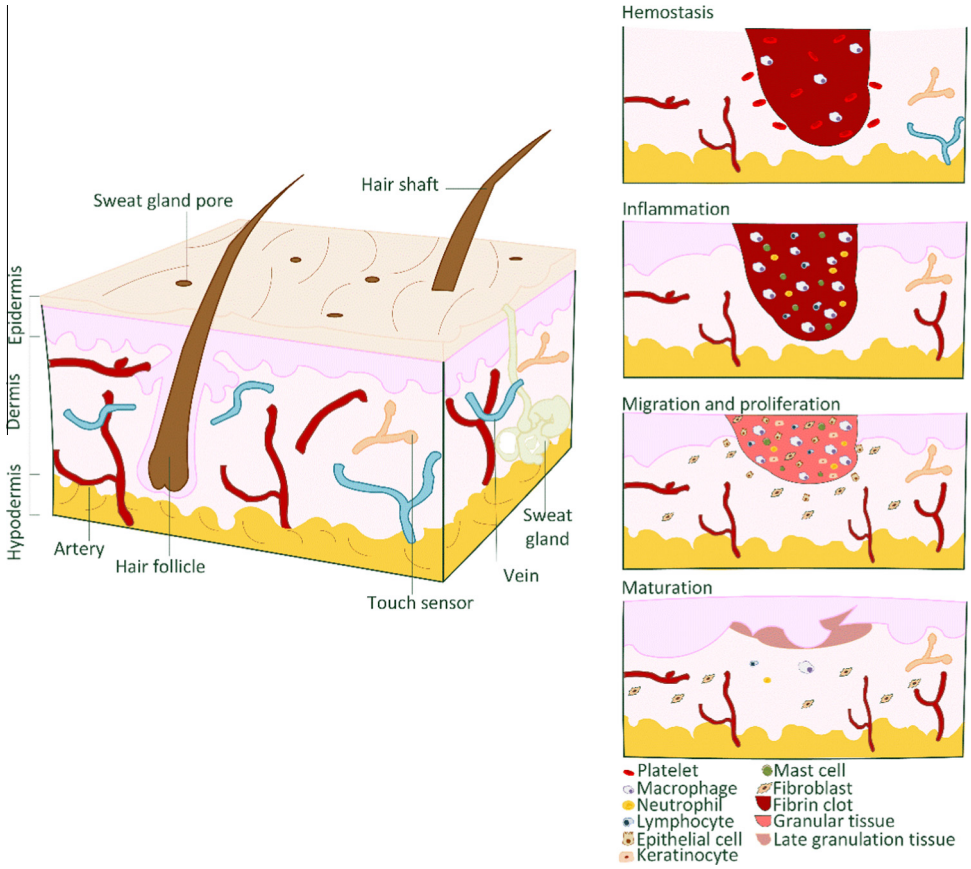

Fig. 1. Skin structure and wound healing phases.

proteolytically sensitive functionalities, and cell differentiation through bound and soluble signaling biomolecules. With relevance for the present topic is the nanometer scale of the several pores and fibers (collagen, hyaluronic acid, elastin, laminin, fibronectin, proteoglycans) that constitute the ECM, highlighting the relevance of mimicking the physical nanometer scale fibrillar nature of this structure through electrospinning. ECM fibers are reported to exhibit diameters between 10 and 300 nm, and the minimum fiber diameter required for fibroblast adhesion and migration, and maximum interfiber distance that fibroblasts are able to bridge, have been described as approximately 10 and 200 μm, respectively, which lie within parameters achievable by electrospinning but hardly achievable using alternative cell culture settings [18,19]. Furthermore, due to their intrinsic ability to synthesize their own ECM, skin cells are known to be able to self-organize even in the absence of molecular cues provided that an adequate 3D nucleation structure exists to enable their self-organization, thereby reinforcing the stimulating role of electrospun nanofibrous structures for skin regeneration [19,20].

When skin damage occurs a consecutive cascade of events called wound healing takes place to restore the skin structure and function [17,21]. A wound can result from burns, contusion, hematoma or a disease process, causing chronic wounds. At present, due to the increasing life expectancy, diseases with high incidence such as diabetes have been considerably increasing the incidence of chronic wounds and thus making it of high social relevance [11,21].

The wound healing process consists, in general, in five different phases, namely hemostasis, inflammation, migration, proliferation and maturation, occurring sequentially after damage [9,21] (Fig 1). During hemostasis, platelets suffer aggregation to promote clotting and stop any bleeding. Delivery of important growth factors to the inflammation process occurs, which trigger the wound healing process through attraction and activation of neutrophils, lymphocytes, macrophages and mast cells [22,23]. The inflammation phase occurs at the same time as hemostasis. In this phase, blood neutrophils followed by phagocytes enter and penetrate inside to the injured area to destroy bacteria and eliminate debris from dying cells and damaged matrix [14,24]. The following phases, migration and proliferation, are considered by several authors as the same phase due to their interdependence [22,25]. Migration is characterized by infiltration of new epithelial cells moving on to the damaged area to replace the dead cells and during the migration the inflammation decreases. The proliferation phase consist on covering all damaged area with epithelial cells and macrophages, while simultaneously fibroblasts and endothelial cells move to the damaged area forming a granular tissue composed by a new matrix and blood vessels, respectively [22,25]. The last phase, maturation, comprises the remodeling process, in which fibroblasts cover all the damaged surface with a

new skin layer and ideally leaving no evidence of scar [14,23]. Through this elaborate process of wound healing the skin has self-regeneration ability although this capacity is strongly reduced in the case of full-thickness lesions, requiring the use of a graft or dressing [11].

3. Skin regeneration products

3.1. Autografts and allografts

When skin lesions result in large full-thickness defects the standard clinical procedure is the autologous skin transplantation based on transplanting split-thickness grafts [7,8,26]. However, this transplantation contains all of the epidermis layer but only a small part of the dermis often leading to scar formation [15]. This process has the obvious restriction of total amount of autologous skin that can be removed and the split-skin donor site takes one week to heal and can be used for split skin harvesting up to 4 times. Frequent harvests also lead to scars in donor sites and hospital stays for long periods of time [6,27,28]. Allografts are grafts removed from other individuals and constitute efficient alternatives to prevent fluid loss and infection, reduce pain and promote the healing of underlying tissues. However, this type of graft presents several ethical problems and is influenced by the donor's availability and potential disease transmission [26].

3.2. Wound dressings

The first procedure when skin damage occurs consists in applying a wound dressing due their efficiency on preventing wound infection and promoting exudate absorption, low cost and availability. The main functions of a dressing are promoting a moist environment in the wound, and protecting the wound against mechanical injury and microbial contamination, especially during the inflammatory stage [7,29]. Ideally, the dressing should be able to fit the wound shape, absorb wound fluid without increasing bacterial proliferation or causing excessive dehydration, provide pressure for hemostasis, and prevent leakage from the bandage. The dressing should also support the wound and surrounding tissues, eliminate pain, promote re-epithelialization during the reparative phase, and be easily applied and removed with minimal injury to the wound [30].

Wound dressings can be categorized according to different characteristics. One possible classification relies in classifying the wound dressings in passive or interactive [9,31]. The passive ones correspond to the common wound dressings and their main function is covering the wound and allowing the regeneration beneath the dressing. Some examples are tulle dressings (made of cotton or viscose gauze impregnated with paraffin) and low-adherence dressings (made of materials as knitted viscose or polyester fabric) [32]. On the other hand, the interactive wound dressings present some advantages like the capability to modify the wound chemical environment facing to the physiological conditions of the wound for a faster healing process. Although in some cases this modification could take long periods of time [9,33]. Commercial available interactive wound dressings, according the widely accept classification, are divided into hydrocolloids, hydrofibers, hydrogels, foams, alginates and bioactive/biological dressings [32].

3.3. Tissue engineering-based products

During the past few years, the progress and evolution on tissue engineering (TE) field have been growing exponentially. This field has been exploring the regeneration of several tissues, including skin, involving knowledge from different disciplines. TE includes the combination of live cells, tissues or organs, with structures and materials designed to mimic the structure of a particular tissue [34,35]. The use of TE strategies for skin tissue regeneration consists essentially in expanding skin cells in the laboratory, cultivating them on a scaffold and applying cell-scaffold construct for restoring the barrier function (first step in burn patients), or to promote wound healing (for instance in chronic non-healing ulcers), thereby reducing pain and promoting optimal conditions for a correct healing [11]. Several products for skin regeneration based on TE are already clinically available that meet the essential requirements for a clinical product, namely be safe for the patient, clinically effective and conveniently handled and applied by health care professionals [6,11].

TE skin substitutes present several advantages when compared with other available solutions including less required vascularisation in the wound bed, increased dermal component of the healed wound, reduced presence of inhibitory factors and faster and safe coverage [8]. TE skin substitutes available in the market can be classified according to different features. The most common classification is related with the anatomical structure to be regenerated, resulting in epidermal, dermal or dermal/epidermal (or composite) substitutes [6,26]. An important phase in the production of epidermal substitutes is the isolation of keratinocytes, obtained through a 2–5 cm^2 skin biopsy from the donor. The epidermis is separated and *in vitro* cultured on top of fibroblasts [6,36]. There are several epidermal substitutes available for clinical applications using cells either of autologous or allogenic origin, with the allogenic products presenting reduced manufacturing costs compared to autologous substitutes. Some of the commercial epidermal substitutes available are MySkin® (CellTran ltd, UK) a synthetic silicone support layer with surface coated and seeded with keratinocytes, Epicel® (Genzyme Biosurgery, USA), sheets of autologous keratinocytes attached to the petrolatum gauze support, and Epidex® (Eurodern GA, Switzerland), an epidermal equivalent from the patient's own outer root sheath, where the keratinocytes are cultured in silicone membranes. Despite

their efficiency in proving epidermal coverage, autologous and allogenic epidermal substitutes are claimed to present poor attachment rates that can lead to blister formation [26].

The development of dermal substitutes emerged due the lack of dermal tissue in full thickness wounds and the poor quality of the scars after treatment with split thickness autografts or cultured epithelial grafts which contain little or no dermal component, respectively [37]. There are several products available in the market that have been demonstrating great effectiveness in dermal regeneration, such as Dermagraft® (Shire Regenerative Medicine, Inc, USA), a cryopreserved human fibroblast-derived dermal substitute, generated by the culture of neonatal dermal fibroblasts onto a bioresorbable poly (lactic-*co*-glycolic acid) (PLGA) mesh scaffold [38], Integra™ (Integra LifeSciences, USA), which is a nanofibrous bilayer mesh specifically designed to be used in conjunction with negative pressure wound therapy, comprising crosslinked bovine tendon collagen and glycosaminoglycan and a semi-permeable polysiloxane layer, and Karoderm™ (Karocell Tissue Engineering AB company, Sweden), a human donated cell free dermis that can also be used as a biological scaffold for autologous keratinocytes.

To mimic skin layers (dermis and epidermis) in the same construct dermal/epidermal substitutes have been explored. Several studies have been carried out with different cell types to evaluate their performance although only autologous keratinocytes were claimed effective to achieve permanent closure of skin defects [6,26]. Dermal/epidermal substitutes available in the market include PermaDerm® (Regenicin Inc., USA), composed by cultured fibroblasts and keratinocytes on an absorbable collagen substrate, and Apligraf® (Novartis, USA), that combines two distinct nanofibrous layers, the lower dermal layer containing bovine type I collagen and human fibroblasts and the upper epidermal layer formed by culturing human keratinocytes.

In spite of the great progress achieved on TE-based skin substitutes several challenges still need to be overcome to achieve the optimal skin substitute, such as: to avoid use animal-derived materials (e.g. serum), to improve the adhesion of cultured keratinocytes to the wound bed, to improve the rate of neovascularization of tissue engineered skin and to enhance the scaffolds materials to resist wound contraction and fibrosis [7,8,34,39,40].

3.4. Advanced skin substitutes

Advanced skin regeneration strategies have been emerging combining cells, growth factors and scaffolds overcoming some of the problems associated to the clinical application of skin grafts, dressings and TE-based products [7]. Scaffolds are a crucial component because the isolated cells on their own are not able to restore the native structure of the skin without support to guide the ECM growth [1]. For scaffolds fabrication, there are two main strategies: the top-down and bottom-up approaches [41,42]. The top-down is considered the traditional approach and is based on cells seeded in a porous scaffold generating a cellular construct, which is later subjected to the maturation process in a bioreactor. With this methodology is expected that the cells adhere, proliferate and differentiate inside the scaffold creating an appropriate ECM stimulated by the growth factors and mechanical or other types of stimulation [41,43]. Most TE products described before are based on this strategy.

The bottom-up approach consists on developing biomimetic modular structures that can be created through self-assembled aggregation, microfabrication of cell-laden hydrogels, fabrication of cell sheets or direct printing with specific microarchitectural features [41,44,45]. The major advantages of this approach are better control over cell seeding, increasing cell density and complexity of microarchitecture than with top-down approaches. Major disadvantages of using bottom-up approaches include the fact that some cell types are unable to produce enough ECM, migrate or form cell-cell junctions, and the great difficulty in developing assembly techniques able to generate engineered tissues with clinically relevant length scales and mechanical properties [7,41,46].

4. Electrospun skin substitutes

Although the electrospinning technique is under growing development in the biomedical field its principles emerged around 1600s. However, since 1980s, several research groups demonstrated that it is possible to produce electrospun fibers with organic polymers increasing, since then, the number of publications exponentially [47,48]. Some of the most important milestones are summarized on Table 1. Further details about electrospinning's history are available elsewhere [47,49–52].

Electrospinning is a technique allowing to create submicron to nanometer scale fibers from polymer solutions or melts and was developed from a basis of electrospraying, widely used for more than 100 years [65,68]. It is also known as electrostatic spinning, with some common characteristics to electrospraying and the traditional fiber drawing process [69].

The conventional setup for an electrospinning system consists of three major components: a high voltage power supply, a spinneret and a collector that can be used with horizontal or vertical arrangement [47,65,70]. The syringe contains a polymeric solution or a melt polymer, pumped at a constant and controllable rate. The polymer jet is initiated when the voltage is turn on and the opposing electrostatic forces overcome the surface tension of the polymer solution. Just before the jet formation, the polymer droplet under the influence of the electric field assumes the cone shape with convex sides and a rounded tip, known as the Taylor cone [59,69,71]. During the jet's travel, the solvent gradually evaporates, and charged polymer fibers are randomly deposited or oriented in the collector [71].

Table 1
Historical milestones of electrospinning.

Year	Author	Historical milestone	Refs.
Around 1600s	Gilbert	Study of the magnetic behaviour and electrostatic phenomena	[49]
Late 1800s	Rayleigh	Investigation of liquid jet hydrodynamic stability, with or without applied electric field	[47,50]
1902	Cooley	Patent registration entitled "Apparatus for electrically dispersing fluids", considered as the first description of a process recognizable as electrospinning	[53,54]
1914	Zeleny	Study of the fluid droplets behaviour at the end of metal capillaries	[51,52]
1934–1944	Formhals	Publication of several patents describing important developments towards electrospinning commercialization	[55–65]
1936	Norton	Patented the use of melted polymers	[49,66]
1964–1969	Taylor	Development of theoretical electrospinning underpinning, which allowed the mathematical modeling of the cone shape formed by the liquid droplet that became known as Taylor's cone	[51,67]

Table 2
Effect of electrospinning parameters in fiber formation.

	Parameter	Effect	Refs.
Solution	Viscosity	Determines the fiber formation	[74,77]
	Surface tension	Determines the applied voltage; it must be higher than surface tension of the solution to initiate the process	[76,78]
	Conductivity	Higher conductivity avoids droplet deposition in the fibers	[75–77]
	Dielectric effect	High dielectric properties reduce bead formation and fiber diameter	[77,78]
Processing	Applied voltage	Influences the jet stretching and acceleration and consequently fiber morphology	[75,77]
	Flow rate	Influences the fiber diameter, its geometry and mesh porosity	[75–77]
	Needle diameter	A small internal diameter reduces droplet formation in the fibers	[77,78]
	Distance needle-collector	Influences the solvent evaporation rate	[75,77]
Ambient	Temperature	The increase of temperature favors the solvent evaporation rate	[67,77]
	Humidity	If too high induces morphological changes increasing the surface heterogeneity and for hydrophilic polymers is unable form fibers and electrospraying occurs	[47,67,77,78]
	Atmosphere types	Some gases are influenced by the electrostatic field blocking the process	[77]
	Pressure	If pressure is lower than atmospheric one the solution exists through the needle causing jet instability	[77]

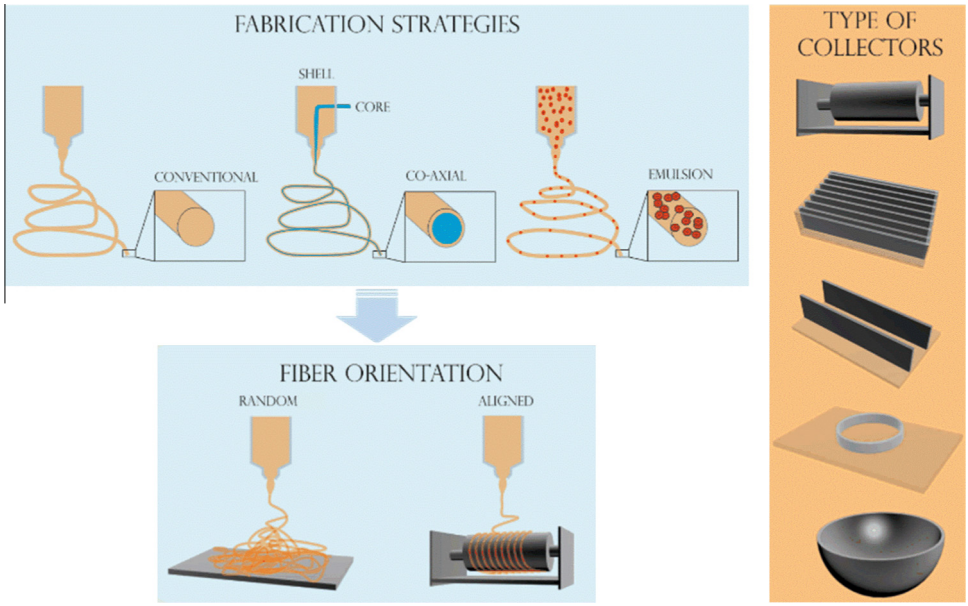

Fig. 2. Electrospinning fabrication strategies, fiber orientation types and types of collectors used.

The electrospinning process can be influenced by several parameters, such as: solution parameters (viscosity, concentration, type of solvent), processing parameters (flow rate, distance between needle and collector, voltage supply, type of collector) and ambient parameters (temperature and humidity), as summarized in Table 2 [47]. It should be emphasized that the acceleration of fiber formation is up to 600 m/s^2, which is much higher than the value of acceleration of gravitational forces on earth (at sea level and at 45° of latitude it corresponds to 9.80665 m/s^2), meaning that gravity does not influence the process [72,73].

The technique is also highly versatile since, in addition to the conventional fiber configuration, it is possible to obtain a variety of other configurations, namely core/shell (co-axial) or emulsion configurations and, according to the fiber orientation, it is possible to produce aligned or randomly oriented fibers depending the type of the collector used (Fig. 2).

The use of electrospinning to regenerate damaged tissues rose in the last decade due to its simplicity to produce meshes and its capacity to mimic the micro-nanostructure of the natural ECM. The nanofibers produced through electrospinning confer a high surface area to the structure, high interconnectivity that is beneficial for regenerative tissue growth and cell migration and great potential for effective delivery of biomolecules, [47,79]. According to tissue engineering principles an ideal scaffold should hold cellular activities, and should disappear over time while tissue regeneration occurs. To enable this, scaffolds should mimic native tissue regarding its structure, appropriate mechanical strength, porosity for cellular infiltration and growth [35,69].

Traditional scaffolding methodologies like solvent casting and particulate leaching, gas foaming, freeze drying and gas foaming have limited ability to form scaffolds that mimic the native tissue nanostructural architecture [80,81]. However, electrospinning presents a unique ability to fabricate nanofiber-based scaffolds that best mimic the nanometer scale of the native ECM as well as the mechanical properties of the native skin. Electrospun skin substitutes have been claimed to have increased potential to promote better cellular attachment, growth and differentiation due the high surface area, high aspect ratio and high microporosity provided by the low fiber diameter structure [35,52,82]. The versatility of this technology further allows tuning of fibrous scaffold design in terms of mechanical properties, fiber diameter, density and orientation to mimic the physical features of the ECM, as shown in several examples ahead.

The mechanical properties of skin *in vitro* and *in vivo* have been evaluated using different techniques (ultrasounds, indentation, tensile tests, suction and torsion) [83–85]. Human skin is a complex tissue due its heterogeneity, viscoelasticity, anisotropy, adhesive properties and non-linear stress-strain behaviour [83,84,86]. Table 3 presents the mechanical properties of skin tissue in comparison to electrospun meshes made by different materials and production strategies, showing that the mechanical properties of electrospun meshes are similar to those of skin, thus demonstrating the potential of this technology to mimic skin tissue due not only due to its similarity in terms of organization (nanofibrous mesh-like structure) but also mechanical properties.

Additionally, the high specific surface area and porosity of electrospun meshes constitute additional functional advantages by providing tunable fluid absorption and drug and biomolecule delivery, adequate oxygen, water and nutrient diffusion coupled with efficient metabolic waste removal.

In spite of the significant advances in electrospinning, in the biomedical field only a few companies provide customized nanofibers production either as single or bi-layers combining different materials. Commercially available products also include cell culture well-plates integrating electrospun structures and meshes for stent coverage [94–96]. Specifically for skin regeneration, a clinical trial was carried out for the treatment of diabetic foot ulcers using a multilayer polyurethane electrospun transdermal patch releasing nitric oxide [97]. However no clinical trials using the electrospinning technique for skin regeneration are ongoing [98].

4.1. Randomly oriented fiber meshes

Conventional electrospinning set-up configuration consists in fibers randomly deposited over the grounded collector, which is usually a metal plate [47,79,99]. The random deposition is a consequence of the jet instability resulting from the electric field applied to overcome the polymeric solution surface tension [51,100].

There are several studies comparing random and aligned deposition strategies in terms of nanofibers morphology, hydrophilicity, mechanical properties and cell adhesion and proliferation [101,102].

In terms of biological response numerous studies demonstrated that aligned fibers usually exert a more relevant influence on cellular behaviour including cell morphology, cellular density and gene expression. In terms of mechanical properties the elongation at break presents better results when fibers are randomly oriented [101–104]. Although both strategies allow producing structures with suitable properties to promote skin regeneration, skin is generally characterized by a meshlike random orientation of fibrils, making random meshes the electrospun structures the more suited to mimic native skin's ECM [18]. Jha and colleagues explored the application of randomly oriented fiber meshes to improve wound healing, in which they assessed skin regeneration promoted by collagen electrospun fibers crosslinked with glutaraldehyde on adult guinea pigs [105]. *In vitro* and *in vivo* results showed that the created wounds closed after 16 days of implantation and no adverse inflammatory reactions or other antigenic complications were observed, showing the great potential of this strategy for dermal reconstruction. Said and co-workers [106,107] also investigated randomly oriented electrospun fibers for wound healing by combining PLGA with different substances as antimicrobial wound dressing. *In vivo* results after application of fusidic acid (FA)-loaded PLGA electrospun ultrafine fibers showed high efficacy of this strategy to promote wound healing and reduced infection (Fig. 3) [106,107]. A study performed by Coskun et al. evaluated the performance of randomly oriented

Table 3
Mechanical properties of skin tissue and electrospun meshes.

Structure	Young's modulus (MPa)	Tensile strength (MPa)	Elongation at break (%)	Refs.
Human skin	2.9–150	1–32	17–207	[87–90]
PCL	21.42 ± 0.04	6.87 ± 0.25	116.0 ± 6.53	[91]
PCL/collagen	82.08 ± 17.86	8.63 ± 1.44	24.0 ± 7.16	[91]
PLCL	47.66 ± 2.24	7.24 ± 0.16	158.54 ± 66.67	[90]
CA/pullulan	2.91 ± 0.21	0.13 ± 0.08	22.2 ± 0.01	[92]
HA/PLGA core/shell	28.0	1.52	60.07	[93]

CA – cellulose acetate; HA - hyaluronic acid; PCL – poly (ε-caprolactone); PLCL – poly(ε-caprolactone-*co*-lactide); PLGA – poly(lactic-*co*-glycolic acid).

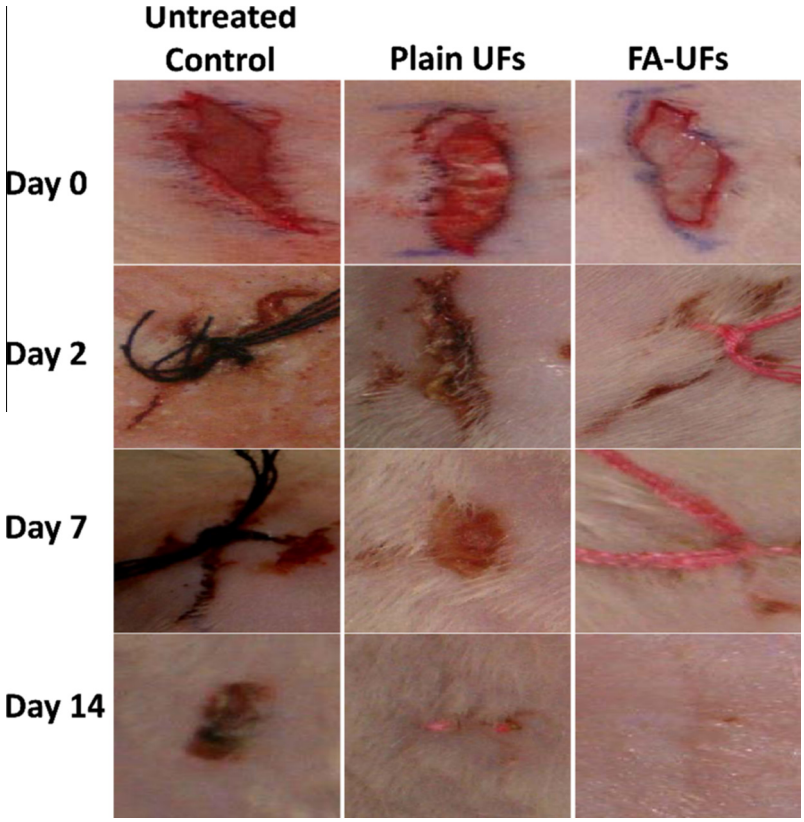

Fig. 3. Effect of plain and fusidic acid loaded PLGA ultrafine fibers on the healing of wounds in rats [107].

electrospun poly (vinyl alcohol)/sodium alginate as wound dressing *in vivo*. This study compared commercially available wound dressings (tulle grass, Eczacibasi), woven cotton antibacterial bactigras (Smith & Nephew) and nonwoven Suprasorb-A (Lohmann) made from calcium alginate fibers to the electrospun meshes during 21 days. In the early time-points (4 and 6 days) no significant differences were observed, although after the following time-points (15 and 21 days) important differences were observed. Electrospun meshes presented the best healing performance as shown through epithelization, epidermis characteristics, vascularization and formation of hair follicles (Fig. 4) [108].

These studies demonstrate the importance of the nanostructure provided by randomly oriented electrospun meshes to promote wound healing. In fact the electrospinning technique allows production of nanostructures with similar diameter (native range between 10 and 300 nm), porosity and random orientation similar to the collagen fibrils in the ECM of skin [18,108].

4.2. Aligned fiber meshes

In the TE field one of the most important criteria to design the optimal scaffolds relies in mimicking the tissue ECM, which may involve a considerable degree of orientation, depending on the tissue type and ECM. Hence, random fiber deposition may not be adequate when mimicking tissues where specific fiber orientation is required [72,79]. Therefore several alternative set-ups to conventional electrospinning have been developed to achieve optimized architectures. To obtain aligned

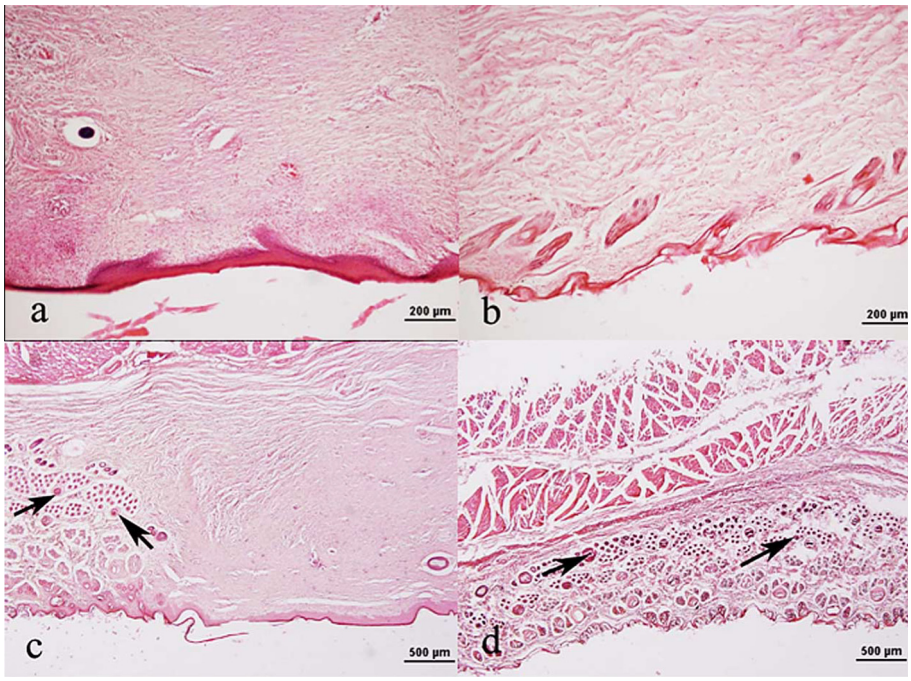

Fig. 4. Histological cross-sections of tissues obtained from regions covered by wound dressings on the 21st postoperative day. (a) Tulle grass. (b) Bactigras. (c) Suprasorb-A. (d) Electrospun poly (vinyl alcohol)/sodium alginate mesh. *Arrows*: hair follicies (reprinted from [108], with permission from IOS Press) [108].

fibers by electrospinning several collectors with varied configurations have been designed to match the desired orientation (Fig. 2). Fiber alignment can also be achieved using near electrospinning or melt electrospinning. In both cases the collector is moving in X and Y directions to induce filament orientation and the process is characterized by short distances between the tip of the needle and the collector. To achieve a stable jet region for controllable deposition the average distance of near electrospinning lies between 500 μm and 3 mm and for melt electrospinning between 3 and 5 cm [109–111].

Compared to randomly oriented fibers, aligned fibers present significantly higher resistance to tensile stress, when tested parallel to fiber alignment, and also exert a distinct influence on cell behaviour [70]. Since a variety of tissues are constituted by oriented fibers the development of support structures capable of influencing cellular behaviour at the right orientation is of significant importance. These tissues include ligaments, tendons, brain, muscles, cardiac and vascular tissues [112]. Recent studies demonstrated the influence of aligned fibers over cell organization and function [113–115].

Despite the general random orientation of native skin tissue, Annaidh and colleagues have reported the relevance of the orientation of collagen fibers in the dermis due to the correlation between their orientation and Langer lines [85]. In the past, Cox and Stark already concluded that the Langer lines have an anatomical basis, since they remained after removal of skin from the body and after tension tests [116,117]. A few studies have investigated the use of aligned fiber meshes to promote wound healing. Patel et al. developed aligned and bioactive nanofibrous scaffolds by immobilizing extracellular matrix protein and growth factor onto poly(L-lactide) (PLLA) nanofibers, which simulated the physical and biochemical properties of native matrix fibrils. The aligned nanofibers significantly induced neurite outgrowth and enhanced skin cell migration during wound healing compared to randomly oriented nanofibers. Furthermore, the immobilized biochemical factors (as efficient as soluble factors) synergized with aligned nanofibers to promote highly efficient neurite outgrowth but had less effect on skin cell migration [118]. Kurpinski and co-authors showed that aligned PLLA nanofibers enhanced bovine aortic endothelial cells (BAECs) infiltration as a result of a high pore openness, which facilitated cell migration across the structure. *In vitro* and *in vivo* tests on a dermal wound healing model showed the importance of nanofiber alignment coupled with the effect of added heparin as effective biophysical and biochemical cues, respectively, to regulate the cellular behaviour and tissue remodeling [119]. In terms of wound size reduction no significant improvements were observed after 7 days. However, histological findings revealed that in aligned fibers the epidermal layer grew, migrating from the wound edge towards nanofibrous graft [119].

4.3. Fibers with core/shell structure

The core/shell technology emerged among the most promising set-ups in the field of electrospinning since it is based on the combination of two different materials or substances. Using this approach, the same filament may have distinct inner

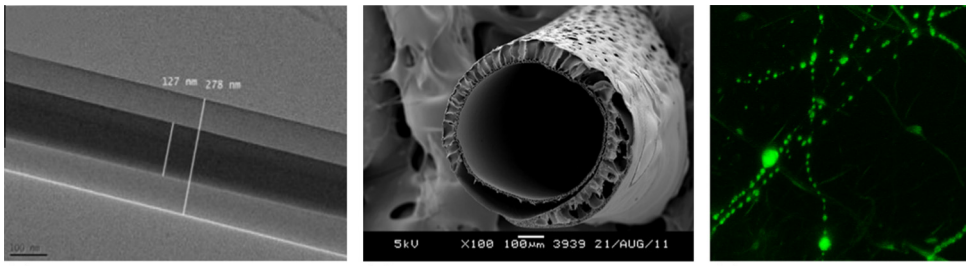

Fig. 5. Core/shell fibers (a) Transmission electron microscopy image of: Core/shell chitosan/poly(lactic acid) electrospun composite nanofibers produced using a co-axial approach [121]. (b) Scanning electron microscopy image of a cross-section of a polycaprolactone (PCL) hollow fiber in water coagulation bath [122]. (c) Confocal microscopy image of a poly(vinyl alcohol) (core)/PCL (shell) nanofiber mesh with encapsulated liposomes (in the core) stained with fluorescein [123].

and outer layers, allowing different compositions such as a material surrounded by another material or by a matrix loaded with dispersed particles [79,120]. This design was developed to incorporate substances (e.g. drugs, enzymes, growth factors or other biomolecules) inside the nanofibers. It presents two main advantages [52]: (i) substances can be incorporated in the inner layer being protected from environmental factors, such as the organic solvents usually used in the electrospinning technique and (ii) and the incorporated substance can be released from the inner layer and past the outer shell layer in a more controlled and sustained pattern [70]. The design parameters, selected materials, thickness and microstructure of the shell will directly influence the release pattern of the substance contained inside of the fibers. The core/shell design is also being widely explored to improve the surface properties of nanofibers, such as the hydrophilicity, which in turn will influence the biological response [70].

There are two different processes to produce core/shell fibers: co-axial electrospinning and emulsion electrospinning. Co-axial electrospinning consists on a capillary concentrically inserted inside the other capillary, resulting in a co-axial configuration in which each capillary is connected to a reservoir containing a given material. Similarly to the conventional electrospinning set-up this approach can work in the vertical or horizontal positions [120]. Through this process, several structures can be produced, such as bicomponent fibers, hollow fibers and fibers with microparticles (Figs. 2 and 5). Bicomponent fibers with core/shell configuration can be obtained from two electrospinnable materials or the combination of a spinable material with other non-spinable. This approach presents as major advantages the obtention of a final fiber presenting unique properties and the use of materials that on their own could not be used in the electrospinning process. Using this approach, the range of materials used in electrospinning considerably increases, overcoming the limitations to obtain electrospun fibers from specific materials due their low molecular weight, limited solubility, unsuitable molecular arrangement, or lack of required viscoelastic properties [120]. For instance, Nguyen and co-workers (2011) developed electrospun meshes of chitosan (CS) (core) and poly(lactic acid) (PLA) (shell) although CS, due to its high molecular weight, high viscosity and polycationic nature, cannot be electrospun on its own, and demonstrated their antibacterial activity and the high potential of these composite nanofibers for applications in the biomedical field [121].

The combination of fibers with drugs, growth factors and other substances or biomolecules also provides novel functionalities to the produced fibers [120]. The entrapment of substances inside the fibers allows controlling the release rate, which is dependent on the degradation rate of the outer fiber polymer, thus smoothing the sudden release [52]. Several research groups have been showing interesting results from substances encapsulation. Maleki et al. reported an easier control of drug release profile through core/shell fibers compared to monolithic fibers using tetracycline hydrochloride (TCH) as core and poly(lactide-*co*-glycolide) (PLGA) as shell [124]. Despite their interesting properties the wide application of liposomes in regenerative medicine is difficult due to their short half-life and inefficient retention at the site of application. Mickova and co-workers claim that these disadvantages could be significantly reduced by their combination with nanofibers [123]. They demonstrated the incorporation potential of liposomes into nanofibers by coaxial electrospinning of poly(vinyl alcohol) (PVA) (core) and polycaprolactone (PCL) (shell). The study validated that the enzymes encapsulated on liposomes dispersed into PVA fibers survived intact to the process fabrication. The potential of this system was also proved by the enhancement of mesenchymal stem cell proliferation, indicating its promising characteristics as drug delivery system [123].

Not many studies are available reporting the use of core-shell nanofibers for skin regeneration. Jin et al. demonstrated that nanofibers composed of gelatin (core)/poly(L-lactic acid)*co*-poly-(e-caprolactone) (PLLCL) (shell) and epidermal induction medium embedded in the core promoted the desired sustained release of the medium without burst release and further induced the differentiation of adipose-derived stem cells into epidermal lineages [125]. According to Xu et al. an efficient delivery system is critical for the success of cellular therapies. To deliver cells to a dynamic organ, the biomaterial vehicle should mechanically match the non-linear elastic behaviour of the host tissue. In this study, non-linear elastic biomaterials have been fabricated from a chemically crosslinked elastomeric poly(glycerolsebacate) (PGS) (core) and the thermoplastic poly(L-lactic acid) (PLLA)(shell) using the core/shell electrospinning technique. Mechanical tests demonstrated values comparable to skin tissue (Table 3) and *ex vivo* and *in vivo* trials shown that the elastomeric mesh supports and fosters the growth of enteric neural crest (ENC) progenitor cells.

Co-axial electrospinning can also be used to produce hollow fibers without the need of a template to be coated, as in the chemical vapor deposition method [126]. In this strategy the core material is dissolved by a specific solvent, at the end of the process or the core interacts with shell forming a hollow fiber during the processing. Wei et al. showed the potential of hollow fibers to act as a drug delivery system using core/shell fibers of PVA (core) and polyethersulfone (PES) (shell) with the core material containing the drug (curcumin). During the fabrication process the core and shell wall interacted forming a hollow fiber bilayer containing the drug on the fiber inner wall [127].

Core/shell fibers can also be produced using emulsions. This approach does not require a special needle with a physical separation between the core and the shell solutions neither such a careful selection of operation parameters as in the co-axial approach. In this case the dispersed drop in the emulsion turns into the core and the continuous matrix become the shell [120,128,129]. Ma et al. reported the formation of core/shell fibers through the emulsion using sodium alginate as core and poly(ethylene oxide) (PEO) as shell. However, when crosslinking occurs it induces changes on fiber morphology and the electrospun mesh looses the configuration and becomes a film. The water-in-oil (w/o) emulsion is being widely explored to encapsulate hydrophilic drugs or bioactive molecules in the core to avoid burst release and prolong the release time [128]. Zhang et al. prepared bovine serum albumin (BSA) entrapped in a water-in-oil emulsion as the core, encapsulated in the shell polymer (methoxy polyethylene glycol-*b*-poly(L-lactide-*co*-e-caprolactone) (PELCL) and poly(L-lactide-*co*-glycolide)(PLGA)) via emulsion-core (EC) coaxial electrospinning. The fibrous membranes reduced the initial burst release of BSA, which can be tailored by changing the composition to PLGA in the core emulsion. The results showed that EC electrospinning performed better than conventional co-axial electrospinning with respect to protein delivery for tissue engineering applications [130].

4.4. Hybrid structures

The characteristic small pore size of nanofibrous meshes produced by electrospinning and the lack of specific groups to interact with cells on the commonly used polymers limits the cellular migration into the scaffold and could results in 2D tissue formation becoming a hindrance to the success on 3D tissue regeneration [131,132]. To overcome these limitations several promising approaches have been developed, either combining different variants of electrospinning or through combination with additive technologies [133,134].

The combination of different electrospinning set-ups allows the fabrication of hybrid structures. Several research works explored the development of hybrid structures combining different fiber diameters [135–137], different materials to improve the properties of the structure [138–140] or combining aligned/random fibers [141]. For skin regeneration most of the available works only explore the combination of materials and different fiber diameters, building structures without gradients.

The droplet formation phenomena, initially considered an handicap to fiber production, is a consequence of the low viscosity of the polymeric solutions used in electrospinning [50,142]. However, exploration of particle formation under influence of an electric field, a new technique was developed, called electrospraying, ensuring that with one entanglement per chain it is possible to obtain particles from micro to nano scale [143]. Particle electrospraying is of great interest for tissue engineering applications by providing encapsulation of biomolecules due its high encapsulation efficiency and increase in the surface area [144,145]. Only a few works are available combining electrospraying with electrospinning, aimed at developing hybrid structures mimicking native tissues. It has been previously demonstrated that combining both techniques it is possible obtain hybrid structures with potential for tissue regeneration due its capacity to promote cell adhesion and proliferation (Fig. 6a) [146–149]. The combination could be an interesting approach to produced meshes for skin regeneration although it has not been explored in that sense yet. As previously explained nanofiber meshes have unique properties to promote skin regeneration although, especially coupled with controlled delivery of relevant therapeutic molecules. This could be achieved using the electrospraying technique that provides advantages over the more widespread use of nanoparticles prepared through conventional techniques, since no emulsion nor high temperatures are required, no further drying step is necessary and it provides an enhanced control over particle size distribution [145,150,151].

Hybrid structures produced through the combination of solution and melt electrospinning is another interesting emerging approach. The use of a molten polymer with electrostatic field was reported for the first time by Larrondo and Mandley [154–156]. However, only recently the use of melt polymers has received attention again rather than polymers dissolved in organic solvents. Although fibers obtained through melt electrospinning usually present relative high diameters, the technology presents important advantages namely not using organic solvents, thus avoiding solvent accumulation and the need to subsequently eliminating them to decrease sample toxicity [109,157]. The combination of solution with melt electrospinning also contributes to solve the problems associated with low cellular infiltration as a consequence of high-density packing of nanofibers, with the microfibers increasing the pore size and porosity required for cell infiltration, and nanofibers contributing to promote cell attachment and growth [145,158]. However, despite the potential of this kind of combination, only few works are available explored this approach, demonstrating that 3D hybrid structures made from PLGA micro and nanofibers show improved mechanical properties, cell attachment and growth than structures composed only by microfibers, thus representing a greater potential for tissue engineering applications, namely for skin regeneration (Fig. 6b) [134,152].

Another strategy to obtain hybrid structures involves additive manufacturing technology combined with electrospinning. Additive manufacturing (AM) techniques have been widely studied for scaffold fabrication due their ability to produce porous structures with high reproducibility, tailored external shape and internal morphology [159–161]. However, the produced scaffolds present lack of nanometer-sized details to mimic the native ECM of tissues. To improve cellular behaviour the combination with electrospun nanofibers is a possibility [131,160,162,163]. The initial works combining both

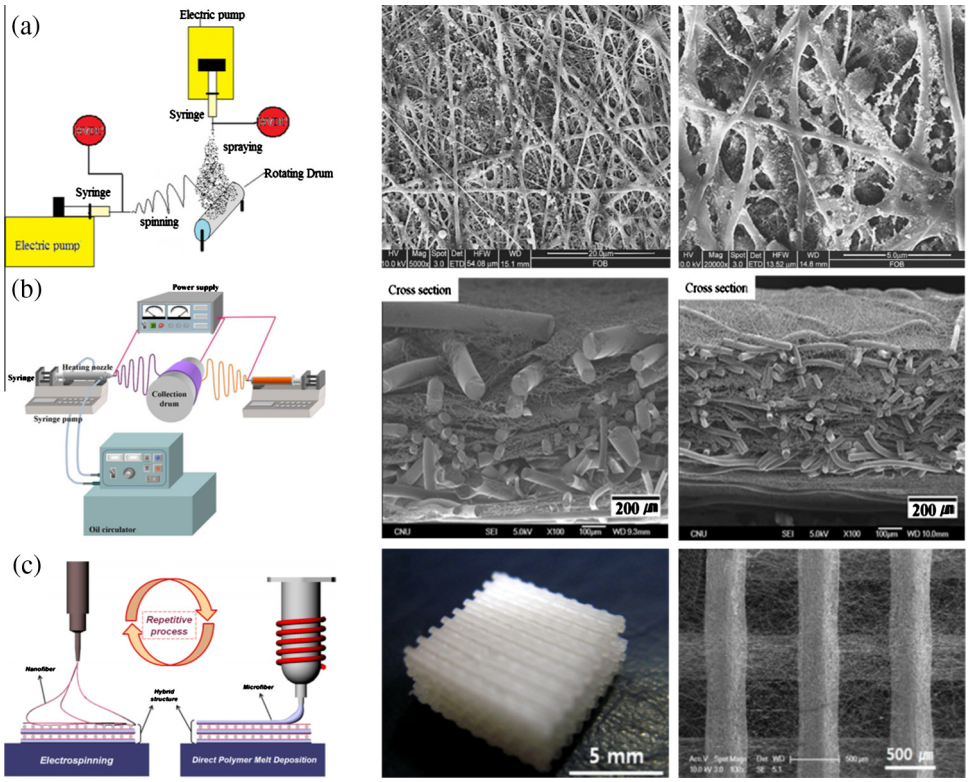

Fig. 6. Hybrid structures produced by combination of: (a) Electrospinning and electrospraying [146,147]. (b) Solution electrospinning and melt electrospinning [152]. (c) 3D printing (FDM) and electrospinning [153].

Table 4
Critical analysis of the essential characteristics of scaffolds produced by additive manufacturing (AM) in comparison with nanofibers produced by electrospinning and their influence on tissue regeneration.

Type of structure	Characteristics	Influence	Refs.
AM scaffolds	Controlled microstructure	Facilitates oxygen and nutrients transport across the structure by increasing the diffusion efficiency	[161,164,173]
	Suitable mechanical properties	Maintains scaffold structural integrity and stability and matches native tissue's mechanical characteristics to expose cells to the correct stress environment	[164,165,174,175]
	Large pore size	Limits cell seeding efficiency	[166,168,171,176]
	Smooth filaments	Inhibits initial cell attachment	[164,166,171]
Electrospun nanofibers	High surface area	Mimics the hierarchical structure of ECM that is critical for cell attachment, spreading and proliferation, as well as for nutrient/waste transportation	[52,79,82,168]
	High porosity	Favors cell attachment, differentiation and mimics the native ECM, facilitating nutrient and waste exchange and vascularization	[70,75,177–179]
	Fibers with low diameter	Fiber diameters match structural properties of the ECM and confer high surface area to volume specific ratio	[50,70,142,180]
	Low mechanical properties	Limits structural and functional integrity and does not provide the correct stress environment to produce neotissues	[70,99,164,167]
	High packing required to obtain 3D structures	Restricts cellular infiltration across the mesh	[160,181,182]

techniques were reported in 2008, demonstrating improved mechanical properties, cell attachment and proliferation of the hybrid structures and their potential for tissue engineering (Fig. 6c) [153,164,165]. Since then, only few additional works have been reported, most of them combining additive techniques based on fused deposition modeling (FDM) with electrospinning, and often using PCL [160,166–172]. Although no works exploring this approach for skin regeneration are available

it would be interesting to integrate the advantages of AM (control of pore size, pore size distribution, interconnectivity and mechanical properties) with electrospun nanofibers. The use of hybrid structures allows combining the advantages of both techniques and reducing or eliminating the disadvantages resulting of the separate use of each technique, as explained in Table 4.

Despite recent advances towards the development of hybrid structures for tissue engineering applications, several challenges still remain. Most of the hybrid structures produced are based on the combination of solution electrospinning together with electrospraying, melt electrospinning or additive manufacturing technologies. Combinations with other techniques, although yet little explored, represent equally exciting potential, even if for specific applications. Pateman and colleagues explored the potential of combining the stereolithography and electrospinning to create channels with oriented fibers supporting the regeneration of injured nerves and guide Schwann cell growth [183]. This approach could be equally interesting for wound dressing development by, for instance, allowing to produce fibers with photocrosslinkable hydrogels that combine the advantages of wound dressings composed by nanofibers (promoting hemostasis, semipermeability, no scar induction, among others) with photocrosslinkable hydrogels that, beyond the advantages of hydrogels in the wound healing process, allow precise control over the diffusion rate of bioactive substances across the structure [9,181,184].

4.5. Cell electrospinning

Scaffolds are critical to support, promote and guide cell growth, thus making the development of structures mimicking the ECM a subject of intense research. To recreate the complex tissue nano-microstructure, modular structures are required providing precise control over the architecture, biomechanical behaviour, cell density and degradation rate [1,7,41]. At present, two main approaches are available to integrate cells into the scaffolds: cell seeding and cell printing/bioprinting, correlated with top-down and bottom-up approaches, respectively. Cell seeding is the most widely used method to integrate cells into 3D structures and consists on seeding cells on scaffolds. However, this approach presents limited control over cell density, localization and spreading, resulting in low seeding efficiency, minimal cell penetration of scaffold walls and not mimicking the cellular organization of native tissues [185–187]. Although different approaches exist for cell seeding, cell printing been attracting great attention due to the possibility of integrating cells directly into the filaments that compose the 3D structure [188,189]. Different cell printing technologies allow the production of 3D structures, in which cells and biomaterials can be positioned in pre-determined places due to the precise control over the internal/external architecture and layer-by-layer fabrication [161,186,189]. The most widely used technologies for cell printing are the inkjet [45,190–192] extrusion [189,193,194], laser [195–197], valve-based [188,198] and acoustic ones [199,200] (Fig. 7).

The biological performance of electrospun meshes, similarly to other structures designed for tissue engineering applications, depends on their ability to incorporate the desired cell types and to promote the intended functionality of the incorporated cells [201]. As previously mentioned, the most common procedure relies in incorporating cells after scaffold production, although recent works have been exploring the combination of electrospinning with bioelectrospraying to seed cells during the production of the structure. The earlier incorporation of a high number of cells was reported to improve structural stability and biochemical composition of engineered tissues [202,203].

Similarly to the previous cell printing technologies mentioned, the cell electrospinning methodology intends to significantly reduce the time needed to generate complex cellularized structures, the non-uniformity in the seeded cells and the time required for cells to fully infiltrate the entire architecture [204]. This concept was pioneered in 2006 by Jayasinghe's research team, when they proposed cell electrospinning with different cell concentrations and using a core-shell set-up and varying flow rates [205]. The cell line used belongs to the neuronal lineage, and hence is more suitable to function under the influence of electric impulses without damage. Since cell suspensions by themselves are not electrospinnable the core-shell approach was used, in which the inner part was composed by a cellular suspension and the outer part by polydimethylsiloxane (PDMS). The outer solution should act as a shield for cells and provide a matrix for cell growth. The cellular viability *in vitro* post electrospinning was evaluated through flow cytometry and showed that cell growth and 100% of confluence in all samples was reached after 3 weeks of culture. *In vivo* tests were performed using real-time bioluminescent imaging in which results showed that the processing did not compromise the ability of the electrospun cells to proliferate [205–207]. However, according to Townsend-Nicholson and colleagues, when the bicomponent filaments (PDMS/cell in suspension) were submerged into the cell growth medium the nanofiber mesh configuration was lost, thus indicating that the cell viability mentioned before corresponded to the cell suspension alone and not to the performance of electrospun meshes incorporating cells. Nevertheless, the study showed the possibility of electrospinning living organisms. The same research team updated the previous work by using the same polymer (PDMS) but increasing the cell concentration from 10^6 to 10^7 - cell/mL and using primary porcine vascular smooth muscle cells and rabbit aorta smooth muscle cells [206]. Although cell viability was described as not affected by the electric field and fibers were electrospun containing high cellular concentrations, no evidence of remaining scaffolds after cell culture was provided. Recently, Sampson and co-workers reported *in vitro* and *in vivo* studies using cell electrospun meshes produced with modified matrigel as shell to the cell suspension. According to their results the cells submitted to the electric discharge showed a similar behaviour to the control ones (not submitted to any discharge), although the matrix was dissolved and cells disassociated from the scaffold before analysis [207].

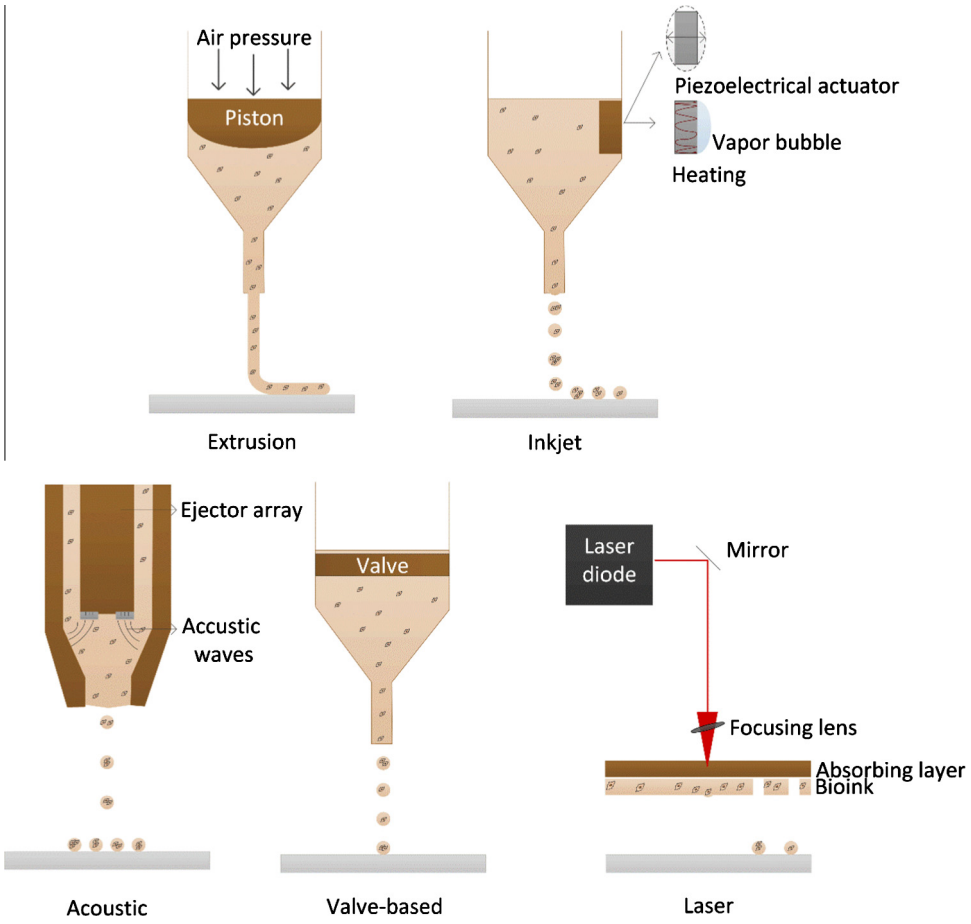

Fig. 7. Cell printing technologies.

Although a few publications already exist on the topic of cell electrospinning, the issues related to cell behaviour in a high electric field, namely the in depth assessment of cellular damage, has not been reported yet. Jayasinghe and his team reported that cells survive the electrospinning process without any major damage, although enough evidence is still missing showing that the 3D structures encapsulating the cells maintain their architecture over time. Another limitation of this process is related with the fiber size. One major advantage of electrospun nanofibers in wound healing is the relatively small fiber diameters (in the order of nanometers), which mimics the native ECM. In suspension cells assume a size of around 10–20 μm, which considerably limits the fiber diameter achievable with the cell electrospinning approach to the micrometer size range, thus compromising the natural advantage of electrospinning to mimic the native fibers of ECM (10–300 nm) compared to other competing technologies such as cell printing.

Therefore, additional studies are required to further address the issues described above. However, in the field of skin regeneration this new approach brings enormous potential, with the possibility of incorporating cells into the core of polymer fibers, thus eventually decreasing the problems associated with low cell infiltration as a consequence of small pore size and high packing associated to electrospun 3D meshes.

4.6. In situ electrospinning

In situ electrospinning is, a new concept that intends to produce appropriate substitutes for tissue repair and regeneration directly on the patient's lesion [7]. To fabricate the adequate substitutes this approach is associated to real-time imaging techniques and path-planning devices for the digitalization of the damaged area and definition of the path for the deposition of biomaterials with or without cells that can be combined with encapsulated cells [7]. The main goal of this approach is to provide a tool to directly create a customized wound dressing to the wound bed, with easy and quick application, painless to remove and at a low cost [208,209]. Xu et al. recently patented an easily handled and portable e-spinning battery-operated apparatus for *in situ* electrospinning (Fig. 8a) [210], allowing the deposition of electrospun meshes, with similar characteristics

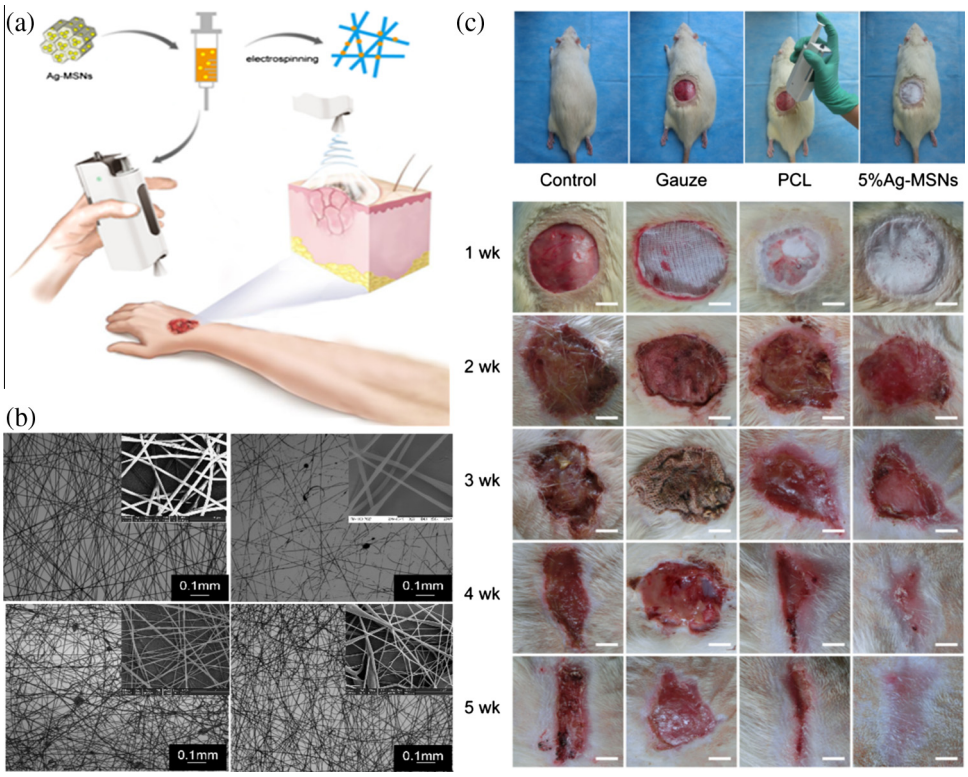

Fig. 8. *In situ* electrospinning concept, (a) portable electrospinning system, (b) SEM of electrospun meshes obtained with portable system, (c) *in vivo* evaluation of *in situ* electrospun mesh, PCL-polycaprolactone, Ag-MSNs -mesoporous silica nanoparticles [208,209].

to the ones obtained by the conventional electrospinning technique, directly to the skin and using varied polymeric micro/nanofibers (Fig. 8b) [208]. More recently, the same team explored the effect of *in situ* electrospinning on the wound healing process. They deposited *in situ* mesoporous silica nanoparticles (Ag-MSNs) dispersed in PCL electrospun fibers and evaluated the antimicrobial activity and biological efficacy in wistar rats. The *in vitro* and *in vivo* results confirmed the antimicrobial activity and bioavailability of 5% Ag-MSNs/PCL electrospun fibers (average diameter of 658 nm). The results showed efficient antibacterial properties against predominant pathogenic bacteria (gram negative *Escherichia coli*) responsible for several burn wound infections. *In vivo* studies clearly showed the improvement of *in situ* deposited nanofibers on wound healing compared to the control groups. After four weeks of post-treatment it was possible to observe significant wound closure and complete re-epithelialization (Fig. 8c) [209]. This new approach can bring considerable advances in the wound care field, allowing a quick deposition of skin substitutes independently of wound size and depth, although some issues still remain to addressed, such as the decrease of fiber diameter (from ca. 650 to 10–300 nm, the average diameter of fibers in native ECM), and the matching of mechanical properties between structures developed and native skin.

5. Concluding remarks and future trends

Nanoscale constructs, and electrospun meshes in particular, have been receiving great attention from the scientific and medical communities for skin regeneration. In the past few years, important advances have been achieved in terms of nanofiber fabrication strategies, and related material synthesis and functionalization, and *in vitro* cell culture procedures. The developments in the field reported so far have been considerably contributing for a more efficient mimicking of the ECM through the combination of materials, growth factors, proteins and biomolecules which, associated to the novel advanced processing strategies, making possible the production of wound dressings with a remarkable potential for skin regeneration. However, recent advances in the specific topic of skin regeneration have been mainly focused on materials rather than in sophisticated fabrication strategies to generate biomimetic and complex constructs that resemble the mechanical and structural properties of skin. Research efforts have been focused on both the development of novel material combinations and the improvement of the biochemical properties of existing materials, for instance, through the use of functionalization procedures and surface modification processes. In general, improved skin substitutes need to be developed to avoid the use of animal-derived materials, improve the adhesion of cultured keratinocytes to the wound bed, improve the rate of neovascularization of tissue engineered skin and enhance the scaffolds materials to resist to the wound contraction and fibrosis.

Several advances on the evolving field of electrospinning can be foreseen with specific application in wound healing, namely:

(i) Development of combined and functional structures using different deposition strategies, such as the multimaterial approach, where two or more materials are deposited at the same time on a single collector, or create a multilayer structure with sequential production. Other interesting strategy is the use of hybrid structures through the combination of filaments produced using different methodologies, such as using emulsions, copolymers, or the core/shell approach.
(ii) Integration of different technologies with electrospinning and different electrospinning approaches to obtain hybrid structures with tunable gradients, properties and functionalities. Combining different materials and fiber compositions, different fiber diameters and nano/microarchitectures to achieve the most suitable mimetic structure to regenerate the skin tissue;
(iii) Cell electrospinning of skin cells (keratinocytes and fibroblasts) needs to be explored to evaluate the electric field influence on the cells viability, proliferation and gene expression. The integration of cells into electrospun fibers will bring forward a new generation of skin substitutes and solve problems of cell infiltration associated to electrospun meshes;
(iv) The *in situ* electrospinning is a promising technology providing the possibility of direct deposition of electrospun nanofibers on the wound with no restriction due to wound size or depth. This technology open considerable possibilities, especially combined with previously mentioned developments, namely the deposition of multilayer structures to build hybrid structures or the integration with cell electrospinning.

Acknowledgments

This work was financed by European Regional Development Fund (ERDF) through the COMPETE 2020 - Operational Programme for Competitiveness and Internationalization (POCI), Norte Portugal Regional Operational Programme (NORTE 2020), under the PORTUGAL 2020 Partnership Agreement, and by Portuguese funds through Portuguese Foundation for Science and Technology (FCT) in the framework of the project Ref. PTDC/BBB-ECT/2145/2014. Juliana Dias is also grateful to FCT for the doctoral grant SFRH/BD/91104/2012.

References

[1] Yildirimer L, Thanh NTK, Seifalian AM. Skin regeneration scaffolds a multimodal bottom-up approach. Trends Biotechnol 2012;30:638–48.
[2] Seal BL, Otero TC, Panitch A. Polymeric biomaterials for tissue and organ regeneration. Mater Sci Eng R 2001;34:147–230.
[3] WHO. The global burden of disease 2004, 2008.
[4] WHO. Fact sheet n°365, 2014.
[5] Brusselaers N, Monstrey S, Vogelaers D, Hoste E, Blot S. Severe burn injury in Europe: a systematic review of the incidence, etiology, morbidity, and mortality. Crit Care 2010;14(R188):1–12.
[6] Shevchenko RV, James SL, James SE. A review of tissue-engineering skin bioconstructs available for skin reconstruction. J R Soc Interface 2010;7:229–58.
[7] Pereira RF, Barrias CC, Granja PL, Bártolo PJ. Advanced biofabrication strategies for skin regeneration and repair. Nanomedicine 2013;8:603–21.
[8] Reddy VJ, Radhakrishnan S, Ravichandran R, Mukherjee S, Balamurugan R, Sundarrajan S, et al. Nanofibrous structured biomimetic strategies for skin tissue regeneration. Wound Rep Reg 2013:211–6.
[9] Zahedi P, Rezaeian I, Ranaei-Sidat SO, Jafari SH, Supaphol P. A review on wound dressings with an emphasis on electrospun nanofibrous polymeric bandages. Polym Adv Technol 2009;21:77–95.
[10] Casey G. The physiology of the skin. Nurs Stand 2002;16:47–51.
[11] MacNeil S. Progress and opportunities for tissue-engineering skin. Nature 2007;445:874–80.
[12] Zhou SS, Li D, Zhou YM, Cao JM. The skin function: a factor of anti-metabolic syndrome. Diabetol Metab Synd 2012;4:1–11.
[13] Lai-Cheong JE, McGrath JA. Structure and function of skin, hair and nails. Medicine 2013;41:317–20.
[14] Timmons J. Skin function and wound healing physiology. Wound Essen 2006;1:9–17.
[15] BÖttcher-Haberzeth S, Biedermann T, Reichmann E. Tissue engineering of skin. Burns 2010;36:450–60.
[16] Scanlon VC, Sanders T. Essentials of anatomy and physiology. 5th ed, 2007.
[17] Tortora GJ, Derrickson B. Principles of anatomy and physiology. 13th ed, 2012.
[18] Molly MS, Juliana HG. Exploring and engineering the cell surface interface. Science 2005;310:1135–8.
[19] Sun T, Norton D, McKean RJ, Haycock JW, Ryan AJ, MacNeil S. Development of a 3D cell culture system for investigating cell interactions with electrospun fibers. Biotechnol Bioeng 2007;97(5):1318–28.
[20] Sun T, Mai S, Norton D, Haycock JW, Ryan AJ, MacNeil S. Self-organization of skin cells in three-dimensional electrospun polystyrene scaffolds. Tissue Eng 2005;11(7/8):1023–33.
[21] Enoch S, Leaper DJ. Basic science of wound healing. Surgery 2007;26:31–7.
[22] Young A, McNaught CE. The physiology of wound healing. Surgery 2011;29:475–9.
[23] Nauta A, Gurtner GC, Longaker MT. Wound healing and regenerative strategies. Oral Dis 2011;17:541–9.
[24] Monaco JL, Lawrence WT. Acute wound healing: an overview. Clin Plastic Surg 2003;30:1–12.
[25] MacKay D, Miller AL. Nutritional support for wound healing. Altern Med Rev 2003;8:359–77.
[26] Groeber F, Holeiter M, Hampel M, Hinderer S, Schenke-Layland K. Skin tissue engineering – in vivo and in vitro applications. Adv Drug Deliv Rev 2011;128:352–66.
[27] Pham C, Greenwood J, Cleland H, Woodruff P, Maddern G. Bioengineered skin substitutes for the management of burns: a systematic review. Burns 2007;33:946–57.
[28] Zhong S, Zhang Y, Lim C. Tissue scaffolds for skin wound healing and dermal reconstruction. WIREs Nanomed Nanobiotechnol 2010;2:510–25.
[29] Vasconcelos A, Gomes AC, Cavaco-Paulo A. Novel silk fibroin/elastin wound dressings. Acta Biomater 2012;8:3049–60.
[30] Wang T, Zhu XK, Xue XT, Wu DY. Hydrogel sheets of chitosan, honey and gelatin as burn wound dressings. Carbohydr Polym 2011;88:75–83.
[31] Weller C, Sussman G. Wound dressings update. J Pharm Pract Res 2006;36:318–24.
[32] Watson NFS, Hodgkin W. Wound dressings. Surgery 2005;23:52–5.

[33] Abdelrahman T, Newton H. Wound dressings: principles and practice. Surgery 2011;29:491–5.
[34] Poinern GEJ, Fawcett D, Ng YJ, Ali N, Brundavanam RK, Jiang ZT. Nanoengineering a biocompatible inorganic scaffold for skin wound healing. J Biomed Nanotechnol 2010;6:497–510.
[35] Pramanik S, Pingguan-Murphy B, Osman NAA. Progress if key strategies in development of electrospun scaffolds: bone tissue. Sci Technol Adv Mater 2012:131. 13pp.
[36] Zhang Z, Michniak-Kohn BB. Tissue engineered human skin equivalents. Pharmaceutics 2012;4:26–41.
[37] Van der Veen VC, van der Wal MB, van Leeuwen MC, Ulrich MM, Middelkoop E. Biological background of dermal substitutes. Burns 2010;36:305–21.
[38] Harding K, Sumner M, Cardinal M. A prospective, multicentre, randomised controlled study of human fibroblast-derived dermal substitute (Dermagraft) in patients with venous leg ulcers. Int Wound J 2013;10:123–37.
[39] MacNeil S. Biomaterials for tissue engineering of skin. Mater Today 2008;11:27–35.
[40] Kearney JN. Clinical evaluation of skin substitutes. Burns 2001;27:545–51.
[41] Nichol JW, Khademohosseini A. Modular tissue engineering: engineering biological tissues from the bottom-up. Soft Matter 2009;5:1312–9.
[42] Bártolo PJ, Domingos M, Patrício T, Cometa S, Mironov V. Biofabrication strategies for tissue engineering. In: Fernandes PJBPR, editor. Advances on modeling in tissue engineering. Berlin: Springer; 2011. p. 137–76.
[43] Nemeno-Guanzon JG, Lee S, Berg JR, Jo YH, Yeo JE, Nam BM, et al. Trends in tissue engineering for blood vessels. J Biomed Biotechnol 2012:956345.
[44] Rustad KC, Sorkin M, Levi B, Longaker MT, Gurtner GC. Strategies for organ level tissue engineering. Organogenesis 2010:61–7.
[45] Jakab K, Norotte C, Marga F, Murphy K, Vunjak-Novakovic G, Forgacs G. Tissue engineering by self-assembly and bio-printing of living cells. Biofabrication 2010;2:02200.
[46] Zamanian B, Kachouie N, Masaeli M, Nichol JW, Khademhosseini A. Self-assembly of cell-laden hydrogels on the liquid-air interface. In: Berthiaume JMF, editor. 3-D tissue engineering. Artech House; 2009. p. 121–32.
[47] Bhardwaj N, Kundu SC. Electrospinning: a fascinating fiber fabrication technique. Biotechnol Adv 2010;28:325–47.
[48] Stanger J, Tucker N, Staiger M. Electrospinning. Rapra review reports. Report 2005;16:190.
[49] Tucker N, Jonathan JS, Staiger MP, Razzaq H, Hofman K. The history of the science and technology of electrospinning from 1600 to 1995. J Eng Fibers Fabr 2012:63–73.
[50] Burger C, Hsiao, Chu B. Nanofibrous materials and their applications. Annu Rev Mater Res 2006;36:333–68.
[51] Teo WE, Ramakrishna S. A review on electrospinning design and nanofibre assemblies. Nanotechnology 2006;17:89–106.
[52] Cui W, Zhou Y, Chang J. Electrospun nanofibrous materials for tissue engineering and drug delivery. Sci Technol Adv Mater 2010;11014108.
[53] Cooley JF. Apparatus for electrically dispersing fluids. US; 1902.
[54] Cooley JF. Electrical method of dispersing fluids. US; 1903.
[55] Formhals A. Process and apparatus for preparing artificial threads, 1934.
[56] Formhals A. Production of artificial fibers, 1937.
[57] Formhals A. Method and apparatus for the production of fibers, 1936.
[58] Formhals A. Artificial fiber construction, 1938.
[59] Formhals A. Method of producing artificial fibers, 1939.
[60] Formhals A. Method and apparatus for the production of artificial fibers, 1939.
[61] Formhals A. Method and apparatus for spinning, 1939.
[62] Formhals A. Artificial thread and method of producing same, 1940.
[63] Formhals A. Production of artificial fibers from fiber forming liquids, 1943.
[64] Formhals A. Method and apparatus for spinning, 1944.
[65] Sill TJ, von Recum HA. Electrospinning: applications in drug delivery and tissue engineering. Biomaterials 2008;29:1989–2006.
[66] Norton C. Method of and apparatus for producing fibrous or filamentary material, 1936.
[67] Vrieze S, Camp TV, Nelvig A, Hagstrom B, Westbroek P, Clerck K. The effect of temperature and humidity on electrospinning. J Mater Sci 2009;44:1357–62.
[68] Fang D, Liu Y, Jiang S, Nie J, Ma G. Effect of intermolecular interaction on electrospinning of sodium alginate. Carbohydr Polym 2011;85:276–9.
[69] Nukavarapu SP, Kumbar SG, Merrell JG, Laurencin CT. Electrospun polymeric nanofibre scaffolds for tissue regeneration. In: Nair L, Laurencin CT, editors. Nanotechnology and tissue engineering: the scaffold. London: Taylor & Francis; 2008.
[70] Shin SH, Purevdorj O, Castano O, Planel JA, Kim HW. A short review: recent advances in electrospinning for bone tissue regeneration. J Tissue Eng 2012;3:1–11.
[71] Li WJ, Xia Y. Electrospinning of nanofibres: reivented the wheel? Adv Mater 2004;16:1151–70.
[72] Braghirolli DL, Steffens D, Pranke P. Electrospinning for regenerative medicine: a review of the main topics. Drug Disc Today 2014;19:743–53.
[73] Reneker DH, Yarin AL, Zussman E, Xu H. Electrospinning of nanofibers from polymer solutions and melts. Adv Appl Mech 2007;41:43–195.
[74] Tiwari SK, Venkatraman SS. Importance of viscosity parameters in electrospinning: of monolithic and core–shell fibers. Mater Sci Eng, C 2012;32(5):1037–42.
[75] Bártolo P, Kruth JP, Silva J, Levy G, Malshe A, Rajurkar K. Biomedical production of implants by additive electro-chemical and physical processes. CIRP Ann - Manuf Technol 2012;61(2):635–55.
[76] Rogina A. Electrospinning process: VERSATILE preparation method for biodegradable and natural polymers and biocomposite systems applied in tissue engineering and drug delivery. Appl Surf Sci 2014;296:221–30.
[77] Ramakrishna S, Fujihara K, Teo WE, Lim TC, Ma Z. An introduction to electrospinning and nanofibers. Singapore: World Scientific; 2005.
[78] Pham QP, Sharma U, Mikos AG. Electrospinning of polymeric nanofibers for tissue engineering applications: a review. Tissue Eng Part B 2006;12(5):1197–211.
[79] Rim NG, Shin CS, Shin H. Current approaches to electrospun nanofibers for tissue engineering. Biomed Mater 2013;8:1–14.
[80] Wiesmann HP, Lammers L. Scaffold structure and fabrication. In: Handschel J, Meyer U, Wieamann HP, Meyer T, editors. Fundamentals of tissue engineering and regenerative medicine. Springer; 2009. p. 539–49.
[81] Yang F, Neeley WL, Moore MJ, Karp JM, Shukla A. Tissue engineering: the therapeutic strategy of the twenty-first century. In: Nair CTLALS, editor. Nanotechnolgy and tissue engineering: the scaffold. Springer; 2008. p. 3–32.
[82] Liu W, Thomopoulos S, Xia Y. Electrospun nanofibres for regenerative medicine. Adv Healthcare Mater 2012;1:10–25.
[83] Boyer G, Molimard J, Tkaya MB, Zahouani H, Pericoi M. Assessment of the in-plane biomechanical properties of human skin using a finite element model updating approach combined with an optical full-field measurement on a new tensile device. J Mech Behav Biomed Mater 2013;27:273–82.
[84] Brown IA. A scanning electron microscope study of the effects of uniaxial tension on human skin. Br J Dermatol 1973;89:383–93.
[85] Annaidh AN, Bruyere K, Destrade M, Gilchrist MD, Otténio M. Characterization of the anisotropic mechanical properties of excised human skin. J Mech Behav Biomed Mater 2012;5:139–48.
[86] Agache PG. Physiologie de la peau et explorations fonctionnelles cutanées. ed. E.M. Internationales; 2000.
[87] Jansen L, Rottier P. Some mechanical properties of human abdominal skin measured on excised strips. Dermatologica 1985;117:65–83.
[88] Vogel H. Age dependence of mechanical and biochemical properties of human skin. Bioeng Skin 1987;3:67–91.
[89] Jacquemoud C, Bruyere-Garnier K, Coret M. Methodology to determine failure characteristics of planar soft tissues using a dynamic tensile test. J Biomech 2007;40(2):468–75.
[90] Pan J-F, Liu N-H, Sun H, Xu F. Preparation and characterization of electrospun PLCL/poloxamer nanofibers and dextran/gelatin hydrogels for skin tissue engineering. PLoS One 2014;9(11):e112885.

[91] Gümüşderelioğlu M, Dalkıranoğlu S, Aydın RST, Çakmak S. A novel dermal substitute based on biofunctionalized electrospun PCL nanofibrous matrix. J Biomed Mater Res Part A 2011;98(A):461–72.
[92] Atila D, Keskin D, Tezcaner A. Cellulose acetate based 3-dimensional electrospun scaffolds for skin tissue engineering applications. Carbohydr Polym 2015;133:251–61.
[93] Lee EJ, Lee JH, Jin L, Jin OS, Shin YC, Oh SJ, et al. Hyaluronic acid/poly(lactic-co-glycolic acid) core/shell fiber meshes loaded with pigallocatechin-3-O-gallate as skin tissue engineering scaffolds. J Nanosci Nanotechnol 2014;14(11):8458–63.
[94] Sigma-Aldrich <http://www.sigmaaldrich.com/labware/labware-products.html?TablePage=109807607> [cited 2016 11/02/2016].
[95] NanofiberSolutions™ <http://www.nanofibersolutions.com/products.html> [cited 2016 11/02/2016].
[96] Zeus <http://www.zeusinc.com/> [cited 2016 11/02/2016].
[97] FundaciónCardiovasculardeColombia. Clinical trial for the treatment of diabetic foot ulcers using a nitric oxide releasing patch: PATHON; 2011 <https://clinicaltrials.gov/ct2/show/NCT00428727?term=electrospinning&rank=2> [cited 2016 11/02/2016; NCT00428727].
[98] ClinicalTrials.gov <https://clinicaltrials.gov/ct2/results?term=electrospinning> [cited 2016 11/02/2016].
[99] Agarwal S, Wendorff JH, Greiner A. Use of electrospinning technique for biomedical applications. Polymer 2008;49:5603–21.
[100] Miloh T, Spivak B, Yarin A. Needleless electrospinning: electrically driven instability and multiple jetting from free surface of a spherical liquid layer. J Appl Phys 2009;106:114910–8.
[101] Meng ZX, Wang YS, Ma C, Zheng W, Li L, Zheng YF. Electrospinning of PLGA/gelatin randomly-oriented and aligned nanofibers as potential scaffold in tissue engineering. Mater Sci Eng, C 2010;30:1204–10.
[102] Schneider T, Kohl B, Sauter T, Kratz K, Lendlein A, Ertel W, et al. Influence of fiber orientation in electrospun polymer scaffolds on viability, adhesion and differentiation of articular chondrocytes. Clin Hemorheol Microcircul 2012;52:325–36.
[103] Jahani H, Kaviani S, Hassanpour-Ezatti M, Soleimani M, Kaviani Z, Zonoubi Z. The effect of aligned and random electrospun fibrous scaffolds on rat mesenchymal stem cell proliferation. Cell J 2012;14:31–8.
[104] Shang S, Yang F, Cheng X, Walboomers XF, Jansen JA. The effect of electrospun fibre alignment on the behavior of rat periodontal ligament cells. Euro Cells Mat 2010;19:180–92.
[105] Jha BS, Ayres CE, Bowman JR, Telemeco TA, Sell SA, Bowlin GL, et al. Electrospun collagen: a tissue engineering scaffold with unique functional properties in a wide variety of applications. J Nanomat 2011:1–15.
[106] Said SS, Aloufy AK, El-Halfawy OM, Boraei NA, El-Khordagui LK. Antimicrobial PLGA ultrafine fibers: interaction with wound bacteria. Euro J Pharm Biopharm 2011;79:108–18.
[107] Said SS, El-Halfawy OM, El-Gowelli HM, Aloufy AK, Boraei NA, El-Khordagui LK. Bioburden-responsive antimicrobial PLGA ultrafine fibers for wound healing. Euro J Pharm Biopharm 2012;80:85–94.
[108] Coşkun G, Karaca E, Ozyurtlu M, Özbek S, Yermezler A, Çavuşoğlu İ. Histological evaluation of wound healing performance of electrospun poly(vinyl alcohol)/sodium alginate as wound dressing in vivo. Bio-Med Mater Eng 2014;24:1527–36.
[109] Hutmacher DW, Dalton PD. Melt electrospinning. Chem Asian J 2011;6:44–56.
[110] Sun D, Chang C, Li S, Lin L. Near-field electrospinning. Nano Lett 2006;6(4):839–42.
[111] Chang C, Limkrailassiri K, Lin L. Continuous near-field electrospinning for large area deposition of orderly nanofiber patterns. Appl Phys Lett 2008;93(12):123111.
[112] Kim HN, Jiao A, Hwang NS, Kim MS, Kang DH, Kim D-M, et al. Nanotopography-guided tissue engineering and regenerative medicine. Adv Drug Deliv Rev 2013;65:536–58.
[113] Cooper A, Bhattarai N, Zhang M. Fabrication and cellular compatibility of aligned chitosan–PCL fibers for nerve tissue regeneration. Carbohydr Polym 2011;85:149–56.
[114] Kenar H, Kose GT, Toner M, Kaplan DL, Hasirci V. A 3D aligned microfibrous myocardial tissue construct cultured under transient perfusion. Biomaterials 2011;32:5320–9.
[115] Wang C-Y, Zhang K-H, Fan C-Y, Mo X-M, Ruan H-J, Li F-F. Aligned natural–synthetic polyblend nanofibers for peripheral nerve regeneration. Acta Biomater 2011;7:634–43.
[116] Cox H. The cleavage lines of the skin. Br J Surg 1941;29(114):234–40.
[117] Stark HL. Directional variations in the extensibility of human skin. Br J Plast Surg 1977;30(2):105–14.
[118] Patel S, Kurpinski K, Quigley R, Gao H, Hsiao BS, Poo MM, et al. Bioactive nanofibers: synergistic effects of nanotopography and chemical signaling on cell guidance. Nano Lett 2007;7(7):2122–8.
[119] Kurpinski K, Stephenson J, Raphael R, Janairo R, Lee H, Li S. The effect of fiber alignment and heparin coating on cell infiltration into nanofibrous PLLA scaffolds. Biomaterials 2010;31(3):3536–42.
[120] Elahi MF, Lu W, Guoping G, Khan F. Core/shell fibers for biomedical applications-a review. J Bioeng Biomed Sci 2013;3:1–14.
[121] Nguyen TTT, Chung OH, Park JS. Coaxial electrospun poly(lactic acid)/chitosan (core/shell) composite nanofibres and their antibacterial activity. Carbohyd Polym 2011;86:1799–806.
[122] Diban N, Haimi S, BolhuisVersteeg L, Teixeira S, Miettinen S, Poot A, et al. Development and characterization of poly(εcaprolactone) hollow fiber membranes for vascular tissue engineering. J Memb Sci 2013;438(2013):29–37.
[123] Mickova A, Buzgo M, Benada O, Rampichova M, Fisar Z, Filova E, et al. Core/Shell nanofibers with embedded liposomes as a drug delivery system. Biomacromolecules 2012;13:952–62.
[124] Maleki M, Latifi M, Amani-Tehran M, Mathur S. Electrospun core-shell nanofibers for drug encapsulation and sustained release. Polym Eng Sci 2013:1770–9.
[125] Jin G, Prabhakaran MP, Kai D, Ramakrishna S. Controlled release of multiple epidermal induction factors through core-shell nanofibres for skin regeneration. Euro J Pharm Biopharm 2013;85:689–98.
[126] Khajavi R, Abbasipour M. Electrospinning as a versatile method for fabricating coreshell, hollow and porous nanofibres. Sci Iran F 2012;19:2029–34.
[127] Wei Z, Zhang Q, Peng M, Wang X, long S, Yang J. Preparation and drug delivery study of electrospun hollow PES ultrafine fibers with a multilayer wall. Colloid Polym Sci 2014;292:1339–45.
[128] Zhang H, Zhao C, Zhao Y, Tang G, Yuan X. Electrospinning of ultrafine core/shell fibers for biomedical applications. Sci China Chem 2010;53:1246–54.
[129] Ma G, Fang D, Liu Y, Zhu X, Nie J. Electrospun sodium alginate/poly(ethylene oxide) core–shell nanofibres scaffolds potential for tissue engineering applications. Carbohyd Polym 2012;87:737–43.
[130] Zhang H, Zhao Y, Han F, Wang M, Yuan X. Controlled release of bovine serum albumin from electrospun fibrous membranes via an improved emulsion-core technique. Abstracts/J Control Rel 2011;152:e133–91.
[131] Wang N, Burugapalli K, Song W, Halls J, Moussy F, Ray A, et al. Electrospun fibro-porous polyurethane coatings for implantable glucose biosensors. Biomaterials 2013;34:888–901.
[132] Sun B, Long YZ, Zhang HD, Li MM, Duvail JL, Jiang XY, et al. Advances in three-dimensional nanofibrous macrostructures via electrospinning. Progr Poly Sci 2014;39:862–90.
[133] Dalton PD, Vaquette C, Farrugia BL, Dargaville TR, Brown TD, Hutmacher DW. Electrospinning and additive manufacturing: converging technologies. Biomater Sci 2013;1:171–85.
[134] Yoon YI, Park KE, Lee SJ, Park WH. Fabrication of microfibrous and nano-/microfibrous scaffolds: melt and hybrid electrospinning and surface modification of poly(ι-lactic acid) with plasticizer. BioMed Res Int 2013:1–10.
[135] Grey CP, Newton ST, Bowlin GL, Haas TW, Simpson DG. Gradient fiber electrospinning of layered scaffolds using controlled transitions in fiber diameter. Biomaterials 2013;2013(34):4993–5006.

[136] Sundararaghavan HG, Burdick JA. Gradients with depth in electrospun fibrous scaffolds for directed cell behavior. Biomacromolecules 2011;12:2344–50.
[137] Abrigo M, Kingshott P, McArthur SL. Electrospun polystyrene fiber diameter influences bacterial attachment, proliferation and growth. Appl Mater Interf 2015;7(14):7644–52.
[138] Tijing LD, Ruelo MTG, Amarjargal A, Pant HR, Park CH, CS K. One-step fabrication of antibacterial (silver nanoparticles/poly(ethylene oxide)) e polyurethane bicomponent hybrid nanofibrous mat by dual-spinneret electrospinning. Mater Chem Phys 2012;2012(137):557–61.
[139] Jin G, Prabhakaran MP, Ramakrishna S. Stem cell differentiation to epidermal lineages on electrospun nanofibrous substrates for skin tissue engineering. Acta Biomater 2011;7:3113–22.
[140] Har-el Y-E, Gerstenhaber JA, Brodsky R, Huneke RB, Lelkes PL. Electrospun soy protein scaffolds as wound dressings: enhanced reepithelialization in a porcine model of wound healing. Wound Med 2014;2014(5):9–15.
[141] Park SH, Kim MS, Lee BJ, Park JH, Lee HJ, Lee NK, et al. Creation of a hybrid scaffold with dual configuration of aligned and random electrospun fibers. Appl Mater Interfaces 2016:1–27.
[142] Garg K, Bowlin GL. Electrospinning jets and nanofibrous structures. Biomicrofluid 2011;5:013403–19.
[143] Shenoy SL, Bates WD, Frisch HL, Wnek GE. Role of chain entanglements on fiber formation during electrospinning of polymer solutions: good solvent, non-specific polymer-polymer interaction limit. Polymers 2005;43:3372–84.
[144] Jaworek A, Krupta A, Lackowski M, Sobczyk AT, Czech T, Ramakrishna S, et al. Electrospinning and electrospraying techniques for nanocomposites non-woven fabric production. Fibres Text Eastern Euro 2009;17:77–81.
[145] Bock N, Dargaville TR, Woodruff MA. Electrospraying of polymers with therapeutic molecules: state of art. Prog Poly Sci 2012;37:1510–51.
[146] Gupta D, Venugopal J, Mitra S, Dev VRG, Ramakrishna S. Nanostructured biocomposite substrates y electrospinning and electrospraying for the mineralization of osteoblasts. Biomaterials 2009;30:2085–94.
[147] Francis L, Venugopal J, Prabhakaran MP, Thavasi V, Marsano E, Ramakrishna R. Simultaneous electrospin–electrosprayed biocomposite nanofibrous scaffolds for bone tissue regeneration. Acta Biomater 2010;6:4100–9.
[148] Li W, Li X, Li W, Wang T, Li X, Pan S, et al. Nanofibrous mats layer-by-layer assembled via electrospun cellulose acetate and electrosprayed chitosan for cell culture. Euro Poly J 2012;48:1846–53.
[149] Zhu W, Masoodb F, O'Brien J, Zhang L. Highly aligned nanocomposite scaffolds by electrospinning and electrospraying for neural tissue regeneration. Nanomed Nanotechnol Biol Med 2015;2015(11):693–704.
[150] Sokolsky-Papkov M, Agashi K, Olaye A, Shakesheff K, Domb AJ. Polymer carriers for drug delivery in tissue engineering. Adv Drug Deliv Rev 2007;59:187–206.
[151] Freiberg S, Zhu X. Polymer microspheres for controlled drug release. Int J Pharm 2004;282:1–18.
[152] Kim SJ, Jang DH, Park WH, Min B-M. Fabrication and characterization of 3-dimensional PLGA nanofiber/microfiber composite scaffolds. Polymer 2010;51:1320–7.
[153] Park SH, Kim TG, Kim HC, Yang DY, Park TG. Development of dual scale scaffolds via direct polymer melt deposition and electrospinning for applications in tissue regeneration. Acta Biomat 2008;4:1198–207.
[154] Larrondo L, Manley JRS. Electrostatic fiber spinning from polymer melts: experimental observations on fiber formation and properties. J Poly Sci Part B 1981;19:909–20.
[155] Larrondo L, Manley JRS. Electrostatic fiber spinning from polymer melts: examination of the flow field in an electrically driven jet. J Poly Sci Part B 1981;19:921–32.
[156] Larrondo L, Manley JRS. Electrostatic fiber spinning from polymer melts; electro static deformation of pendent drop of polymer melt. J Poly Sci Part B 1981;19:933–40.
[157] Dalton PD, Klee D, Möller M. Electrospinning with dual collection rings. Polymer 2005;46:611–4.
[158] Ekaputra AK, Prestwich GD, Cool SM, Hutmacher DW. The three-dimensional vascularization of growth factor-releasing hybrid scaffolds of poly(e-caprolactone)/collagen fibers and hyaluronic acid hydrogel. Biomaterials 2011;32:8108–17.
[159] Bártolo PJ, Almeida HA, Rezende RA, Laoui T, Bidanda B. Advanced processes to fabricate scaffolds for tissue engineering. In: Bidanda B BP, editor. Virtual prototyping & bio manufacturing in medical applications. New York: Springer; 2008. p. 149–70.
[160] Mota C, Puppi D, Dinucci D, Errico C, Bártolo P, Chiellini F. Dual-scale polymeric constructs as scaffolds for tissue engineering. Materials 2011;4:527–42.
[161] Mota C, Puppi D, Chiellini F, Chiellini E. Additive manufacturing techniques for the production of tissue engineering constructs. J Tissue Eng Regen Med 2012;9:174–90.
[162] Mitchell GR, Ahn K-H, Davis FJ. The potential of electrospinning in rapid manufacturing processes. Virt Phys Prot 2011;6:63–77.
[163] Wang X, Ding B, Li B. Biomimetic electrospun nanofibrous structures for tissue engineering. Mater Today 2013;16:229–41.
[164] Kim GH, Son JG, Park SA, Kim WD. Hybrid process for fabricating 3D hierarchical scaffolds combining rapid prototyping and electrospinning. Macrom Rapid Commun 2008;29:1577–81.
[165] Giannitelli SM, Mozetic P, Trombetta M, Rainer A. Combined additive manufacturing approaches in tissue engineering. Acta Biomater 2015;2015 (24):1–11.
[166] Ahn SH, Koh YH, Kim GH. A three-dimensional hierarchical collagen scaffold fabricated by combined solid freeform fabrication (SFF) and electrospinning process to enhance mesenchymal stem cell (MSC) proliferation. J Micromech Microeng 2010;20:1–7.
[167] Centola M, Rainer A, Spadaccio C, Porcellinis SD, Genovese JA, Trombetta M. Combining electrospinning and fused deposition modeling for the fabrication of hybrid vascular graft. Biofabrication 2010;2:1–11.
[168] Martins A, Chung S, Pedro AJ, Sousa RA, Marques AP, Reis RL, et al. Hierarchical starch-based fibrous scaffold for boné tissue engineering applications. J Tissue Eng Regen Med 2009;3:37–42.
[169] Vaquette C, Fan W, Xiao Y, Hamlet S, Hutmacher DW, Ivanovski S. A biphasic scaffold design combined with cell sheet technology for simultaneous regeneration of alveolar bone/periodontal ligament complex. Biomaterials 2012;33:5560–73.
[170] Yan F, Liu Y, Chen H, Zhang F, Zheng L, Hu Q. A multi-scale controlled tissue engineering scaffold prepared by 3D printing and NFES technology. AIP Adv 2014;4. 031321-1.
[171] Yu YZ, Zheng LL, Chen HP, Chen WH, Hu QX. Fabrication of hierarchical polycaprolactone/gel scaffolds via combined 3D bioprinting and electrospinning for tissue engineering. Adv Manuf 2014.
[172] Canha-Gouveia A, Costa-Pinto AR, Martins AM, Silva NA, Faria S, Sousa RA, et al. Hierarchical scaffolds enhance osteogenic differentiation of human Wharton's jelly derived stem cells. Biofabrication 2015;2015(7):1–13.
[173] Rogers C, Morris G, Gould T, Bail R, Toumpaniari S, Harrington H, et al. A novel technique for the production of electrospun scaffolds with tailored three-dimensional micro-patterns employing additive manufacturing. Biofabrication 2014;6(3):035003.
[174] Sahoo N, Pan YG, Li L, He CB. Nanocomposites for bone tissue regeneration. Nanomedicine 2013;8(4):639–53.
[175] Pon-On W, Charoenphandhu N, Teerapornpuntakit J, Thongbunchoo J, Krishnamra N, Tang I-M. Mechanical properties, biological activity and protein controlled release by poly(vinyl alcohol)–bioglass/chitosan–collagen composite scaffolds: a bone tissue engineering applications. Mater Sci Eng, C 2014;2014(38):63–72.
[176] Pfister A, Landers R, Laib A, Hubner U, Schmelzeisen R, Mulhaupt R. Biofunctional rapid prototyping for tissue-engineering applications: 3D bioplotting versus 3D printing. J Polym Sci, Part A: Polym Chem 2004;42:624–38.
[177] Khadka D, Haynie D. Protein- and peptide-based electrospun nanofibers in medical biomaterials. Nanomedicine 2012;8(8):1242–62.
[178] Cipitria A, Skelton A, Dargaville T, Daltonac D, Hutmacher D. Design, fabrication and characterization of PCL electrospun scaffolds—a review. J Mater Chem 2011;21:9419.

[179] Bártolo P, Chua C, Almeida H, Chou S, Lim A. Biomanufacturing for tissue engineering: present and future trends. Virt Phys Prot 2009;4(4):203–16.
[180] Ji W, Sun Y, Yang F, van den Beucken J, Fan M, Chen Z, et al. Bioactive electrospun scaffolds delivering growth factors and genes for tissue engineering applications. Pharm Res 2011;28:1259–72.
[181] Leong M, Chan W, Chian K, Rasheed M, Anderson J. Fabrication and in vitro and in vivo cell infiltration study of a bilayered cryogenic electrospun poly (D, L-lactide) scaffold. J Biomed Mater Res A 2010;94A(4):1141–9.
[182] Goh K, Listrat A, Béchet D. Hierarchical mechanics of connective tissues: integrating insights from nano to macroscopic studies. J Biomed Nanotechnol 2014;10(10):2264–507.
[183] Pateman C, Plenderleith R, Daud M, Harding A, Christmas C, Boisannade F, et al. 3D micro-printing of nerve guides for peripheral nerve repair. Euro Cells Mater 2013;26(suppl. 7):78.
[184] Stephens-Altus JS, Sundelacruz P, Rowland ML, West JL. Development of bioactive photocrosslinkable fibrous hydrogels. J Biomed Mater Res A 2011; A:1–10.
[185] Melchels FPW, Barradas AMC, van Blitterswijk CA, Boer J, Feijen J, Grijpma DW. Effects of the architecture of tissue engineering scaffolds on cell seeding and culturing. Acta Biomater 2010;6:4208–17.
[186] Melchels FPW, Domingos MAN, Klein TJ, Malda J, Bártolo PJ, Hutmacher DW. Additive manufacturing of tissues and organs. Prog Polym Sci 2012;37:1079–104.
[187] Villalona GA, Udelsman B, Duncan DR, McGillicuddy E, Sawh-Martinez RF, Hibino N, et al. Cell-seeding techniques in vascular tissue engineering. Tissue Eng Part B 2010;16(3):341–50.
[188] Tasoglu S, Demirci U. Bioprinting for stem cell research. Trends Biotechnol 2013;31(1):10–9.
[189] Ferris CJ, Gilmore KG, Wallace GG, Panhuis M. Biofabrication: an overview of the approaches used for printing of living cells. Appl Microbiol Biotechnol 2013;97:4243–58.
[190] Boland T, Xu T, Damon B, Cui X. Application of inkjet printing to tissue engineering. Biotechnol 2006;1:910–7.
[191] Nakamura M, Kobayashi A, Takagi F, Watanabe A, Hiruma Y, Ohuchi K, et al. Biocompatible inkjet printing technique for designed seeding of individual living cells. Tissue Eng 2005;11(11–12):1658–66.
[192] Smith CM, Stone AL, Parkhill RL, Stewart RL, Simpkins MW, Kachurin AM, et al. Three dimensional bioassembly tool for generating viable tissue engineered constructs. Tissue Eng A 2004;10:1566–76.
[193] Chung JHY, Naficy S, Yue Z, Kapsa R, Quigley A, Moulton SE, et al. Bio-ink properties and printability for extrusion printing living cells. Biomater Sci 2013;1:763–73.
[194] Wang X, Yan Y, Pan Y, Xiong Z, Liu H, Cheng J, et al. Generation of three-dimensional hepatocyte/gelatin structures with rapid prototyping system. Tissue Eng A 2006;12:83–90.
[195] Odde DJ, Renn MJ. Laser-guided direct writing for applications in biotechnology. Trend Biotechnol 1999;17:385–9.
[196] Ma Z, Pirlo RK, Wan Q, Yun JX, Yuan X, Xiang P, et al. Laser-guidance-based cell deposition microscope for heterotypic single-cell micropatterning. Biofab 2011;3:034107.
[197] Gaebel R, Ma N, Liu J, Guan J, Koch L, Klopsch C, et al. Patterning human stem cells and endothelial cells with laser printing for cardiac regeneration. Biomaterials 2011;32:9218–30.
[198] Moon SJ, Hasan SK, Song YS, Xu F, Keles HO, Manzur F, et al. Layer by layer three-dimensional tissue epitaxy by cell-laden hydrogel droplets. Tissue Eng Part C 2010;16(1):157–66.
[199] Demirci U, Montesano G. Cell encapsulating droplet vitrification. Lab Chip 2007;7:1428–33.
[200] Fang Y, Frampton JP, Raghavan S, Sabahi-Kaviani R, Luker G, Deng CX, et al. Rapid generation of multiplexed cell cocultures using acoustic droplet ejection followed by aqueous two-phase exclusion patterning. Tissue Eng Part C 2012;18(9):647–57.
[201] Beachleya V, Wena X. Polymer nanofibrous structures: fabrication, biofunctionalization, and cell interactions. Prog Polym Sci 2010;35:868–92.
[202] Vunjak-Novakovic G, Obradovic B, Martin I, Bursac PM, Langer R, Freed LE. Dynamic cell seeding of polymer scaffolds for cartilage tissue engineering. Biotechnol Progr 1998;14:193–202.
[203] Carrier RL, Papadaki M, Rupnick M, Schoen FJ, Bursac N, Langer R, et al. Cardiac tissue engineering: cell seeding, cultivation parameters, and tissue construct characterization. Biotechnol Bioeng 1999;64:580–9.
[204] Jayasinghe SN. Cell electrospinning: a novel tool for functionalising fibres, scaffolds and membranes with living cells and other advanced materials for regenerative biology and medicine. Analyst 2013;138:2215–23.
[205] Townsend-Nicholson A, Jayasinghe SN. Cell electrospinning: a unique biotechnique for encapsulating living organisms for generating active biological microthreads/scaffolds. Biomacromolecules 2006;7:3364–9.
[206] Jayasinghe SN, Irvine S, McEwan JR. Cell electrospinning highly concentrated cellular suspensions containing primary living organisms into cell-bearing threads and scaffolds. Nanomedicine 2007;2(4):555–67.
[207] Sampson SL, Saraiva L, Gustafsson K, Jayasinghe SN, Robertson BD. Cell electrospinning: an in vitro and in vivo study. Small 2014;10(1):78–82.
[208] Xu S-C, Qin C-C, Yu M, Dong R-H, Yan X, Zhao H, et al. A battery-operated portable handheld electrospinning apparatus. Nanoscale 2015;7:12351–5.
[209] Dong R-H, Jia Y-X, Qin C-C, Zhan L, Yan X, Cui L, et al. In-situ deposition of personalized nanofibrous dressing via a handy electrospinning device for skin wound care. Nanoscale 2016:1–6.
[210] Xu S-C, Qin C-C, Yu M, Dong R-H, Yan X, Zhao H, et al. A battery-operated portable handheld e-spinning apparatus (BOEA). China; 2012.

Juliana R. Dias is currently Ph.D. candidate on Biomedical Sciences at the i3S-Instituto de Investigação e Inovação em Saúde, University of Porto, Portugal. Her main research focus is on hierarchical electrospun nanostructures for skin regeneration. Her main interests focus is on biomaterials, biofabrication, electrospinning and tissue engineering.

Pedro L. Granja is presently Scientific Coordinator of Instituto de Engenharia Biomédica (INEB), group Leader at Instituto de Investigação e Inovação em Saúde (i3S, University of Porto-UP), Associate Professor at Instituto de Ciências Biomédicas Abel Salazar (ICBAS, UP) and Invited Auxiliary Professor at Faculty of Engineering of UP (FEUP). He is also Editor-in-Chief of the Biomaterials Network (Biomat.net), and Editor-in-Chief of the recently launched journal Biomatter.

Paulo J. Bártolo is Chair Professor in Advanced Manufacturing at the School of Mechanical, Aerospace and Civil Engineering, Director of the Manchester Biomanufacturing Centre, Principal Investigator at the Manchester Institute of Biotechnology, University of Manchester (UK). He is further Visiting Professor at the Nanyang University (Singapore) and fellow of the International Academy of Production Engineering. He is also Editor-in-Chief of both Virtual and Physical Prototyping Journal and biomanufacturing Reviews.

RESEARCH ARTICLE

A new design of an electrospinning apparatus for tissue engineering applications

Juliana R. Dias[1,2,3,4], Cyril dos Santos[2], João Horta[2], Pedro Lopes Granja[1,3,4,5] and Paulo Jorge Bártolo[6*]

[1] Instituto de Investigação e Inovação em Saúde (i3S), Universidade do Porto, Porto, Portugal
[2] Centre for Rapid and Sustainable Product Development (CDRsp), Polytechnic Institute of Leiria, Leiria, Portugal
[3] Instituto de Engenharia Biomédica (INEB), Universidade do Porto, Porto, Portugal
[4] Instituto de Ciências Biomédicas Abel Salazar (ICBAS), Universidade do Porto, Porto, Portugal
[5] Faculdade de Engenharia da Universidade do Porto (FEUP), Porto, Portugal
[6] School of Mechanical, Aerospace and Civil Engineering & Manchester Institute of Biotechnology, University of Manchester, UK

Abstract: The electrospinning technique is being widely explored in the biomedical field due to its simplicity to produce meshes and its capacity to mimic the micro-nanostructure of the natural extracellular matrix. For skin tissue engineering applications, wound dressings made from electrospun nanofibers present several advantages compared to conventional dressings, such as the promotion of the hemostasis phase, wound exudate absorption, semi-permeability, easy conformability to the wound, functional ability and no scar induction. Despite being a relatively simple technique, electrospinning is strongly influenced by polymer solution characteristics, processing parameters and environmental conditions, which strongly determine the production of fibers and their morphology. However, most electrospinning systems are wrongly designed, presenting a large number of conductive components that compromises the stability of the spinning process. This paper presents a new design of an electrospinning system solving the abovementioned limitations. The system was assessed through the production of polycaprolactone (PCL) and gelatin nanofibers. Different solvents and processing parameters were considered. Results show that the proposed electrospinning system is suitable to produce reproducible and homogeneous electrospun fibers for tissue engineering applications.

Keywords: biofabrication, electrospinning, fibers, polymer solutions, tissue engineering

*Correspondence to: Paulo Jorge Bártolo, School of Mechanical, Aerospace and Civil Engineering & Manchester Institute of Biotechnology, University of Manchester, UK; Email: paulojorge.dasilvabartolo@manchester.ac.uk

Received: January 29, 2017; **Accepted**: April 10, 2017; **Published Online**: May 15, 2017

Citation: Dias J R, dos Santos C, Horta J, *et al.*, 2017, A new design of an electrospinning apparatus for tissue engineering applications. *International Journal of Bioprinting*, vol.3(2): 1–9. http://dx.doi.org/10.18063/IJB.2017.02.002.

1. Introduction

Electrospinning is an electrostatic fibre fabrication technique that has been attracting increasing interest due to its versatility and potential for applications in different fields[1]. In the biomedical field, electrospinning has been used to produce biosensors, filtration devices, scaffolds for tissue engineering, wound dressing, drug delivery and enzyme immobilization systems[2,3]. In tissue engineering, electrospun meshes have a great potential due to their high surface area and interconnectivity and are beneficial for tissue ingrowth and cell migration, coupled with controlled delivery of incorporated biomolecules[4–6].

The conventional setup of a solution electrospinning system consists of three major components: a high voltage power supply, a spinneret and a collector that can be used in a horizontal or vertical arrangement[5,7,8]. The syringe contains a polymeric solution, pumped at a constant and controlled rate. The polymer jet is initiated when the voltage is turned on and the opposing electrostatic forces overcome the surface tension of the polymer. Just before the jet formation, the polymer droplet under the influence of the electric field assumes a cone shape with convex sides and a rounded tip, known as the Taylor cone[2,9,10]. During the jet's travel, the solvent gradually evaporates, and charged polymer fibers are deposited in the collector[10].

Several laboratory-type and industrial scale electrospinning systems are commercially available[11–13]. However, laboratory-type systems are still relatively expensive, and, due to its low complexity, most research laboratories assembled their own systems[14–16].

The solution electrospinning process is influenced by several parameters, such as: solution parameters (*e.g.*, viscosity, polymer concentration, solvent type), processing parameters (*e.g.*, flow rate, distance between needle and collector, voltage, type of collector) and ambient conditions (*e.g.*, temperature and humidity)[17]. For tissue engineering applications, where hydrogels are commonly used, it is fundamental to control the fabrication environment. However, this is not possible with most commercial available laboratory-type systems that present several limitations such as:

- metallic parts in contact with the electric field and thus affecting it, inducing the formation of secondary jets, and consequently, the deposition of fibers was not only on the collector surface but also over all metallic components. Moreover, non-stable jets can induce solvent drop deposition over the electrospun meshes, making them toxic;
- flow rate control exerted by a step motor that limits the accurate control of flow rate compared to the use of a syringe pump;
- fiber production mostly limited to horizontal mode strategies.

These drawbacks limit the versatility and reproducibility of this technique by compromising the stability of the electric field. To solve some of these limitations a new design of an electrospinning system is presented and evaluated.

2. Materials and Methods

2.1 New Design of an Electrospinning System

The digital representation of the new design of a solution electrospinning system is presented in Figure 1.

In this new system a significant number of non-conductive components were introduced. The box of the equipment (1) is made in acrylic, with a main hole to allow solvent evaporation. This structure incorporates a door to access to the equipment inner part and some additional entry spot to allow the entrance of the infusion tubes supplying the polymeric solution. The base of the equipment (3) is made in cork (Corecork TB40, Amorim, Portugal) due to its adequate mechanical re- sistance and machinability properties, insulation characteristics and eco-friendly nature. An acrylic part (2) is used to support the rod (4) made of teflon. The collector (5) is a grounded copper plate. The needle support (6) is made of acrylonitrile butadiene styrene (ABS) and slides on to adjust the distance between the needle (single or core/shell) and the collector. The collector (5) is static but its fixation system allows its easy replacement by other type of collectors. Items (1), (2), (4) and (5) were purchased and items (3) and (6) produced using a computer numeric control machine (CNC, from INAUTOM, Portugal) and an additive manufacturing system (Dimension machine from Stratasys). Additionally, the new system includes a syringe pump (model Pump 11Elite, Harvard apparatus) to supply the polymeric solution, a polymeric tube connecting the syringe and the needle, a Liquid Crystal Display (LCD) to control the voltage, an emergency button and a high voltage source (model PS/MJ30P0400-11, Glassman High Voltage, Inc).

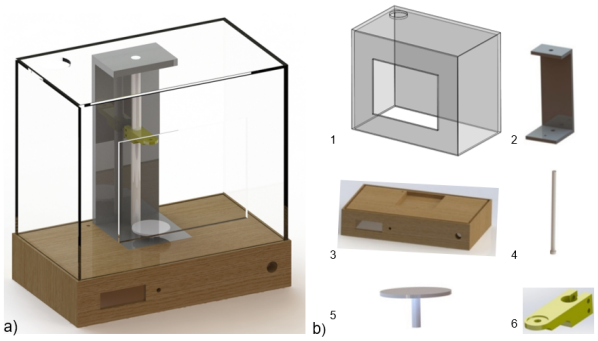

Figure 1. New design of electrospinning system. (**A**) Computer-aided design (CAD) model of electrospinning system proposed; (**B**) Main components:1 – acrylic box, 2 – acrylic support, 3 – cork base, 4 – teflon rod, 5 – collector, 6 – needle support.

The assembled electrospinning, which corresponds to a more versatile, flexible and user-friendly system, is shown in Figure 2. Key features of this system are:

- Allowing the preparation of samples using vertical or horizontal configurations;

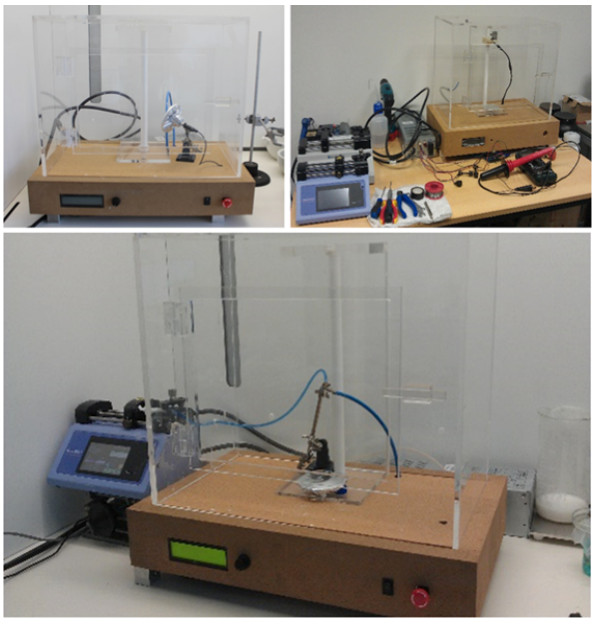

Figure 2. Assembled electrospinning apparatus

- Keeping the jet stable, not presenting secondary jets; due to the selection of non-conductive materials the jet is kept stable, and not presenting secondary jets;
- Providing accurate regulation of voltage due to the addition of a controller to the high voltage source.

2.2 Materials

Poly (ε-caprolactone) (PCL) (Mw 50,000 (g/mol), bulk density: 1.1 g.cm^{-3}) was kindly supplied by Perstorp (UK) and dissolved in dimethyl Ketone (DMK) (Sigma-Aldrich), and acetic acid (AA) (PanReac AppliChem). Gelatin powder from pig skin (type A, 300 bloom, 60 mesh) were kindly supplied by Italgelatine (Italy). For polymers dissolution, different solvents were explored as indicated in Table 1. In order to increase the conductivity of the solutions prepared with acetic acid, 2 % v/v of triethylamine (TEA, Sigma Aldrich) was added. After optimization, 1,4-butanediol diglycidyl ether (BDDGE, Alpha Aesar, Germany) was used as the gelatin crosslinker.

2.3 Electrospinning of Nanofiber Meshes

Polymeric meshes were processed using a single jet approach. Table 1 presents the processing parameters used to produce the meshes. Non-woven electrospun meshes were obtained at room temperature and relative humidity of 40–50%. Crosslinking of electrospun gelatin fibers were produced through the incorporation of BDDGE on the gelatin solution immediately before fiber electrospinning to avoid the loss of configuration that is induced through a crosslinking bath after fiber production.

2.4 Physico-chemical Characterization

2.4.1 Morphology and Fiber Diameter

The morphology of the produced meshes was examined by scanning electron microscopy (SEM) using a Quanta 400 FEG ESEM/EDAX Genesis X4M (FEI Company, USA). Prior to examination, samples were coated with a gold/palladium (Au/Pd) thin film, by sputtering, using the SPI module sputter coater equipment. SEM images were also used to measure the fiber diameter using Image J software. For each condition, three individual samples were analyzed and fifty measurements per image were carried out.

2.4.2 Structure

Fourier transform infrared (FTIR) spectroscopy with attenuated total reflectance (ATR) was used to evaluate the chemical composition of the materials and to detect possible structural changes. FTIR analyses were carried out using an Alpha-P Brucker FTIR-ATR spectrometer, in the range of 4000–500 cm^{-1}, at a 4 cm^{-1} resolution with 64 scans.

2.5 *In Vitro* Studies

Human dermal neonatal fibroblasts (hDNF) isolated from the foreskin of healthy male newborns (ZenBio, US) were cultured, expanded, and maintained in Dulbecco's modified eagle medium (DMEM) (Gibco, US), at 37 °C in a humidified atmosphere of 5% CO_2. The culture medium was changed twice a week and cells were trypsinized (0.25 % trypsin/0.05 % ethylenediamine tetraacetic acid (EDTA)/0.1% glucose in PBS (pH 7.5)) when they reached 70 %–80 % of confluence. Cells from passages between 8 and 11 were used in this study.

To assess cytotoxicity, electrospun meshes were tested in direct (samples) and indirect (leachables) contact with different pre-conditions (washed and non-washed in ultrapure water). Samples were sterilized with UV light followed by washing during 24 hours. hDNF cells were seeded in culture wells for 24 hours at a density of 2×10^4 cells/well. 24 hours later, samples (direct contact) and culture medium in contact with samples (indirect contact) were incubated with cells for another 24 hours. The culture medium was then removed from the wells and fresh basal medium with 20 % v/v resazurin (Sigma-Aldrich) was added. Cells were incubated (37°C, 5% v/v CO_2) for an additional period of 2 hours, after which 300 µL per well were transferred to a black 96-well plate and measured (Ex at 530 nm, Em at 590 nm) using a micro-plate reader (Synergy MX, BioTek, US). The control consisted in cells alone.

For the quantification of the total double-stranded DNA (dsDNA) content, the cell pellets were recovered from the wells and washed with phosphate-buffered saline (PBS). The suspension was then centrifuged (10,000 rpm, 5 min) and then stored at –20 °C until further analysis. The dsDNA quantification was

Table 1. Parameters tested to optimized the electrospun mesh production

Polymer	Solution parameters		Processing parameters		
	Solvent system	Polymer concentration (wt%)	Distance between collector and needle(cm)	Voltage (kV)	Flow rate (mL/h)
PCL	AA/TEA (2% v/v) DMK	6, 11, 17	7, 10, 12	7, 10, 12	0.72, 3.17
Gelatin	AA/TEA(2% v/v)	5, 10, 15			0.4, 0.72

performed using the Quant-iT PicoGreen dsDNA kit (Molecular Probes, Invitrogen, US), according to the manufacturer's protocol. Briefly, the samples were thawed and lysed in 1% v/v Triton X-100 (in PBS) for 1 hour at 250 rpm at 4 °C. Then, they were transferred to a black 96-well plate with clear bottom (Greiner) and diluted in Tris-EDTA (TE) buffer (200 mM Tris–HCl, 20 mM EDTA, pH 7.5). Finaly, samples were incubated for 5 min at room temperature in the dark, and fluorescence was measured using a microplate reader (Ex at 480, Em at 520 nm).

2.6 Statistical Analyses

All data points were expressed as mean ± standard deviation (SD). Statistical analysis (Levene's and T- test) was carried out using IBM SPSS Statistics 20.0 with 99 % confidence level for cytotoxicity assays. The results were considered statistically significant when $p \leq 0.05$ (*).

3. Results and Discussion

3.1 Microscopic and Macroscopic Characterization of Electrospun Meshes

SEM images of the different produced meshes are presented in Figure 3 and Figure 4. For simplicity, only the tested conditions that resulted in fibers without beads or drops are presented in these figures.

Results show that a stronger electric field increased the amount of produced fibers per time, which is correlated to the higher amount of charges into the solution, thereby increasing the jet velocity and, consequently, supplying more solution to the collector. The distance between the needle tip and the collector also determines the fiber diameter. By increasing this distance, the flight time is longer, allowing the solvent to evaporate, resulting in higher polymer chain stretching, which leads to a decrease in fiber diameter. These results show that the designed electrospinning is able to process proper meshes, being particularly relevant the production of gelatin meshes, which is strongly affected by ambient parameters, namely the relative humidity.

Concerning the PCL and gelatin meshes, according to the parameters tested significant differences were observed in terms of fiber diameter or morphology. Thus, for further analyses, the following requirements were selected, providing (i) longer distance to promote solvent evaporation and high chain stretching, (ii) high density of fibers per area, requiring less production time and (iii) continuous and uniform fiber production enhancing mechanical performance. Therefore, the following fiber production parameters were selected: 17 wt% of PCL dissolved in DMK, produced with a flow rate of 3.17 mL/h, 12 cm distance between needle and collector and 10 kV of voltage; 15 wt% of gelatin dissolved in AA and 2% v/v of TEA, produced with a flow rate of 0.4 mL/h, a 12 cm distance between needle and collector and 12 kV of voltage. Moreover as gelatin is a water-soluble protein, a crosslinking is needed to improve its mechanical properties and to increase its stability in aqueous medium[19]. Gelatin fibers were *in situ* crosslinked with BDDGE, according a protocol previously established[20]. The morphology of selected meshes are shown in Figure 5A–C. The fiber diameter measurements, the reduced standard deviation observed and the homogeneity of the obtained fibers demonstrates the stability of the system in producing nanoscale meshes. From Figure 5E it is also possible to observe that the developed system improves fiber deposition in the collector.

FTIR-ATR spectra, used to evaluate possible structural changes in the electrospun meshes, are shown in Figure 5D. The spectrum of PCL meshes presents a 1720.7 cm^{-1} peak, corresponding to the C=O bond, characteristic to esters, and additional peaks between 750 and 1500 cm^{-1}, corresponding to the CH_2 groups of PCL chain. Two other peaks at 2863.69 cm^{-1} and 2941.57 cm^{-1} can also be observed, corresponding to the CH bonds. The FTIR spectrum of gelatin shows prominent peaks in four different amide regions, namely at 1700–1600 cm^{-1}, corresponding to amide I; 1565–1520 cm^{-1}, corresponding to amide II; 1240–670 cm^{-1}, corresponding to amide III; and 3500–3000 cm^{-1}, corresponding to amide A. The absorption of amide I contains contributions from the C=O stretching vibration of amide group and a minor contribution from the C-N stretching vibration. Amide II absorption is related to N-H bending and C-N stretching vibrations. Amide III presents vibrations from C-N stretching attached to N-H in-bending with weak contributions from C-C stretching and C=O in-plane bending. At 2930 and 2890 cm^{-1}, it is possible to observe two peaks associated to the contribution of aliphatic moieties from BDDGE, confirming the incorporation of BDDGE into the gelatin matrix (Figure 5D). For both samples no solvent residues were detected and no structural changes were observed.

3.4 Cytotoxicity of Nanofibers Produced

Cytotoxicity of the produced electrospun meshes system was assessed to demonstrate the process stability, as a stable jet allows to produce electrospun meshes without solvent deposition. According to the obtained results (Figure 6), fibroblasts cultured on the electrospun meshes remained metabolically active for both PCL and gelatin meshes. After 24 hours, no cytotoxicity was observed either in direct or indirect contact assays. In direct contact assays no statistical significance was observed between control and samples, meaning that

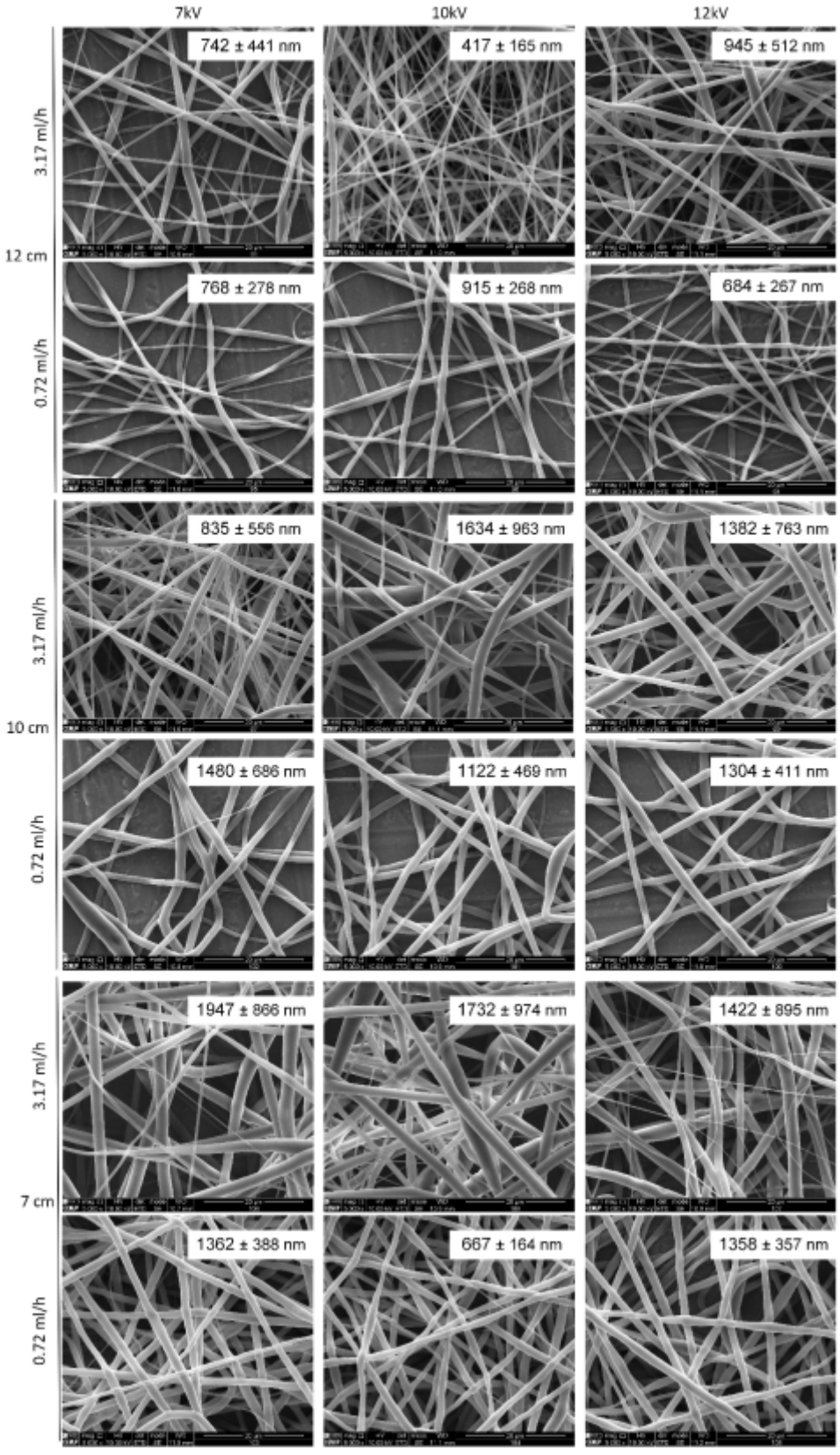

Figure 3. Electrospun PCL meshes (17 wt%, dissolved in DMK) obtained using different flow rates, distances between needle and collector and voltage. For each mesh it is presented the average fiber diameter. Scale bar: 20 μm.

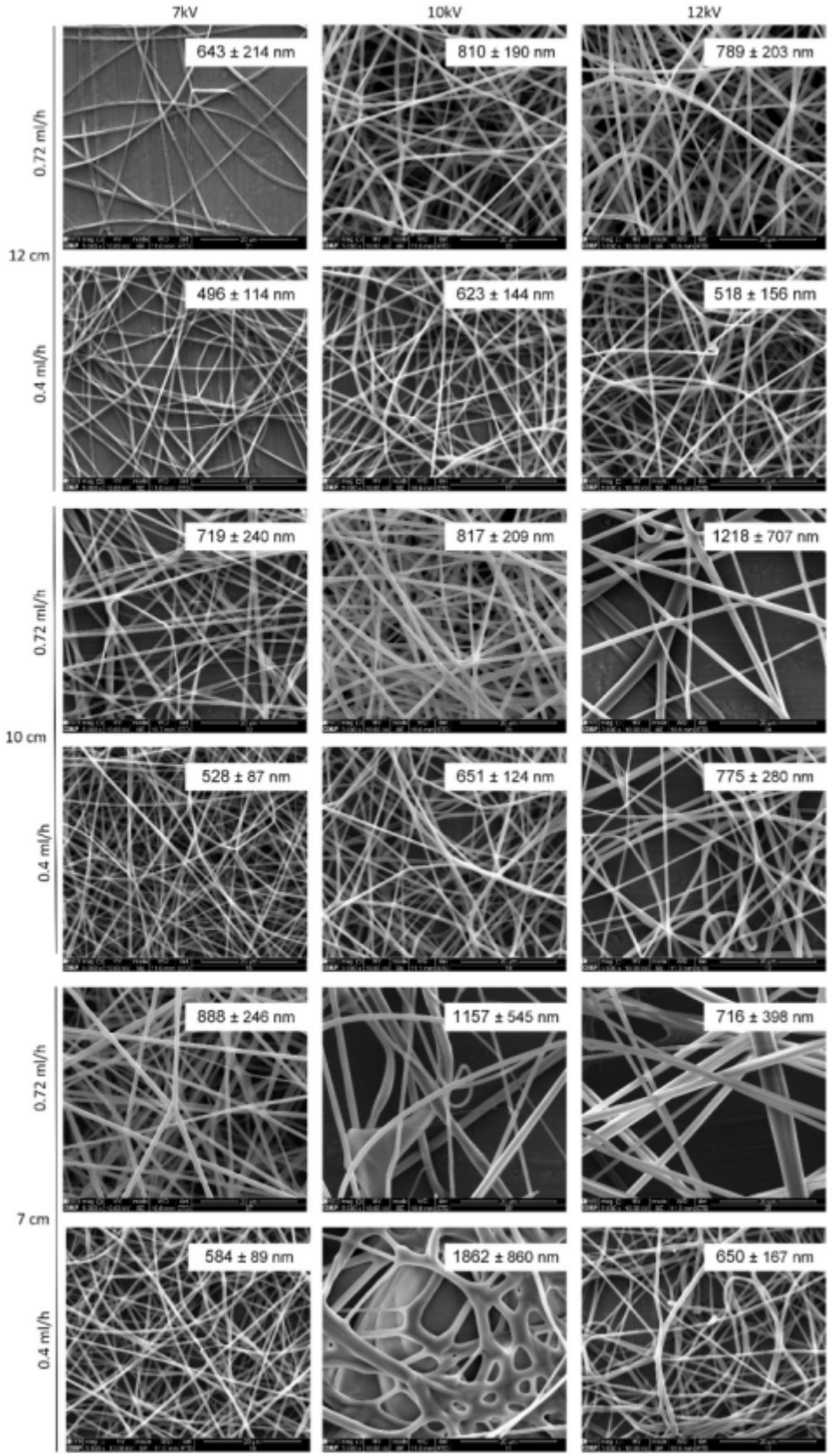

Figure 4. Electrospun gelatin meshes (15 wt%, dissolved AA/TEA 2% v/v) obtained using different flow rates, distances between needle and collector and voltage. For each mesh it is presented the average fiber diameter. Scale bar: 20 μm.

the structures, when in contact with cells, does not induce any toxicity. Regarding indirect contact assay, no leachables delivered from the samples to the medium presented toxicity.

4. Conclusions

This paper introduces a solution electrospinning system developed to produce electrospun meshes for applications in tissue engineering and more specifically for wound dressing applications. For the fabrication of the electrospinning system non-conductive materials (cork and polymers) were used to replace metallic ones, allowing to obtain a feasible and versatile laboratory-scale apparatus with ability to produce reproducible nanofiber meshes from materials with distinct characteristics. The system was used to produce nanofibers from two distinct polymers, using two different solvents, demonstrating its versatility of the new reassembled apparatus. The fabrication of gelatin meshes is particularly relevant; as like other natural polymers, it is a material very sensitive to the environmental conditions, in particular the relative humidity. Keeping the processing parameters stable is key to obtain high quality and reproducible meshes, *i.e.*, with no beads, resulting in filaments with constant diameter and in meshes with high porosity between pores. Meshes did not show any presence of remaining solvents, which can be correlated to the lack of toxicity detected through the biological assays.

The two selected materials are particularly relevant for skin applications. PCL presents high mechanical properties but, due to its hydrophobic nature, presents

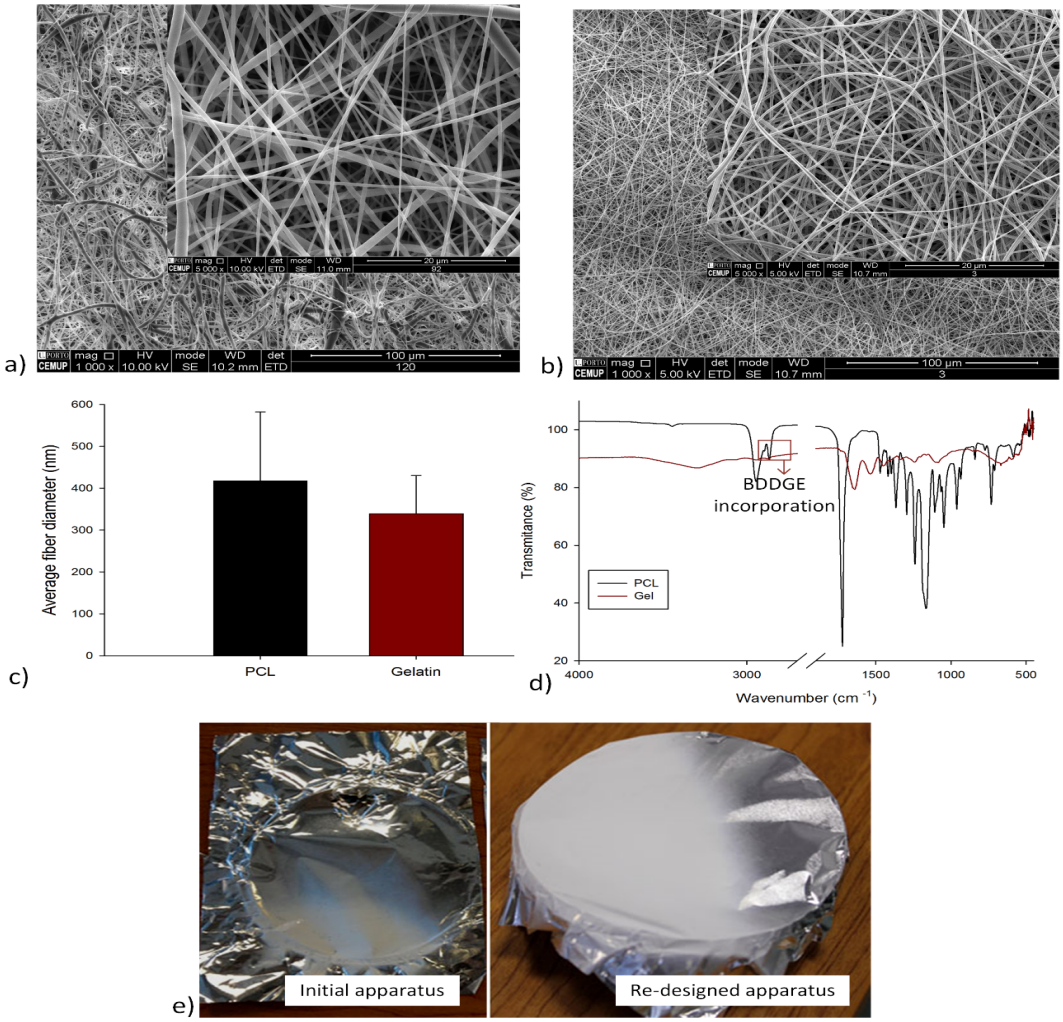

Figure 5. Characterization of PCL and gelatin electrospun meshes selected for further analysis. (**A**) Fiber morphology with 1000× and 5000× magnifications of PCL meshes; (**B**) Fiber morphology with 1000× and 5000× magnifications of gelatin meshes crosslinked with BDDGE; (**C**) Comparison between PCL and gelatin average fiber diameter; (**D**) FTIR spectra of PCL and crosslinked gelatin and (**E**) Influence of the purpose electrospinning system on fiber deposition over the collector in comparison with initial one comprising a significant metallic components.

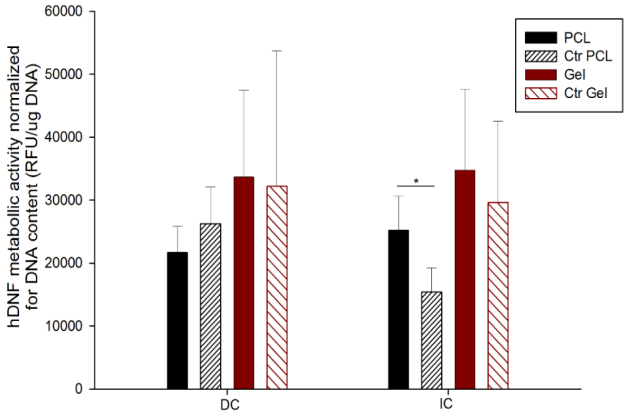

Figure 6. Cytotoxicity assay of PCL and gelatin electrospun meshes in direct contact (DC) and indirect contact (IC) with fibroblasts (hDNF cells), using as control cells seeded on the well. Statistical significance for $p \leq 0.05$ (*).

low interaction with cells. Contrary, gelatin displays many integrin-binding sites for cell adhesion, migration, proliferation, and differentiation due to the abundant Arg–Gly–Asp (RGD) amino acid sequences in its protein chain, which has been claimed to favor cell behavior. The combination of both materials may allow to produce meshes with improved properties.

Conflict of Interest and Funding

No conflict of interest was reported by the authors. This study was supported by the Project PTDC/BBB-ECT/2145/2014 and UID/Multi/04044/2013, financed by European Fonds Européen de Développement Régional (FEDER) through the Portuguese national programs Programa Operacional Factores de Competitividade (COMPETE), Portugal2020 and Norte2020, and by Portuguese funds through Fundação para a Ciência e a Tecnologia (FCT). This work is also supported by a research grant (SFRH/BD/91104/2012) awarded to Juliana Dias by FCT.

Acknowledgements

The authors thank CEMUP, University of Porto for the SEM images.

References

1. Bártolo P, Kruth J-P, Silva J, *et al.*, 2012, Biomedical production of implants by additive electro-chemical and physical processes. *CIRP Annals — Manufacturing Technology*, vol.61(2): 635–655. https://dx.doi.org/10.1016/j.cirp.2012.05.005
2. Teo W E and Ramakkrishna S, 2006, A review on electrospinning design and nanofibre assemblies. *Nanotechnology*, vol.17(14): 89–106. https://dx.doi.org/10.1088/0957-4484/17/14/R01
3. Ramakrishna S, Fujihara K, Teo W-E, *et al.*, 2005, *An Introduction to Electrospinning and Nanofibers*, World Scientific, Singapore.
4. Rim N G, Shin C S and Shin H, 2013, Current approaches to electrospun nanofibers for tissue engineering. B*iomedical Materials*, vol.8(1): 014102.
5. Bhardwaj N and Kundu S C, 2010, Electrospinning: a fascinating fiber fabrication technique. *Biotechnology Advances*, vol.28(3): 325–347. https://dx.doi.org/10.1016/j.biotechadv.2010.01.004
6. Niu H and Lin T, 2012, Fiber generators in needleless electrospinning. *Journal of Nanomaterials*, vol.12: 1–13. https//dx.doi.org/10.1155/2012/725950.
7. Sill T J and von Recum H A, 2008, Electrospinning: applications in drug delivery and tissue engineering. *Biomaterials*, vol.29(13): 1989–2006. https://dx.doi.org/10.1016/j.biomaterials.2008.01.011
8. Shin S H, Purevdori O, Castano O, *et al.*, 2012, A short review: recent advances in electrospinning for bone tissue regeneration. *Journal of Tissue Engineering*, vol.3(1): 1–11. https://dx.doi.org/10.1177/2041731412443530
9. Nukavarapu S P, Kumbar S G, Merrell J G, *et al.*, 2014, Electrospun polymeric nanofibre scaffolds for tissue regeneration, in Laurencin C T and Nair L S (eds.), *Nanotechnology and Tissue Engineering: The Scaffold*, 2nd edition, Taylor & Francis, London, 229–254.
10. Li W J and Xia Y, 2004, Electrospinning of nanofibres: reinventing the wheel? *Advanced Materials*, vol.16(14): 1151–1170. https://dx.doi.org/10.1002/adma.200400719
11. IME Technologies, n.d., *IME Technologies: Your partner in electrospinning*, viewed January 5, 2017, <https://www.imetechnologies.com>
12. Inovenso, n.d. *Inovenso*. viewed January 8, 2017, <http://inovenso.com/about/>
13. Elmarco, n.d., *NanoSpiderTM Electrospinning Technology*, viewed January 16, 2017, <http://www.elmarco.com/electrospinning/electrospinning-technology/>
14. Har-el Y-E, Gerstenhaber J A, Brodsky R, *et al.*, 2014, Electrospun soy protein scaffolds as wound dressings: enhanced reepithelialization in a porcine model of wound healing. *Wound Medicine*, vol.5: 9–15. https://dx.doi.org/10.1016/j.wndm.2014.04.007
15. Liu S-J, Kau Y-C, Chou C-Y, *et al.*, 2010, Electrospun

PLGA/collagen nanofibrous membrane as early-stage wound dressing. *Journal of Membrane Science*, vol. 355(1–2): 53–59. https://dx.doi.org/10.1016/j.memsci.2010.03.012

16. Gümüşderelioğlu M, Dalkıranoğlu S, Aydın R S T, *et al.*, 2011, A novel dermal substitute based on biofunctionalized electrospun PCL nanofibrous matrix. *Journal of Biomedical Materials Research Part A*, vol.98A(3): 461–472. https://dx.doi.org/10.1002/jbm.a.33143
17. Dias J R, Granja P L and Bártolo P J, Advances in electrospun skin substitutes. *Progress in Materials Science*, vol.84: 314–334. https://dx.doi.org/10.1016/j.pmatsci.2016.09.006
18. R Core Team, 2014, R: a language and environment for statistical computing, R Foundation for Statistical Computing, Vienna, Austria, viewed January 27, 2017 <http://www.R-project.org/>
19. Ward A G and Courts A, 1977, *The Science and Technology of Gelatin*, London:Academic Press, Inc., London.
20. Dias J R, Granja P L and Bártolo P J, 2016, Internal crosslinking evaluation of gelatin electrospinning fibers with 1,4-butanediol Diglycidyl ether (Bddge) for skin regeneration, in *10th World Biomaterials Congress, Montréal*, Canada, 17–22 May, 2016. https://dx.doi.org/10.3389/conf.FBIOE.2016.01.00896

CHEMICAL ENGINEERING TRANSACTIONS
VOL. 32, 2013
A publication of AIDIC
The Italian Association of Chemical Engineering
Online at: www.aidic.it/cet
Chief Editors: Sauro Pierucci, Jiří J. Klemeš

ISBN 978-88-95608-23-5; **ISSN** 1974-9791
DOI: 10.3303/CET1332170

Influence of the Rheological Behaviour in Electrospun PCL Nanofibres Production for Tissue Engineering Applications

Juliana R. Dias[a*], Filipe E. Antunes[b], Paulo J.Bártolo[a]

[a] Centre for Rapid and Sustainable Product Development, Polytechnic Institute of Leiria, Marinha Grande, Portugal
[b] Department of Chemistry, University of Coimbra, Coimbra, Portugal;
juliana.dias@ipleiria.pt

A strategy to obtain functional tissues engineering with desired biomechanical properties was used to develop scaffolds with morphologies mimicking the native environment to guide tissue regeneration. Non-woven scaffolds, with fibre dimensions at a nanometre scale, can mimic the physical structure of natural extracellular matrices (ECM). Though its clinical application is yet limited, nano/micro fibrous scaffolds produced by electrospinning gains more and more interest in different Tissue Engineering fields. The electrospinning technique is controlled by several parameters, such as polymer solution and processing ambient, being one of the most important parameters the solution viscosity, which allows defining the minimum viscosity needed to obtain fibres.
This research work investigates the rheological behaviour of PCL solutions to produce nanoscale fibre meshes for cartilage application. Poly (ε-caprolactone) (PCL) solutions were prepared using glacial acetic acid (AA) and glacial acetic acid with triethylamine (AA/TEA) at different concentrations. It was necessary to double the value of the critical concentration (c*), that is 10 wt% for PCL/AA and 9,6wt% for PCL/AA/TEA, to prepare suitable fibres. Results also show that a more homogenous mesh can be produced by adding TEA.

1. Introduction

Tissue engineering is a multidisciplinary field, combining efforts of biologists, engineers and clinicians towards the development of biological substitutes to maintain, restore or improve tissue and organ function. Tissue engineering comprises three main strategies: i) cell-based strategies, which involves the direct in vivo implantation of isolated cells or cel scaffold that provides a substrate for implanted cells and a physical support to organize the formation of the new tissue (Meyer *et al*, 2009, Ringeisen *et al*, 2008).
A variety of techniques have been proposed to produce scaffolds from biomaterials being one of these the electrospinning (Yang *et al*, 2008). Electrospinning is a technique to create submicron to nanometre scale fibres from a polymer solution or melt with some common characteristics to electrospraying and the traditional fibre drawing process (Nukavarapu *et al*, 2008). The sub-micron range spun fibres produced by this process offer several advantages like high surface area to volume ratio, harmonious porosity and the ability to manipulate nanofibre composition in order to get desired properties and function (Bhardwaj *et al*, 2010).
The electrospun meshes by this technique have fine filaments that appear to promote the communication between the matrix and the cells which leads to increased cellular adhesion and proliferation due to a greater number of anchor points (Kuo *et al*, 1991, Saetone *et al*, 1994, Moore *et al*, 1995) . However, it is clear from the literature that the physical and mechanical properties of the electrospun polymer meshes are very dependent on the solvent used in the electrospinning process. For instance, Kanani et al. (2011), studied the effect of different solvents (glacial acetic acid, 90% acetic acid, methylene chloride/dimethyl formamide, glacial formic acid and formic acid/acetone) on the morphology of PCL nanofibrous meshes (Kanani *et al*, 2011). They found that the use of glacial acetic acid as solvent led to the formation of fibers with nonuniform distribution of fibre diameters. Scheren et al. (2011) have also evaluated the use of solvents such as chloroform, formic acid, acetic acid, methanol and ethanol in the preparation of PCL Scaffolds (Scheren *et al*, 2011). They emphasised the major potential of the solvent mixture formic acid/

Please cite this article as: Dias J., Antunes F., Bartolo P., 2013, Influence of the rheological behaviour in electrospun pcl nanofibres production for tissue engineering applications, Chemical Engineering Transactions, 32, 1015-1020 DOI: 10.3303/CET1332170

acetic acid for the electrospinning of PCL. In this work we propose to understand the dependence of the type of solvent, as well as of the polymer concentration, on the type of PCL fibers and the suitability of such fibres for their use in tissue engineering. This was carried out by dissolving different concentrations of PCL in solvents with different polarities and observe the fiber formation. Our physicochemical interpretation underlines the importance of having PCL solutions above the polymer overlap concentration to get fibers.

2. Materials and Methods

2.1 Materials

For nanofibres meshes preparation was used PCL (Mw 50000[g/mol]), by Perstorp Company (CAPA 6500), dissolved AA (Mw 60.05 [g/mol]), by Labsolve company and AA added with 2wt% of TEA (Mw 101.19 [g/mol]), obtained from Sigma-Aldrich. After solutions preparation with different concentrations (1.5wt%, 3wt%, 6wt%, 9wt% and 11wt %) were placed in a shaking incubator during 24 hour, and heated between 25ºC and 65ºC, with a heating rate of 5ºC/min.

2.2 Methods

2.2.1 Rheology

The rheological analysis, allow us to estimate the molecular organization of the polymeric solutions and also to predict its dynamic properties, i.e. the viscosity. Solutions were analyzed using Reologica StressTech Rheometer at different temperatures: 15ºC, 20ºC and 25ºC.

2.2.2 Electrospinning

Electrospun meshes were produced using the homemade system shown in Figure 4. The following processing conditions were considered: syringe volume – 2.5 mL; needle diameter – 0. 6 mm; applied voltage – 10 kV; distance between the needle and the collector – 10 cm and flow rate - 0.72 mL/h.

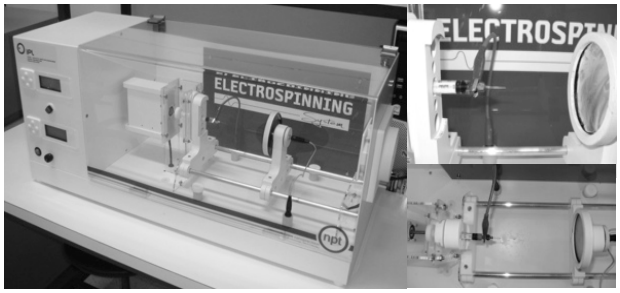

Figure 1. Equipment of Electrospinning process.

2.2.3 Scanning Electron Microscopy (SEM)

Each mesh of electrospun fibres was examined by scanning electron microscopy (model: FEI Quanta 600F) using a Cambridge Instruments S360 SEM. The samples were coated with gold prior to examination. The SEM images were used to evaluate the morphology of each mesh and the diameter distribution within each mesh.

3. Results and Discussion

3.1 Rheology

Homogenous solutions were readily prepared up to a concentration of PCL of 11wt% for systems based on AA and those prepared with AA and 2% of TEA.

The Figure 2a shows the variation of the zero-shear viscosity of the PCL solutions as a function of the polymer concentration with acetic acid as the solvent. The viscosity increases with the concentration of PCL until a cross-over point at c ~ 5.0 for solutions dissolved in AA and c ~ 4.8 for solutions dissolved in AA/TEA, where the rate of increase of the viscosity with concentration markedly increases. This happens because of the transition from dilute to semi-dilute regime where the polymer chains form entanglements. Figure 2b shows the equivalent data for the solutions containing TEA. Shenoy *et al.* (2005) have argued

that the critical concentration for the formation of fibres by electrospinning is twice of the cross-over concentration (Shenoy et al, 2005).

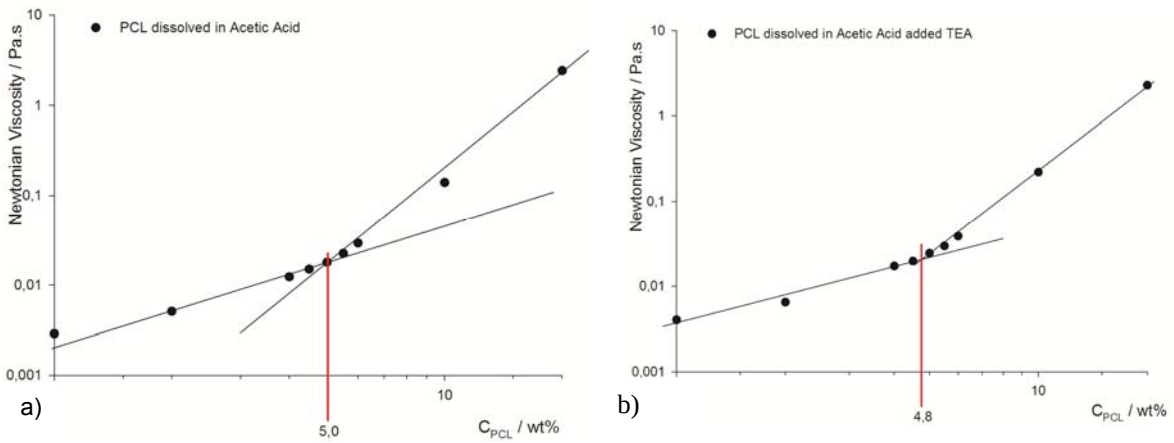

Figure 2. Plots of the zero shear viscosity against polymer concentration for solutions of (a) AA and (b) AA with 2% of TEA.

According the Table 1 it is possible to observe the influence of the temperature and the viscosity of the solutions. With increasing of the temperature the viscosity decreases, because of the higher polymer dynamics and increase the concentration, consequently the viscosity increase too, because there are more polymer chains. With rheological measurements was possible observed that the solutions presents a Newtonian behaviour, that is, the viscosity is independent of the shear rate applied.

Table 1: Viscosity measurements with temperature influence

	Concentration (wt%)	η15º (Pa.s)	η20º(Pa.s)	η25º(Pa.s)
PCL/AA	11	1.582E-01	1.383E-01	1.208E-01
	9	7.164E-02	6.363E-02	5.582E-02
	6	2.454E-02	2.153E-02	1.950E-02
	3	8.987E-03	8.237E-03	7.599E-03
	1.5	5.337E-03	5.000E-03	4.752E-03
PCL/AA/TEA	11	1.511E-01	1.328E-01	1.145E-01
	9	6.427E-02	5.653E-02	4.958E-02
	6	2.710E-02	2.408E-02	2.114E-02
	3	8.093E-03	7.023E-03	6.470E-03
	1.5	5.356E-03	4.145E-03	3.959E-03

3.2 SEM

The morphologies of the electrospun mats produced from acetic acid based solutions of PCL for the two different syringe flow rates are shows in Figure 3. For solution concentrations below 9 wt% only irregular shaped particles are observed of ~ 1μm in size. The morphology appears to arise from largely spherical droplets merging to form larger aggregates. For solutions contain 9wt% PCL and with the higher flow rate produce a small number of fibres (diameter ≈ 38.5 nm) amongst a high level of particles. For the highest concentration both feed rates produce a more continuous morphology.

Figure 4 shows the morphologies of the electrospun mats produced from PCL solutions based on acetic acid and triethylamine. In contrast to the solutions of acetic acid only, electrospraying only happens for 1.5wt% and 3wt% concentration when TEA is added with an increase in concentration to 6 wt%, there are already some fibres but widely dispersed especially with the higher flow rate. For a 9 wt% concentration, we can observe the presence of many fibres although there are also highly interconnected particles; owing to the charges these particles have which attract the fibres for those places. The highest concentration

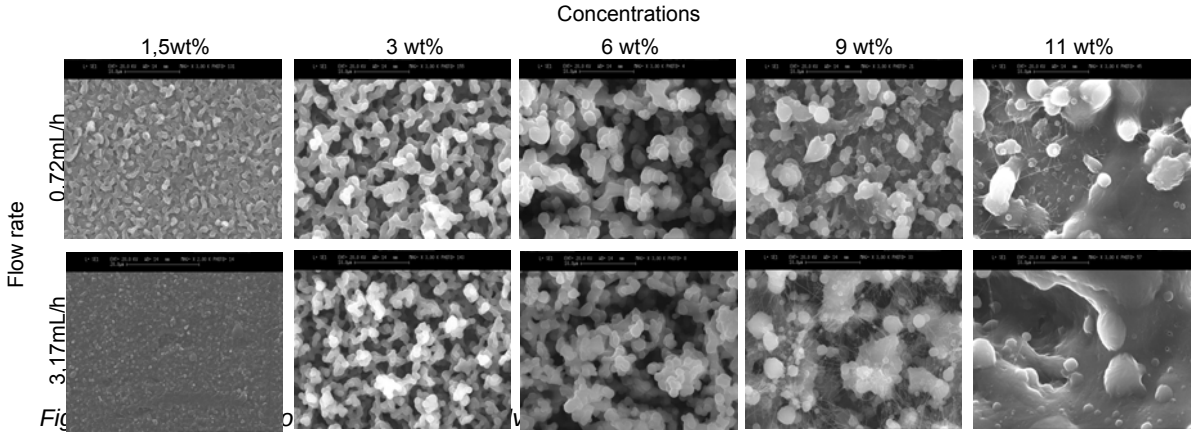

Fig[illegible]o[illegible]w

solutions (11 wt %), produce meshes of filaments with excellent quality and with little beading especially for the higher flow rate. This suggests that we are close to the flow rate and processing conditions appropriate for this solution.

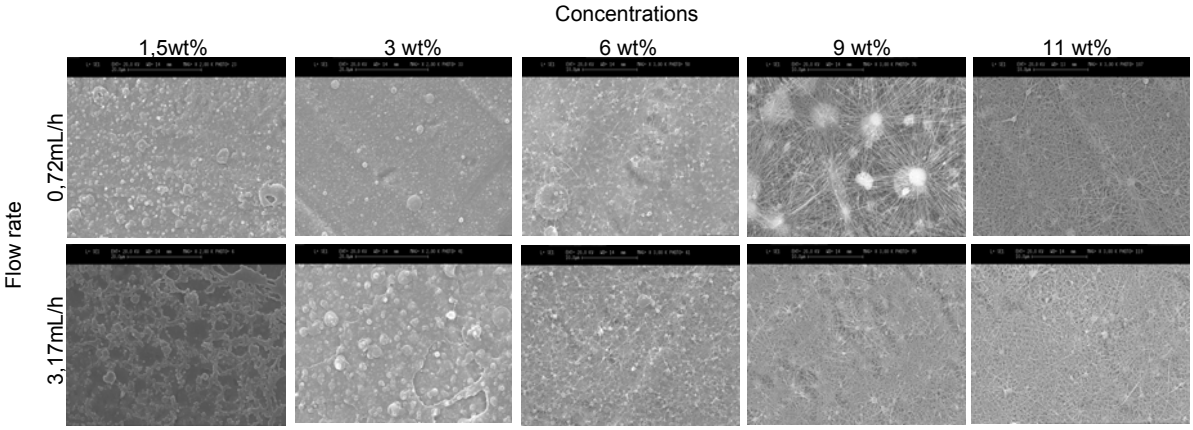

Figure 4. Morphology of PCL meshes dissolved in AA/TEA.

Figure 5 shows a plot of the average fibre diameter against the zero shear viscosity for fibres prepared from PCL solutions in Acetic acid and TEA. In calculating the average we have not included any beading or other aggregates. The trend can observe, such as in the bibliography, the diameter average increase when the viscosity increase too (Bhardwaj *et al*, 2010, Homayoni *et al*, 2009).

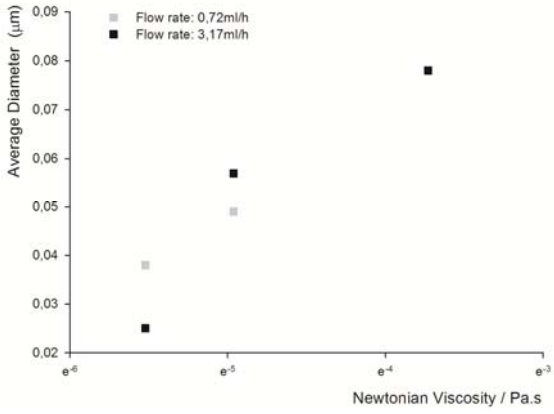

Figure 5. Newtonian viscosity vs Average diameter.

The viscosity of the solution has an effect on the electrospinning and the resultant fibre morphology. In general, the viscosity of the solution is connected to the extent of the entanglement of the polymer molecule chains within the solution. When the viscosity of the solution is too low, electrospraying may occur and polymer particles are formed instead of fibres. At a lower viscosity, where usually the polymer chain entanglements are lower, there is a higher similar that beaded fibres are obtained instead of smooth fibres. Therefore, factors that affect the viscosity of the solution will also affect the electrospinning process and the resultant fibres.

From the electrospinning data, the minimum concentration to obtain fibres is 10wt% for the Acetic Acid – PCL system and 9.6wt% for the Acetic Acid + TEA – PCL system. These values are c.a. twice of the values obtained for the overlap concentration, c* (intersection between the two lines in Figure 2). This critical concentration refers to the onset of the chain overlapping and to a transition from a dilute to semi-dilute regime. This comparison clearly indicates that the polymer system needs to be well above the overlap concentration to avoid problems as spraying or heterogeneous beads. When the polymer concentration is twice the overlap concentration, the network is established and the overlapping rejects any kind of spraying.

This work main objective was to propose a mesh of nanofibres for tissue engineering, so we need a mesh to put in to a scaffold to increase the adhesion surface, and consequently increase the area for cellular adhesion. This will lead to a faster regeneration of the tissue. We also need that the nanofibres present adequate mechanical properties to achieve the desired behaviour.

Through rheology (Figure 2 a) and b)), we can observe that for an increase in concentration the viscosity increases too, as there are more chains of polymers and the arrangements of molecules in the solution are minor, the solution became more viscous. Consequently the fibre diameter is higher as the solution has more chain of polymers.

The polymer concentration determines the spinnability of a solution, whether a fibre forms or not. The solution to occur must have a high enough polymer concentration for chain entanglement. Though, the solution cannot be either too dilute or too concentrated. The polymer concentration influences both the viscosity and the surface tension of the solution, and consequently the diameter of fibres. If the solution is too dilute then the polymer fibres will break up into droplets before reaching the collector, due to the effects of surface tension. However, if the solution is too concentrated, then fibres cannot be formed due to the high viscosity, which makes it difficult to control the solution flow rate through the capillary. With the c* determination we defined the minimum viscosity needed for fibres production when uses solution of PCL dissolved in Acetic acid and acetic acid with TEA.

Through the rheologic analyse we can define three different zones: the first corresponding to the solutions that only allow produce beads, the second zone we can produce a mix of beads and fibres and, finally, the third zone we can produce only fibres. The importance of this knowledge is known the c*, critical concentration, through this we can guarantee the production of fibres using the minimum viscosity in any kind of equipment for solutions with PCL.

Rheological studies were carried out to determine the viscosity of all solutions. For the acetic acid solutions the results shows a Newtonian behaviour, i.e., a linear relation between stress and shear rate. Additionally it was verify, as expected, a decrease of the viscosity with temperature and increase with solution concentration. Those relationships are important not only to optimise the process but also for simulation propose. The viscosity of the acetic acid solution without TEA is higher than the viscosity of the solution with TEA, as this amine is also a solvent diluting the solution.

The characteristics of the meshes depend on the solution viscosity as shown by this work. If the viscosity is too low it is not possible to produce any kind of meshes, occurring an electrospraying phenomenon (spray of small droplets). This was observed with the solution of acetic acid without TEA, where the viscosity was too low for the flow rates used.

From this work it is possible to conclude that the use of PCL dissolved in acetic acid with TEA is adequate to produce meshes for tissue engineering applications. TEA can also be used to control the viscosity of the solutions.

4. Conclusions

The addition of small quantities of triethylamine to solutions of PCL/acetic acid transforms the process from electrospraying to electrospinning leading to the formation of nanoscale fibres suitable for tissue regeneration applications. Through this work, is possible to known that for this solvent system is necessary have to 9.6wt% of PCL to produce electrospun meshes without beads.

Acknowledgments

Juliana Dias thanks the Centre for Rapid Development and Sustainable Product for the research grant awarded for the work. The authors also thank the Centre for Advanced Microscopy, University of Reading and in particular Dr. Chris Stain and Dr. Geoffrey Mitchell for the SEM micrographs of the electrospun meshes, to the Chemistry Department, University of Coimbra for the rheological measurements and the support by Foundation for Science and Technology through the strategic project PES-OE/EME/UI4044/2011.

References

Bhardwaj N, Kundu SC , 2010, Electrospinning: A fascinating fiber fabrication technique, Biotechnology Advances, 28, 325-347, DOI:10.1016/j.biotechadv.2010.01.004

Homayoni H, Ravandi SAH, Valizadeh M, 2009, Electrospinning of chitosan nanofibres: processing optimization, *Carbohydrate Polymers* ,77, 656-661, DOI:10.1016/j.carbpol.2009.02.008

Kanani AG, Bahrami SH, 2011, Effect of changing solvents on Poly (e-caprolactone) nanofibrous webs morphology, Journal of Nanomaterials, 2011,1-10, DOI: 10.1155/2011/724153

Kuo JW, Swann DA, Prestwich GD, 1991, Chemical modification of hyaluronic acid by carboiimides. *Bioconjugate Chem,* 2,232-241, DOI: 10.1021/bc00010a007

Meyer U., 2009, The History of Tissue Engineering and Regenerative Medicine in Perspective. In: Meyer U, Handschel J, Meyer T, Wiesmann HP (ed)Fundamentals of Tissue Engineering and Regenerative Medicine, Springer, Berlim, pp 5-12.

Moore AR, Willoughby DA, 1995, Hyaluronan as a drug delivery systems for diclofenac: a hypothesis for mode of action, *Int. J. Tissue React.,* 17, 153-156, DOI: 10.1159/000080213

Nukavarapu SP, Kumbar SG, Merrell JG, Laurencin CT, 2008, Electrospun Polymeric nanofibres Scaffolds for Tissue Regeneration, In: Laurencin CT, Nair LS (ed) Nanotechnology and Tissue Engineering: The scaffold, Taylor & Francis, Boca Raton, pp 199-219.

Ringeisen BR, Barron JA, Young D, Othon CM, Ladoucuer D, Wu PK, Spargo BJ, 2008, Laser priting cells, In: Bidanda B, Bártolo PJ (ed) Virtual Prototyping & Bio Manufacturing in Medical Applications, Springer,New York, pp 207-228.

Saetone MF, Monti D, Torraca MT, Chetoni P, 1994, Mucoadhesive ophthalmic vehicles: evaluation of polymeric low-viscosity formulations, *Journal of Ocular Pharmacology and Therapeutics*, 10, 83-92, DOI:10.1089/jop.1994.10.83

Schueren LV, Schoenmaker B, Kalaoglu OI, Clerck K ,2011, An alternative solvent system for the steady state electrospinning of polycaprolactone, *European Polymer Journal, 47, 1256-1263,* DOI: 10.1016/j.eurpolymj.2011.02.025

Shenoy SL,Bates WD, Frisch HL, Wnek GE, 2005, Role of chains entanglements on fiber formation during electrospinning of polymer solutions: good solvent, non-specific polymer-polymer interaction limit, Polymer, 46, 3372-3384, DOI:10.1016/j.polymer.2005.03.011

Yang F, Neeley W L, Moore M J, Karp J M, Shukla A, Langer R, 2008, Tissue Engineering: The therapeutic strategy of the twenty-first centuary, In: Laurencin CT, Nair LS (ed) Nanotechnology and Tissue Engineering: The scaffold, Taylor & Francis, Boca Raton, pp 3-32.

Available online at www.sciencedirect.com

SciVerse ScienceDirect

Procedia CIRP 5 (2013) 216 – 221

www.elsevier.com/locate/procedia

The First CIRP Conference on Biomanufacturing

Morphological characteristics of electrospun PCL meshes – the influence of solvent type and concentration

J. Dias[a], P.Bártolo[a]*

[a]*Centre for Rapid and Sustainable Product Development, Polytechnic Institute of Leiria, Centro empresarial da Marinha Grande, Rua de Portugal – zona industrial,2430-028 Marinha Grande, Portugal*

* Corresponding author. Tel.: +351-244-569-441; fax: +351-244-569-444.*E-mail address*: paulo.bartolo@ipleiria.pt

Abstract

Fibrous scaffolds, with fiber dimensions on the nanometer scale, are ideal for tissue engineering applications as they can mimic the physical structure of natural extracellular matrix. This paper investigates the effect of the solvent type and the solvent concentration on the morphological and hydrophobic characteristics of Polycaprolactone (PCL) meshes. Acetone and acetic acid with triethylamine (TEA) were used as solvents with different concentrations of PCL. Results show that its use allows the formation of meshes with high surface roughness, less surface friction and less hydrophobicity.

Selection and/or peer-review under responsibility of Professor Mamoru Mitsuishi and Professor Paulo Bartolo

Keywords: Electrospinning; Nanofibers; Polycaprolacone; Tissue Engineering.

1. Introduction

Biodegradable constructs for medical applications can be used in the form of meshes, films or three-dimensional porous scaffolds. These structures can be produced in a wide range of synthetic and natural materials trough the use of a large number of techniques [1-3].

Electrospinning is one of the most important electro-chemical processes to produce micro to nanoscale fiber meshes for medical applications [1, 4-6]. The basic requirements of an electrospinning system comprise a capillary tube with a needle, a high power voltage supply, a collector and electrical wires connecting the power voltage supply with both the capillary tube and the collector (Fig. 1). Two strategies can be considered [1,4-6]: solution electrospinning and melt electrospinning. Melt electrospinning requires the polymeric melt to be cooled, while the solution electrospinning relies on the fast evaporation of the solvent to produce the meshes [1].

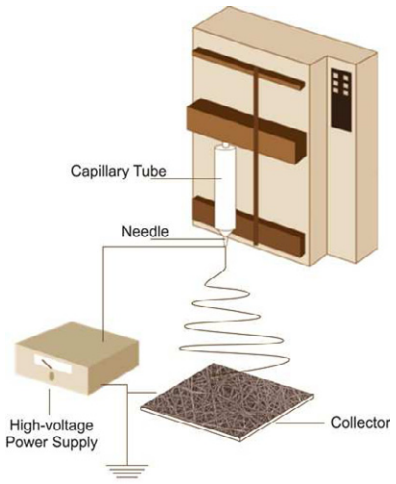

Fig. 1. Components of an electrospinning apparatus

The electrospinning process requires the control of a large number of parameters. Non-optimised processes produce non-homogeneous meshes with a significant number of material aggregates (beads) (Fig. 2) or

2212-8271
Selection and/or peer-review under responsibility of Professor Mamoru Mitsuishi and Professor Paulo Bartolo
doi:10.1016/j.procir.2013.01.043

spraying mechanisms without producing fibres (Fig. 3).

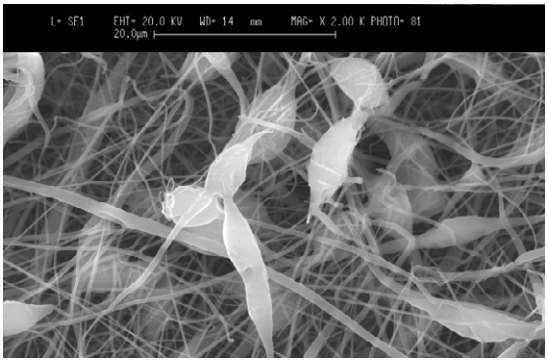

Fig 2. Non-homogeneous electrospun mesh.

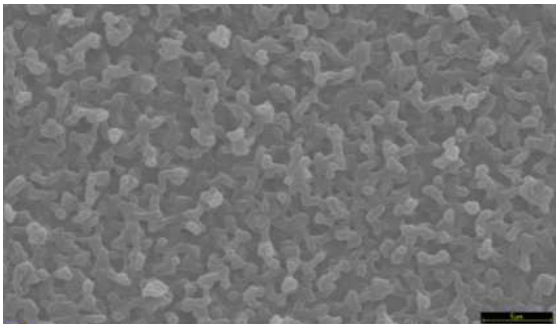

Fig 3. Electrosprayed surface.

Electrospun meshes close mimic the extracellular matrix of native tissues, providing a network structure with high surface area for cell attachment, proliferation and differentiation.
This paper focuses on the use of a solution electrospinning process to produce PCL meshes, investigating the effect of the solvent type and solvent content on the morphology and hydrophobicity characteristics of the produced meshes.

2. Materials and Methods

2.1. Materials

PCL (Mw 50000[g/mol]), from Perstorp (CAPA 6500), was dissolved in two different solvents:

i) acetone (Mw 58.08 [g/mol]), from Sigma-Aldrich
ii) acetic acid (Mw 60.05 [g/mol]), from Labsolve mixed with 2wt% of triethylamine (Mw 101.19 [g/mol]) supplied by Sigma-Aldrich.

Solutions with different concentrations (1.5wt%, 3wt%, 6wt%, 9wt%, 11wt % and 17wt% of PCL) were placed in a shaking incubator during 24 hours, and heated between 25ºC and 65ºC, with a heating rate of 5ºC/min.

2.2. Methods

2.2.1 Electrospinning apparatus

Electrospun meshes were produced using the homemade system shown in Fig. 4. The following processing conditions were considered: syringe volume - 2,5ml; needle diameter - 0, 6 mm; applied voltage - 10kV; distance between the needle and the collector - 10cm and flow rate - 0.72ml/h.

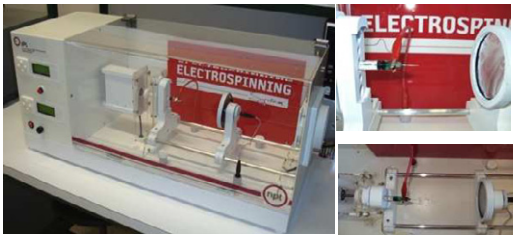

Fig 4. Electrospinning apparatus.

2.2.2 Characterisation techniques

Produced meshes were characterised using the following techniques:

- Scanning electron microscopy (SEM);
- Atomic force microscopy (AFM);
- Contact angle (CA).

SEM tests were performed to evaluate the mesh structure and the diameter of the fibres, using the FEI QUANTA 600F system (FEI Company, USA). Samples were coated with gold prior observation.
AFM uses a flexible cantilever as a type of spring, to measure the force between the tip and the sample, was used to determine surface roughness. All measurements were obtained using the NanoWizard system (maximum scan range: 100x100 µm; z-range: 15 µm; spring constant: 2N/m) with the TopViewOptics software (JPK instruments, Germany).
Water contact angle was used to measure the hydrophobicity of the produced meshes. A contact angle below 90º means a hydrophilic surface, while a contact angle above 90º corresponds to hydrophobic surfaces [7]. The contact angle was measured by delivering a droplet of water to the surface and determining its height and width (Fig. 5), according to the following equation [7]:

$$\tan\left(\frac{\theta s}{2}\right) = \frac{h}{(x)} \qquad (1)$$

where Θs is the static contact angle, h is the water droplet height, and x corresponds to the half of the water droplet width.

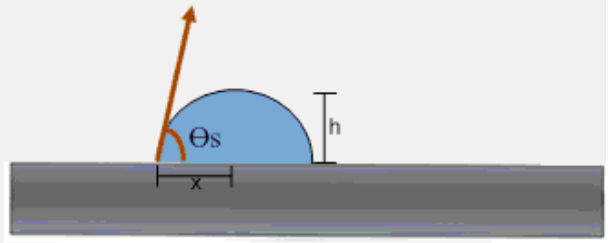

Fig 5. The water contact angle.

Contact angle measurements were performed using the Optic Tensiometer model Theta (Paralab, Portugal).

3. Results and Discussion

3.1. Scanning Electron Microcopy (SEM)

Figures 6 and 7 shows the obtained structures. Better electrospun meshes were produced with solutions containing 17wt% of PCL dissolved in acetone (Fig. 8) and 11wt% of PCL dissolved acetic acid with triethylamine (Fig. 9). In the first case, the average diameter of the fibers is 876 nm, while in the second case is 47 nm. Results show, that for low polymer concentrations no spinning is obtained.

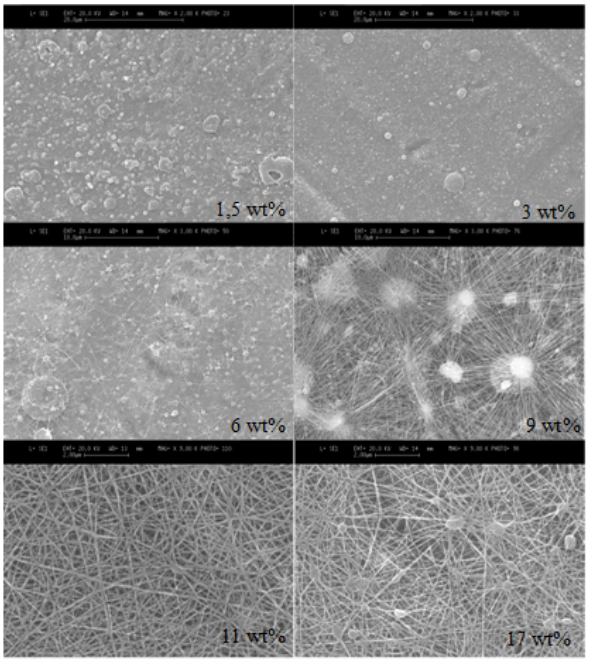

Fig 6. Morphology of the structures produced with solutions containing different concentrations of PCL dissolved in acetone.

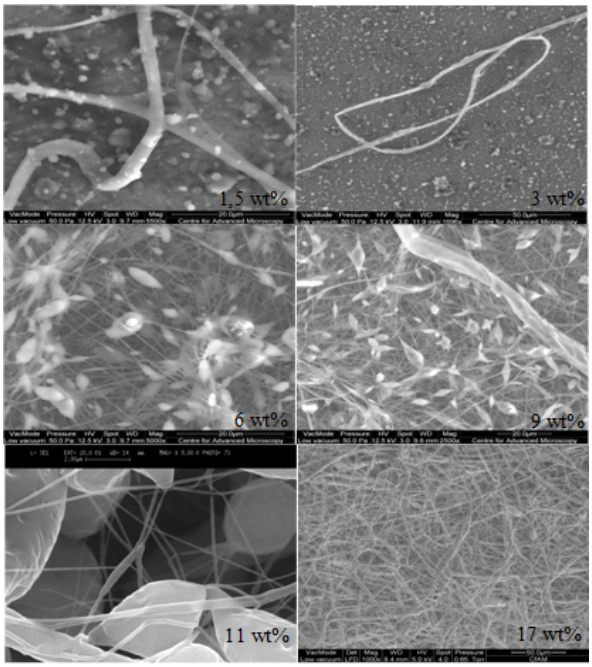

Fig 7. Morphology of the structures produced with solutions containing different concentrations of PCL dissolved in acetic acid with triethylamine.

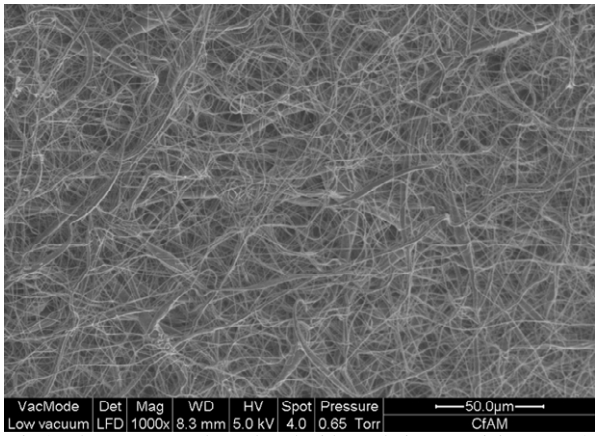

Fig 8. Electrospun mesh produced with a solution containing 17wt% of PCL dissolved in acetone.

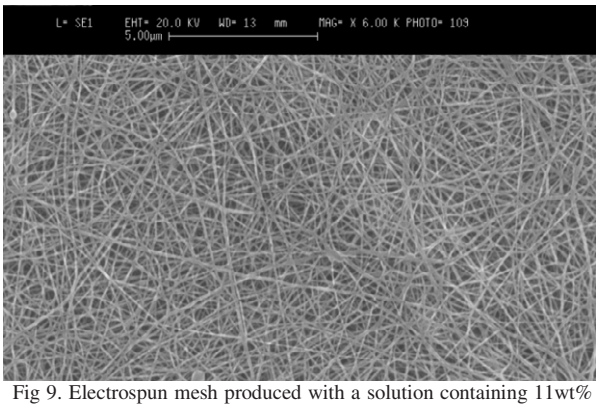

Fig 9. Electrospun mesh produced with a solution containing 11wt% of PCL dissolved in acetic acid with triethylamine.

The addition of triethylamine to the acetic acid allows the formation of a salt that increases the dielectric constant and the volatility of the solvent, which facilitates the electrospinning process [8]. Results also show that for the PCL solution in acetic acid with triethylamine, there is a critical concentration value after which non-homogeneous meshes were produced.

3.2. Atomic Force Microscopy

AFM measurements enable to determine different mechanical and adhesive properties by determining three fundamental parameters (Fig. 10): height (represents the surface roughness), slope (represents the stiffness of the sample) and adhesion (represents surface friction).
Figures 11 and 12 show the topography of the meshes produced by solution containing 17wt% of PCL dissolved in acetone and a solution containing 11wt% of PCL dissolved in acetic acid with triethylamine. Slope and adhesion values are indicated in Figures 13 and 14.

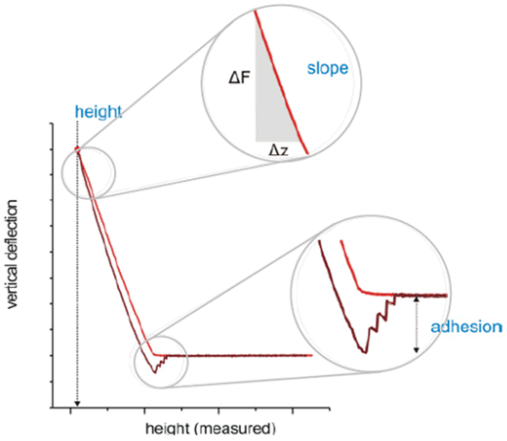

Fig 10. AFM measured parameters.

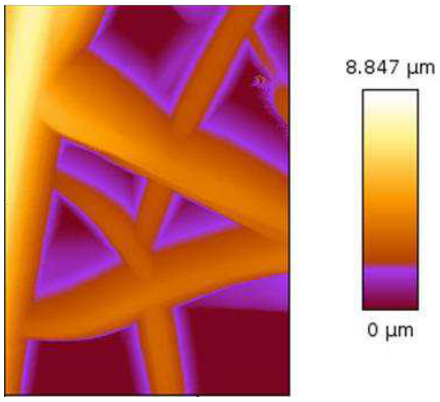

Fig. 11. Surface topography of a mesh produced using a solution containing 17wt% of PCL dissolved in acetone.

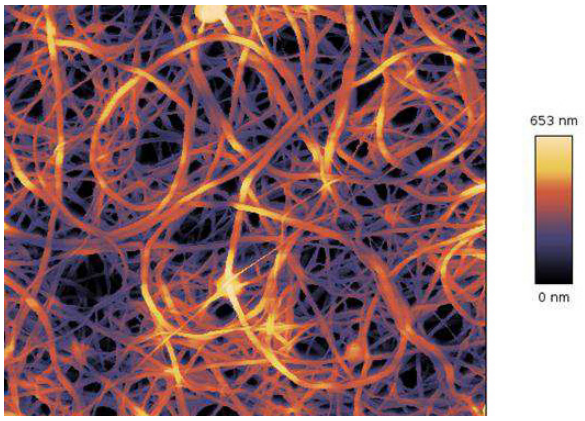

Fig. 12. Surface topography of a mesh produced using a solution containing 11wt% of PCL dissolved in acetic acid with triethylamine.

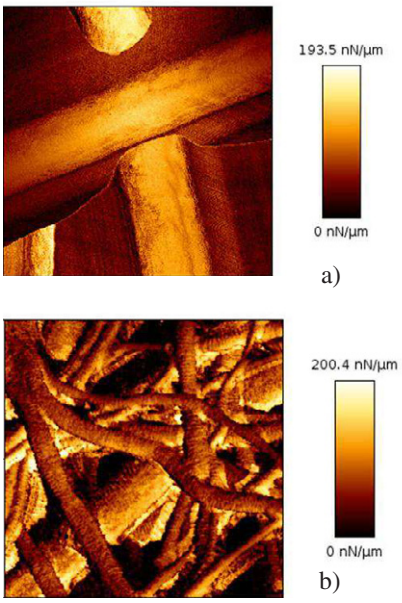

Fig. 13. Slope variation of a) mesh produced using a solution containing 17wt% of PCL dissolved in acetone; b) mesh produced using a solution containing 11wt% of PCL dissolved in acetic acid with triethylamine.

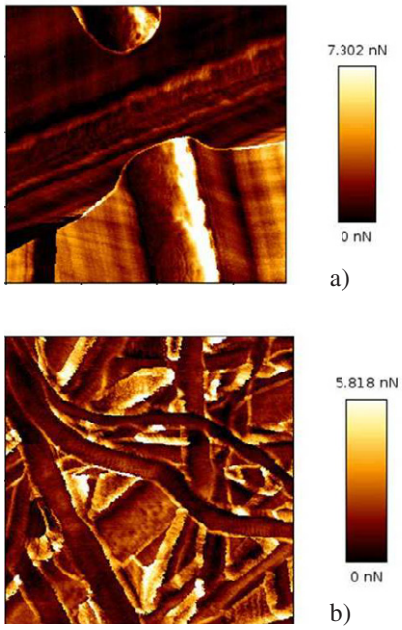

Fig. 14. Adhesion variation of a) mesh produced using a solution containing 17wt% of PCL dissolved in acetone; b) mesh produced using a solution containing 11wt% of PCL dissolved in acetic acid with triethylamine.

Results show that the meshes produced, using a solution containing 17wt% of PCL dissolved in acetone, present a smooth structure. This mesh is also a stiffer and higher friction structure compared to the meshes produced using a solution containing 11wt% of PCL, dissolved in acetic acid with triethylamine.

3.3 Contact Angle

The contact angle photographs (Fig. 15 and Fig. 16) show that the produced meshes are hydrophobic, as expected. However, the use of acetic acid with triethylamine enables the fabrication of less hydrophobic meshes, as indicated in Table 1.

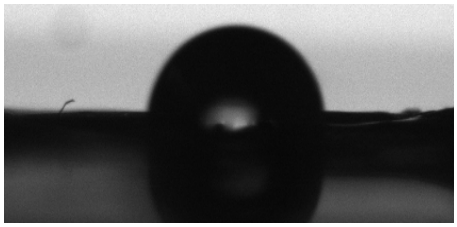

Fig. 15. Contact angle on the mesh produced with a solution containing 17wt% of PCL dissolved in acetone.

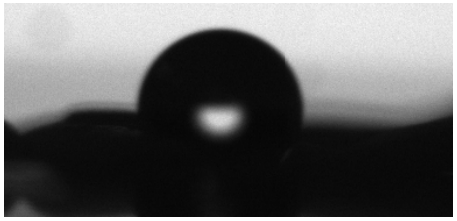

Fig. 16. Contact angle on the mesh produced with a solution containing 11wt% of PCL dissolved in acetic acid with triethylamine.

Table 1. Contact angle values.

Sample	Contact Angle (º)	95% Confidence interval mean
17wt% PCL dissolved in acetone	101,1 ±0,94	[83,35; 93,92]
11wt% PCL dissolved in acetic acid with triethylamine	83,64±2,72	[100,94; 101,18]

4. Conclusions

Results show that the type and concentration of the solvent strongly determine the characteristics of the produced meshes. The use of a solvent with high dielectric constant (acetic acid with triethylamine) allows the formation of electrospinning meshes with low PCL concentration. These meshes are also characterised by high surface roughness, less surface friction and less hydrophobicity.

Acknowledgments

The Strategic Project (PEST-OE/EME/UI4044/2011) funded by the Portuguese Foundation for Science and Technology supported this work. Authors also acknowledge the support provided by JPK Instruments (Germany) and Paralab (Portugal).

References

[1] Bartolo, P., Kruth, J.-P., Silva, J., Levy, G., Malshe, A., Rajurkar, K., Mitsuishi, M., Ciurana, J., Leu, M., 2012. Biomedical production of implants by additive electro-chemical and physical processes. *CIRP Annals - Manufacturing Technology* 61, p. 635.

[2] Melchels, F.P.W., Domingos, M.A.N., Klein, T.J., Malda, J., Bartolo, P.J., Hutmacher, D.W., 2012. Additive manufacturing of tissues and organs. *Progress in Polymer Science*, 37, p. 1079

[3] Bartolo, P.J., Chua, C.K., Almeida, H.A., Chou, S.M., Lim, A.S.C., 2009. Biomanufacturing for tissue engineering: present and future trends. *Virtual and Physical Prototyping*, 4, p. 203

[4] Teo, W.E., Inai, R., Ramakrishna, S., 2011. Technological advances in electrospinning of nanofibres. *Science and Technology of Advanced Materials*, 12, p.1

[5] Cipitria, A., Skelton, A., Dargaville, T.R., Dalton, P.D., Hutmacher, D.W., 2011. Design, fabrication and characterization of PCL electrospun scaffolds – a review. *Journal of Materials Chemistry*, 21, p. 9419

[6] Mitchell, G.R., Ahn, Kyung-hwa, Davis, Fred J., 2011. The potential of electrospinning in rapid manufacturing processes. Virtual and Physical Prototyping, 6, p. 63.

[7] Goddard, J.M., Hotckiss, J.M., 2007. Polymer surface modification for the attachment of bioactive compounds. *Progress in Polymer Science*, 32, p. 698

[8] Dias, J., Mitchell, G., Bártolo, P., 2011. Nanofibres development for cartilage tissue through electrospinning process.

Advanced Materials Research Vol 683 (2013) pp 137-140 *Online: 2013-04-24*

doi:10.4028/www.scientific.net/AMR.683.137

Mechanical and Biological characteristics of electrospun PCL meshes – the influence of solvent type and concentration

Dias, Juliana[1, a], Gloria, Antonio[2,b] and Bártolo, Paulo[1,c]

[1] Centre for Rapid and Sustainable Product Development, Polytechnic Institute of Leiria, Marinha Grande, Portugal

[2]Institute of Composite and Biomedical Materials - Research Council - P.le Tecchio 80, 80125 – Naples, Italy

[a]juliana.dias@ipleiria.pt, [b] angloria@unina.it, [c]paulo.bartolo@ipleiria.pt

Keywords: Electrospinning; Nanofibers; Polycaprolacone; Tissue Engineering.

Abstract. Non-woven scaffolds, with fiber dimensions at a nanometer scale, can mimic the physical structure of natural extracellular matrices, being ideal construts for Tissue Engineering applications. This research work explores solution electrospinning to produce nanoscale meshes. Different Poly (ε-caprolactone) (PCL) solutions were considered and the influence of both polymer concentration and type of solvent studied regarding the fabrication of polymeric meshes and their mechanical and biological properties. PCL solutions were prepared using two different solvents: glacial acetic acid with triethylamine (AA/TEA)) and Acetone (DMK) at different concentrations. PCL/AA/TEA meshes present better mechanical properties and good cell viability and proliferation.

Introduction

Tissue engineering is a multidisciplinary field, combining efforts of biologists, engineers and clinitians towads the development of biological substitutes to mantain, restore or improve tissue and organ function [1]. Tissue engineering comprises three main strategies: i) cell-based strategies, which involves the direct in vivo implantation of isolated cells or cel scaffold that provides a substrate for implanted cells and a physical support to organize the formation of the new tissue [2-4].This paper focuses on the use of a solution electrospinning process to produce PCL meshes, investigating the effect of the solvent type and solvent content on the mechanical properties and biological characteristics of the produced meshes.

Materials and Methods

Materials

Two different solvents were used to dissolved PCL (Mw 50000[g/mol]) supplied by Perstorp (CAPA 6500):

i) acetone (Mw 58.08 [g/mol]), from Sigma-Aldrich

ii) acetic acid (Mw 60.05 [g/mol]), from Labsolve mixed with 2wt% of triethylamine (Mw 101.19 [g/mol]) supplied by Sigma-Aldrich.

Solutions with different concentrations (1.5wt%, 3wt%, 6wt%, 9wt%, 11wt % and 17wt% of PCL) were placed in a shaking incubator during 24 hours, and heated between 25ºC and 65ºC, with a heating rate of 5ºC/min.

Methods

Electrospinning apparatus

Electrospun meshes were produced using the homemade system shown in Fig. 1. The following processing conditions were considered: syringe volume - 2,5ml; needle diameter - 0, 6 mm; applied voltage - 10kV; distance between the needle and the collector - 10cm and flow rate - 0.72ml/h.

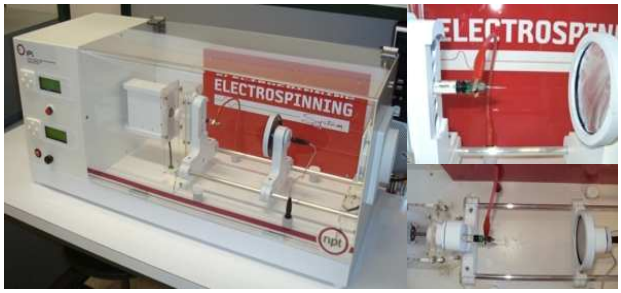

Fig. 1: Electrospinning apparatus.

Characterisation techniques

Produced meshes were characterised using the following techniques:

- Scanning electron microscopy (SEM);
- Atomic force microscopy (AFM);
- Biological test.

SEM tests were performed to evaluate the mesh structure and the diameter of the fibres, using the FEI QUANTA 600F system (FEI Company, USA). Samples were coated with gold prior observation.

AFM uses a flexible cantilever as a type of spring, to measure the force between the tip and the sample. It was used to determine the Young modulus of the meshes. All measurements were obtained using the NanoWizard system (maximum scan range: 100x100 µm; z-range: 15 µm; spring constant: 2N/m) with the TopViewOptics software (JPK instruments, Germany).

Biological tests were performed to evaluate cell viability and proliferation using the Alamar Blue™ assay. Human mesenchymal stem cells (hMSCs) were used.

Results and Discussion

Scanning Electron Microcopy (SEM)

Figures 2 a) and b) shows the obtained structures. Better electrospun meshes were produced with solutions containing 17wt% of PCL dissolved in acetone (Fig. 3 a)) and 11wt% of PCL dissolved in acetic acid with triethylamine (Fig. 3 b)). In the first case, the average diameter of the fibers is 876 nm, while in the second case is 47 nm. Results show, that for low polymer concentrations no spinning was obtained. The addition of triethylamine to the acetic acid allows the formation of a salt that increases the dielectric constant and the volatility of the solvent, which facilitates the electrospinning process [5]. Results also show that for the PCL solution in acetic acid with triethylamine, there is a critical concentration value after which non-homogeneous meshes were produced.

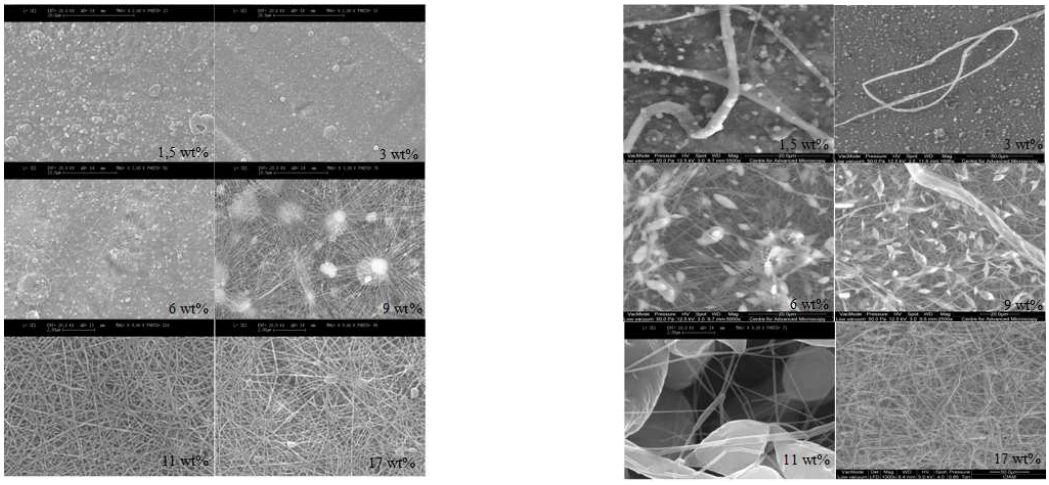

Fig. 2: a) Morphology of the structures produced with solutions containing different concentrations of PCL dissolved in acetone; b) Morphology of the structures produced with solutions containing different concentrations of PCL dissolved in acetic acid with triethylamine.

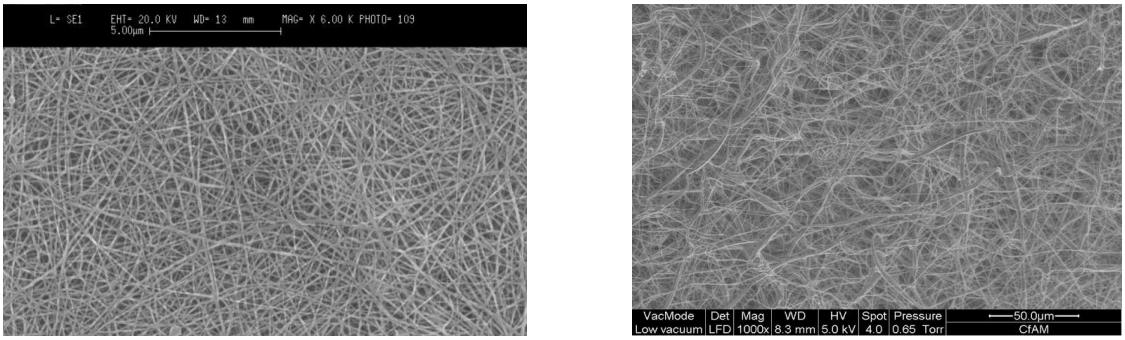

Fig. 3: a) Electrospun mesh produced with a solution containing 17wt% of PCL dissolved in acetone; b) Electrospun mesh produced with a solution containing 11wt% of PCL dissolved in acetic acid with triethylamine.

Atomic Force Microscopy

AFM measurements enable to evaluate surface roughness and mechanical properties by determining three fundamental parameters (Fig. 4): height (represents the surface roughness), slope (represents the stiffness of the sample) and adhesion (represents surface friction).Table 1 show the Young's Modulus of the meshes produced by using a solution containing 17wt% of PCL dissolved in acetone and a solution containing 11wt% of PCL dissolved in acetic acid with triethylamine. Results show that the Young modulus of PCL/AA/TEA meshes is higher than PCL/DMK ones. The obtained values are close to the value of cartilage and tendon [6].

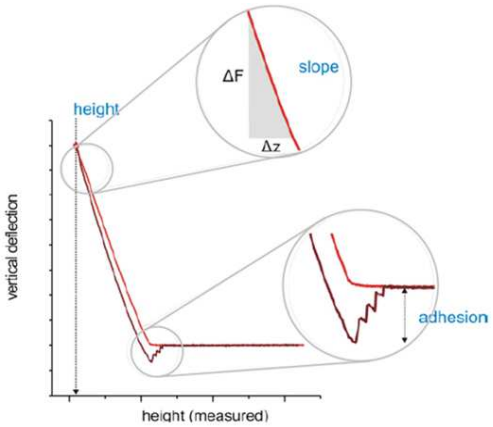

Fig. 4: AFM measured parameters.

Table 1: Young's Modulus.

Sample Type	Young's modulus (MPa)	Interval of 50% of samples (10^6)
PCL/AA/TEA	2,7±2,2	[1,1;3,7]
PCL/DMK	0,6±0,28	[0,4;0,8]

Biological test

Two kinds of disk-shaped meshes (PCL/DMK and PCL/AA/TEA) with a diameter of 6.0 mm were seeded with human mesenchymal stem cells (hMSCs). Cell viability and proliferation were evaluated by using the Alamar Blue™ assay. This assay is based on a redox reaction that occurs in the mitochondria of the cells; the colored product is transported out of the cell and can be measured spectrophotometrically. The number of viable cells correlates with the magnitude of dye reduction and is expressed as a percentage of Alamar Blue™ reduction [7].

During the assay it was possible observe a "mesh contraction" due to cell attachment process. Results also show that both meshes present no toxicity (Figure 5). However, better cell proliferation results were obtained with PCL/DMK samples.

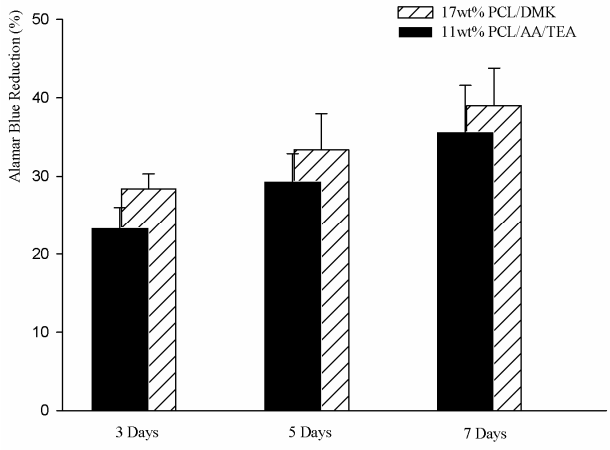

Fig. 5: AlamarBlue^{TM} reduction.

Conclusions

Results show that the type and concentration of the solvent strongly determine the characteristics of the produced meshes. The use of a solvent with high dielectric constant (acetic acid with triethylamine) allows the formation of electrospinning meshes with low PCL concentration. These meshes are also characterised by high mechanical properties and good cellular viability and proliferation.

Acknowledgments

The Strategic Project (PEST-OE/EME/UI4044/2011) funded by the Portuguese Foundation for Science and Technology supported this work. Authors also acknowledge the support provided by JPK Instruments (Germany) and Paralab (Portugal).

References

[1] Melchels, F.P., Domingos, M.A., Klein, T., Malda, J., Bartolo, P.J., Hutmacher, D.W., "Additive manufacturing of tissues and organs", Progress in Polymer Science, 37(2012), 1079-1104
[2]Meyer, Ulrich, Handschel, Thomas Meyer Jorg and Wiesmann, Hans Peter. Fundamentals of Tissue Engineering and Regenerative Medicine. Springer, 2009.
[3] Bidanda, B. e Bártolo, P.J. 2008. Virtual Prototyping & Bio Manufacturing in Medical Applications. Springer, 2008.
[4] Maya, Horst, Madduri, S., Rita, G., Tullio, S., Hall, H., Eberli, D. Scaffolds for the Engineering of funcrional bladder tissues. In Daniel Eberli.(eds)*, Tissue Engineering,* In-tech , 2010, pp. 119-140.
[5] Dias, J., Mitchell, G., Bártolo, P., 2011. Nanofibres development for cartilage tissue through electrospinning process.
[6]Sabir, M.I., Xu, X., A review on biodegradable polymeric materials for bone tissue engineering applications, J. Materials Sci,44 (2009) 5713-5724;
[7] Russo,T., Gloria, A., D'Antò, V., D'Amora, U., Ametrano, G., Bollino, F., De Santis, R., Ausanio, G., Catauro, M., Rengo, S., Ambrosio, L.. "Poly(ε-caprolactone) reinforced with sol-gel synthesized organic-inorganic hybrid fillers as composite substrates for tissue engineering". J Appl Biomater Biomech, 8(2010) 146-152.

Advanced Materials and Engineering Materials II
10.4028/www.scientific.net/AMR.683

Mechanical and Biological Characteristics of Electrospun PCL Meshes – the Influence of Solvent Type and Concentration
10.4028/www.scientific.net/AMR.683.137

European Polymer Journal 95 (2017) 161–173

Contents lists available at ScienceDirect

European Polymer Journal

journal homepage: www.elsevier.com/locate/europolj

In situ crosslinked electrospun gelatin nanofibers for skin regeneration

J.R. Dias[a,b,c,d,*], S. Baptista-Silva[e], C.M.T. de Oliveira[a,c,f], A. Sousa[a,c], A.L. Oliveira[e], P.J. Bártolo[h], P.L. Granja[a,c,d,g]

[a] Instituto de Investigação e Inovação em Saúde (i3S), Universidade do Porto, Porto, Portugal
[b] Centre for Rapid and Sustainable Product Development (CDRsp), Polytechnic Institute of Leiria, Leiria, Portugal
[c] Instituto de Engenharia Biomédica (INEB), Universidade do Porto, Porto, Portugal
[d] Instituto de Ciências Biomédicas Abel Salazar (ICBAS), Universidade do Porto, Porto, Portugal
[e] Center for Biotechnology and Fine Chemistry (CBQF), School of Biotechnology, Portuguese Catholic University, Porto, Portugal
[f] Escola Superior de Tecnologia da Saúde do Porto (ESTSP/IPP), Porto, Portugal
[g] Faculdade de Engenharia da Universidade do Porto (FEUP), Porto, Portugal
[h] School of Mechanical, Aerospace and Civil Engineering & Manchester Institute of Biotechnology, University of Manchester, UK

ARTICLE INFO

Keywords:
In situ crosslinking
Electrospun fibers
Gelatin
BDDGE
Wound dressing

ABSTRACT

Due to its intrinsic similarity to the extracellular matrix, gelatin electrospun nanofibrous meshes are promising scaffold structures for wound dressings and tissue engineering applications. However, gelatin is water soluble and presents poor mechanical properties, which generally constitute relevant limitations to its applicability. In this work, gelatin was *in situ* crosslinked with 1,4-butanediol diglycidyl ether (BDDGE) at different concentrations (2, 4 and 6 wt%) and incubation time-points (24, 48 and 72 h) at 37 °C. The physico-chemical and biological properties of BDDGE-crosslinked electrospun gelatin meshes were investigated. Results show that by changing the BDDGE concentration it is possible to produce nanofibers crosslinked *in situ* with well-defined morphology and modulate fiber size and mechanical properties. Crosslinked gelatin meshes show no toxicity towards fibroblasts, stimulating their adhesion, proliferation and synthesis of new extracellular matrix, thereby indicating the potential of this strategy for skin tissue engineering.

1. Introduction

Skin is the largest vital organ in the body, protecting it against the external environment [1–5]. Although skin has a self-regeneration ability, this capacity is strongly reduced in the case of full-thickness lesions, making necessary the use of grafts or dressings [1]. The usual procedure when skin damage occurs consists in the application of a wound dressing due their efficiency, low cost and availability [6,7]. Wound dressings made from electrospun nanofibers present advantageous properties compared to conventional dressings such as the potential to promote the hemostasis phase, wound exudate absorption, semi-permeability, easy conformability to the wound, functional ability and no scar induction [8].

Gelatin, derived from collagen, is a natural mimic of the extracellular matrix (ECM) of human tissues and organs and is widely used in the tissue engineering field due to of its excellent biological origin, biocompatibility, biodegradability non-immunogenicity,

* Corresponding author at: Biomaterials for Multistage Drug & Cell Delivery Group, Instituto de Investigação e Inovação em Saúde, Universidade do Porto, Rua Alfredo Allen, 208, 4200-135 Porto, Portugal.
E-mail address: juliana.dias@ineb.up.pt (J.R. Dias).

http://dx.doi.org/10.1016/j.eurpolymj.2017.08.015
Received 8 April 2017; Received in revised form 25 July 2017; Accepted 4 August 2017
Available online 07 August 2017
0014-3057/

cell-interactivity and commercial availability [9,10]. However, gelatin is a water-soluble protein derived from partial hydrolysis of collagen and crosslinking is usually needed to improve its mechanical properties and stability, making gelatin scaffolds insoluble in biological environments [10]. Several gelatin crosslinking methods are available, such as enzymatic using transglutaminase [11,12], or chemical using fructose [13], dextran dialdehyde [14], diepoxy [15], formaldehyde [16], glutaraldehyde [13,16,17], genipin [15,18,19], diisocyanates [20], or carbodiimides [21]. The widely used aldehyde-based crosslinking strategy has provided a powerful tool to tailor the physical properties of gelatin films [22–24] although the assumed toxicity of such chemicals makes their use uncertain [22]. Epoxy compounds are preferred as a stabilizing agent of collagen-based materials for biomedical applications due to their lower toxicity compared to commonly used dialdehydes [25–27].

The search for alternative crosslinkers presenting low toxicity and good stability is the main objective of this research work. Amongst water-soluble polyepoxides, 1,4-butanediol diglycidyl ether (BDDGE) is commercially available as a crosslinking agent in dermal filler formulations [26]. Although un-reacted BDDGE should be considered from slightly to moderately toxic [27], residual BDDGE might undergo hydrolysis yielding a diol-ether (3,3′(butane-1,4-diylbis(oxy)) bis propane-1,2-diol), which has been proven non-toxic, thus limiting safety risks [26]. This study evaluates the ability of BDDGE to crosslink electrospun gelatin nanofibers and provides the first insights on the physicochemical and in vitro biological performance of produced scaffolds in the context of skin tissue engineering applications.

2. Materials and methods

2.1. Materials

Gelatin powder of pig skin (type A, 300 bloom, 60 mesh) was kindly supplied by Italgelatine (Italy). Acetic acid (AA) glacial was purchased from PanReac AppliChem, triethylamine (TEA) from Sigma Aldrich, and 1,4-butanediol diglycidyl ether (BDDGE) from Alpha Aesar. All materials used were of reagent grade and used without any further purification.

2.2. Electrospinning of crosslinked gelatin nanofiber meshes

A gelatin/AA/TEA solution was prepared by dissolving gelatin (15 wt%) in AA and then adding 2 wt% of TEA to the solution and stirring at 37 °C overnight. TEA was added to increase the solution's conductivity. Crosslinking of electrospun gelatin fibers was carried out through the incorporation of BDDGE on the gelatin solution immediately before fiber electrospinning to avoid the loss of configuration that is induced through a crosslinking bath after fiber production. The effect of different BDDGE concentrations (2, 4 and 6 wt%) at varied time-points (24, 48 and 72 h) was tested.

Gelatin nanofibrous meshes were processed using a home-made electrospinning apparatus. Non-woven gelatin electrospun meshes were obtained at room temperature (RT) and relative humidity of 40–50% with a constant flow rate of 0.4 mL/h (SP11Elite, Harvard Apparatus) and 11 kV of voltage. A grounded copper plate was used as collector and it was positioned 12 cm away from the needle tip.

2.3. Physico-chemical characterization

2.3.1. Apparent density and porosity

The apparent density and porosity of gelatin electrospun meshes were calculated using Eqs. (1) and (2) [28], respectively, and the mesh thickness was measured using a micrometer.

$$\text{Apparent density } (\text{g}\cdot\text{cm}^{-3}) = \frac{\text{mesh mass (g)}}{\text{mesh thickness (cm)}\cdot\text{mesh area (cm}^2\text{)}} \tag{1}$$

$$\text{Mesh porosity} = \left(1 - \frac{\text{Mesh apparent density } (\text{g}\cdot\text{cm}^{-3})}{\text{Bulk density of gelatin } (\text{g}\cdot\text{cm}^{-3})}\right)\cdot 100\% \tag{2}$$

2.3.2. Morphology and fiber diameter

The morphology of each electrospun fibrous mesh was examined by scanning electron microscopy (SEM) using a Quanta 400 FEG ESEM/EDAX Genesis X4M (FEI Company, USA). Prior to examination samples were coated with a gold/palladium (Au/Pd) thin film, by sputtering, using the SPI Module Sputter Coater equipment. SEM images were also used to evaluate the fiber diameter distribution using Image J software. To each condition three individual samples were analyzed and fifty measurements per image were carried out.

2.3.3. Mesh structure

Fourier transform infrared (FTIR) spectroscopy with attenuated total reflectance (ATR) was used to evaluate the chemical composition of the materials and to detect possible structural changes. FTIR analyses were carried out using an Alpha-P Brucker FTIR-ATR spectrometer, in the range of 4000–500 cm^{-1}, at a 4 cm^{-1} resolution with 64 scans.

2.3.4. Crosslinking extent

The ninhydrin (NHN) assay was used to quantify the number of amino groups involved in the crosslinking reaction through UV–vis spectrometry. Crosslinked gelatin electrospun meshes with different crosslinker percentages and dried after different periods of time were tested. A precise amount of sample (10.5 ± 0.5 mg) was heated with ninhydrin solution (200 mg/100 mL) for 10 min in a water bath at 90 °C. Afterwards, 5 mL of ethanol was added to 100 μL of each sample and the absorbance recorded on a spectrophotometer (lambda 35 from Perkin Elmer, USA) at a wavelength of 570 nm with glycine as standard. Linear regression was performed with a correlation of 0.9976. The extent of crosslinking was defined according to Eq. (3):

$$\text{Crosslinking degree } (\%) = \left(1 - \frac{NH_t}{NH_0}\right) \cdot 100 \tag{3}$$

where NH_0 is the amount of free amino groups in the gelatin before crosslinking and NH_t is the amount of free amino groups after crosslinking [29].

2.3.5. Dissolvability and water uptake

To assess the dissolvability, samples were dried for 24 h before weight determination, followed by incubation in distilled water and sodium azide (0.02%) as bacteriostatic agent. After 24 h of incubation samples were removed from the distilled water solution and weighted again to evaluate the swelling degree (Eq. (4)). Then, the samples were dried for an additional 24 h period at 37 °C and weighted to evaluate their dissolvability (Eq. (5)).

$$\text{Degree of sweeling } (\%) = \frac{W_w - W_d}{W_d} \cdot 100, \tag{4}$$

where W_w is the wet weight and W_d is the dry weight.

$$\text{Dissolvability } (\%) = \frac{W_0 - W_d}{W_0} \cdot 100 \tag{5}$$

where W_0 is the initial weight and W_d is the dry weight.

2.3.6. Water vapor permeability

To evaluate the water permeation rate of electrospun meshes, glass bottles with the same size and type were filled with PBS solution and the electrospun meshes were fixed on their openings. The area available for vapor permeation was 2.39 cm^2. Evaporation of water through the mesh was monitored by the measurement of weight loss according to standard test methods for water vapor transmission [30]. Briefly, each set was weighted and kept at 32 °C during 24 h, after which the weight of each set was recorded again to quantify the amount of water evaporated.

2.3.7. Mechanical properties

The tensile strength and modulus of crosslinked electrospun gelatin samples were determined both in the dry and wet state using a texturometer (TA.XT Plus model, Stable Micro System SMD, England) with a 5 N load cell. Mechanical tests were carried out in a controlled environment at RT and relative air humidity of 45%. The gauge length was 15 mm and the test speed was 1 mm s^{-1}. At least five individual samples were tested from each group and measurements were reported as mean ± standard deviation according the statistical method used (mixed effect model).

2.4. In vitro studies

Human dermal neonatal fibroblasts (hDNF) isolated from the foreskin of healthy male newborns (ZenBio) were cultured, expanded, and maintained in Dulbecco's modified eagle medium (DMEM) (Gibco), at 37 °C in a humidified atmosphere of 5% CO_2. The culture medium was changed twice a week and cells were trypsinized (0.25% trypsin/0.05% ethylenediamine tetraacetic acid (EDTA)/0.1% glucose in PBS (pH 7.5)) when they reached 70–80% of confluence. Cells from passages between 8 and 11 were used in this study.

2.4.1. Cytotoxicity

To assess cytotoxicity, electrospun meshes were tested in direct (samples) and indirect (leachables) contact under different preconditions (washed and non-washed in ultrapure water). Samples were sterilized with UV light followed by washing during 24 h. hDNF cells were seeded in culture wells for 24 h at a density of 2×10^4 cells/well. 24 h later, samples (direct contact) and culture medium having been in contact with samples (indirect contact) were incubated with the cells for another 24 h. The culture medium was then removed from the wells and fresh basal medium with 20% v/v resazurin (Sigma) was added. Cells were incubated (37 °C, 5% v/v CO_2) for an additional 2 h period, after which 300 μL per well were transferred to a black 96-well plate and measured (Ex at 530 nm, Em at 590 nm) using a micro-plate reader (Synergy MX, BioTek). The control consisted in cells alone.

For the quantification of the total double-stranded DNA (dsDNA) content, the cell pellets were recovered from wells and washed with phosphate buffered saline (PBS). The suspension was then centrifuged (10,000 rpm, 5 min) and then stored at −20 °C until further analysis. The dsDNA quantification was performed using the Quant-iT PicoGreen dsDNA kit (Molecular Probes, Invitrogen), according to the manufacturer's protocol. Briefly, the samples were thawed and lysed in 1% v/v Triton X-100 (in PBS) for 1 h at

250 rpm at 4 °C. Then, they were transferred to a black 96-well plate with clear bottom (Greiner) and diluted in Tris-EDTA buffer (200 mM Tris–HCl, 20 mM EDTA, pH 7.5). After adding the Quant-iT PicoGreen dsDNA reagent, samples were incubated for 5 min at RT in the dark, and fluorescence was measured using a microplate reader (Ex at 480, Em at 520 nm).

2.4.2. Cell metabolic activity and proliferation

Cell metabolic activity and proliferation assays were performed using hDNF cells seeded on electrospun meshes at a cell density of 1×10^4 cells per sample. To promote an efficient cell penetration into the mesh the seeding was performed with only 10 μL. After 2 h medium up to 500 μL was added and cultured during 7 days. Metabolic activity was estimated using the resazurin-based assay, using electrospun meshes without cells as control. For the proliferation assay samples were tested in direct contact with hDNF cells and pre-washed with ultrapure water. Afterwards, they were cultured for 7 days, and their metabolic activity was measured at days 1, 3 and 7.

2.4.3. Cell morphology and fibronectin deposition

For the same time-points as for the cell metabolic activity (1, 3 and 7 days), cells seeded in electrospun meshes were stained for filamentous actin (F-actin), nuclei (Dapi) and fibronectin (FN) deposition. Briefly, samples were washed with PBS, fixed for 20 min in 4 wt% paraformaldehyde (PFA, Sigma), and permeabilized with 0.2% Triton X-100 (Sigma) for 7 min. Samples were then incubated for 1 h with 1 wt% bovine serum albumin (BSA, Merck) in PBS. For FN staining, electrospun meshes were incubated overnight at 4 °C with rabbit anti-fibronectin (f3648, Sigma, 1: 300) and then with the goat anti-rabbit secondary antibody Alexa Fluor® 488F(ab′)$_2$ fragment (Molecular Probes-Invitrogen, 1:2000, 2 h at RT). Subsequently, samples were incubated with the conjugated probe phalloidin/Alexa Fluor® 594 (Molecular Probes-Invitrogen, 1:40, 1 h at RT) for F-actin staining. Samples were then washed three times with the PBS solution and nuclei were counterstained with 40,6-diamidino-2-phenylindole dihydrochloride (DAPI, Sigma, 0.1 mg mL^{-1}) in vectashield (vector), just before confocal visualization (CLSM, Leica SP2AOBS, Leica Microsystems) using LCS software (Leica Microsystems). The scanned Z-series were projected onto a single plane and pseudo-colored using ImageJ. The cells cultured in electrospun meshes were also visualized trough SEM to evaluate their morphology. Briefly, samples were washed with PBS, fixed for 30 min in 2.5 wt% glutaraldehyde (GA, Fluka), and dehydrated with a successive graded ethanol series (40, 50, 70, 90 and 100%) for 15 min each. After that, critical point drying (CPD7501, Polaron Range) was performed to ensure the complete dehydration of samples.

2.5. Statistical analyses

All data points were expressed as mean ± standard deviation (SD). Statistical analysis (Levene's and T test) was carried out using IBM SPSS Statistics 20.0 with 99% confidence level for extent of crosslinking and cytotoxicity assays. Linear mixed model (LMM) was used to test differences between the effects of concentration, time and environment (wet and dry) in Young's Modulus, tensile strength at break and elongation at break. Concentration, time and environment were treated as a fixed factor and replication experiment was treated as a random factor to take into account possible heterogeneity of the samples in each set. Parameters estimation were performed by lme package and multiple comparison adjustment were performed by mulcomp package from the R statistical software [31]. The results were considered statistically significant when $p \leq 0.05$ (*).

3. Results and discussion

3.1. Macroscopic and morphological characterization

An optimal scaffold requires a highly porous (> 60–90%) and fully interconnected structure to provide a large surface area for cell ingrowth, uniform cell distribution, easy access to oxygen and nutrients by the cells, facilitating vascularisation [32–35]. The porosity of electrosopun meshes can be influenced by several parameters such as the fiber diameter and fibers density per area. The theoretical values calculated for the porosity of electrospun meshes produced (Table 1) range between 97.37 (2% v/v BDDGE,72 h) and 98.76% (4% v/v BBDGE, 24 h). The results showed that higher diameters yield slightly high mesh porosity values as a consequence of less fibers packing, leaving larger spaces between fibers. However, all sample demonstrated a high degree of porosity.

SEM morphological analyses of electrospun gelatin meshes with and without BDDGE are presented in Fig. 1. The results show that the obtained electrospun meshes present an uniform random deposition, with well-defined filaments and without beads. The *in situ* crosslinked fibers keep their morphology after incorporating BDDGE in the polymeric solution prior to fiber spinning. Fiber diameters strongly depend on both the amount of crosslinker and the incubation time (Table 1). For all samples, the fiber diameter generally decreased with increasing the crosslinking reaction time in BDDGE as a consequence of new bonds formation, bringing the molecular chains closer and thereby decreasing the fiber diameter. Using 2% of BDDGE the diameter decreased from 346 ± 158 nm at 24 h to 284 ± 120 nm at 72 h of incubation. With 4% of BDDGE the diameter decreased from 378 ± 137 nm at 24 h to 339 ± 91 nm at 72 h of incubation and with 6% of BDDGE there is a reduction from 341 ± 134 nm at 24 h to 276 ± 88 nm at 72 h. At 48 h of crosslinking reaction a non-agreement with the general trend was observed, which can be correlated with the instability associated to an incomplete reaction.

This seems to be confirmed by the fact that samples are more stable when incubated during 72 h with 4% or 6% of BDDGE, corresponding to 65.94% and 72.81% of crosslinking degree and a decrease of fiber diameter of 34.56% and 46.72%, respectively, compared to the non-crosslinked gelatin mesh (518 ± 165 nm) (Table 1 and Fig. 1a). Effectively, the decrease of standard deviation

Table 1
Characterization of gelatin electrospun meshes produced. Mechanical properties correspond to tests performed on wet samples only. Statistical significance for $p < 0.05$, (a) compared to 6% of BDDGE at the same incubation time, (b) compared to 4% of BDDGE at the same incubation time and (c) compared to 2% of BDDGE at the same incubation time.

BDDGE (%)	Crosslinking duration (h)	Crosslinking degree (%)	Apparent density	Porosity (%)	Average fiber diameter (nm)	Swelling degree (%)	Dissolvability (%)	Water vapor permeability (g/m^2/day)	Elastic modulus (MPa)	Tensile strength (MPa)	Elongation at break(%)
2	24	9.55 ± 1.31[a]	0.01222	98.30	346 ± 158	460.01 ± 317.36	53.60 ± 18.58	2425.49 ± 137.71	0.77 ± 0.45	0.26 ± 0.15	35.45 ± 5.88
	48	25.49 ± 0.59[a,b]	0.01250	98.26	261 ± 170	380.65 ± 84.28	15.27 ± 6.23	2359.52 ± 91.13	0.42 ± 0.23	0.05 ± 0.02	23.80 ± 10.81
	72	43.45 ± 0.52[a,b]	0.01893	97.37	284 ± 120	615.68 ± 31.34	30.68 ± 10.67	2462.43 ± 100.52	0.31 ± 0.11	0.08 ± 0.06	25.20 ± 8.99
4	24	35.19 ± 0.61[a]	0.00893	98.76	378 ± 137	644.40 ± 158.78	24.83 ± 1.56	2582.86 ± 46.80	0.67 ± 0.45	0.16 ± 0.15	45.01 ± 9.46
	48	42.75 ± 0.60[b,c]	0.01471	97.96	157 ± 88	468.48 ± 227.89	23.91 ± 5.33	2647.62 ± 54.22	0.60 ± 0.26	0.12 ± 0.10	33.23 ± 19.67
	72	65.94 ± 0.23[b]	0.01579	97.81	339 ± 91	567.22 ± 124.63	17.21 ± 10.19	2292.69 ± 147.36	0.30 ± 0.15	0.04 ± 0.03	29.10 ± 11.60
6	24	59.53 ± 0.97[b,c]	0.01339	98.14	341 ± 134	2375.48 ± 274.11	52.65 ± 4.61	2111.36 ± 115.50	0.16 ± 0.19	0.03 ± 0.02	15.04 ± 8.32
	48	67.57 ± 2.04[b,c]	0.01676	97.67	398 ± 198	1291.11 ± 142.93	38.06 ± 4.72	2160.13 ± 141.19	0.33 ± 0.15	0.04 ± 0.02	26.12 ± 7.76
	72	72.81 ± 1.70[c]	0.01798	97.50	276 ± 88	820.79 ± 90.90	28.43 ± 7.99	2299.82 ± 101.10	0.43 ± 0.24	0.02 ± 0.01	35.67 ± 15.35

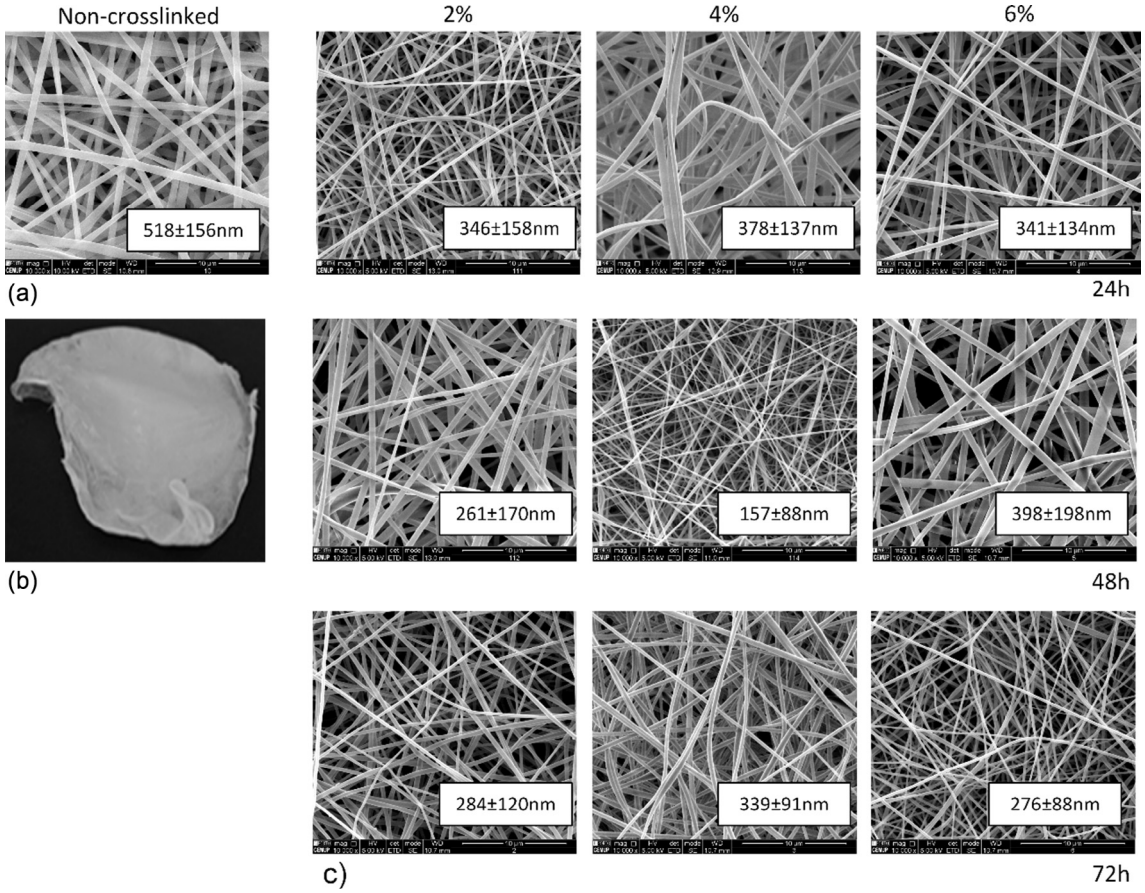

Fig. 1. Morphological evaluation of gelatin electrospun meshes. (a) Uncrosslinked sample, (b) Electrospun mesh at macroscale. (c) Electrospun gelatin nanofibrous meshes crosslinked with different concentrations of BDDGE at different time-points. Average fiber diameter is indicated in white background. Scale bars correspond to 10 μm.

at the end of 72 h suggests the stabilization of the reaction.

3.2. Physico-chemical and structural characterization

Fourier transform infrared spectroscopy with attenuated total reflection (FTIR-ATR) analyses were performed to evaluate the

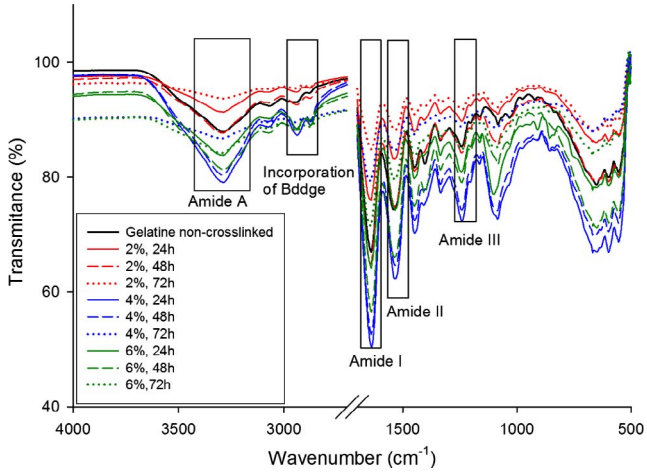

Fig. 2. FTIR spectra of uncrosslinked and gelatin crosslinked with BDDGE at different crosslinking degrees.

Table 2
Ratio between non-crosslinked and crosslinked samples at 2930 and 2890 cm^{-1}, ratio ≥1 means presence of BDDGE.

BDDGE (%)	Crosslinking duration (h)	Ratio between intensity of non-crosslinked and crosslinked samples (a.u.)	
		2930 cm^{-1}	2890 cm^{-1}
2	24	1.41	2.34
	48	0.99	2.47
	72	1.01	2.08
4	24	1.02	2.23
	48	1.01	2.34
	72	1.01	1.70
6	24	0.99	1.63
	48	0.98	2.49
	72	1.02	2.35

interaction between gelatin and BDDGE on electrospun meshes using uncrosslinked gelatin as control. The different spectra obtained are shown in Fig. 2. The FTIR spectrum of gelatin (uncrosslinked) is characterized by strong and sharp peaks that include prominent absorption bands directly associated with the protein's secondary structure [36]. The FTIR spectra of crosslinked gelatin samples shows prominent peaks in four different amide regions, namely at 1700–1600 cm^{-1} corresponding to amide I, at 1565–1520 cm^{-1}, corresponding to amide II, at 1240–670 cm^{-1} corresponding to amide III, and at 3500–3000 cm^{-1} corresponding to amide A [36–40]. The absorption of amide I contains contributions from the C═O stretching vibration of amide group and a minor contribution from the C−N stretching vibration [36]. Amide II absorption is related to N−H bending and C−N stretching vibrations. Amide III presents vibrations from C−N stretching attached to N−H in-bending with weak contributions from C−C stretching and C═O in-plane bending [41]. In samples crosslinked with BDDGE, at 2930 and 2890 cm^{-1}, it is possible to observe intensity changes compared to the uncrosslinked gelatin spectrum, which are associated to the contribution of aliphatic moieties from BDDGE, confirming the incorporation of BDDGE into the gelatin matrix (Fig. 2 and Table 2) [39].

The extension of crosslinking reaction was also assessed through UV/Vis used to quantify the crosslinking degree as a function of the amount of crosslinker and incubation time at different time-points. As expected, higher crosslinker amount and longer incubation times resulted in higher crosslinking degrees, showing that the crosslinking degree, and thus the properties of the obtained meshes can be easily tuned by simply varying the amount of crosslinker and the incubation time. For instance, using 2% of BDDGE incubated for 72 h resulted in a crosslinking degree of 43.45%, although using 4% of BDDGE incubated for only 48 h resulted in a similar crosslinking degree (42.75%). It is important to highlight that the maximum crosslinking degree reached was 72.81%, corresponding to samples crosslinked in 6% of BDDGE and incubated for 72 h. The reaction between BDDGE and gelatin occurs in acidic conditions due to the AA/TEA solution used to dissolve the gelatin, which results in protonation of the carboxylic acid groups (Fig. 3), and thereby limiting the achievement of 100% of crosslinking degree [39,42,43].

3.3. Water uptake, swelling, dissolvability and water vapor permeability

The water uptake of biodegradable polymers is an important indicator of their hydrophilic/hydrophobic character and, therefore, their susceptibility to degrade by hydrolysis [44]. The water uptake makes the materials more flexible and promotes changes in the dimensions of the implant material [45]. Table 1 shows the correlation between the water uptake and the crosslinker concentration and incubation time. The uncrosslinked samples were not evaluated due to their high dissolvability in aqueous medium. The capability to absorb water is known to decrease with the increase of crosslinking degree as the polymer chains become closer due the new bond formation, making the mesh more dense, with higher retraction forces [39,46]. This trend was also observed in this work, using gelatin crosslinked with BDDGE (4 and 6% v/v) for different reaction times. A less predictable behavior was observed, using 2% v/v of BDDGE, where an instability associated to incomplete reaction was observed.

On the other hand, keeping the reaction time and increasing the crosslinker amount was observed an increase of swelling that can be correlated to the increase of solution pH that affect directly how the crosslinking reaction occurs. In fact the pH of gelatin solution (15 wt% of gelatin in AA/TEA) and BDDGE is 2.5 and 7, respectively. Consequently, higher amount of crosslinker induces a slightly increase of solution pH leaving less protons available, increasing anion-anion repulsive forces and allowing the absorption of an increasing water volume [47,48].

The dissolvability assay represents the amount of uncrosslinked material immediately dissolved by the medium. Similarly, to the swelling degree the dissolvability decreased with the increase of crosslinking degree due the presence of less unreacted components. Samples with the lowest crosslinking degree (9.55 ± 1.30%), corresponding to 2% of BDDGE at 24 h, present 53.60 ± 18.58% of dissolved matter. Samples with the highest crosslinking degree (72.81 ± 1.70%) present only 28.43 ± 7.99% of dissolved material. Results show a clear evolution of swelling degree with the dissolution of samples with 4% and 6% of BDDGE.

An ideal wound dressing should control the water loss evaporation at an optimal rate. It should be permeable to maintain a moist environment avoiding wound dehydration. Therefore, the water vapor permeability (WVP) is one of the most important characteristics of wound dressings [49]. A wound with a dry environment causes tissue desiccation and consequently the tissue matrix becomes dehydrated, the cells die and a hard scab is formed [50]. Subsequently the keratinocytes have to pass beneath this scab to

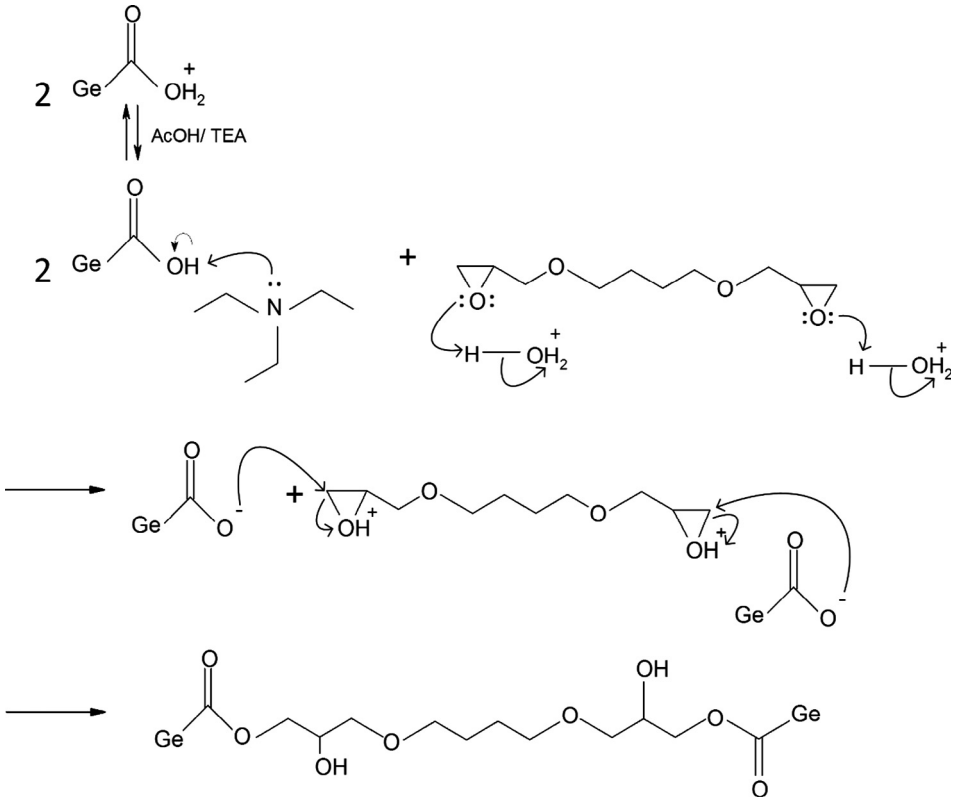

Fig. 3. Characteristic reaction between BDDGE and gelatin under acidic pH.

reach viable tissue, which consumes energy and time, and delays the wound healing process [49]. However, it is important to underline that a moist wound environment is not a wet wound environment, since excess of exudates will lead the patient to hypergranulation tissue formation in the wound bed and macerated periwound skin [49,50]. Therefore, an important objective in providing topical wound care relies in selecting a dressing which can maintain a moist wound surface and, at same time, remove exudates [49–51]. The common permeation rate for healthy skin is 204 g/m^2/day, while for injured skin can range from 279 g/m^2/day, for a first-degree burn, to 5138 g/m^2/day, for a granulating wound [52,53]. For an ideal wound dressing a rate of 2500 g/m^2/day is recommended to provide an adequate level of moisture without risking wound dehydration [49,52,54]. The water vapor permeability through the gelatin electrospun meshes ranges between 2111.36 ± 115.5 and 2647.62 ± 54.22 g/m^2/day, which is in the range of recommended values. The WVP of dressings is influenced by the pore size and interconnectivity between pores, with meshes with small pores and packed fibers resulting in low permeability to water vapor [55]. From Table 1 it is possible to observe that there's a general tendency for a decrease in WVP values with the increase in crosslinking degree from 2 to 6% of BDDGE, which can be correlated with both the reduction in the fiber diameter and the increase in packing of the fibers.

3.4. Mechanical characterization

The mechanical properties of crosslinked electrospun gelatin meshes were also investigated as a function of amount of crosslinker and incubation time. Representative stress–strain curves for samples tested in the dry and wet state are shown in the Fig. 4a. From those curves, it was possible to obtain the Young's modulus, the tensile strength and the elongation at break. As expected, in the dry state gelatin electrospun meshes show the distinctive behaviour of brittle and rigid materials, having high values of Young's modulus and low values of elongation at break, as a consequence of a rigid protein network [39]. In the dry state, the Young's modulus of all samples (Fig. 4b) decrease by increasing the incubation time in BDDGE from 24 to 72 h. The same trend was observed for samples in the wet state (Fig. 4b), except for samples crosslinked with 6% of BDDGE, which showed a slight increment from 24 to 72 h although not statistically significant. This decrease of the Young's modulus is related to the new bonds formed between polymer chains upon crosslinking, which increases the elasticity of the structure. It is worthwhile mentioning that samples in the wet state exhibited Young's modulus values between 0.16 ± 0.19 and 0.77 ± 0.45 MPa, in comparison to 25.61 ± 9.71 to 113.09 ± 63.85 MPa in the dry state, clearly demonstrating that an hydrogel was formed after crosslinking with BDDGE, directly improving the elasticity of the produced meshes. Samples in the dry state present low elongation at break values due their rigid nature without water (Fig. 4c). According to independent works of van Wachem and Zeeman, crosslinking of collagen with BDDGE at acidic pH promoted higher tensile strength and elongation at break values than the crosslinking reaction under alkaline conditions [56,57]. In the wet state, the

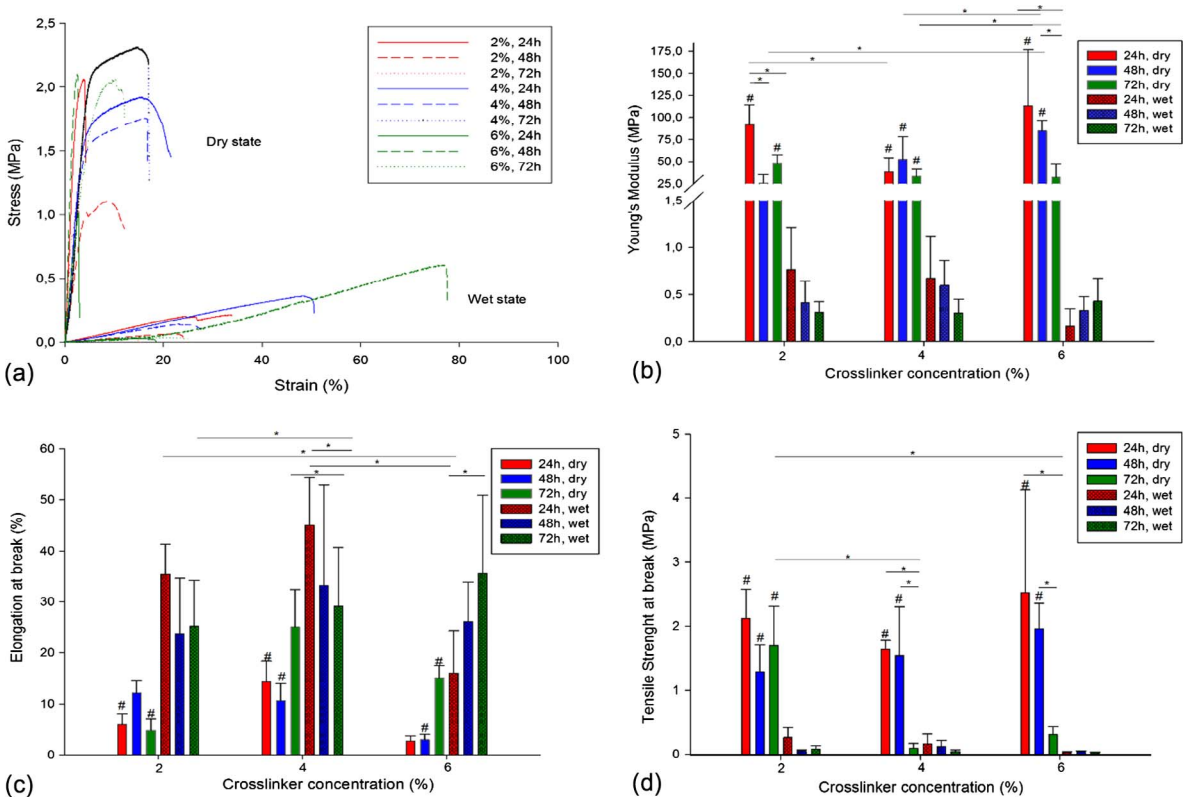

Fig. 4. Mechanical behaviour of electrospun gelatin meshes in the wet and dry state. (a) Stress–strain representative curves. (b) Young's Modulus. (c) Elongation at break. (d) Tensile strength at break. Statistical significance for $p \leq 0.05$ (*) and statistical significance for $p \leq 0.05$ compared to the same condition in wet state (#).

elongation at break, up to 4% of crosslinker, decreased with the incubation time, while an increase was observed when 6% of BDDGE was used, as a consequence of the higher crosslinking degree achieved, leading to a denser and more compact structure. However for incomplete reactions (24 h and 48 h), at lower concentrations (2% and 4% v/v of BDDGE), the elongation and tensile strength was higher due to the plasticizing provided by the secondary hydroxyl groups and hydroxyl-terminated pendant groups from hydrolyzed un-reacted epoxides of BDDGE [39].

The tensile strength at break (TSB) is characterized by the maximum tensile stress supported before sample break. In both states (dry and wet) the TBS values decreased with the incubation time for each set and from the lower crosslinker concentration to the higher concentration. These variations can be attributed to the hydroxyl compounds from hydrolyzed un-reacted epoxides of BDDGE that may be attached to gelatin and can take part in weakening the interactions between protein chains, consequently enhancing the mobility of the macromolecules, reducing the Young's modulus and tensile strength and enhancing the elongation of electrospun meshes crosslinked with BDDGE [39].

For the human skin values of 2.9–150 MPa for Young's Modulus, 1–32 MPa for Tensile Strength and 17–207% for elongation at break can be considered as reference [58–61]. Several works have been demonstrating the similarity between the mechanical properties of skin tissue and electrospun meshes made by different materials and production strategies [62–64]. In terms of mechanical properties, the gelatin electrospun meshes developed here exhibit values generally lower than natural skin, although this behavior can be easily improved by developing hybrid structures to mimic the mechanical properties of the skin.

3.5. Biological behavior

The cytotoxicity of the electrospun meshes was assessed using samples crosslinked in BDDGE at different concentrations (2, 4 and 6%) during only 48 h which, according to the previous results, are representative of low, medium and high crosslinking degrees (35.18%, 42.75% and 65.94%, respectively).

The results presented in Fig. 5 show that fibroblasts remained metabolically active in all considered cases. After 24 h no cytotoxicity was observed even for samples with high amount of crosslinker and the additional washing step did not influence the toxicity, either in direct or indirect contact assays. In direct contact assays differences between samples with 2 and 6% of BDDGE exhibited statistical significance to the control (pre-washed or not). In indirect contact assays statistically significant differences were observed between samples with 2% BDDGE (control and washed) and between samples with 6% BDDGE (control and non-washed samples). In indirect contact assays results show an increased metabolic activity of cells in indirect contact with samples compared to the control, which can eventually be explained by the release of uncrosslinked gelatin to the medium. Gelatin displays many integrin-binding sites

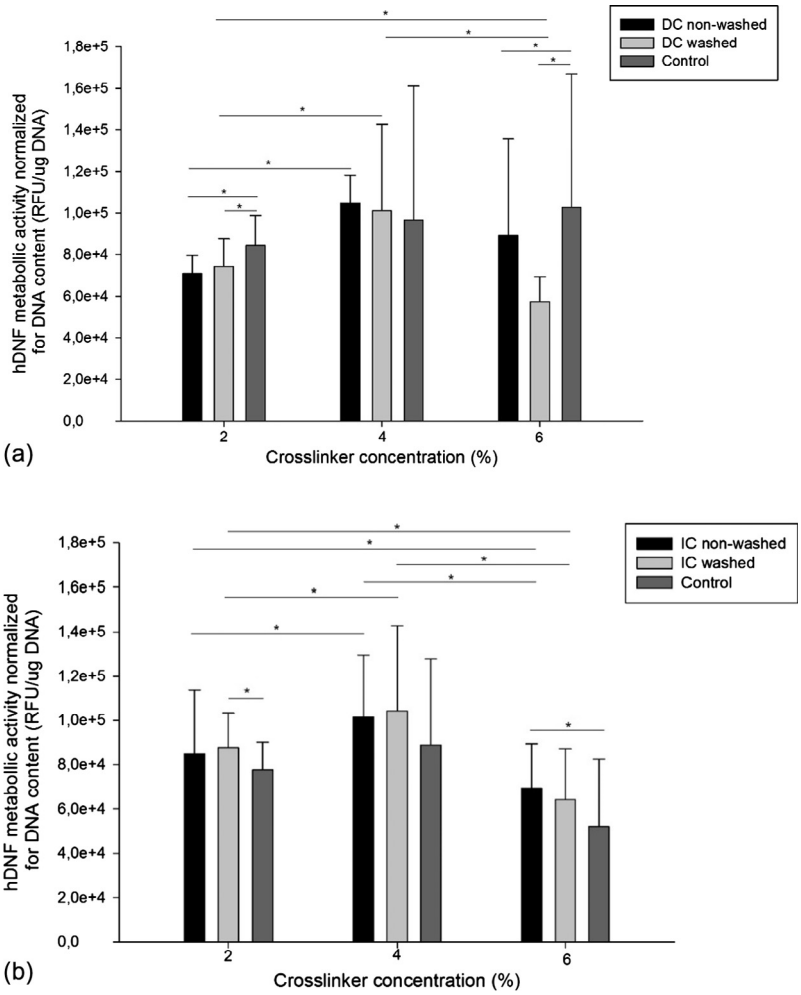

Fig. 5. Cytotoxicity assessment of electrospun gelatin meshes crosslinked with 2, 4 and 6% of BDDGE for 48 h. (a) Direct contact (DC) and (b) Indirect contact (IC) with hDNF cells, using as cells alone as control. Statistical significance for $p \leq 0.05$ (*).

for cell adhesion, migration, proliferation, and differentiation due to the abundant Arg–Gly–Asp (RGD) amino acid sequences in its protein chain, which may enhance the metabolic activity of cells [65].

The proliferation of fibroblasts seeded on the electrospun gelatin meshes crosslinked with 4% of BDDGE (72 h) during 7 days was accessed using the metabolic activity assay and cell morphology was further observed by SEM and confocal microscopy. Samples with 4% BDDGE (72 h crosslinking) were selected according to the previous results. Since no samples showed cytotoxic effects the selection was based on the combination of adequate crosslinking degree, stability and mechanical properties but providing the lower amount of crosslinker. As shown in Fig. 6a fibroblasts cultured on the crosslinked gelatin electrospun meshes proliferated throughout the 7 days of culture. SEM images (Fig. 6b) show the intimate interaction between the cells and the nanofibrous structures. From day 1 to day 7, in agreement with metabolic activity assessment, it is possible to observe an increase in cell number, as well as the integration and spreading of cells in the filamentous electrospun mesh. According to Jin and co-authors (2014) the integrin-binding sites available on gelatin promote cell adhesion and proliferation, and the nano-sized fibers encourage better cell proliferation and signaling [65].

Electrospinning presents a unique ability to fabricate nanofiber-based scaffolds that best mimic the nanometer scale of the native ECM of skin [66]. Consequently, electrospun skin substitutes have been claimed to have increased potential to promote better cellular attachment, growth and differentiation due the high surface area, high aspect ratio and high microporosity provided by the low fiber diameter structure [67–69], which seems to be confirmed in the present work. Confocal microscopy images (Fig. 6b) of cells cultured on the electrospun meshes show the capability of fibroblasts to adhere and proliferate across the 7 days of culture and that they exhibit a proper phenotype, with a typical fibroblastic morphology. Additionally, after 7 days of culture, the production of fibronectin by the fibroblasts is clearly observed, sowing their ability to synthesize new ECM. Fibronectin is a large glycoprotein which plays an essential role in development, wound healing and angiogenesis [70].

Gelatin is a cost-effective, biocompatible, biodegradable and cell-interactive material, known for not causing any adverse immune response [65]. However, its fast degradation in aqueous media, associated to usually low mechanical properties, considerably limit its

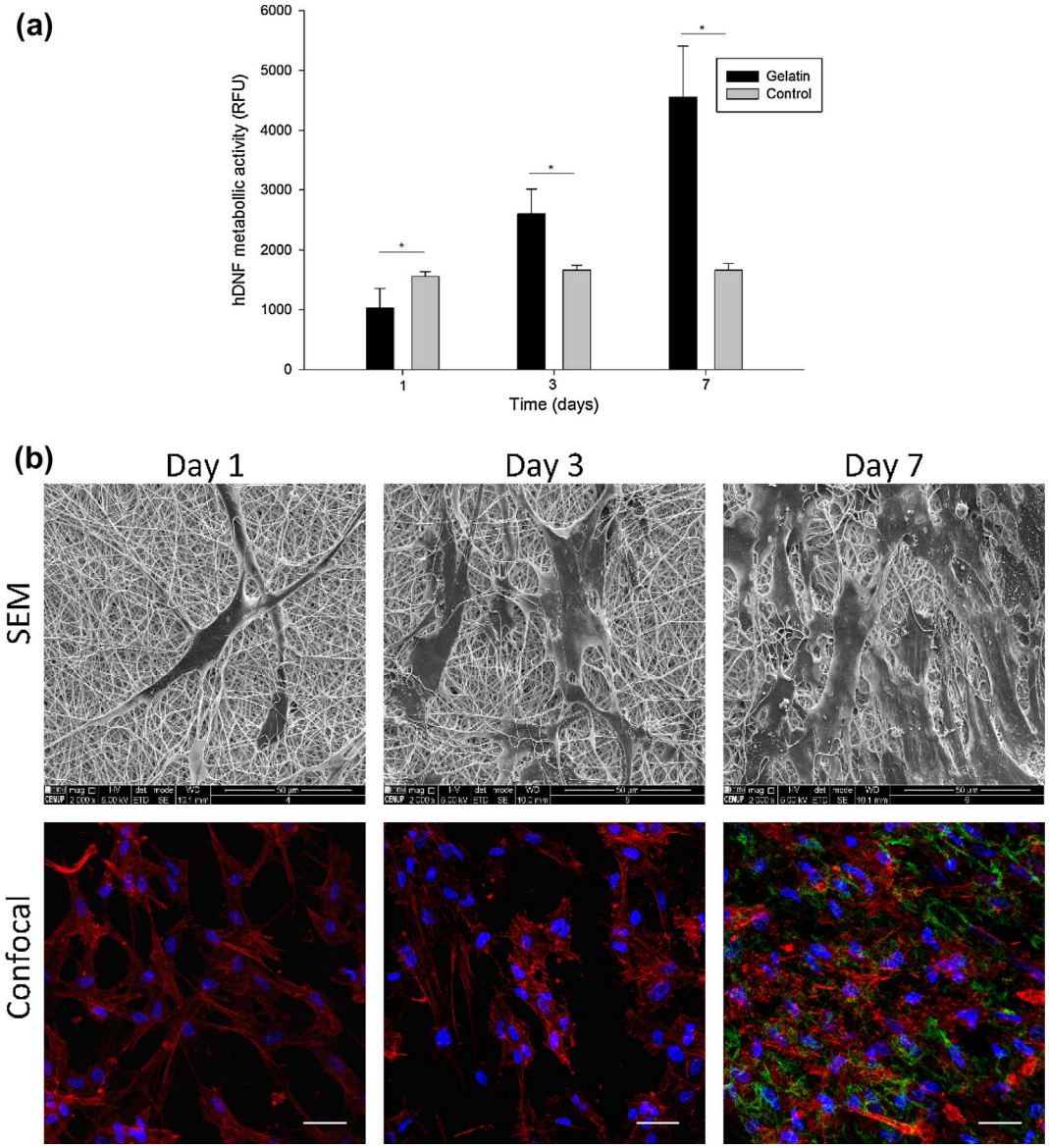

Fig. 6. Proliferation of hDNF cells on electrospun gelatin meshes. (a) Metabolic activity, using electrospun meshes without cells as control. Statistical significance for $p \leq 0.05$ (*). Scale bars correspond to 50 μm; (b) SEM and confocal microscopy images of cells cultured on electrospun meshes (blue: nuclei; red: actin; green: fibronectin). Scale bars correspond to 50 μm. (For interpretation of the references to colour in this figure legend, the reader is referred to the web version of this article.)

application [71]. Hence, new non-toxic gelatin crosslinkers are fundamental to improve the potential application of this biomaterial for tissue engineering applications. BDDGE is a widely used crosslinker in hyaluronic fillers already available in the market for several years. FDA determined that the use of unreacted BDDGE below 2 ppm is safe since those trace amounts are prone to hydrolysis ultimately yielding CO_2 and water [26]. Martucci and colleagues (2015) described for the first time the use of BDDGE as crosslinker of gelatin for preparing biodegradable films for food packaging. According to this study, the films produced by casting with different percentages of BDDGE (0.5, 1 and 3%), revealed a great potential for food packing due to their non-toxicity and enhanced mechanical properties [39]. However, this paper reports for the first time the use of BDDGE as *in situ* crosslinker of electrospun gelatin nanofibers for biomedical applications. Due to its similarity with the native ECM, gelatin electrospun meshes have been previously investigated as dressings for wound healing and drug release, revealing promising properties [9]. However, most of the crosslinkers used are toxic and/or non-stable, inducing changes in the fiber morphology due to the crosslinking bath/vapor used after fibers production [9,72]. The *in situ* crosslinking method used here represents a more effective crosslinking strategy than the traditional vapor crosslinking due to the homogenous mixing between polymer and crosslinker at the syringe prior to fiber formation [73]. The current study further demonstrates the possibility of modulating fiber diameter by controlling the *in situ* crosslinking parameters. Furthermore, the obtained electrospun meshes kept their morphology after the crosslinking process. Ultimately, gelatin electrospun meshes crosslinked

with BDDGE show great potential as wound dressings due to their ideal water vapor permeability rate, stability on aqueous medium, adequate swelling degree, non-toxicity and capability to promote fibroblasts attachment, proliferation and production of ECM proteins.

4. Conclusions

The main purpose of this research work was to explore, for the first time, the potential of crosslinking gelatin fibers with BDDGE, improving its stability in aqueous media and mechanical properties. BDDGE-crosslinked gelatin meshes were synthesized, characterized and tested regarding their toxicity and potential as wound dressing. Electrospun gelatin fibers crosslinked with BDDGE were successfully produced, allowing to obtain meshes with a well-defined morphology and random deposition. The crosslinking degree could be tuned changing the amount of crosslinker and the incubation time, which allowed the control of both fiber diameter and mechanical properties. 4% and 6% BDDGE (both incubated for 72 h) provided gelatin fibers with high crosslinking degree and stable diameters of 339 ± 91 and 276 ± 88 nm, respectively, although 4% BDDGE resulted in the best combination of mechanical properties. Cytotoxicity assays revealed no toxicity and proliferation assays showed that fibroblasts were able to attach and proliferate, producing new extracellular matrix within the electrospun meshes. Overall, this study demonstrated the potential of BDDGE as an alternative gelatin crosslinker due its non-toxicity and capability to tailor gelatin's mechanical and physical properties.

Acknowledgements

This study was supported by the Projects PTDC/BBB-ECT/2145/2014 and UID/Multi/04044/2013, financed by European Fonds Européen de Développement Régional (FEDER) through the Portuguese national programs Programa Operacional Factores de Competitividade (COMPETE), Portugal2020 and Norte2020, and by Portuguese funds through Fundação para a Ciência e a Tecnologia (FCT). This work is also supported by the research grants SFRH/BD/91104/2012 awarded to Juliana Dias and SFRH/BPD/90047/2012 awarded to Aureliana Sousa by FCT, and by the Investigator FCT program IF/00411/2013, awarded to Ana L. Oliveira. The authors thanks to CEMUP, University of Porto for the SEM images and, to Victoria Leiro and Marco Araújo for their support in chemical reactions interpretation.

References

[1] S. MacNeil, Progress and opportunities for tissue-engineering skin, Nature 445 (2007) 874–880.
[2] G. Casey, The physiology of the skin, Nursing Standard 16 (2002) 47–51.
[3] S.S. Zhou, D. Li, Y.M. Zhou, J.M. Cao, The skin function: a factor of anti-metabolic syndrome, Diabetol. Metab Syndrom. 4 (2012) 1–11.
[4] L. Yildirimer, N.T.K. Thanh, A.M. Seifalian, Skin regeneration scaffolds a multimodal bottom-up approach, Trends Biotechnol. 30 (2012) 638–648.
[5] V.J. Reddy, S. Radhakrishnan, R. Ravichandran, S. Mukherjee, R. Balamurugan, S. Sundarrajan, S. Ramakrishna, Nanofibrous structured biomimetic strategies for skin tissue regeneration, Wound Rep. Reg. (2013) 211–216.
[6] P. Zahedi, I. Rezaeian, S.O. Ranaei-Sidat, S.H. Jafari, P. Supaphol, A review on wound dressings with an emphasis on electrospun nanofibrous polymeric bandages, Polym. Adv. Technol. 21 (2009) 77–95.
[7] A. Vasconcelos, A.C. Gomes, A. Cavaco-Paulo, Novel silk fibroin/elastin wound dressings, Acta Biomater. 8 (2012) 3049–3060.
[8] R.F. Pereira, C.C. Barrias, P.L. Granja, P.J. Bártolo, Advanced biofabrication strategies for skin regeneration and repair, Nanomedicine 8 (2013) 603–621.
[9] Y.Z. Zhang, J. Venugopal, Z.M. Huang, C.T. Lim, S. Ramakrishna, Crosslinking of the electrospun gelatin nanofibers, Polymer 47 (2006) 2911–2917.
[10] A.G. Ward, A. Courts, The Science and Technology of Gelatin, Academic Press, Inc,, London, 1977.
[11] E.P. Broderick, D.M. O'Halloran, Y.A. Rochev, M. Griffin, R.J. Collighan, A.S. Pandit, Enzymatic stabilization of gelatin-based scaffolds, J. Biomed. Mater. Res. B Appl. Biomater. 72 (2005) 37–42.
[12] C.W. Yung, L.Q. Wu, J.A. Tullman, G.F. Payne, W.E. Bentley, T.A. Barbari, Transglutaminase crosslinked gelatin as a tissue engineering scaffold, J. Biomed. Mater. Res. Part A. 83 (2007) 1039–1046.
[13] K. Ulubayram, E. Aksu, S.I.D. Gurhan, K. Serbetci, N. Hasirci, Cytotoxicity evaluation of gelatin sponges prepared with different cross-linking agents, J. Biomater. Sci. Polym. (2002) 1203–1219.
[14] J.P. Draye, B. Delaey, A. Van de Voorde, A. Van Den Bulcke, B. De Reu, E. Schacht, In vitro and in vivo biocompatibility of dextran dialdehyde cross-linked gelatin hydrogel films, Biomaterials (1998) 1677–1687.
[15] H.W. Sung, D.M. Huang, W.H. Chang, R.N. Huang, J.C. Hsu, Evaluation of gelatin hydrogel crosslinked with various crosslinking agents as bioadhesives: In vitro study, J. Biomed. Mater. Res. (1999) 520–530.
[16] R.R. Ray, S.C. Jana, G. Nanda, Immobilization of β-amylase from Bacillus megaterium B6 into gelatin film by cross-linking, J. Appl. Bacterial (1995) 157–162.
[17] S. Matsuda, H. Iwata, N. Se, Y. Ikada, Bioadhesion of gelatin films crosslinked with glutaraldehyde, J. Biomed. Mater. Res. (1999) 20–27.
[18] S.M. Lien, W.T. Li, T.J. Huang, Genipin-crosslinked gelatin scaffolds for articular cartilage tissue engineering with a novel crosslinking method, Mater. Sci. Eng. Biomim. Mater. Sens. Syst. (2008) 36–43.
[19] C.H. Yao, B.S. Liu, C.J. Chang, S.H. Hsu, Y.S. Chen, Preparation of networks of gelatin and genipin as degradable biomaterials, Mater. Chem. Phys. 204–8 (2004).
[20] A.A. Apostolov, D. Boneva, E. Vassileva, J.E. Mark, S. Fakirov, Mechanical properties of native and crosslinked gelatins in a bending deformation, J. Appl. Polym. Sci. (2000) 2041–2048.
[21] Y. Ming-Kung, L. Yan-Ming, C. Kuang-Ming, D. Niann-Tzyy, L. Cheng-Che, Y. Jenn-Jong, A novel cell support membrane for skin tissue engineering: Gelatin film cross-linked with 2-chloro-1-methylpyridinium iodide. Polymer (2011) 996–1003.
[22] A. Bigi, G. Cojazzi, S. Panzavolta, K. Rubini, N. Roveri, Mechanical and thermal properties of gelatine films at different degrees of glutaraldehyde crosslinking, Biomaterials 763–768 (2001).
[23] J.F. Martucci, A. Accareddu, R.A. Ruseckaite, Preparation and characterization of plasticized gelatin films cross-linked with low concentrations of glutaraldehyde, J. Materials Sci. (2012) 2382–3292.
[24] J. Guo, L. Ge, X. Li, C. Mu, D. Li, Periodate oxidation of xanthan gum and its crosslinking effects on gelatin-based edible films, Food Hydrocolloids 243–250 (2014).
[25] D. Enea, F. Henson, S. Kew, J. Wardale, A. Getgood, R. Brooks, N. Rushton, Extruded collagen fibres for tissue engineering applications: effect of crosslinking method on mechanical and biological properties, J. Mater. Sci.: Mater. Med. (2011) 1569–1578.
[26] K. De Boulle, R. Glogau, T. Kono, M. Nathan, A. Tezel, J.-X. Roca- Martinez, S. Paliwal, D. Stroumpoulis, A review of the metabolism of 1,4-butanediol diglycidyl ether–crosslinked hyaluronic acid dermal fillers, Dermatolog. Surg. (2013) 1758–1766.

[27] J. Zhang, X. Ma, D. Fan, C. Zhu, J. Deng, J. Hui, P. Ma, Synthesis and characterization of hyaluronic acid/human-like collagen hydrogels, Mater. Sci. Eng., C (2014) 547–554.
[28] W. He, Z. Ma, T. Yong, W.E. Teo, S. Ramakrishna, Fabrication of collagen-coated biodegradable polymer nanofiber mesh and its potential for endothelial cells growth, Biomaterials 7606–761 (2005).
[29] M.-K. Yeh, Y.-M. Liang, K.-M. Cheng, N.-T. Dai, C.-C. Liu, J.-J. Young, A novel cell support membrane for skin tissue engineering: Gelatin film cross-linked with 2-chloro-1-methylpyridinium iodide, Polymer 996–1003 (2011).
[30] I. ASTM, Standard test methods for water vapor transmission of materials, in: E96/E96M-10.
[31] R.C. Team, R: A language and environment for statistical computing., ed. R.F.f.S. Computing, Vienna, Austria, 2014.
[32] F.J. O'Brien, Biomaterials & scaffolds for tissue engineering, Mater. Today 14 (2011) 88–95.
[33] C.A. Léon y Léon, New perspectives in mercury porosimetry, Adv. Coll. Interface. Sci. 76-77 (1998) 341–372.
[34] T. Garg, O. Singh, S. Arora, R.S.R. Murthy, Scaffold: A novel carrier for cell and drug delivery, Crit. Rev.™ Therap. Drug Carrier Syst. 29 (2012) 1–63.
[35] T.M. Freyman, I.V. Yannas, L.J. Gibson, Cellular materials as porous scaffolds for tissue engineering, Prog. Mater. Sci. 46 (2001) 273–282.
[36] N. Cebi, M.Z. Durak, O.S. Toker, O. Sagdic, M. Arici, An evaluation of Fourier transforms infrared spectroscopy method for the classification and discrimination of bovine, porcine and fish gelatins, Food Chem. 190 (2016) 1109–1115.
[37] M. Nagarajan, S. Benjakul, T. Prodpran, P. Songtipya, H. Kishimura, Characteristics and functional properties of gelatin from splendid squid (Loligoformosana) skin as affected by extraction temperatures, Food Hydrocolloids 29 (2012) 389–397.
[38] D. Hashim, M.Y. Che, R. Norakasha, M. Shuhaimi, Y. Salmah, Z. Syahariza, Potential use of Fourier transform infrared spectroscopy for differentiation of bovine and porcine gelatins, Food Chem. 118 (2010) 856–860.
[39] J.F. Martucci, J.P. Espinosa, R.A. Ruseckaite, Physicochemical properties of films based on bovine gelatin cross-linked with 1,4-butanediol diglycidyl ether, Food Bioprocess Technol. 1645–1656 (2015).
[40] R. Núñez-Flores, B. Giménez, F. Fernández-Martín, M.E. López-Caballero, M.P. Montero, M.C. Gómez-Guillén, Physical and functional characterization of active fish gelatin films incorporated with lignin, Food Hydrocolloids 39 (2013) 243–250.
[41] J. Bandekar, Amide modes and protein conformation, Biochim. Biophys. Acta 1120 (1992) 123–143.
[42] L. Shecter, J. Wynstra, R.P. Kurkjy, Glycidyl ether reactions with amines, Ind. Eng. Chem. 48 (1956).
[43] R.G. Paul, A.J. Bailey, Chemical stabilisation of collagen as a biomimetic, Sci. World J. 3 (2003) 138–155.
[44] M.M. Hohmann, M. Shin, G. Rutledge, M.P. Brenner, Electrospinning and electrically forced jets I stability theory, Phys. Fluid. (2001) 2201–2220.
[45] H.S. Azevedo, M.G. Francisco, R.L. Reis, In vitro assessment of the enzymatic degradation of several starch based biomaterials, Biomacromol. 4 (2003) 1703–1712.
[46] G. Vargas, J.L. Acevedo, J. López, J. Romero, Study of cross-linking of gelatin by ethylene glycol diglycidyl ether, Mater. Lett. 62 (2008) 3656–3658.
[47] N.V. Gupta, H.G. Shivakumar, Investigation of swelling behavior and mechanical properties of a ph-sensitive superporous hydrogel composite, Iranian J. Pharm. Res. 11 (2012) 481–493.
[48] H.K. Ju, S.Y. Kim, Y.M. Lee, pH/temperature-responsive behaviors of semi-IPN and comb-type graft hydrogels composed of alginate and poly(N-iso-propylacrylamide), Polymer 42 (2001) 6851–6857.
[49] S.-Y. Gu, Z.-M. Wang, J. Ren, S.-Y. Zhang, Electrospinning of gelatin and gelatin/poly(L-lactide) blend and its characteristics for wound dressing, Mater. Sci. Eng., C 29 (2009) 1822–1828.
[50] C.K. Field, M.D. Kerstein, Overview of wound healing in a moist environment, Am. J. Surgery 16 (1994) 2–6.
[51] M. Abrigo, S.L. McArthur, P. Kingshott, Electrospun nanofibers as dressings for chronic wound care: advances, challenges, and future prospects, Macromol. Biosci. 14 (2014) 772–792.
[52] L.O. Lamke, G.E. Nilsson, H.L. Reithner, The evaporative water loss from burns and the water-vapour permeability of grafts and artificial membranes used in the treatment of burns, Burns 3 (1977) 159–165.
[53] R. Dave, H.M. Joshi, V.P. Venugopalan, Biomedical evaluation of a novel nitrogen oxides releasing wound dressing, J. Mater. Sci.: Mater. Med. 23 (2012) 3097–3106.
[54] S. Gustaitea, J. Kazlauskea, J. Bobokalonova, S. Perni, V. Dutschkc, J. Liesienea, P. Prokopovich, Characterization of cellulose based sponges for wound dressings, Colloids Surfaces A: Physicochem. Eng. Aspects 480 (2015) 336–342.
[55] P.I. Morgado, A.A. Ricardo, I.J. Correia, Asymmetric membranes as ideal wound dressings: An overview on production methods, structure, properties and performance relationship, J. Membrane Sci. 490 (2015) 139–151.
[56] P.B. van Wachem, R. Zeeman, P.J. Dijkstra, J. Feijen, M. Hendriks, P.T. Cahalan, M.J.A. van Luyn, Characterization and biocompatibility of epoxy-crosslinked dermal sheep collagens, J. Biomed. Mater. Res. 47 (1999) 270–277.
[57] R. Zeeman, P.J. Dijkstra, P.B. van Wachem, M.J.A. van Luyn, M. Hendriks, P.T. Cahalan, J. Feijen, Crosslinking and modification of dermal sheep collagen using 1,4-butanediol diglycidyl ether, J. Biomed. Mater. Res. 46 (1999) 424–433.
[58] H. Vogel, Age dependence of mechanical and biochemical properties of human skin, Bioeng. Skin 3 (1987).
[59] L. Jansen, P. Rottier, Some mechanical properties of human abdominal skin measured on excised strips, Dermatologica 117 (1985) 65–83.
[60] C. Jacquemoud, K. Bruyere-Garnier, M. Coret, Methodology to determine failure characteristics of planar soft tissues using a dynamic tensile test, J. Biomech. 40 (2007) 468–475.
[61] J.-F. Pan, N.-H. Liu, H. Sun, F. Xu, Preparation and characterization of electrospun PLCL/poloxamer nanofibers and dextran/gelatin hydrogels for skin tissue engineering, PLoS ONE 9 (2014) e112885.
[62] M. Gümüşderelioğlu, S. Dalkıranoğlu, R.S.T. Aydın, S. Çakmak, A novel dermal substitute based on biofunctionalized electrospun PCL nanofibrous matrix, J. Biomed. Mater. Res. Part A 98 (2011) 461–472.
[63] D. Atila, D. Keskin, A. Tezcaner, Cellulose acetate based 3-dimensional electrospun scaffolds for skin tissue engineering applications, Carbohyd. Polym. 133 (2015) 251–261.
[64] E.J. Lee, J.H. Lee, L. Jin, O.S. Jin, Y.C. Shin, S.J. Oh, J. Lee, S.-H. Hyon, D.-W. Han, Hyaluronic acid/poly(lactic-co-glycolic acid) core/shell fiber meshes loaded with pigallocatechin-3-O-gallate as skin tissue engineering scaffolds, J. Nanosci. Nanotechnol. 14 (2014) 8458–8463.
[65] G. Jin, Y. Li, M.P. Prabhakaran, W. Tian, S. Ramakrishna, In vitro and in vivo evaluation of the wound healing capability of electrospun gelatin/PLLCL nanofibers, J. Bioactive Compatible Polym. 29 (2014) 628–645.
[66] J.R. Dias, P.L. Granja, P.J. Bártolo, Advances in electrospun skin substitutes, Prog. Mater Sci. 84 (2016) 314–334.
[67] W. Cui, Y. Zhou, J. Chang, Electrospun nanofibrous materials for tissue engineering and drug delivery, Sci. Technol. Adv. Mater (2010) 11014108.
[68] S. Pramanik, B. Pingguan-Murphy, N.A.A. Osman, Progress if key strategies in development of electrospun scaffolds: bone tissue, Sci. Technol. Adv. Mater. 131–13 (2012).
[69] W. Liu, S. Thomopoulos, Y. Xia, Electrospun nanofibres for regenerative medicine, Adv. Healthcare Mater. 1 (2012) 10–25.
[70] A. Hielscher, K. Ellis, C. Qiu, J. Porterfield, S. Gerecht, Fibronectin deposition participates in extracellular matrix assembly and vascular morphogenesis, PLoS ONE 11 (2016) e0147600.
[71] A. Kasuya, S. Sobajima, M. Kinoshita, In vivo degradation and new bone formation of calcium phosphate cement–gelatin powder composite related to macroporosity after in situ gelatin degradation, J. Orthop. Res. 30 (2012) 103–1111.
[72] S.R. Gomes, G. Rodrigues, G.G. Martins, M.A. Roberto, M. Mafra, C.M.R. Henriques, J.C. Silva, In vitro and in vivo evaluation of electrospun nanofibers of PCL, chitosan and gelatin: A comparative study, Mater. Sci. Eng., C 46 (2015) 348–358.
[73] A.P. Kishan, R.M. Nezarati, C.M. Radzicki, A.L. Renfro, J.L. Robinson, M.E. Whitely, E.M. Cosgriff-Hernandez, In situ crosslinking of electrospun gelatin for improved fiber morphology retention and tunable degradation, J. Mater. Chem. B. 3 (2015) 7930.

Europass-Curriculum Vitae

Informação pessoal

Apelido(s) / Nome(s) próprio(s)	**Dias, Juliana Rosa**
Morada(s)	Rua da charneca nº798 Moinhos de carvide, 2425-371 Carvide, Portugal
Telefone(s)	n.a. Telemóvel: 919483792
Fax(es)	n.a.
Correio(s) electrónico(s)	jrdias.juliana@gmail.com
Nacionalidade	Portuguesa
Data de nascimento	22/09/87
Sexo	Feminino

Experiência Profissional

• *Datas (de – até)*	2013-2017
• *Nome e endereço do empregador*	Fundação para a Ciência e Tecnologia (FCT) 1º e 2º ano – Centro para o Desenvolvimento Rápido e Sustentado de Produto do Instituto Politécnico de Leiria, Marinha Grande, Portugal; 3º e 4º ano – Instituto de Investigação e Inovação em Saúde da Universidade do Porto, Porto, Portugal;
• *Tipo de empresa ou sector*	Investigação
• *Função ou cargo ocupado*	Aluna premiada com bolsa de doutoramento (SFRH/BD/91104/2012) para o desenvolvimento do projeto :" Hybrid electrospun fibers for skin regeneration. O projeto baseia-se no desenvolvimento de um curativo que colmate as necessidades do mercado para este tipo de dispositivo médico. O curativo é composto por uma estrutura híbrida de nanofibras de polímeros naturais e sintéticos. Para a produção das mesmas foi feita uma nova assemblagem da tecnologia de electrospinning e o processamento otimizado. As estruturas produzidas foram alvo de profundas caracterizações em termos de propriedades mecânicas, físicas, químicas , morfológicas e biológicas de forma a selecionar a estrutura ideal para a utilização como curativo para a regeneração da pele.

• *Datas (de – até)*	2011 – 2013
• *Nome e endereço do empregador*	Centro para o Desenvolvimento Rápido e Sustentado do Produto Centro empresarial da Marinha Grande Rua de Portugal – Zona Industrial 2430-028 Marinha Grande
• *Tipo de empresa ou sector*	Centro de Investigação

• *Função ou cargo ocupado*	• Responsável-técnico do Laboratório de Materiais Neste âmbito realizavam-se caracterizações químicas, físicas e mecânicas (FTIR, DSC, Texturometro, Micro-CT, Angulo de contacto, entre outras) a materiais poliméricos, quer no âmbito de projetos industriais quer no âmbito de projetos de investigação. • Preparação e submissão de candidaturas no âmbito do 7FP e Horizonte2020 a entidades como o QREN e IAPMEI. Estreita colaboração com as empresas para preparação de candidaturas sólidas e inovadoras. Submissão de candidaturas a vales I&DT, projetos individuais e de co-promoção com empresas como 3DTech, Moliporex, Derovo, Farmi, Vibeiras, 3DCAD, entre outras.
• *Datas (de – até)*	23-03-2009 – 2011
• *Nome e endereço do empregador*	Centro para o Desenvolvimento Rápido e Sustentado do Produto Centro empresarial da Marinha Grande Rua de Portugal – Zona Industrial 2430-028 Marinha Grande
• *Tipo de empresa ou sector*	Centro de Investigação
• *Função ou cargo ocupado*	Bolseira de Investigação
• *Principais actividades e responsabilidades*	Desenvolvimento de nanofibras para aplicações médicas; Caracterização de Biomateriais; Organização de Conferências e Workshops; Elaboração de candidaturas a projectos.

Educação e formação

Datas	De 2008 a 2011
Designação da qualificação atribuída	Mestrado em Engenharia da Conceção e Desenvolvimento do Produto
"Principais disciplinas/competências profissionais	**Domínio Geral** Proporciona um conjunto integrado de competências dinâmicas, solidamente alicerçadas em conhecimentos técnicos e científicos imprescindíveis ao desenvolvimento de produtos de qualidade, de forma rápida e inovadora, com elevado grau de sucesso e valor acrescentado. Confere uma formação multidisciplinar e versátil, que permita ao profissional desempenhar funções estratégicas e/ou supervisão em empresas industriais ou de serviços, bem como entidades públicas ou privadas. **Domínio específico** **1º Ano** Design do Produto; Design Sustentável; Materiais de Elevado Desempenho; Modelação e Simulação do Produto; Marketing de Novos Produtos; Introdução à Investigação; Comportamento em Serviço de Componentes Mecânicos, Prototipagem e Fabricação Rápida; Eficiência Energética e Ambiente; Reciclagem de Materiais; Tecnologias Avançadas de Produção; Automatização e Robótica; **2º Ano** Dissertação: "Nanofibres Development for cartilage tissue through electrospinning process"
Nome e tipo da organização de ensino ou formação	Instituto politécnico de leiria Escola superior de tecnologia e gestão de Leiria Morro do Lena Apartado 4163-2411-901 Alto do Vieiro, Leiria

Classificação obtida nacional ou internacional	Dezoito valores (18)
Classificação obtida nacional ou internacional	n.a.

Educação e formação

Datas	De 12-01-2010 a 30-03-2010
Designação da qualificação atribuída	Certificado de Competências Pedagógicas (CCP, antigo CAP);
"Principais disciplinas/competências profissionais	- Dotar os profissionais de competências com vista ao planeamento, organização e animação de acções de formação.
Nome e tipo da organização de ensino ou formação	Grupo Pessoas & Soluções
Classificação obtida nacional ou internacional	n.a.

Educação e formação

Datas	De 2005 a 2008.
Designação da qualificação atribuída	• Licenciatura em Biomecânica;
"Principais disciplinas/competências profissionais	**Domínio geral:** - Projecto de 1º ano de mestrado intitulado: Sistema multifuncinal para a reabilitação humana – Rehabstairs"; - Fortes conhecimentos em imagiologia médica; - Elevadas competências nas técnicas aditivas utilizadas em biofabricação; - Dissertação do Projecto Biomecânico intitulado "Hidrogeis: caracterização e libertação de fármacos"; - Conhecimentos bastante aprofundados em Electrospinning; - Elevadas capacidades na caracterização de materiais poliméricos; - Anatomia e fisiologia, - Modelação computacional; - Biomecânica do movimento; - Biomateriais, - Ergonomia e Conforto; - Higiene e Segurança no trabalho; - Biofabricação; - Biomecânica dos tecidos; - Antropometria; - Simulação computacional; - Biomimética; - Engenharia de Tecidos.
Nome e tipo da organização de ensino ou formação	Instituto politécnico de leiria Escola superior de tecnologia e gestão de Leiria Morro do Lena Apartado 4163-2411-901 Alto do vieiro, Leiria
Classificação obtida nacional ou internacional	Quinze valores (15)

Outra(s) língua(s)

Auto-avaliação	Compreensão				Conversação				Escrita	
Nível europeu (*)	Compreensão oral		Leitura		Interacção oral		Produção oral			
Inglês	B1	Utilizador independente	B1	Utilizador independente	B1	Utilizador independente	B1	Utilizador independente	B1	Utilizador independente

(*) Nível do Quadro Europeu Comum de Referência (CECR)

Aptidões e competências sociais	- Iniciativa/Auto motivação; -Trabalho em equipa; - Planeamento/organização; - Gestão de tempo; - Liderança; - Dinamismo; - Versatilidade; - Boa capacidade de comunicação.
Aptidões e competências de organização	• Organização de diversas conferências e workshops: - 5th and 6th International Conference on Advanced Research in Virtual and Rapid Prototyping (VR@P2011/2), Leiria, Portugal, - 1ª e 2ª Conferencia Internacional SIM, 2011/3; - 1º, 2º, 3º e 4ºCurso Internacional Avançado em Medicina regenerativa(2011-4) - 3º Workshop do Centro para o Desenvolvimento Rápido e Sustentado de produto, 2010; • Sentido de organização e planeamento; • Gestão de recursos e tempos; • Capacidade de liderança.
Aptidões e competências técnicas	- Equipamentos laboratoriais utilizados na caracterização de polímeros: - DSC, - STA 6000; - Identipol; - DMA; - TG, - Texturometro, - FTIR; - Micro-CT; - Reómetro de pratos, - Espectrofotómetro UV-VIS; - Análises biológicas; - Microscópios eletrónicos e confocais.
Aptidões e competências informáticas	Domínio de diversos softwares como: - Word; - Exel; - Powerpoint; - Image J; - Visio; - Solidworks; - Invensalius; - Mimics; - Geomagic; - Labview; - Twido.
Carta de condução	Carta de condução de categoria B.

Informação adicional

Publicações

JR Dias, C dos Santos, J Horta, PL Granja, PJ Bártolo A new design of an electrospinning apparatus for tissue engineering applications, International Journal of Bioprinting, 2017, DOI 10.18063 /IJB. 2017. 02 .002.

JR Dias, PL Granja, PJ Bártolo, Advances in electrospun skin substitutes. Progress in Materials Science, 84, 2016, 314–334

JR Dias, FE Antunes, PJ Bártolo, Influence of the rheological behaviour in electrospun PCL nanofibres production for tissue engineering applications, Chemical Engineering Transactions, 32, 2013, 1015-1020;

E Gomez, JR Dias , U D'Amora, C A Rodríguez, A Gloria, PJ Bártolo. Morphological and mechanical evaluation of hybrid scaffolds for bone regeneration, Advanced Materials Research, 749, 2013, 429-432;

JR Dias, PJ Bártolo, Morphological characteristics of electrospun pcl meshes – the influence of solvent type and concentration, Procedia CIRP, 5,2013, 216-221;

JR Dias, A Gloria, PJ Bártolo,Mechanical and biological characteristics of electrospun PCL meshes – the influence of solvent type and concentration, Advanced Materials Research, 683,2013, 137-140 ;

JR Dias, I Reis, PJ Bártolo (2013) Potencial do electrospinning para aplicações industriais, Revista O Molde, 96, 35-38;

G Rodriguez, J Dias, M A d'Ávila, P Bártolo, Influence of Hydroxyapatite on Extruded 3D Scaffolds, Procedia Engineering 59,2013, 263 – 269;

Dias, Juliana; Antunes, Filipe; Mitchell, Geoffrey; Bártolo, Paulo Jorge: "Electrospun PCL meshes for cartilage regeneration", 5th International Conference: Advanved research in Virtual and Rapid Prototyping (VR@P2011), Leiria, 2011;

Dias, Juliana; Antunes, Filipe; Mitchell, Geoffrey; Bártolo, Paulo Jorge: "Produção de nanofibras em PCL para a cartilagem através de Electrospinning", 4° Congresso de Biomecânica,Coimbra, 2011;

Dias, Juliana; Mitchell, Geoffrey; Bártolo, Paulo Jorge: "Avaliação do processo de Electrospinning para produção de scaffolds em PCL para Engenharia de Tecidos", Confeng10, Covilhã, 2009;

Dias, Juliana; Mitchell, Geoffrey; Bártolo, Paulo Jorge: "Avaliação do processo de Electrospinning para produção de scaffolds em PCL para Engenharia de Tecidos"; 1as Jornadas do Curso de Mestrado em Concepção e Desenvolvimento de Produto, Marinha Grande, 2009;

Dias, Juliana, Patrício, Tatiana; Sousa, Inês; Sousa, João; "Automatização do Sistema Multifuncional para a Reabilitação Humana – Rehabstairs" 1as Jornadas do Curso de Mestrado em Concepção e Desenvolvimento de Produto, Marinha Grande, 2009.

Livros

P.J. Bártolo, A.C. de Lemos, A.P. Tojeira, A. Mateus, C. Capela, C. da Silva, D.M. Freitas, F. Domingues, H. Bártolo, H.A. Almeida, M. Domingos, J.R.Dias, N.M. Alves & R. Pereira (Eds.), INNOVATIVE DEVELOPMENTS IN VIRTUAL AND PHYSICAL PROTOTYPING, CRC Press.

Capítulos de livro

Dias, Juliana; Almeida, Henrique, Bártolo, Paulo Jorge; "Sinterização Laser"; Fascículo do livro para a rede Ibero-Americana BIOFAB, 2010.

Patentes

I. Sousa, J. Sousa, J. Dias, T. Patrício, P.J. Bártolo, N.M. Alves, C. Capela, A. Mendes, H.A. Almeida, N. André, SISTEMA MULTIFUNCIONAL PARA REABILITAÇÃO HUMANA, Modelo de utilidade Nacional n° 104470.

Orador Convidado

- 28 de Março, 2017: "Hierarchical electrospun nanostructures for skin regeneration", School of Bioengineering, Universidade Católica, Porto;

- 19 de Abril,2017: "Nanofibras como base de desenvolvimento de estruturas híbridas para a regeneração da pele ", VI Biomechanics day, School of technology and Management, Instituto Politécnico de Leiria, Leiria;

Arguência Provas

- 28 de Março, 2017, The effect of sonication on electrospun Silk Fibroin/PEO membranes for periodontal regeneration", Candidato ao grau de Mestre em Engenharia Biomédica, Aluno Ricardo Serôdio, School of Bioengineering, Universidade Católica, Porto;

Seminários/Workshops

- 18 de Fevereiro, 2013: Design of Advanced Prostheses and 3D Multifunctional Scaffolds with Enhanced and Tailored Properties, Doctor Antonio Gloria, Institute of Composite and Biomedical Materials – National Research Council of Italy, and Universidade de Nápoles "Federico II", Itália

- 16 de Abril, 2013: "Biomaterials for Neurosciences @ INEB", Doctor Ana Paula Pêgo, Instituto de Engenharia Biomédica (INEB);

- 17 de Abril, 2013: "Contribuições da neuroengenharia em aplicações à Epilepsia e ao Estudo do Tremor", Doctor Paula Faria, Departamento de Matemática, ESTG – Instituto Politécnico de Leiria | Centro para o Desenvolvimento Rápido e Sustentado de Produto – IPL;

- 3 de Maio, 2013: "Educação e Formação para o Século XXI – "Aprendizagem através da Tecnologia", Doctor António Augusto Fernandes, Distance Learning Consulting Company;

- 12 de Junho, 2013: Engenharia em Português: interessante em tempos de crise? Há futuro?, Eng.º Rodolfo Martins, Evoleo Technologies, Lda company;

- 10 de Julho, 2013: Bioengineering strategies to modulate stem cell differentiation and improve cell engraftment, Doctor Lino Ferreira, BIOCANT.

- 17 de Junho, 2014: "Bioelectronic Medicines: treating diabetes by targeting the peripheral nervous system", Professor Maria Pedro Guarino, School of Health Sciences, Polytechnic Institute of Leiria;

- 10 de Setembro, 2014: Physics and its Boundaries - in Imaging and Display Technologies – Personal Experience", Professor David Ezra, DE Technologies Ltd and Centre for Advanced Microscopy, Reading University, UK;

- 22 de Dezembro, 2014 : "The thermography and its applications for health: Experience in using this resource for research" Professor Luis Carrao, School of Human Kinetics, University of Lisbon, School of Health Sciences, Polytechnic Institute of Leiria;

- 20 de Maio, 2015: NPY Signalling Pathway in Bone Homeostasis: Y1 Receptor as a Potential Drug Target, Daniela Sousa, Post-Doctoral Investigator, INEB;

- 27 de Maio, 2015: siRNA loaded nanoparticles to the blood-brain barrier – permeability through an in vitro BBB model and nanosystem improvement", Maria João Gomes, PhD student, INEB;

- 3 de Junho, 2015, "Impact of trimethyl chitosan nanoparticles degradation rate on their performance as a DNA vector" Carla Gomes, PhD student, INEB;

- 17 de Junho, 2015, "A 3D in vitro model to explore the inter-conversion between epithelial and mesenchymal states during EMT and its reversion", Sílvia Bidarra, Post-Doctoral Investigator, INEB;

- 28 de Outubro, 2015, "Thermo-Analysis 2015", Francesc Català,Product Specialist TA-Metler Toledo;

- 4 de Novembro, 2015, "Surface-immobilized Antimicrobial Peptides (AMPs) for prevention of implanted-related infections" Fabíola Costa Moutinho, PhD student, INEB;

- 2nd of December, 2015, "A Innovative Micro-and Nano Composites for Biomedical Applications" Helder A. Santos, Division of Pharmaceutical Chemistry & Technology, Faculty of Pharmacy, University of Helsinki, Finland;

- 14 de Março, 2015, " Silk fibroin-based scaffolds for tissue engineering", Viviana , PhD student at University of Minho, Seminar at Catholic University;

- 5 de Abril, 2016, " Our 10 year jouney with an endoplasmatic reticulum chaperone: from infection to cell biology", Sandra Sousa, I3S - IBMC, Group of molecular microbiology;

- 6 de Abril, 2016, "Novel modified collagen/ hydroxyapatite nanoparticles composites (coll/nanoha) for guided bone regeneration,Christiane Laranjo Salgado, I3S - INEB, Biocomposites;

-19 de Abril, 2016, "Bioengineered nanomedicines for modulation of mucosal drug delivery", Bruno Sarmento, Biomaterials for Multistage Drug & Cell Delivery group, i3S;

-21 de Abril, 2016, " Challenges of the application of chitosan in Tissue Engineering and Drug Delivery", Professor Juilio San Román from CSIC, Madrid. Seminar took place at Catholic University;

-11 de Maio, 2016, "GLP-1 nanotechnology based systems for diabetes therapy" Francisca Araújo - i3S/INEB, Biocarrier Group (Biomedical Sciences PhD Program, ICBAS)

-30 de Maio, 2016, " Natural-based hydrogels and liquefied microenvironments for biomedical applications", João Mano, CICECO, Research at University of Aveiro, Seminar took place at Catholic University;

- 7 de Junho, 2016, "An overview of the research presently being developed by the "BIOCOMPOSITES" Research Group (I3S)",Fernando Jorge Monteiro, i3S - INEB, Biocomposites Group

-6 de Julho, 2016, "An injectable Sr-Releasing Hybrid System to Promote Bone Regeneration" Ana Lourenço - Microenvironments for New Therapies group, i3S/INEB

Conferences/ Courses

3 – 6 de Março, 2013: 1st CIRP Conference on BioManufacturing, Tokyo, Japan;

2-5 de Junho, 2013: 11th International conference on Chemical & Process Engineering (ICheaP-11), Milan, Italy;

6 -8 de Junho, 2013: 3rd International Conference on Tissue Engineering (ICTE), Leiria, Portugal (Organizing committee);

1 – 5 de Outubro, 2013: International Conference on Advanced Research in Virtual and Rapid Prototyping (VRAP 2013), Leiria, Portugal;

- 21 – 23 de Maio, 2014: 2nd Hydrozones Training course, Utrecht, Netherlands;

- 12 de Dezembro, 2014: REMED- 4th Advanced Course on Regenerative Medicine, Centre for Rapid and Sustainable Product Development (CDRSP);

- 25 -27 de Junho 2015: 4th International Conference on Tissue Engineering (ICTE), Lisboa, Portugal, (oral presentation);

- 29 – 31 de Julho, 2015: 2nd CIRP conference on Biomanufacturing (CIRP-Bio 2015), Manchester, UK; (Oral presentation)

- 11 de Dezembro, 2015: REMED- 5th Advanced Course on Regenerative Medicine, Centre for Rapid and Sustainable Product Development (CDRSP);

-17 – 22 de Maio, 2016, WBC2016 – 10th world Biomaterials Congress, Montréal, Canadá, Poster presentation : Internal crosslinking evaluation of gelatin electrospinning fibers with 1,4 – butanediol Diglycidyl ether;

-30 de Junho – 1 de Julho, 2016, MDA2016 – 1st International conference on Materials design and applications, Oral presentation (Pedro Granja): "Evaluation of Gelatin Electrospun Fibers Crosslinked with 1,4 – butanediol Diglycidyl Ether for Skin Regeneration".

-28 de Junho – 1 de Julho, 2016, Electrospin2016 – 4th International Conference on Electrospinning 2016, Otranto, Italy, Oral presentation: Hybrid electrospun meshes for skin regeneration.